

ASPECTS OF COMBUSTION OF SOLID FUELS
IN FLUIDIZED BED COMBUSTORS

by

FOLORUNSHO OLAYIWOLA AKINBODE

A thesis
submitted for the
Degree of
Doctor of Philosophy

Department of Mechanical and Production Engineering
The University of Aston in Birmingham, England

OCTOBER 1984

THE UNIVERSITY OF ASTON IN BIRMINGHAM

ASPECTS OF COMBUSTION OF SOLID FUELS IN FLUIDIZED BED
COMBUSTORS

by

FOLORUNSHO OLAYIWOLA AKINBODE

A THESIS SUBMITTED FOR THE DEGREE OF DOCTOR OF PHILOSOPHY
1984

SUMMARY

The work reported here represents an experimental study of the mechanism of combustion of solid fuels in fluidized bed combustor. Many such combustors burn coal particles in a bed of sand typically at 1073 - 1173^oK.

Past work on mechanisms of combustion in fluidized bed combustors has concentrated on combustion of residual carbon. Study in the present work is concentrated on the combustion of volatile matter in the fuel.

Initially some ancillary experiments were conducted at ambient temperature to obtain a little insight into the mixing of volatiles with air in the above-bed region. Combustion experiments were then performed using bituminous and non-bituminous coals and also wood in shallow (circa 100 mm deep) fluidized bed combustor. Both steady state and batch burning experiments were performed. The effect of fuel particle size on the time taken for emission of the volatile matter and combustion of it, was observed together with simultaneous measurements of temperatures, oxygen, carbon dioxide, carbon monoxide and unburnt hydrocarbon concentrations in the off-gas.

When burning coal, it was found that feeding secondary air into the above bed region did not enhance combustion, but feeding the same amount of air into the bed did. When burning wood the reverse was found.

In steady state tests, fuel, air and exhaust gas concentrations were used to estimate heat released by the fuel both in the bed and the above bed zone. These results were compared with predictions of a model developed by Merrick, and a different model developed in the course of this work. It showed that Merrick's model could be extended into FBC field.

Data showed that the amount of heat released in the above bed zone was very dependent upon the type of fuel and its particle size. The importance of this in relation to distribution of heat transfer surfaces is discussed.

VOLATILES COMBUSTION, TEMPERATURE, COAL, WOOD, FLUIDIZED BEDS.

ACKNOWLEDGEMENTS

An acknowledgement of deepest gratitude, appreciation and sincere thanks is made to Dr J R Howard who taught the author much on combustion and much more on life itself. His active supervision, constant encouragement, guidance, inspiration, suggestion and invaluable advice throughout this work have been of immense help.

A great deal of encouragement, guidance, invaluable advice and assistance came from Mr W L Flint particularly during the experimental tests and preparation of this work.

The author wishes to thank and acknowledge:- Dr Alex Gaines, Solid Research Laboratory, Department of Chemistry, University of Aston, for his advice, suggestions and assistance in analysing the coal and wood samples. Mr Neil Owen, technical staff of the same department for conducting the chromatography tests. Dr Eric Smith, Department of Chemical Engineering, University of Aston for his suggestions and assistance in analysing the samples. Dr H H Sheena of the same department for his assistance in conducting the proximate analysis tests on wood and coal samples. The technical staff, Department of Mechanical and Production Engineering, University of Aston for their active cooperation and assistance for the experimental work, particularly Mr John Scattergood, for his help in procuring materials, Mr Alan Evitts for his help in providing facilities for the experimental work, also Messrs P Pizer

and L. Beddall for constructing the experimental set-up and Messrs N. Moss, M. D. Clark and T. Horton for their help in the laboratory at different times.

Special thanks are due to Mr Peter Hickman who was always prepared to help during the experimental runs whenever he was needed. Financial help from the Federal Government of Nigeria is also gratefully acknowledged.

The author also would like to express his gratitude to his friend Mr Adesola Adediran for his encouragement, moral and financial support throughout the work. Finally, the author wishes to thank his wife Mojisola for her patience, understanding, encouragement and loving support throughout the work. To these people I am much indebted.

DEDICATED TO

My parents, my wife and children, who despite putting up with pre-occupation with energies, variation etc. over a long period, gave me the love and happiness necessary to pursue this arduous, but enjoyable career.

NOMENCLATURE

Ar	Archimedes number, $dp^3 \rho_g (\rho_p - \rho_g) g / \mu_g^2$.	
A	Surface area for heat transfer calculations	m^2
CV	Calorific value	kJ/kg
C	Specific heat at constant pressure.	kJ/kg
d_o	Coal particle diameter.	m
d_p	Particle diameter.	m
ϵ	Emissivity.	
g	Acceleration due to gravity	m/s^2
Gr	Grashof number $g \beta \rho^2 \Delta T L^3 / \mu^2$.	
H_R	Enthalpy of the reactants.	kJ/kg
H_P	Enthalpy of combustion products.	kJ/kg
h_{cond}	Conductive component of heat transfer.	$W/m^2 K$

h_{conv}	Convective component of heat transfer.	$\text{W/m}^2\text{K}$
h_{rad}	Radiative component of heat transfer.	$\text{W/m}^2\text{K}$
h_{Total}	Total components of heat transfer.	$\text{W/m}^2\text{K}$
k	Thermal conductivity.	W/m K
L	Characteristic length of the system.	m
M	Mass.	kg
\dot{M}	Mass flow rate.	kg/s
N	Number of particles.	
Nu	Nusselt number hdp/k_g .	
ΔP_D	Pressure drop across bed.	N/m^2
ΔP_D	Pressure drop across distributor.	N/m^2
Pr	Prandtl number, $C_p \mu_g / k_g$.	
Q	Heat transfer to the system.	kJ/kg

Re	Reynolds number, $d_p U_g \rho_g / \mu_g$.	
Re _{mf}	Reynolds number based on U _{mf} .	
R	Universal gas constant.	
T	Temperature	K
T _b	Temperature of bed	K
T _s	Temperature of heat transfer surface.	K
ΔT	Temperature difference.	K
t _c	Burn out time of a coal particle	s
t _{bdiffusion}	Burn out time of particle under diffusionally controlled rate of combustion.	s
t _{bkinetic}	Burn out time of particle under completely kinetically controlled rate of combustion.	s
U	Superficial gas velocity.	m/s
U _{mf}	Gas velocity at which bed becomes fluidized.	m/s

V	Volume	m^3
\dot{V}	Volumetric flow rate	litre/min
X	Mass fraction.	
Z	Bed height	m
ϵ_b	Emissivity of bed.	
ϵ_m	Modified emissivity allowing for effect of immersed surface on adjacent bed temperature.	
ϵ_{mf}	Voidage at minimum fluidization.	
ϵ_r	Reduced emissivity.	
ϵ_s	Emissivity of surface.	
Φ_s	Particle sphericity in Ergun equation.(2.4) see Addendum	
ρ_f	Density of fluid	kg/m^3
ρ_g	Density of gas	kg/m^3

ρ_p Density of particle kg/m^3

μ_g Viscosity of gas. kg/ms

ν Kinematic viscosity. kg/ms

SUBSCRIPTS

a air.

b bed.

c coal.

f fuel.

g gas.

in inlet.

mf minimally fluidized.

o datum.

out outlet.

APPENDIX

p particle.

r reduced emissivity.

res residual char.

rc raw coal.

s surface or sphericity

st stoichiometric, Air/Fuel Ratio.

Vm Volatile matter.

Ratio of the surface area of the sphere per unit volume of the particle to the surface area of the particle.

CONTENTS

	Page
TITLE PAGE	
SUMMARY	
ACKNOWLEDGEMENTS	
DEDICATION	
NOMENCLATURE	
CONTENTS LIST	
LIST OF FIGURES	
LIST OF TABLES	
CHAPTER ONE: INTRODUCTION	1
CHAPTER TWO: REVIEW OF LITERATURE	5
2.1 Components of a fluidized bed	5
2.2 Bed behaviour	9
2.3 Regime of fluidization	11
2.4 Minimum Fluidizing Velocity, U_{mf}	11
2.5 Heat transfer in Fluidized bed	14
2.6 Particle motion in Fluidized bed	17
2.7 Mixing of particles in bed	20
2.8 Mixing of gas in bed	22
2.9 Mixing of gas in freeboard region	23
2.10 Combustion of a single coal particle in an air stream	23
2.11 Combustion of a single coal particle in a Fluidized bed.	27
2.12 Combustion of Devolatilised char	34
2.13 Conclusion on Review of Literature on combustion of a single coal particle	36

and Devolatilised char	
2.14 The combustion of Volatiles hydrocarbon	37
2.15 Combustion of volatiles in Fluidized bed	40
2.16 Conclusion on Review of Literature on Volatile combustion	45

CHAPTER THREE: THEORETICAL CONSIDERATION

PART A

3.1 Thermodynamic Analysis of heat release	46
3.2 Heat extraction requirements	54
3.3 Consequent Modification to the Model	57
3.4 Mixing concepts.	60

PART B

3.5. A Mathematical model for combustion of volatile matter - Mass balance.	63
3.5.1. Introduction.	63
3.5.2. Development of model.	64
3.5.2.1. Composition of volatile matter.	64
3.5.2.2. Assumption.	65
3.5.2.3. Structure of the model.	66
3.5.3. Theoretical investigation.	72
3.5.4. Validation of the model.	73
3.5.4.1. Experimental Result and Discussion	74
3.5.4.2. Conclusions.	75

CHAPTER FOUR: DEVOLATILIZATION RATES OF	
COAL PARTICLES IN SHALLOW BEDS	
4.1. Introduction	78
4.2. Experimental equipment.	78
4.2.1. Experimental fluidized bed combustor.	78
4.2.2. Fluidizing gas.	79
4.3. Rate of devolatilization Experiments - Test procedure.	79
4.3.1. Batch burning experiments.	79
4.3.2. Devolatilization Rate Experiments - Result and Discussion.	81
4.3.2.1. Effect of bed temperature.	81
4.3.2.2. Effect of charge mass.	82
4.4. Conclusion.	84
4.5. Development of Plume of Volatiles.	84
4.5.1. Plume model.	85
4.5.2. Assumptions of the plume model.	85
4.6. Experiments to obtain better insight into mixing of volatiles with combustion air in above bed region.	88
4.6.1. Introduction.	88
4.6.2. Cold bed test with solid CO ₂ block-free and restrained in the bed.	
4.6.3. Result and discussion.	89
4.6.4. Experiments with solid blocks of	92

CO₂ in hot bed - Analogous to
more rapid devolatilization.

CHAPTER FIVE: COMBUSTION EXPERIMENTS WITH CONTINUOUS FEED OF COAL PARTICLES IN FLUIDIZED BEDS	
5.1. Introduction.	109
5.2. Experimental equipments.	109
5.2.1. Experimental fluidized bed combustion.	109
5.2.2. Distribution of coal particles in the bed.	110
5.2.3. Effect of coal feed systems in distribution of coal particles in the bed.	111
5.2.3.1. Ancilliary Experiments.	112
5.2.4. Bed Inert Material.	114
5.2.5. Fluidizing gas.	114
5.2.6. Analysis of products of combustion.	114
5.2.7. Response Time of the Instruments.	115
5.2.7.1. Introduction.	115
5.2.7.2. Response of Instruments.	116
5.2.7.3. Experimental procedure.	117
5.3. Combustion Experiments.	121
5.3.1. Combustion test procedure.	121
5.3.2. Experimental Results and Discussions.	122
5.3.2.1. Freeboard Reaction.	122

5.3.2.2. Initial Tests.	122
5.3.2.3. Second Tests.	123
5.3.2.4. Test with Bituminous Coal.	124
5.3.2.5. Test with Anthracite Coal.	125
5.3.2.6. Effect of insulation when burning small coal particles.	126
5.3.2.7. Effect of using large coal particles - only with insulated bed.	127
5.3.2.8. Influence of Excess Air.	130
5.3.2.9. Effect of using large coal particles.	133
5.3.3. Energy Balance.	134
5.3.4. Comparison of enthalpy balance with intrinsic limit (Merrick's data)	136
5.4. Combustion Experiments with wood.	138
5.4.1. Introduction.	138
5.4.2. Experimental technique.	140
5.4.2.1. Wood burning unit.	140
5.4.2.2. Wood sample used.	140
5.4.2.3. Analytical method.	140
5.4.3. Experimental Results.	141
5.4.3.1. Analysis of wood.	141
5.4.3.2. General behaviour of wood combustion and gas analysis.	141

5.4.4. Discussion of the results.	143
5.4.4.1. General nature of wood combustion.	143
5.4.4.2. Effect of secondary air.	144
5.4.4.3. Effect of bed temperature.	146
5.4.4.4. The nature of combustion products.	146
5.4.4.5. Heat in bed and freeboard.	147
5.4.4.6. Modes of heat transfer.	149
5.4.4.7. Freeboard reaction.	150
5.4.4.8. Comparison of Fluidized bed combustion of wood with fixed grate	150
5.4.4.9. Conclusions from the table of observations.	151
CHAPTER SIX: GENERAL DISCUSSION ON PRESENT EXPERIMENTAL FINDINGS	175
CHAPTER SEVEN: SUMMARY OF CONCLUSIONS.	177
CHAPTER EIGHT: RECOMMENDATIONS FOR FURTHER WORK.	178
APPENDICES:	
APPENDIX A: Theoretical Investigation.	181
APPENDIX B: Combustion Experiment with Coal.	187
APPENDIX C: Experiments with Solid CO ₂ .	190
APPENDIX D: Calculation of Enthalpy Balance.	191

ADDENDUM

r_1	Mass of oxygen	in the air	kg
r_2	" " nitrogen	" " "	"
r_3	0		
r_4	" " carbon	" " fuel	"
r_5	" " hydrogen	" " "	"
r_6	" " oxygen	" " "	"
r_7	" " nitrogen	" " "	"
r_8	" " sulphur	" " "	"
d_1	the volume fraction of CO_2 in the dry products		
d_2	" " "	" CO	" " " "
d_3	" " "	" HC	" " " "
d_4	" " "	" O_2	" " " "
d_5	the carbon to hydrogen ratio in the fuel by mass		
Φ_s	Ratio of the surface area of the sphere per unit volume of the particle to the surface area of the particle.		

APPENDIX E:	Calculations of r 's from the fuel and air.	215
APPENDIX F:	Evaluation of Energy balance using Merrick's Data.	218
REFERENCES.:		230

LIST OF FIGURES

	Page
Figure 1.1. The importance of volatiles - same heat removal required to control temperatures but distribution of heat removal between bed and freeboard zones depend on volatiles content of fuel.	4
Figure 2.1. Main components of a fluidized bed.	8
Figure 2.2. Fluidized bed behaviour with increasing gas velocity.	10
Figure 2.3. Variation in effective emissivity, ϵ , of a non-isothermal alumina bed of small particles with both the temperature of transfer surface, T_s , and bed, T_b , Botterill (4).	17
Figure 2.4. Geldart's powder classification diagram for fluidization by air (ambient conditions) Botterill (14).	19

Figure 2.5.	Some evidence to suggest that when the particles are very small, their temperature is hotter than during most of their life.	25
Figure 3.1.	Illustrating a steady-flow Chemical Reacting System.	50
Figure 3.2.	Refractory lined bed showing heat leakage.	51
Figure 3.3.	Enthalpy - temperature diagram used in the discussion of steady-flow combustion process.	53
Figure 3.4.	Fluidized bed combustor with heat transfer tubes in the bed and a heat exchanger in the off-gas stream.	54
Figure 3.5.	Graph of surface area against the fraction of heat in fuel released in bed.	56
Figure 3.6.	Shallow bed burning low volatile fuel.	59
Figure 3.7.	Shallow bed burning high volatile fuel.	59
Figure 3.8.	Set of linear equations for predicting the fraction of burnt carbon and hydrogen in the fuel.	71

Figure 4.1.	Experimental fluidized bed combustor.	95
Figure 4.2.	Typical concentration profile of volatiles in the plume.	86
Figure 4.3.	To show qualitatively the significant differences in freeboard mixing patterns	90
Figure 4.4.	Experimental result of batch charge of coal particle at bed temperatures 800°C and 900°C.	96
Figure 4.5.	Concentration of CO ₂ at various freeboard levels with CO ₂ block unrestrained.	97
Figure 4.6.	Concentration of CO ₂ at various freeboard levels with CO ₂ block restrained.	98
Figure 4.7.	Average of composition of CO ₂ at each level.	99
Figure 4.8.	Time average concentration of CO ₂ in air by volume.	100
Figure 4.9.	Concentration of CO ₂ at various freeboard levels with CO ₂ block unrestrained	101

Figure 4.10.	Concentration of CO ₂ at various freeboard levels with CO ₂ block restrained.	102
Figure 4.11.	Average % composition of CO ₂ at each level.	103
Figure 4.12.	Time average concentration of CO ₂ in air by volume.	104
Figure 4.13.	Comparison between restrained with unrestrained block of CO ₂ (same bed temperature).	105
Figure 4.14.	Comparison between restrained with unrestrained block of CO ₂ (same bed temperature).	106
Figure 4.15.	Restrained block of CO ₂ in hot bed compared with restrained block in cold bed.	107
Figure 4.16.	Unrestrained block of CO ₂ in hot bed compare with unrestrained block in cold bed.	108
Figure 5.1.	Experimental fluidized bed combustor	152

Figure 5.2.	Photograph of the cone shaped chimney with the extended chute and the attached cone.	153
Figure 5.3.	Photograph showing secondary air nozzles	154
Figure 5.4.	Photograph of coal distribution in the bowl of water.	155
Figure 5.5.	Photograph of coal distribution in the bowl of water.	155
Figure 5.6.	Photograph of coal distribution in the bowl of water.	156
Figure 5.7.	Photograph of coal distribution in the fluidized bed of sand.	156
Figure 5.8.	Schematic diagram of the water technique apparatus.	113
Figure 5.9.	Schematic diagram of water technique apparatus with the chute extended and the attached cone.	113
Figure 5.10.	Photograph of the experimental apparatus.	157

Figure 5.11.	Schematic diagram for the instrument response experiments .	117
Figure 5.12.	CO ₂ output response curves by air/combustion products input.	119
Figure 5.13.	Response time of sampling probe in the steel tube.	120
Figure 5.14.	Temperature measurement from burning bituminous coal experiment(Uninsulated condition)	158
Figure 5.15.	Temperature measurement from burning bituminous coal experiment (Insulated condition).	159
Figure 5.16.	Gas concentrations from burning bituminous coal experiment (Uninsulated condition).	160
Figure 5.17.	Gas concentrations from burning anthracite coal experiment (Uninsulated condition)	161
Figure 5.18.	Sankey diagram using author's model and Merrick's data (Uninsulated condition).	162
Figure 5.19.	Sankey diagram using author's model and Merrick's data (Insulated condition).	163
Figure 5.20.	The effect on heat release in the two zones.	130

Figure 5.21.	Gas concentrations from burning bituminous coal experiment.(Insulated condition)	164
Figure 5.22.	Photograph showing the sintered bed surface.	165
Figure 5.23.	Photograph showing the burn out of pilot burner.	166
Figure 5.24.	Flow diagram showing energy losses in the reactor.	136
Figure 5.25.	Temperature measurement from burning wood experiment.(Uninsulated condition)	167
Figure 5.26.	Gas concentrations from burning wood experiment. (Uninsulated condition)	168
Figure 5.27.	Temperature measurement from burning wood experimrnt.(Insulated condition)	169
Figure 5.28.	Gas concentrations from burning wood experiment. (Insulated condition)	170
Figure 5.29.	Temperature measurement from wood experiment. (Insulated condition)	171
Figure 5.30.	Gas concentrations from burning	172

bituminous coal experiment.(Insulated condition)

Figure 5.31. Temperature measurement from burning 173
bituminous coal experiment.
(Uninsulated condition)

Figure 5.32. Gas concentrations from burning 174
bituminous coal experiment.
(Uninsulated condition)

LIST OF TABLES

	Page
Table 3.1. National Coal Board rank 101 anthracite supplied as washed.	53
Table 3.2. Equilibrium products of complete combustion from combustion of coal described in table (3.1) with 25% excess air.	53
Table 3.3. Hot water surface area required to maintain bed temperature at 850°C.	56
Table 3.4. Equilibrium products of burning fraction of fuel in the bed from combustion of coal described in table (3.1) with 25% excess air.	58
Table 3.5. Characteristics of coal used.	72
Table 3.6. Theoretical values of products of combustion.	73
Table 3.7. Fraction of carbon and hydrogen converted and unburnt carbon.	73
Table 3.8. Characteristics of ^{bituminous} coal used	76

Table 3.9.	Products of combustion	77
Table 3.10.	Fraction of carbon and hydrogen converted and unburnt carbon.	77
Table 4.1.	Experimental results of batch charge of coal particles at bed temperatures of 800°C and 900°C.	83
Table 4.2A.	Average gas fraction of CO ₂ at each level.	93
Table 4.2B.	Time average concentration of CO ₂ in air by volume.	94
Table 5.1.	Summary of results with coal.	128
Table 5.2.	Summary of results with wood.	143
Table 5.3.	Observation of combustion in freeboard.	151

CHAPTER ONE

INTRODUCTION

Increasingly high costs of fossil fuels and the ultimate prospect of an energy shortage have led to much attention being given to utilizing the presently abundant coal reserves, low grade fuel and wastes, particularly in the United Kingdom where there are very large coal reserves. Of all the fuel reserves, coal most merits effort being spent on overcoming pollution problems associated with its use and exploiting its cheapness per heat unit compared with oil and gas.

Fluidized bed combustion offers a method for utilising a wide variety of coals and low grade fuels, which is relatively insensitive to fuel quality and capable of satisfactory control of emission of sulphurdioxide, at less capital cost than scrubbers and controlling oxides of Nitrogen. This capability for low pollution levels which allows high sulphur fuels to be used, renders a greater proportion of the world's inventory of fossil fuel to be usable. This is of great importance to those countries which do not have high quality low sulphur coal which is found in the United Kingdom but do possess supplies of poor quality, high sulphur coal.

The fluidized bed combustion process also offers high heat transfer rate from the bed to its containment or immersed surfaces, high combustion intensity with the possibility of smaller plant for a given thermal output than conventional coal fired plant.

Fluidized bed utilisation of coal goes back further than

the catalytic cracker. Winkler of Germany having patented it for gasifiers in 1921, used it extensively as a source of synthesis gas from coal, successfully handling a wide variety of coal types(1).

There was significant research and development in U.K. of fluidized combustion systems during the early '50s at BCURA and N.C.B(1,2) and early '60s by the late Professor Douglas Elliott then at the C.E.G.B. laboratories at Marchwood(1,3). The motive was to exploit the inherently good gas/solid contacting to deal with relatively unreactive low grade fuels, especially those with a very high ash content, to fractionate coal into an ash free volatile part, which would be used as gas turbine fuel and a char part, which could be used as a boiler fuel(1).

Despite this however, the mechanism of combustion of the volatile matter component in coal ^{burnt} in fluidized beds, has not yet been fully investigated. On the other hand, combustion of the residual carbon has been extensively studied. Volatile matter contributes significantly to the calorific value of the fuel so that information on this component of the fuel will assist the design of fluidized bed combustion systems and affect the design of future control systems for them. The importance of volatile matter in coal may be illustrated as follows:

If the fuel contains only a small fraction of volatile matter then most of the heat released from the fuel will take place in the bed. If excessive bed temperature and bed sintering are to be avoided, a significant amount of this heat release will have to be removed from the bed either by in-bed cooling tubes or provision of a large amount of

excess air.

This arises from the first law of thermodynamics applied to combustion. Fig. 1.1.

On the other hand if the fuel contains a large fraction of volatiles, these may escape from the bed unburnt and be ignited in the freeboard region. In this case in-bed cooling tubes may not be necessary, because of only a fraction of the heat is released in ^{the} bed; but extra cooling surface may be required downstream of the bed, yet chilling of flame is undesirable. Furthermore, combustion of volatiles in the freeboard region may be accompanied by radiation from the flames back to the bed, affecting the heat balance there; deposition of soot on the heat transfer surfaces in the freeboard zone can occur, reducing their effectiveness, while incomplete combustion reduces the thermal efficiency.

None of these features has been properly investigated so their influence on design is not known, particularly in a quantitative way. The objectives of the present work are:

- (i) to identify and specify the problems more clearly.
- (ii) to explore the implications for design of fluidized bed combustors of changing from low volatile fuels to high volatile fuels.

Because there were no satisfactory models in existence and there was relatively little experimental data on combustion of volatiles covering a range of variables found in current fluidized bed combustion systems, it was decided to approach the problem by analysing thermodynamically the heat release from known fuel in a simple prescribed system and then compare such data with the experimental results. Also by making experimental measurements on a simple combustor using

different fuels of known analyses data might be obtained which might be used to help design a combustor for fuels of different volatile matter contents and to develop a model for predicting performance. Experimental experience should in any case advance knowledge and provide insight into the process.

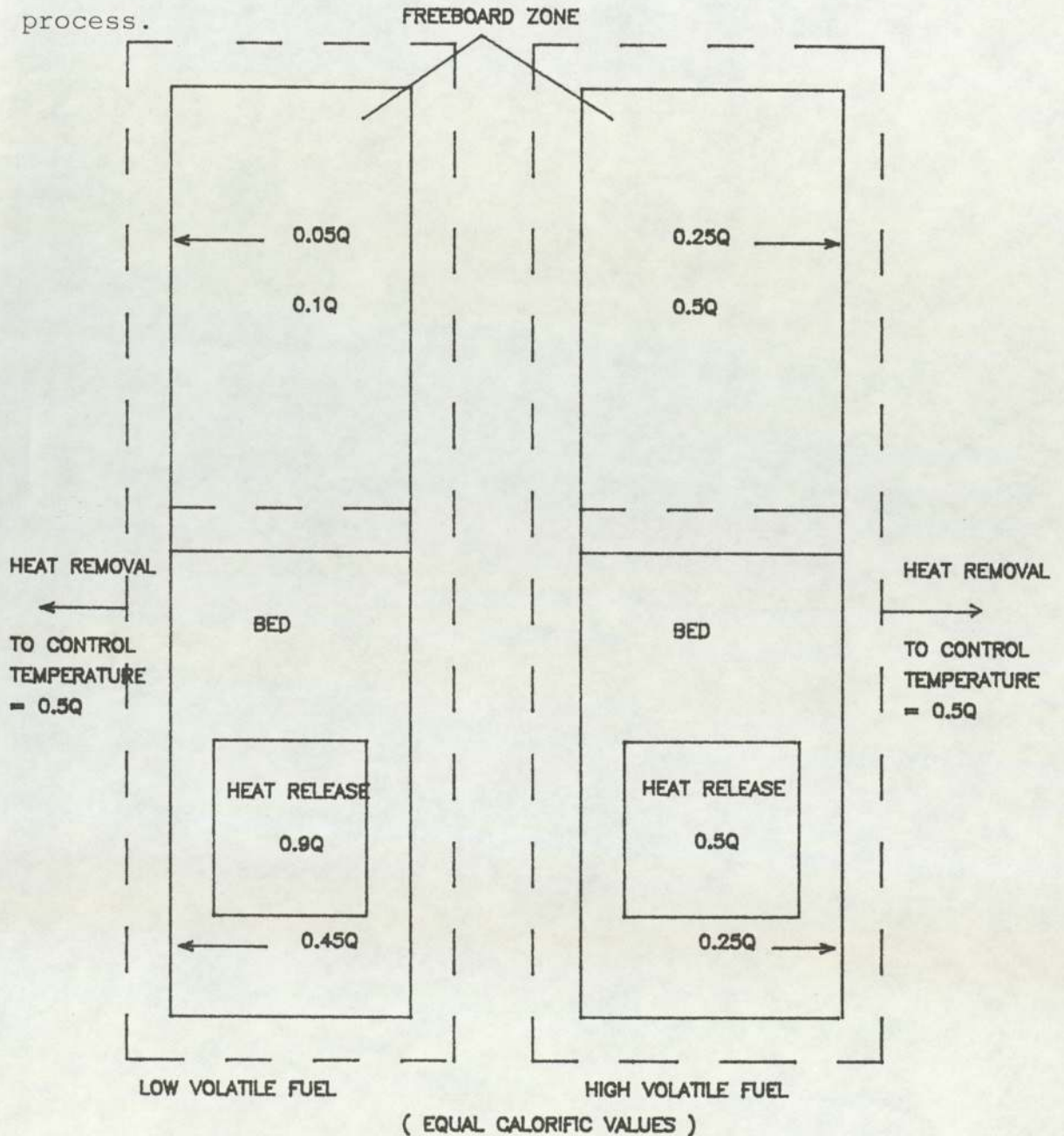


FIG.1.1 THE IMPORTANCE OF VOLATILES - SAME HEAT REMOVAL REQUIRED TO CONTROL TEMPERATURES BUT DISTRIBUTION OF HEAT REMOVAL BETWEEN BED AND FREEBOARD ZONES DEPEND ON VOLATILES CONTENT OF FUEL

CHAPTER TWO

REVIEW OF LITERATURE

INTRODUCTION

Any study of the fluidized bed combustion requires an understanding of the phenomenon of fluidization. The literature surveyed below has yielded fundamental information on the following.

2.1 Components of a Fluidized Bed

A fluidized bed consists of a vertical containment vessel in which a bed of particles is maintained in suspension by a gas passing evenly upwards through it via a distributor plate in the base, see Fig.2.1. The choice of materials for construction (depending upon the operating conditions) ranges from refractory brick lining as for large high-temperature kilns to unlined steel vessels, according to circumstances. A metal containment surface may be used as a heat transfer surface if it is necessary to add or remove heat using an external heat transfer medium. However, the area of the containing surface may be insufficient or inappropriate for this purpose and so it will be necessary to immerse tubes within the bed to provide the necessary heat transfer surface area.

At the base of the vessel is a distributor. This equipment has the very important function of presenting sufficient resistance to gas flow to ensure the uniformity of gas flow into the bed. This is necessary because there is no self-regulatory change in pressure drop across the fluidized bed should gas flow increase in one region at the expense of another; the pressure drop across the bed in the fluidized

condition remaining very closely equal to the bed weight per unit area regardless of the gas flow through it. However, the pumping power cost of significant distributor pressure drop can be very expensive when dealing with large gas flows and so excessive pressure has to be avoided.

Botterill(4) suggested that

For deeper beds

$$\frac{\Delta P_D}{\Delta P_b} \sim 0.15 \quad \text{for} \quad \frac{U}{U_{mf}} \quad \text{in the range} \quad 1 \rightarrow 2 \quad (2.1)$$

and

$$\frac{\Delta P_D}{\Delta P_b} \sim 0.015 \quad \text{for} \quad \frac{U}{U_{mf}} \gg 1 \quad (2.2)$$

For shallow beds (<150mm deep), however, the ratio is higher and often close to 1

The following types of distributor are commonly used.

- (1) The pipe grid - this is the simplest form.
- (2) Tuyeres - used in large installations where low pressure drop is important.
- (3) Perforated plate and Bubble caps - used for low pressure drop systems.
- (4) Porous ceramic tiles and Metal sinters - used for high pressure requirements.

While the perforated plates can produce a more even distribution of smaller bubbles, bubble caps need to be designed to reduce particle seepage into the plenum chamber; such particles would mill around in the turbulent gas flow conditions and cause erosion damage to both the plenum chamber and the underside of the distributor. However, if porous tiles are used the underside can be quickly blocked should there be particulates in the fluidizing gas stream.

Beneath the distributor plate is the plenum chamber from which fluidizing gas passes ^{through} the distributor into the bed.

Above the bed is the freeboard zone. This is to promote the disengagement of particles thrown up by bubbles bursting at the bed surface. Though the cross-sectional area in the space above the bed may be enlarged to reduce further the superficial gas velocity there, the smallest particles will still tend to be entrained into the gas stream. Accordingly, it will be necessary to provide disengaging devices for high velocity systems.

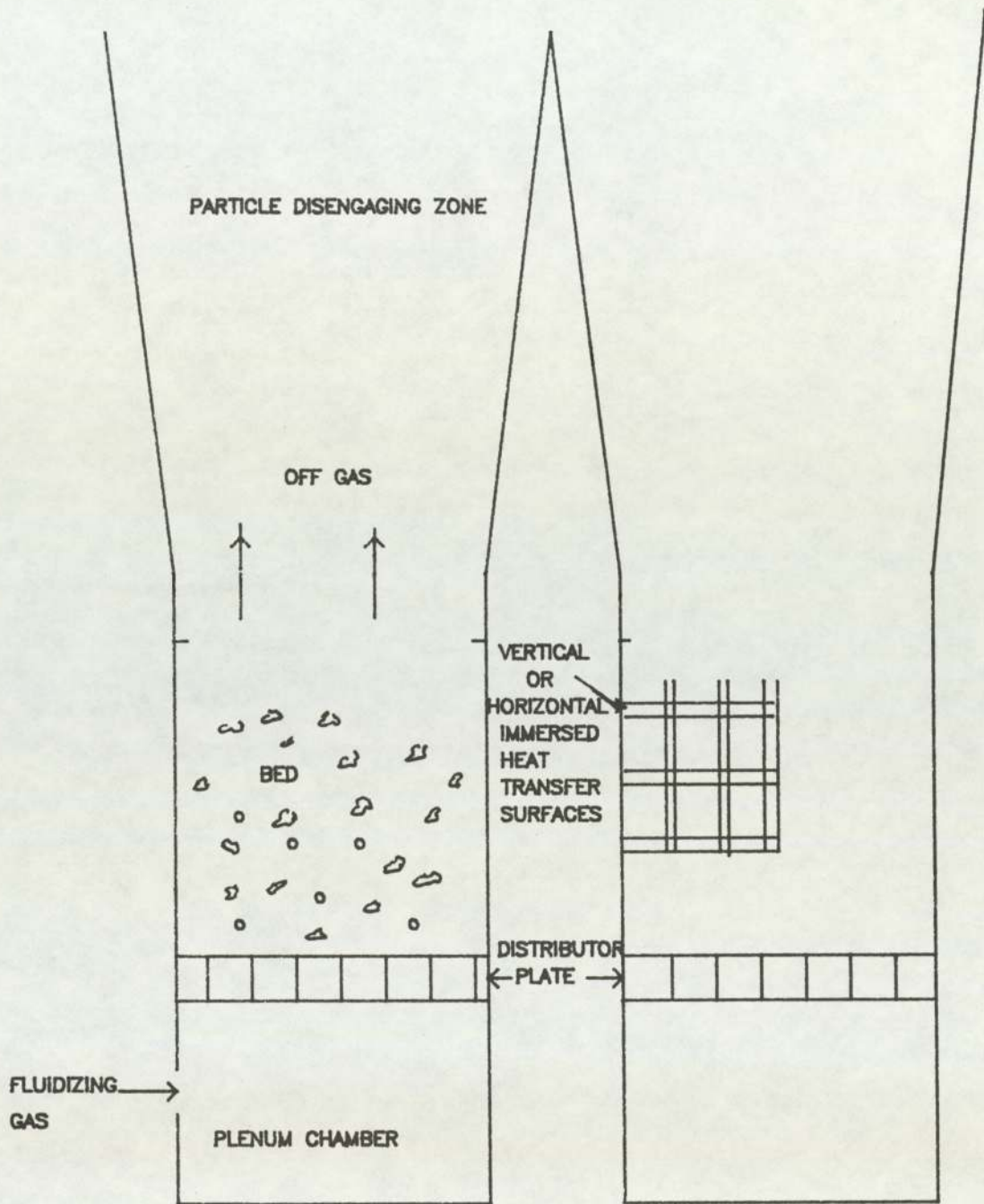


FIG.2.1 MAIN COMPONENTS OF A FLUIDIZED BED.

2.2 Bed Behaviour.

At very low flow rate, fluid simply passes through the void spaces between stationary particles without the particles changing position or interacting with the gas flow. This is a packed bed. As the velocity of flow increases, at first the particles tend to rearrange themselves to accommodate the flow, but with further increase they are thrown into a state of motion similar to that of a boiling liquid because the excess gas flow passes through as bubbles. If the particles are not large the bed will expand in depth corresponding to the limit of stability of a packed bed and marking its transition to a fluidized bed. It is known that beds consisting of particles of small size or having a continuous particle size distribution generally show a greater bed expansion (Matheson et al(5)). With further increase of upward fluid velocity, expansion continues until a stage is reached when the drag forces exerted on the particles will be sufficient to support the weight of the particles. (Fig.2.2). In this state, the bed of solid particles takes on fluid-like properties and it is referred to as incipient fluidization; the gas velocity needed to achieve this is referred to as the minimum fluidizing velocity, U_{mf} (Fig.2.2). As the gas velocity increases beyond U_{mf} , the excess gas passes through the bed as bubbles. Bubbles erupting at the surface generate pressure fluctuations and throw a spray of particles into the freeboard space above the bed. Many are carried away in the gas stream according to the particle size distribution and the gas velocity in the freeboard region above the bed. Furthermore it is known that plug flow and/or channelling

may occur in systems in which attraction forces between the particles are large, as in beds of fine powder; there is as yet no generally accepted explanation for these phenomena and no dependable correlation can be given for the onset of fluidization of a bed of powder. The significance of these phenomena can be better appreciated in relation to the classification of particulate matter by its fluidization characteristics which Geldart(6) suggested. This is based on particle density and size from tests under ambient conditions which will be discussed in section 2.5

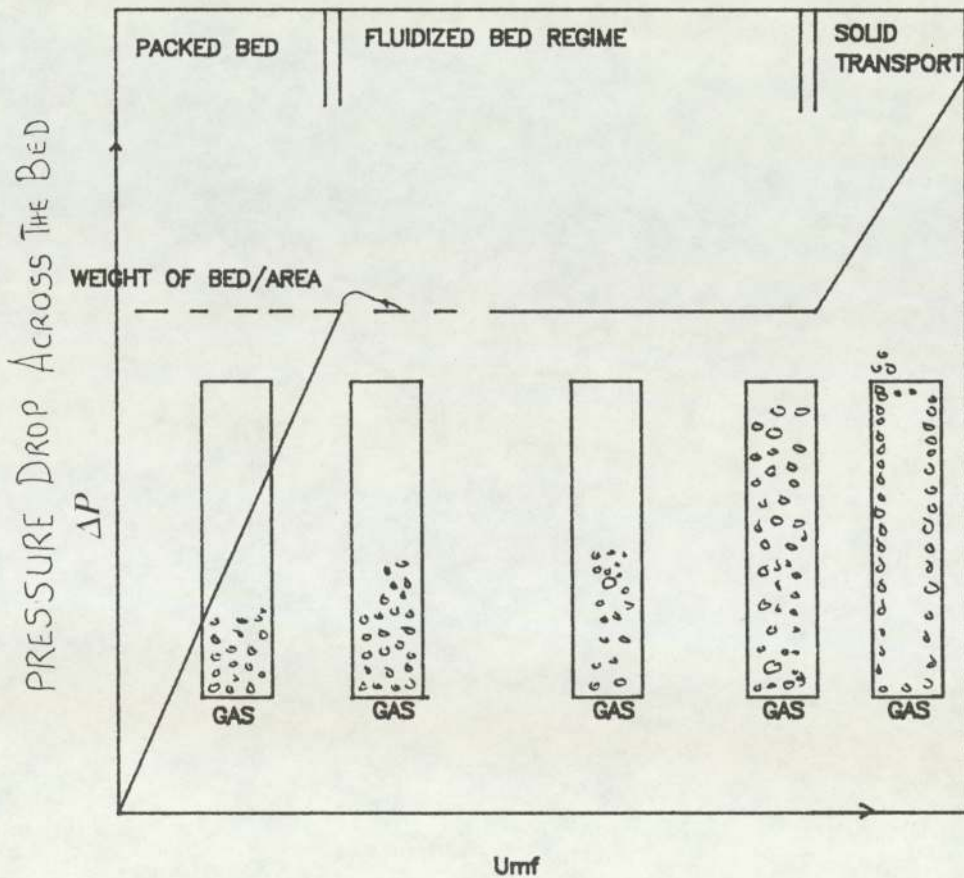


FIG.2.2 FLUIDIZED BED BEHAVIOUR WITH INCREASING GAS VELOCITY

2.3 Regimes of fluidization.

The physical appearance of a fluidized bed is qualitatively described as either being particulate or aggregative(7).

If upon increasing the fluid velocity through a bed of solid particles, the bed expands uniformly, the operating condition is referred to as "Particulate Fluidization"; this is generally obtained with liquid-fluidization systems.

Beyond the onset of fluidization, known as minimum fluidization velocity, the fluid passes through the bed of particles in a stream of bubbles; this condition is referred to as "Aggregative Fluidization" and is obtained with gas-fluidized systems.

2.4 Minimum Fluidizing Velocity U_{mf} .

It is generally accepted that for a given bed geometry and particle density, the most important variables are the total weight of the bed material, distributor pressure drop and the particle diameter. These variables interact in a complex manner to govern bed start-up, minimum fluidization and the upper limit of fluidized bed operation beyond which a significant quantity of particles become entrained in the gas leaving the bed. This transport of fine particles is termed "elutriation".

Minimum fluidization velocity, U_{mf} , is defined as the superficial fluid velocity at which the particles are all just supported by the drag forces exerted by the fluid. At this condition the pressure drop across the bed is just sufficient to support the weight of the bed of particles.

$$\Delta P_b = z_{mf} (1 - \epsilon_{mf}) (\rho_s - \rho_g) g \quad (2.3)$$

Because U_{mf} is one of the principal parameters of the fluidized state, many attempts have been made to develop correlations for the gas velocity at which transition from packed bed to fluidized state will take place.

Notable among the early workers was **Ergun**(8) who estimated minimum fluidizing velocities by relating the pressure drop through a packed bed when the bed was at the voidage of minimum fluidization to the weight of the bed per unit area.

He produced equation for predicting U_{mf} .

$$\frac{\Delta z_g}{z_b} = \frac{150(1-\epsilon)^2 \mu_g U_{mf}}{\epsilon^3 (\Phi_s d_p)^2} + \frac{1.75(1-\epsilon) \rho_g U_{mf}}{\epsilon^3 \Phi_s d_p} \quad (2.4)$$

for the pressure drop.

However, although the particle size, solid and fluid densities and viscosity are usually known, the particle shape factor (required for non-spherical particles) and voidage at the beginning of fluidization are not generally known accurately and very difficult to measure. As can be seen from the form of equation (2.4), a small change in voidage, ϵ , can produce a large change in the solution of this equation for U_{mf} (if the right hand side is known). Particle shape and size can have a number of different definitions, but in fluidization surface-volume ratio are pertinent(9). Hence the suggestion of **Wen and Yu** (10), by modifying these expressions empirically to be of greater practical use because they attempted to average out the effects of size and shape. The accuracy of such correlations is not high, $\pm 30\%$ at best.

Wen and Yu found from experimental results of packed beds that

$$\frac{1}{\Phi_s^3 \epsilon_{mf}^3} \approx 14 \text{ and}$$

$$\frac{1 - \epsilon_{mf}}{\Phi_s^2 \epsilon_{mf}^3} \approx 11$$

which when replaced in the equations (2.3) and (2.4) above give

$$Re_{mf} = \frac{d_p U_{mf} \rho_g}{\mu} = [33.7^2 + 0.0408 d_p^3 \rho_g (\rho_s - \rho_g) g]^{0.5} - 33.7 \quad (2.5)$$

μ_g^2

for the whole range of Reynolds numbers.

For small particles

$$U_{mf} = \frac{d_p^2 (\rho_s - \rho_g) g}{1650 \mu} \quad Re < 20 \quad (2.6)$$

and for large particles

$$U_{mf} = \frac{d_p (\rho_s - \rho_g) g}{24.5 \rho_g} \quad Re > 100 \quad (2.7)$$

The above equations give the minimum fluidizing velocity, U_{mf} , in terms of specified, viz. particle and fluid densities, particle size and gas viscosity.

Goroshko et al (11) found that provided the value of ϵ_{mf} was chosen to fit the correlation, the effect of change in gas pressure and temperature could be accommodated by obtaining an interpolation formula for determining the critical velocity for onset of fluidization.

The formula is

$$Re_{mf} = \frac{Ar}{150 \frac{1 - \epsilon_{mf}}{\epsilon_{mf}^3} + \sqrt{\frac{1.75}{\epsilon_{mf}^3}} Ar} \quad (2.8)$$

and it is valid over a wide range of Ar. However it should be noted that these correlations are based on experiments at

ambient temperature and pressure, so that they should be used with the greatest caution at elevated temperature.

In general the best way of determining U_{mf} is to measure it experimentally with the actual particles to be used.

2.5 Heat Transfer in Fluidized bed.

(a) Gas-to-Particle heat transfer.

In the process of designing or evaluating a fluidized bed combustor capable of achieving the required exhaust gas temperature, it is necessary to take into account a significant amount of heat that will be lost from the red hot particles. However, gas-to-particle heat transfer coefficients based on the total particle surface area are always small; a fluidized bed particle is capable of exchanging heat very effectively with the fluidizing gas because of the very large surface area exposed by the particles.

Extensive studies and many correlations for the heat transfer coefficient have been developed over a wide range of operating conditions.

Botterill(12) has reviewed heat transfer correlations and concluded that the reliability of such correlations for general predictive purposes is poor, because these correlations are frequently applicable only at temperatures close to ambient and only on the particular piece of equipment on which they are measured.

Because of their high thermal heat capacity, the temperature of the solids dominates the thermal behaviour, the gas temperature that follows that of the particles not vice versa.

(b) Particle to Immersed Surface.

Although gas fluidized beds have the uniformity of temperature because of good mixing and good heat transfer properties, there are instances when heat transfer remains the limiting factor in the design of a given fluidized system. Often, however, the area of a containing surface will be insufficient to remove heat at the desired rate. In order to overcome such a heat transfer problem, horizontal or vertical tubes are sometimes installed within the bed to give the necessary additional heat transfer surface. This solution is common especially when heat has to be removed from a highly exothermic reaction and the bed volume is too large for the containing surface to offer sufficient heat transfer area.

Various investigators (13), (14) have approximated the heat transfer coefficient between the particles and immersed surface under conditions of ordinary fluidization to be the sum of three components. These are

i The coefficient of conductive heat transfer, h_{cond} .

ii The coefficient of convective heat transfer, h_{conv} .

iii The coefficient of radiant heat transfer, h_{rad} .

Thus

$$h_{\text{total}} = h_{\text{cond.}} + h_{\text{conv.}} + h_{\text{rad.}} \quad (2.9)$$

There are various factors (for example, particle diameter) that affect both the conductive and convective components of heat transfer coefficients differently. Furthermore although these components are often taken as being independent of each other, there is evidence to suggest that at high temperatures the increase in $h_{\text{rad.}}$ may be at the expense of $h_{\text{conv.}}$ so that these two components equation (2.9) are not strictly additive, Botterill (14). However, for initial design purposes it is sufficient to treat these components as being independent.

Radiative heat transfer is the most difficult to estimate especially at temperature above 600°C but it increases progressively with temperature and reaches about 20% of the heat transfer at about 1000°C . The radiative component can be estimated by using absolute temperature and adopting the Stefan-Boltzman equation (2.10) in the form

$$h = \frac{5.673 \times 10^{-8} E_r (T_b^4 - T_s^4)}{T_b^4 - T_s^4} \quad (2.10)$$

where E_r is a reduced emissivity to take into account the different emissivity properties of the surface ϵ_s and the bed ϵ_b given by

$$E_r = \frac{1}{(1/E_s + 1/E_b) - 1} \quad (2.11)$$

and T_b is the bed temperature adjacent to the surface. Since E_r is not generally known a modified ϵ_m of the order of 0.6 together with the bulk bed temperature (14) following Baskakov et al (15) may be used Fig.2.3.

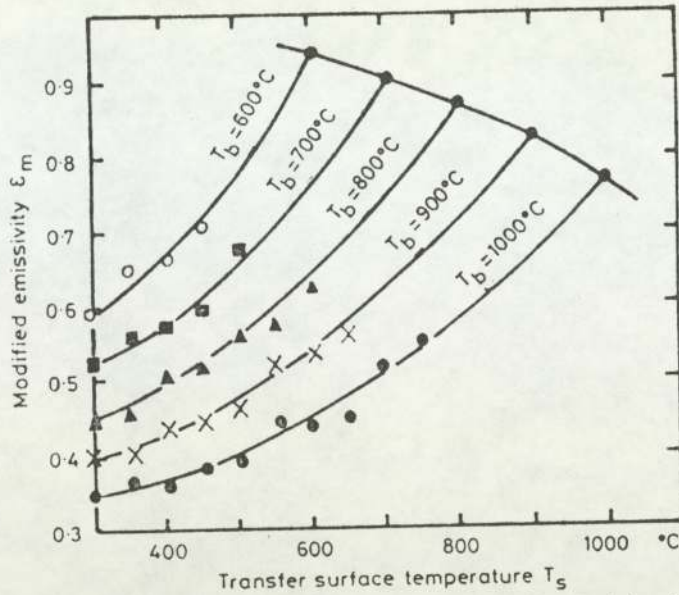


FIG.2.3 VARIATION IN EFFECTIVE EMISSIVITY, ϵ , OF A NON-ISOTHERMAL ALUMINA BED OF SMALL PARTICLES WITH BOTH THE TEMPERATURE OF TRANSFER SURFACE, T_s , AND BED, T_b , Botterill (14)

2.6 Particle Motion in Fluidized Beds.

Particle motion in fluidized beds is due mainly to the non-uniformity of the flow round the particles and the non-uniformities caused by the passage of bubbles. When a bed becomes fluidized the extent of particle motion increases with fluidizing velocity and is very apparent indeed at 3 to 4 times U_{mf} . Particles spend most of their time moving downward slowly but occasionally are swept up in the wake of bubbles - Rowe (16) and this contributes greatly to mixing of particles. There is a relationship between the motions of the particles and the fluid in a fluidized bed. As the bed becomes fluidized, the particle motion commences after reaching a sufficient large fluid velocity.

According to Rowe (16), bubbles appear only at fluidization indices $N = > 1.3$. In this sense

the motion of fluid becomes of primary importance. However, moving particles, particularly aggregates of particles can entrain some fluid with themselves and thus lead to mixing of it. For example, the downward motion of the particles around the walls causes the fluid (gas) at the walls to move in ^{the} opposite direction to the main stream.

Geldart (6) approached the problem by classifying particles into four broad groups associated with particular applications.

GROUP	SIZE RANGE	DENSITY
A	20 to 100 μ m	<1400 kg/m ³
B	40 to 500 μ m	1400 to 4000 kg/m ³
C	<30 μ m	Lower density
D	>600 μ m	Higher density

Group A is used extensively in petrochemical industry but is too light to be used in heat recovery applications because it has very low entrainment velocity.

Group B exhibits much less stable bed expansion and free bubbling occurring at or a little over minimum fluidizing velocity. This might be suitable for heat recovery purposes.

Group C is of lower density so that gravity has less effect than the interparticle forces hence it is very difficult to fluidize.

Group D is dense and fluidizes unstably.

Correct choice of particles and fluidizing velocities is essential for a well designed fluidized bed system particularly where the performance depends strongly upon heat transfer and particle mixing. The particle size range with which fluidized beds operate satisfactorily is relatively narrow so that the particles size may have to be

prepared by crushing before use in a fluidized bed.

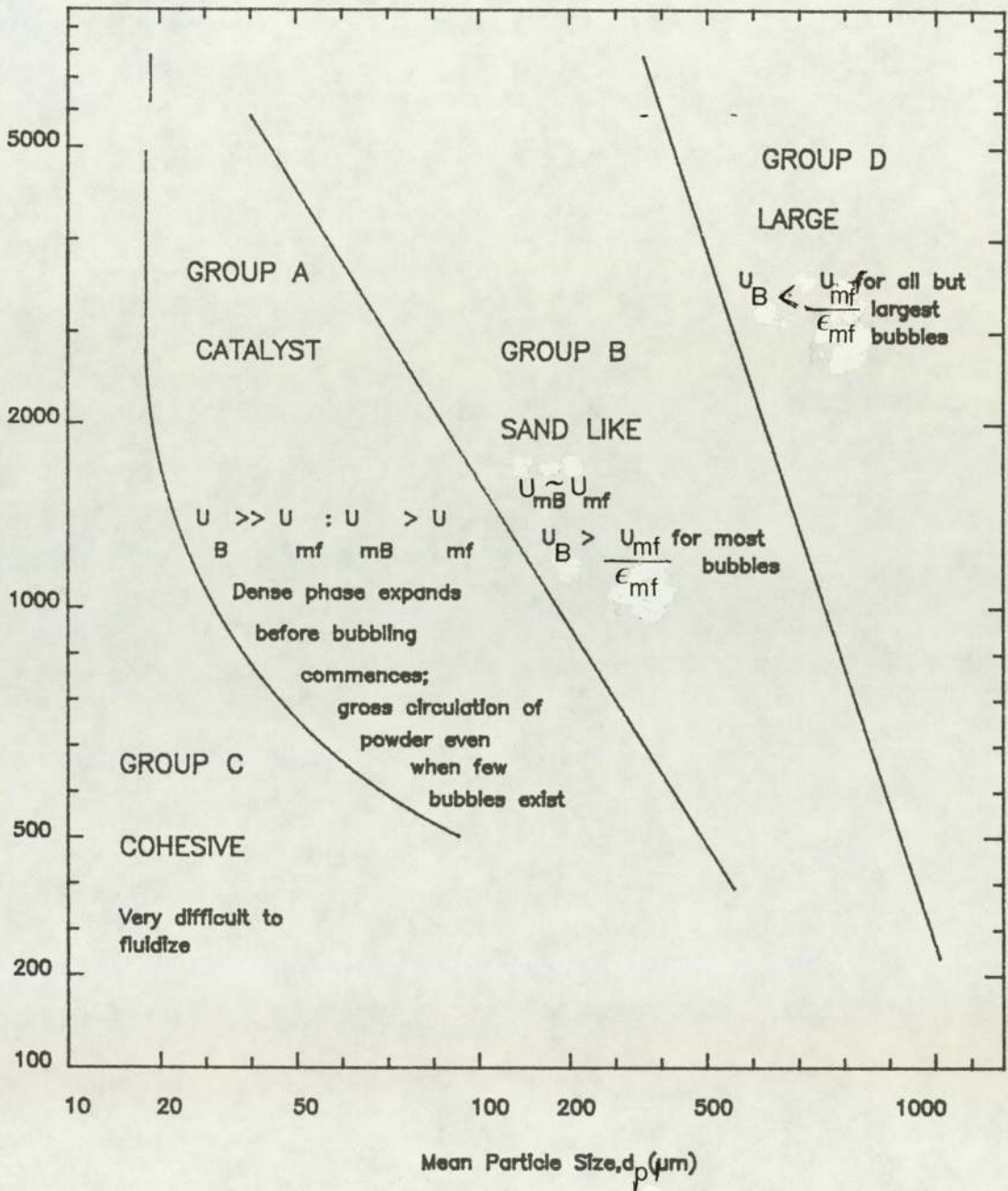


FIG.2.4 GELDART'S POWDER CLASSIFICATION DIAGRAM FOR FLUIDIZATION
BY AIR (ambient conditions) BOTTERILL (14)

2.7 Mixing of Particles in Bed.

The importance of mixing in a fluidized ^{bed} depends on the application. For instance, heating a fluidized bed by direct injection of fuel at a single point may produce a very uniform bed temperature because mixing may be so effective that heat generated by combustion will be dispersed rapidly and if insufficient fuel is being burnt to overcome heat losses from the bed, combustion will not be sustained. If it is desired to reduce the fuel flow then mixing will have to be reduced, perhaps by slumping part of the bed in the regions distant from the fuel injection point so that heat is not dispersed throughout the bed. This method of slumping the bed is sometimes used to control the combustor.

Several investigators have made studies of mixing of solid particles in fluidized bed.

Rowe and Sutherland (17) reported experiments in which nickel shot was used as tracer material in a bed of 0.1397m diameter and at bed height of 1.2192m. Their results showed that no particle mixing occurred at gas velocities up to 1.2 times U_{mf} and that the rate of mixing depended on the rate of bubbling.

Rowe et al (18) reported experiments in which copper and nickel were used as tracer materials. They concluded that in a gas-fluidized beds, mixing was caused solely by the bubbles and the patterns of particle movement was predictable once the pattern of bubbling was known.

Sutherland(19) reported experiments at ambient temperature

and pressure in which he compared solids mixing in tapered and un-tapered gas-fluidized beds. His main aim of the experiment was to establish whether or not the effect of tapering the bed would reduce the vertical mixing rate of solids. He used glass ballotini in a bed of uncoloured material and also the nickel tracer technique in a bed of copper shot. He concluded that tapering the bed only appeared to stabilise the just fluidized state throughout the depth of the bed, rather than changing of any fundamental solids mixing behaviour.

Lewis et al (20) in their experimental findings of heat transfer and solids mixing in beds of fluidized solids, found that there was a preferential circulation of the solids up the central region and downward along the walls.

Tailby and Cocquerel (21) made a study of residence time of solids in ^{an} air fluidized bed of glass beads. They observed that the direction of solids flow in their two experiments had effects on the flow patterns, and concluded that increasing the air flow rate led to perfect mixing.

Fan et al (22) made an extensive review of solids mixing. They compared the three proposed mechanisms of mixing (diffusion, convection and shear) and concluded that the mechanism of mixing was similar to diffusion of particles in gas and liquid phases; diffusion was the mechanism for lateral mixing.

A measure of mixing is the diffusion coefficient (m/s)

2.8 Mixing of gas in bed.

Solid mixing which takes place in fluidized beds promotes a degree of temperature control not readily obtainable in other types of reactor. However, this solids mixing causes mixing of the products of reaction with the entering reactants and permits some bypassing of reactants, so that the relative speed of reaction and diffusion is not uniform. Whereas solid fuels mix laterally across the bed from the point of injection, gas is carried through the bed by the combustion air with almost no lateral mixing. Because of this it is necessary to introduce this fuel at many points across the area of the air distributor. Since the mixing of gases in the bed is relatively poor and the gas residence time is short, premixing the gas with the air at air inlet has the advantage of allowing a uniform combustion to occur in the bed. However, these premixed gases can bypass the bed without burning thereby prevent^{ing} the bed from reaching combustion temperatures (Broughton(23), Pillai(24)). Gas mixing and bypassing lead to a decreased reaction rate and nonuniformity of products, both of which are generally undesirable. The effect of these nonuniformities in gas flow becomes increasingly serious as the desired degree of conversion increases.

There have been several experimental studies done to determine the nature and extent of gas-mixing in fluidized beds.

Gilliland and Mason (25) in their experimental findings concluded that the back-mixing of gas in small fluidized beds with large height to diameter (L/D) ratios was relatively small and in the case of most reactions not

particularly detrimental.

Gilliland et al (26) in their studies of residence time concluded that gas flow and hence chemical conversion in small fluidized beds depart from that corresponding to gas motion without backmixing as the L/D ratio decreases.

2.9 Mixing of gas in Freeboard Region.

The freeboard region provides not only the height for the disengagement of solids but also for additional reaction between the projected particles and the gas and volatile matter from solid fuels and air. While ^{the} freeboard region does not have the thermal capacity of the bed itself, there is no further gas by-passing (except the gases are not well mixed), and as a result gas/solid contacting becomes very efficient. At the two extremes of immediate delayed combustion, the volatiles combustion rate is controlled in the first case by the rate of coal pyrolysis and in the second case, by the rate of mixing with additional air. Since significant combustion of volatiles (which represent as much as half the calorific value of the coal) occurs in the freeboard region, adequate air is needed to mix with the volatiles and burn completely there. This area has not been identified to date and hence knowledge and information are lacking here.

2.10. Combustion of a single coal particle in an air stream.

The combustion of coal particle is a physically controlled process, but chemical kinetic factors often impose further constraints.

Broughton and Howard (27), Pillai (28), Chakraborty and Howard (29), Avedesian and Davidson (30), Campbell and Davidson (31) and Basu (32) describe the following stages in the burning of a single coal particle:

i The bed temperature decreases slightly as the coal enters the bed.

ii A few milliseconds later a luminous, tall flame can be seen surrounding the particle. Coal particle temperature is rising but the particle remains black relative to the bed while this flame continues. This is the period during which a flame is visible and is taken as the time during which volatiles are being evolved and burnt. This devolatilization process is not a simple physical evaporation such as occurs with a liquid, but is the result of chemical reactions which may be endothermic and irreversible.

iii After the volatile flames have extinguished, the residual carbon ignites when it reaches ignition temperature and oxidizes relatively slowly to release its heat.

iv As the carbon burns, there is an increase in particle temperature; the colour increases in brilliance to bright red. The greater the amount of oxygen reaching the surface, the brighter the particle glows. The local heat balance of the reactive particle determines the particle temperature. (The temperature reached by the fuel particle is important because any ash bound in with the fuel may melt and cause agglomeration if the temperature is too high).

Oxidation of the carbon continues until it is all consumed or the remaining particle is small enough to be entrained in gas stream.

The above sequence is illustrated in Fig.2.5 below.

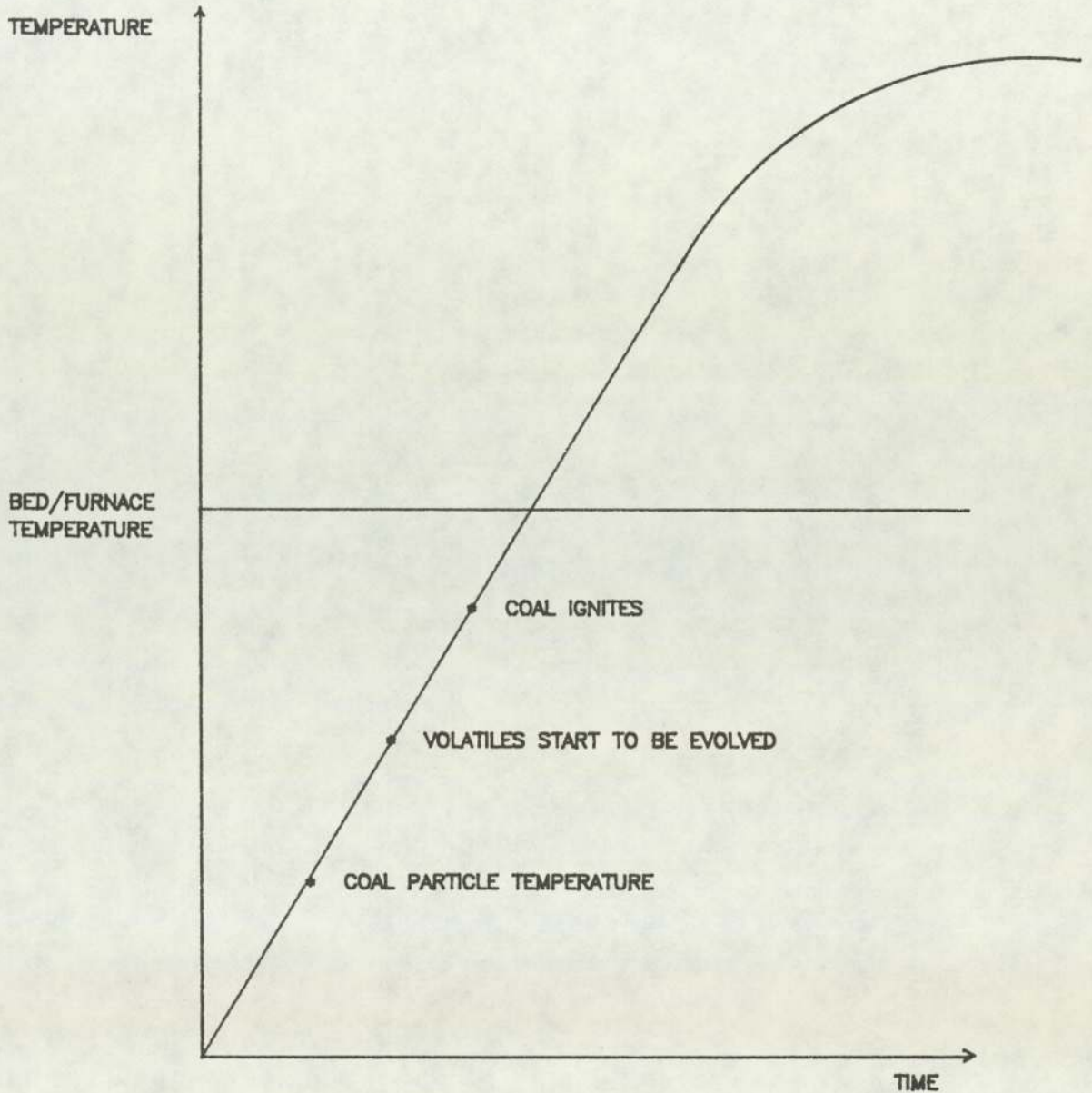


FIG.2.5 SOME EVIDENCE TO SUGGEST THAT WHEN THE PARTICLES ARE VERY SMALL THEIR TEMPERATURE IS HOTTER THAN DURING MOST OF THEIR LIFE

Theoretical and experimental studies of the combustion of a single coal particle in air have been made by a number of investigators to establish the mechanism of combustion and to determine the products of combustion at different temperatures.

Field et al (33) carried out extensive investigation of the combustion of a single coal particle. They noted the difference between gas-phase reaction and heterogeneous reaction and concluded that diffusion of oxygen to the surface was the controlling step in the oxidation of carbonmonoxide to carbondioxide.

Essenhigh and Perry (34) in their review of combustion and gasification likened the reaction of volatiles evolving from a coal surface to the combustion of oil when the liquid vapourizes and reacts in the gas phase at a distance from the liquid surface. Using Nusselt square law, they showed that the burnout time t_c was proportional to the square of the diameter of the coal particle (d_o).

$$t_c = Kd_o^2 \quad (2.12)$$

Mulcahy and Smith (35) made an extensive review of the combustion kinetics of a single particle and concluded that at about 1200K to 2300K, the rate of combustion of carbon particles greater than 100um in size would be controlled by the rate at which oxygen was able to diffuse towards the carbon surface, equation 2.13, while the rate of combustion of particles less than 100um in size would be controlled by

chemical kinetics equation 2.14.

$$t_{b\text{Diffusion}} \propto d_1^2 \quad (2.13)$$

$$t_{b\text{Kinetic}} \propto d_1 \quad (2.14)$$

2.11 Combustion of a single coal particle in a fluidized bed

The combustion of a coal particle in air resembles to some extent the combustion of a coal particle in a bed of hot inert particles fluidized with air. The main difference is that in a fluidized bed the coal particle temperature is lower. In the case of a coal particle burning in a hot air stream, the ash bound in with the particle may melt and cause agglomeration if the particle temperature is too high.

In the fluidized bed, the temperature of the burning particle surface can be controlled at a value less than the ash fusion temperature, due to the fact that heat transfer coefficient between the burning particle surface and inert particles is at least five times greater than the normal convective heat transfer coefficient between the particles and a free air stream (**Broughton and Howard (27)**).

Despite these investigations, the literature reveals no accurate model, either fundamental or empirical, of the burning of coal particles in a fluidized bed from which to predict burning rates or surface temperatures.

Basu et al (36) studied the mechanism of combustion of coal particles burning in a fluidized bed of sand at 1123K. They used Phosphorous Oxychloride (POCl_3) to suppress the oxidation reaction between carbon monoxide and oxygen and

recorded a rise in carbon-monoxide and a fall in carbon-dioxide concentrations in the products of combustion. Their results suggested that oxygen diffuses and reacts on the carbon surface to produce carbon-monoxide and carbon-dioxide initially, while carbon-monoxide diffuses away and burns with a spherical diffusion flame around the particle. They also performed a heat balance on the combustion mechanism of particles in the emulsion phase of a fluidized bed. Their results showed that more heat was radiated away from the particle than was conducted back to its surface from the reaction zone. Thus insufficient heat seemed to be reaching the surface to sustain the gasification reaction, which suggests that the proposed mechanism does not support the combustion model presented by **Avedesian and Davidson** (30) and supported by **Campbell and Davidson** (31).

Gibbs and Hedley (37) studied combustion of large coal particles in a 0.3m square in section, 1.83m high fluidized bed of sand operating at a bed depth of 0.6m and at temperatures between 700 and 850°C. Their result was then compared with those of the same combustor fired by a < 1.4mm crushed coal for the same operating conditions. Their off-gas concentrations of carbon-dioxide and oxygen showed that as the size of the coal feed was increased, less combustion occurred in the lower half of the bed, and more in the freeboard region of the bed. They also measured the freeboard temperature some 600mm above the bed surface, finding it to be 50 K higher with the large coal than for

the crushed coal under the same operating conditions. This rise in temperature can be attributed to feeding of large coal particles onto the surface of hot fluidized bed where some of the fuel volatiles will be released and escape into the freeboard. The subsequent combustion of these volatiles in the vicinity of the freeboard region, where the oxygen concentration is high results in temperature rise. Furthermore, large coal particles are not as well mixed vertically in the bed as a crushed coal especially in a deep bed, and only a few large particle will be present in the lower region of the bed.

The significance of this is that less heat is being released in the bed and this temperature rise can cause sintering of elutriated ash as it passes through the freeboard region. With the combustor operating at temperatures between 700 and 850°C and ^{at} 825°C for large and crushed coal respectively; their results showed that more heat was being released in the freeboard region for large coal than crushed coal.

Sinha et al (38) studied method of predicting coal burning rate in fluidized bed of sand at a temperature of 850°C using two mean sizes of bed materials, 0.43 and 0.80mm. They concluded that ^{for this range} the larger the bed inert particle size, the higher the burning rate of carbon. They also analysed the combustion gases and concluded that most of the oxygen was consumed in the bed while a small amount of carbon burnt in the freeboard region.

Campbell and Davidson (31) carried out an experimental study in a fluidized bed combustor operated at temperatures

between 700 and 850°C, feeding both batch charges and continuous charges. They concluded that reactions in fluidized beds were diffusion controlled. They extended the model of **Avedesian and Davidson** (30) for particle burning to when a finite concentration of carbon-dioxide in the particulate phase of the fluidized bed was considered. The reaction model assumed remains the same as that of **Avedesian and Davidson**, but in reality, carbon-dioxide concentration in particulate phase will be finite in fluidized beds of carbon particles and for **Avedesian and Davidson's** model to be valid with increased radius of reaction zone, the surrounding ash will pick up much of the heat from the reaction zone and the surface temperature will not be high enough for the endothermic gasification reaction between carbon and carbon-dioxide to occur there.

Campbell and Davidson (31) also conducted experiments on particle size distribution by charging coal, char and coke particles. Their results on coke particles are in good agreement with the theoretical predictions but those on coal and char particles do not agree well with the theory. This suggests that their assumption of perfect mixing in their theory neglects both attrition and entrainment factors which may be very significant especially attrition in case of char and small size coal particles.

Pyle (39) reviewed fluidized combustion modelling ^{by} five authors but was disappointed because of ^{the} low experimental content. He then summarised a number of topics which needed closer ^{examination} in order to develop more generally applicable and useful models. These include bubbling and fluidization, particle combustion and system analysis. He then concluded

that though the existing models could give useful guides to the behaviour and designs, theory and experiment must go hand in hand if more comprehensive models were to be developed and used.

Horio and Wen (40) developed a fluidized bed combustor model for estimating combustion efficiency and axial temperature profile. Experimental results reported by the National Research Development Corporation, England and National Coal Board, England were used in their simulation study. Their calculated data on the effects of excess air on combustion efficiency was compared with the NCB fluidized bed. They found that carbon loss was mainly caused by elutriation and concluded that combustion rate for a particular type of coal, as well as the elutriation characteristics was very important for estimating the combustion efficiency. They also found that an increase in heat release rate per unit volume of the bed would increase the nonuniformity of the bed temperature.

Gibbs et al (41) studied the combustion of coal and formation of NO in a 300mm square sectioned fluidized bed coal combustor of inert silica-based clinker sized 1.68 to 0.25mm at temperatures between 650 and 850°C. Spatial distribution of CO₂, CO, O₂ and NO and of temperatures were measured both in the bed and in the freeboard.

Their results showed that there was an increase of about 25°C in the freeboard temperature upto 450mm above the bed and beyond 450mm of the bed surface, the freeboard temperature fell below the bed temperature. Their off gas concentration measurements showed that they were nearly uniform over the cross section of the bed except in the

proximity of the walls where the CO_2 concentration was higher and the O_2 concentration lower than farther away from the walls. It was also shown from the off gas measurements in the bed and freeboard region that the main reaction taking place above the bed was the oxidation of unburnt CO and the extent of this oxidation was dependent on both the bed temperature and excess air. They concluded that(1) most of the combustion in the bed took place in the particulate phase resulting in a particulate phase oxygen concentration which may approach zero and is significantly lower than that of the bubble phase; bubbles continually supply oxygen to the burning particles in the particulate phase as they ascend through the bed and hence the oxygen concentration in the bubble phase decays as the bed surface is approached.

(2) Combustible loss decreases with increasing bed temperature and increasing excess air.

(3) The carry over loss is increased when low volatile coal or coarse coal is used as feed to the bed; in the first instance because of the lower reactivity of the feed and in the second because of the loss of large particles from the bed as a result of "splashing".

(4) The NO emission is only slightly dependent upon the input air-fuel ratio when compared with other modes of coal combustion (Stoker or pulverised fuel). Their results show a small increase in emission of NO_x with increasing excess air, which offsets the dilution effect such that the concentration is not affected by excess air. This indicates a strong relationship between NO_x and bed temperature.

Gibbs (42) developed a mechanistic model for predicting the

performance of a fluidized bed combustor. The model was based on the two phase theory of fluidization as proposed by Davidson and Harrison, and material balances of shrinking particles. His model was tested with operating conditions and the results showed that

(i) Combustible loss decreases with excess air.

(ii) The larger the bubble diameter in the bed the more combustibles accumulate in the bed and the higher the combustible loss.

(iii) Rate of attrition in the bed may have a significant effect on the combustion efficiency.

He concluded that though the model was highly adaptive without any limitation to burning, attrition, elutriation and splashing rate equations, it would not be useful until reliable data on the above limitation become available to test the validity of the model.

Beer(43) reviewed the fundamental and engineering aspects of fluidized combustion of coal, and concluded that in order to have a break through in the industrial application of fluidized combustion, the study and understanding of start up, load following, deposit on turbine blades corrosion of superheater tubes immersed in the bed etc have to be made.

Rajan and Wen(44) developed a comprehensive model for the simulation of the fluidized bed coal combustors. The model was capable of predicting the combustion efficiency, char, particle size distribution in the bed, elutriation and entrainment of materials, solid withdrawal rate, bed temperature, exhaust gases and volatiles. The validity of their model was tested under a set of operating conditions

based on the experimental data reported by the National Coal Board(1971), Gibbs and his associates in Sheffield(1975),the Exxon and Research and Engineering Company USA(1976) and NASA Lewis Reseach Centre Cleveland,Ohio(1978).

The results of their model simulation on particle distribution and elutriated material indicated close agreement with the experimental data of NCB, while the model on temperature and carbon concentration profiles did not when tested with NASA data. This was attributed to the closely packed horizontal tubes, and hence poor solid mixing which in turn affected the temperature profile.

2.12 COMBUSTION OF DEVOLATILISED CHAR.

Smith (45) reported experimental measurements of combustion rates of pulverised fuels of various types and sizes over the temperature range 1200 - 2270 K. His experiments showed that combustion rates were controlled by combined effects of pure diffusion and chemical reaction at the pore structure of the particles.

Field (46) measured the burning rates of pulverised coal chars in the range of 28 - 105 μ m over the particle temperature range 1200 -2000 K in a stream of hot gas. His experiments showed that at gas temperature more than 1500 K, the burning rates of this size of char particle was controlled by the rate at which oxygen diffused towards the surface.

Chakraborty and Howard (29) studied the mechanism of combustion of char in a shallow fluidized bed of sand electrically heated at 1073 -1173 K. They used a wide range

of particle sizes and superficial fluidizing velocity. Their results suggested that between 1223 and 1323 K, combustion of char particle was influenced by both chemical kinetics and the diffusion of oxygen towards the surface. They also showed that the larger the bed inert particle size, the higher the burning rate of carbon.

Garbett and Hedley(47) developed a mathematical model of an AFBC for combustion of carbon. They described the effects of (1) transfer of oxygen to the particulate phase (11) diffusion through the gas within the interstices between the inert particles round each carbon particles (111) chemical rate control at the surface of each carbon particle.

They used the two phase theory of Davidson and Harrison together with a combustion mechanism based on the experimental results of Avedesian and Davidson that concluded that the effect of chemical rate control at the surface of each carbon particle is negligible on account of high carbon temperature.

They concluded that using the model to predict the performance of a FBC fed with monosized coal, the carbon loading was shown to be highly dependent on bed temperature, particle temperature and bubble diameters.

Jung and LaNauze(48) studied the combustion of two types of carbon of widely different character in a fluidized bed of sand (102mm diameter) heated by external electrical elements and an electrically heated 76mm diameter bed of sand. In their results, they observed that for both carbons, mass

loss by attrition was 5% for the irregular particles and less than 3% for spherical particles.

They concluded that the change in particle size with burn-off might be modelled as a shrinking sphere of constant density despite oxygen penetration into the particle.

Yagi and Kunii(49) studied the combustion of carbon particles in flames and fluidized beds. They developed the general theory of combustion of single carbon particle in flame and that of pure carbon particles in fluidized bed. They then estimated the controlling factor for combustion under various conditions by comparing the value of chemical reaction rate coefficient of a carbon particle with that of the mass transfer coefficient of boundary film around the particle. Their findings showed that chemical reaction rate coefficient did not differ much from the mass transfer coefficient through the boundary film when the temperature was about 1300K and the diameter of the particle was 1mm in flames. But in the case of fluidized beds where the formation of the boundary layer around the particle was suitable to be prevented by the highly turbulent mixing, it might be assumed that the chemical reaction rate was controlling when $T < 1300K$ and particle diameter $D_p < 1mm$, if complete contact of all particles with gas stream was assumed.

They also carried out experimental combustion of pitch coke in fluidized beds and analysed the results with their theoretical equations which were found to be in agreement.

2.13 Conclusions on Review of Literature on combustion of a single coal particle and Devolatilised char.

The above review suggests that the combustion of large carbon particles will be controlled by the diffusion of oxygen towards the particle surface, while that of the small carbon particles will be chemically controlled.

2.14 The combustion of Volatiles Hydrocarbon.

The combustion of volatile products has received very little attention in the past; this may be attributed to the complex reaction mechanism involved. Recent development on the coal conversion processes has focused attention to the combustion of coal volatiles. Volatiles are important because they can be responsible for almost 50% of the heat released by coals and will be discussed in section 2.15.

Several investigators have proposed reaction mechanism of volatiles combustion, but this needs further investigation.

Field et al (33) reviewed and discussed the combustion of volatiles. They described the composition of volatiles as well as giving information on soot formation and burning.

Numerous authors (50,51,52,53) have reviewed coal devolatilization, composition of volatiles products and their combustion; a particularly comprehensive survey is that of **Anthony and Howard**(54). They presented several experimental methods of slow and rapid heating which yield the same types of product components. These components include tar, various gases (CC_2 , CO, CH_4 , H_2 and others) and water.

Thurgood and Smooth (55) developed a model of volatile combustion based on a reaction mechanism for methane oxidation. They found that a majority of the reactions involved in a complete methane oxidation scheme were also found in mechanisms for other volatiles. They also found that oxidation reactions for carbon monoxide, and hydrogen were included in reaction sequences for methane systems, and any water vapour formed must be included in overall mechanisms.

They also reviewed the earlier workers' mechanism of methane oxidation, made comparison with theirs and concluded that with methane oxidation a similar mechanism could be applied to predict the burning rate of other hydrocarbons.

Howard and Essenhigh (56) studied the mechanism of solid-particle combustion with simultaneous gas-phase volatile combustion in a furnace by burning Pittsburgh seam coal up to 200 μ m in size. They found that at about 0.15 seconds after ignition had occurred, 50% of the fixed carbon had burned and about 95% of the volatile matter had either evolved and burned as gases or burned in-situ as solid material. They concluded that particles larger than about 65 μ m in size experienced gas-phase, volatile combustion while smaller particles experienced simultaneously both rapid, gas-phase, volatiles combustion and heterogeneous combustion. Similarly particles less than 15 μ m in size experienced heterogeneous combustion during

rapid volatiles evolution.

Howard and Essenhigh (56) also presented a model for burning fuel particle. Their model was adopted from the theory of oil-drop combustion. Despite this, the predictions from their model agreed well with their experimental findings. Their experimental results suggested that gas-phase and heterogeneous combustion are not interdependent. But what Howard & Essenhigh failed to discover was how fast these volatiles^{were} being released, their burning time and where the reaction does occur. The oil drop model used was to estimate the screening influence of evolution volatiles rather than to estimate burning times.

Merrick(57) developed a mathematical model of volatile release. The model describes the calculation of the final yields of volatile species, the kinetics of volatile matter release and by considering a full range of volatile species enables the prediction of the char yield and composition to be made by element balances.

In order to determine values for the parameters in the model, Merrick did a series of experimental tests on a range of U.K. coals of maximum particle size 3mm in a 0.12m long and 0.03m diameter tubular steel pot. The coal was heated by placing the pot in a 3KW electric muffle furnace, the maximum sample temperature being 950°C with heating rates of 3 to 8K/min.

His results suggest that increasing the heating rate increases the temperature at which the maximum loss occurs

but has little effect on the maximum rate of mass loss as expressed as S^{-1} .

He also noted that application of the model to coals of a different nature and origin, should therefore be treated with caution unless additional experimental data were available for validation. He concluded that the model could be used as the basis of a computational procedure provided the ultimate and proximate analysis of the coal and the heating profile were known. However his volatile evolution rate in the pot is very slow compared with that in the fluidized bed combustion which is very fast, nevertheless it could be extended to fluidized bed combustion.

2.15 Combustion of volatiles in fluidized beds.

The conditions of combustion of volatiles in fluidized beds are some what different from those in more conventional coal burners.

Since the volatile matter content of coal may account for as much as 40% of the total heat released in the combustors, the location at which volatiles burn depends interactively on the bed depth, coal feeding methods, and gas velocity, as well as particle size and composition. For example shallow beds tend to have larger numbers of small bubbles whereas in the upper regions of deep beds coalescence causes smaller numbers of bubbles but of larger size; this bubbling mechanism gives rise to a gas by-pass mechanism which tends to bursting of bubble at the surface flinging solid particles into the freeboard space above,

and under some circumstances, leads to loss of combustion within the bed. Hence a generous freeboard is desirable to ensure complete combustion.

In deep beds, the volatile component of the coal is released into the particulate phase zone and some burns there if oxygen is present. After gas mixing, the volatiles ^{might} also burn inside the bubbles.

Combustion in the bed is incomplete because there is little oxygen in the upper part of the particulate phase and therefore volatiles released there are unable to burn. Since interchange with the bubble phase gas is relatively poor in the upper part of the bed, these volatiles leave the bed unburned.

Stubington (58) studied the release of coal volatiles in fluidized bed combustion. He noted that variation of oxygen concentration within the bed affected the combustion rate of solid particles, since particles within the evolution region experienced very low or zero concentrations. This, he noted was in marked contrast with models for carbon particle combustion, which assume a uniform oxygen concentration across the bed and concluded that the proposed physical picture for the evolution and combustion of volatiles was more realistic than the models, though the accuracy of the picture needed to be tested experimentally.

Atimtay (59) conducted a combustion experiment with coal in a shallow (83mm static depth) fluidized bed of coal ash, mean diameter of 550 μ m at 1173K. She found that

burning of volatiles took place more in the freeboard region than in the bed.

Atimtay (59) also presented a model to calculate the radial velocity of the gases coming out of the particles during devolatilization process as shown by equation 2.11 below.

$$V_R = Q/4\pi R^2 N \quad 2.11$$

The main limitation of this model is that at fluidizing velocities commonly encountered, the flame is swept away from the coal and volatiles burn in the freeboard.

She concluded that the burnout time of volatiles increased with charged masses, particle size and volatile matter content but decreased with the air velocity.

Park et al (60) proposed a plume model for large particle fluidized-bed combustors. The model was based on the assumptions that since coal devolatilization is fast (1sec. for a 200um particle) compared with both particle circulation (about 15sec. for complete mixing) and char combustion (60sec. for a 300um particle), the coal particle entering at the distributor will devolatilize practically instantaneously and the volatiles will rise in the plug flow as plumes with the same velocity as the fluidizing gas. Thus a plume of volatiles was envisaged as rising from each coal entry port and burning with air at the plume boundary as in the case of a diffusion flame.

Pattipati and Wen(61) studied the devolatilization of coal particles and combustion of coke particles in a 13.2cm diameter and 28.5cm high fluidized bed of silica sand made of mild steel. In their devolatilization experiment, they noted that at different oxygen concentrations, the volatiles formed a detached flame near ^{the} coal surface while the coal surface itself was at much lower temperature than the bed itself. They also observed the floating of the coal particles on the bed surface while devolatilization was taking place and that the particles tend to segregate and move to the bed wall.

In their combustion tests, they observed the glowing of coke particles which were at higher temperatures than the bed. The tests also showed a definite reduction in size after combustion. Their results indicate that devolatilization is not entirely chemical reaction controlled and at higher temperatures, the rate of combustion of char is under a diffusion control regime.

Pattipati and Wen(61) also developed a single particle combustion model in fluidized bed. They then compared their proposed model with model predictions of Avedesian and Davidson (1973), Basu et al (1975), Howard and Chakraborty (1979), Sinha et al (1980). They found that Avedesian and Davidson's model and Basu's model underpredict combustion rates while Sinha's model overpredicts the combustion rates. Howard and Chakraborty's model underpredicts the combustion rates of char particles larger than 5mm.

They concluded that,

(i) both kinetic and diffusional resistances are important in determining the combustion rates of large coal particles

at sizes greater than 2mm.

(ii) devolatilization time for large coal particles were considerably higher than the mixing time in FBC and must be considered in modelling and designing of FBC systems; devolatilization of coal particles increases sharply with particle size and decreases with increase in bed temperature.

(iii) combustion rate increases with increase in inert particle size, increase in temperature and in char particle size but decreases with carbon loading in the bed.

(iv) their proposed model predicted combustion rates of char particle within $\pm 25\%$ error range.

Yates et al(62) examined the mechanism of coal devolatilization by suspending a piece of bituminous coal in a fluidized bed of fine particles ($d_p = 200\mu\text{m}$) at 850°C and observed by means of X-rays the formation and development of bubbles. Visual observation of the coal by means of a scintillation screen showed a stream of such bubbles rising continuously for about one minute after its immersion in the bed. At the end of this time no more bubbles could be seen and it was assumed that the coal had by then become devolatilised and had begun to burn as char. They concluded that volatiles released from coal early in its period of residence in a hot fluidized bed of fine particles flew in ^{the} form of bubbles and that combustion of volatiles in this case would appear to have followed the same pattern as that of any other combustible gas admitted as bubbles to the lower region of a hot fluidized bed.

LaNauze(63) developed a mathematical model for coal devolatilization in fluidized combustors. He suggested that for coal particle sizes used in fluidized bed combustors, the rate of devolatilization was controlled by the rate of diffusion of volatiles through the char and not by the kinetics of the decomposition processes. He tested the model by using the experimental data of Jung and Stanmore and concluded that devolatilization times were generally of the same order or longer than the time scale for the dispersion of solids, so volatiles release could be expected throughout the bed for most sizes of coal feed used in practice.

2.16 Conclusions on Review of Literature on Volatile Combustion.

The above review of combustion of volatiles either in hot air or in fluidized beds clearly shows that the actual mechanism has not yet been firmly established and that there is disagreement between findings of different workers. Also evolution rate of volatiles, their burning rate and the temperature at which they evolve and burn under different fluidized bed design and operating conditions have certainly not been quantified nor the controlling parameters understood. The existing published experimental work and models have only dealt with evolution of volatiles with little mention of their combustion. Hence the intention of the present work was to elucidate the role of coal volatiles in combustion processes and to discuss the effects on the design of industrial fluidized bed combustor systems.

CHAPTER THREE

PART A

3. Theoretical Consideration

3.1 Thermodynamic Analysis of Heat Release.

When a fluidized bed combustor is being designed the combustion reaction and accompanying heat release rate must be considered. Heat release per unit time within the bed is dependent upon the amount of fuel resident in the bed and the reaction rates of the fuel. These are dependent upon the fuel type, temperature and controlling mechanism (e.g. whether limited by chemical kinetics or diffusion of oxygen to the reacting fuel). The role of combustible volatiles is important in that a fraction may burn in the bed, a fraction may burn in the freeboard, some may not be burnt at all or only decomposed. Qualitative assessment of this heat release can be accomplished by applying the First Law of Thermodynamics to the combustion system Fig.3.1

Consider a practical case of a coal fired fluidized bed combustor burning a typical United Kingdom coal and operating with a bed temperature 850° C at atmospheric pressure of 1 bar with sufficient excess air for satisfactory combustion. The exhaust gases will leave the bed at about 850° C. The thermal capacity of the bed particles is many times larger than that of the fluidizing gas so that the gas will tend to follow the temperature of

the particles rather than vice versa. When combustible gases are being burnt, they can burn in the interstitial spaces and/or in the bubbles. This situation may give locally high gas temperature, because mixing of gases and particles is imperfect, but the assumption that the off-gas temperature has the same value as bed temperature may be sufficient for first order purposes.

First law analysis shows that in the steady state, a significant fraction (maybe 50%) of the heat liberated from the fuel may have to be removed from the bed if all combustion takes place within the bed. Cooling tubes can be installed into the bed to remove sufficient of the heat generated and maintain a bed temperature of 850° C. The alternative to installation of cooling tubes is to increase the amount of excess air, which acts as a coolant. The latter is undesirable in boilers because the excess air merely lowers the boiler efficiency. However, since it is seldom possible to mix the fuel and air in complete uniformity, some excess air must be provided in order to avoid the still less desirable phenomenon of incompletely - burned fuel passing out of the system in the exhaust gases.

If however, all combustion does not occur in the bed and a significant part of the combustion occurs in the above - bed region, then less heat has to be extracted from the bed so that less tube surface area is required there, but more will then be required downstream of the bed.

Stubington (58) in his demonstration example of oxygen availability limit, suggested that even though the process of oxygen transfer from bubble to particulate phase and gas phase mixing is rapid, about 72% of volatile matter will

burn above the bed region.

A significant amount of heat is lost from the bed by radiation from the surface and this is absorbed by the hot gases rising through the freeboard zone and by the walls of the freeboard, while a little heat leaks through the bed containment (refractory lining) Fig. 3.2.

Considering the chemically reacting system shown in Fig.3.1, the steady flow energy equation is

$$H_R + Q = H_P \quad (3.1)$$

where H_R = Enthalpy of the reactants, (air + fuel)

H_P = Enthalpy of the combustion products.

Q = Heat transfer to the system. (- Q for heat loss)

The enthalpies H_R and H_P depend on their temperatures. The datum temperature, T_0 for H_R and H_P is 25°C (298K)

Considering Figs.3.2 and 3.3, the reactants enter the system at temperature T_1 and the products of combustion leave at bed temperature T_2 .

From equation 3.1 the heat transfer, Q , to the system from the surroundings is

$$Q = H_P - H_R \quad (3.2)$$

Using the notation H_{P2} to mean enthalpy of the products at temperature T_2 , etc, (T_0 = Datum temperature, 25°C (298 K)) equation 3.2 becomes

$$Q = (H_{P2} - H_{P0}) + (H_{P0} - H_{R0}) + (H_{R0} - H_{R1}) \quad (3.3)$$

$$= (H_{P2} - H_{P0}) + (\Delta H_0) - (H_{R1} - H_{R0}) \quad (3.4)$$

where $(\Delta H_o) = (H_{PO} - H_{RO}) =$ Higher calorific value of the fuel.

Enthalpy $H = mh$ where $m =$ mass of the product or reactant and

$h =$ specific enthalpy of the reactant or product.

A summary of the results of theoretical analysis is provided in tables 3.1 and 3.2 but details of calculations in Appendices A1 to A2.

Similarly taking the specific heats, C , of coal and air as 0.98 kJ/kgK and 1.005 kJ/kgK respectively, the enthalpy of the reactants at T_1 can be found from

$$(H_{R1} - H_{RO}) = (M_{\text{coal}} C_{\text{coal}} + M_{\text{air}} C_{\text{air}})(T_1 - T_o) = -132.5 \text{ kJ/kgK} \quad (3.5)$$

$$(H_{p2} - H_{po}) = \text{Addition of the quantities in the last column of table 3.2} = 14379.3 \text{ kJ/kg fuel} \quad (3.6)$$

$$(\Delta H_o) = \text{Higher Calorific value of the fuel} = -27000 \text{ kJ/kg} \quad (3.7)$$

To obtain the heat transfer to the bed from the surroundings, adding equations (3.5), (3.6) and (3.7) will give

$$Q = -12753.2 \text{ kJ/kg fuel} \quad (3.8)$$

the negative sign means that heat has to be lost from the system. Therefore, for a fuel flow rate of 0.0308 kg/s , ^{used here,} the rate of heat loss, Q , from the bed must be

$$Q = 0.0308 \text{ kg/s fuel} \times 12753.2 \text{ kJ/kg fuel} \\ = 393 \text{ kW.}$$

... and details of calculations in Appendices A1 to A2

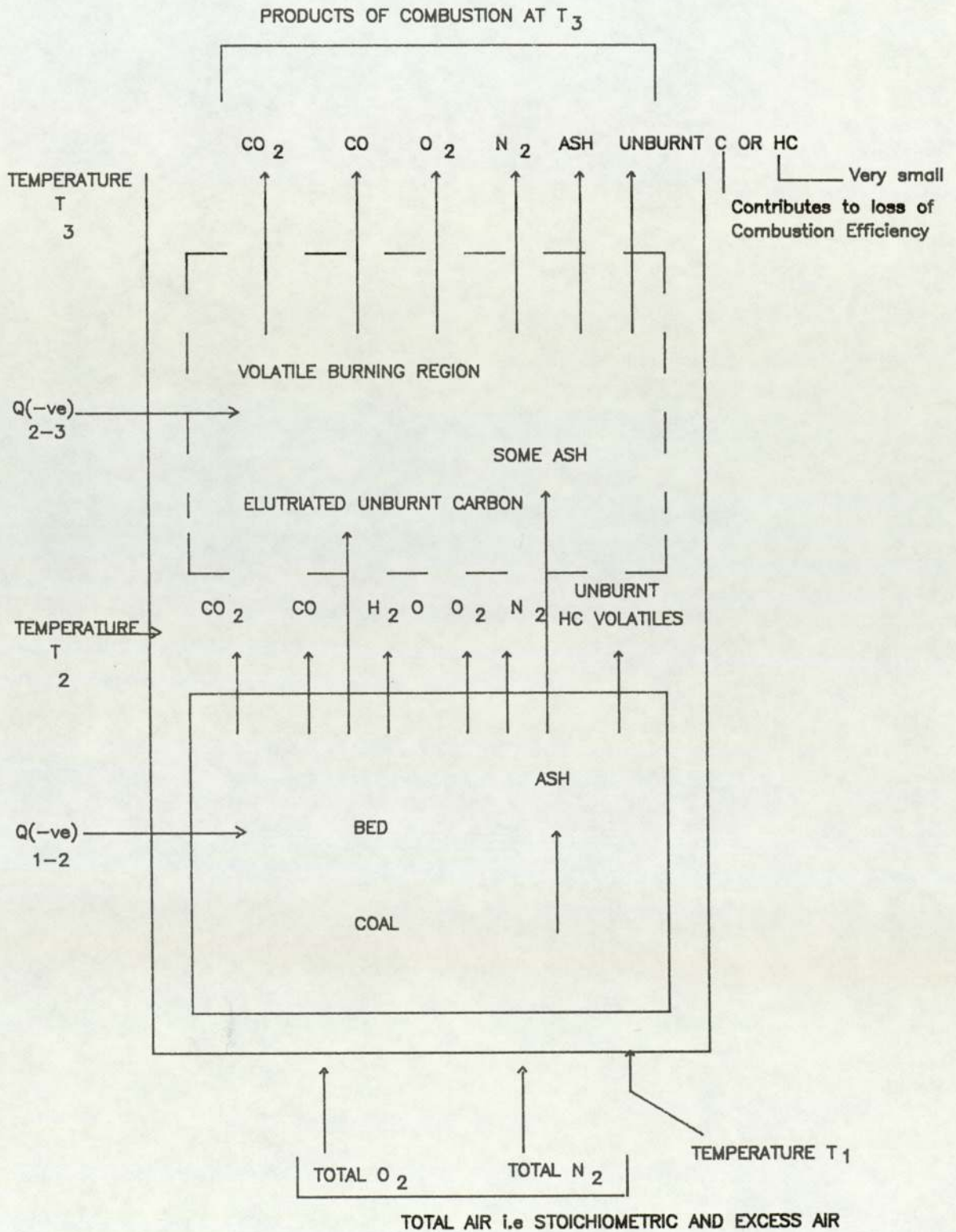


FIG.3.1 ILLUSTRATING A STEADY - FLOW CHEMICAL REACTING SYSTEM.

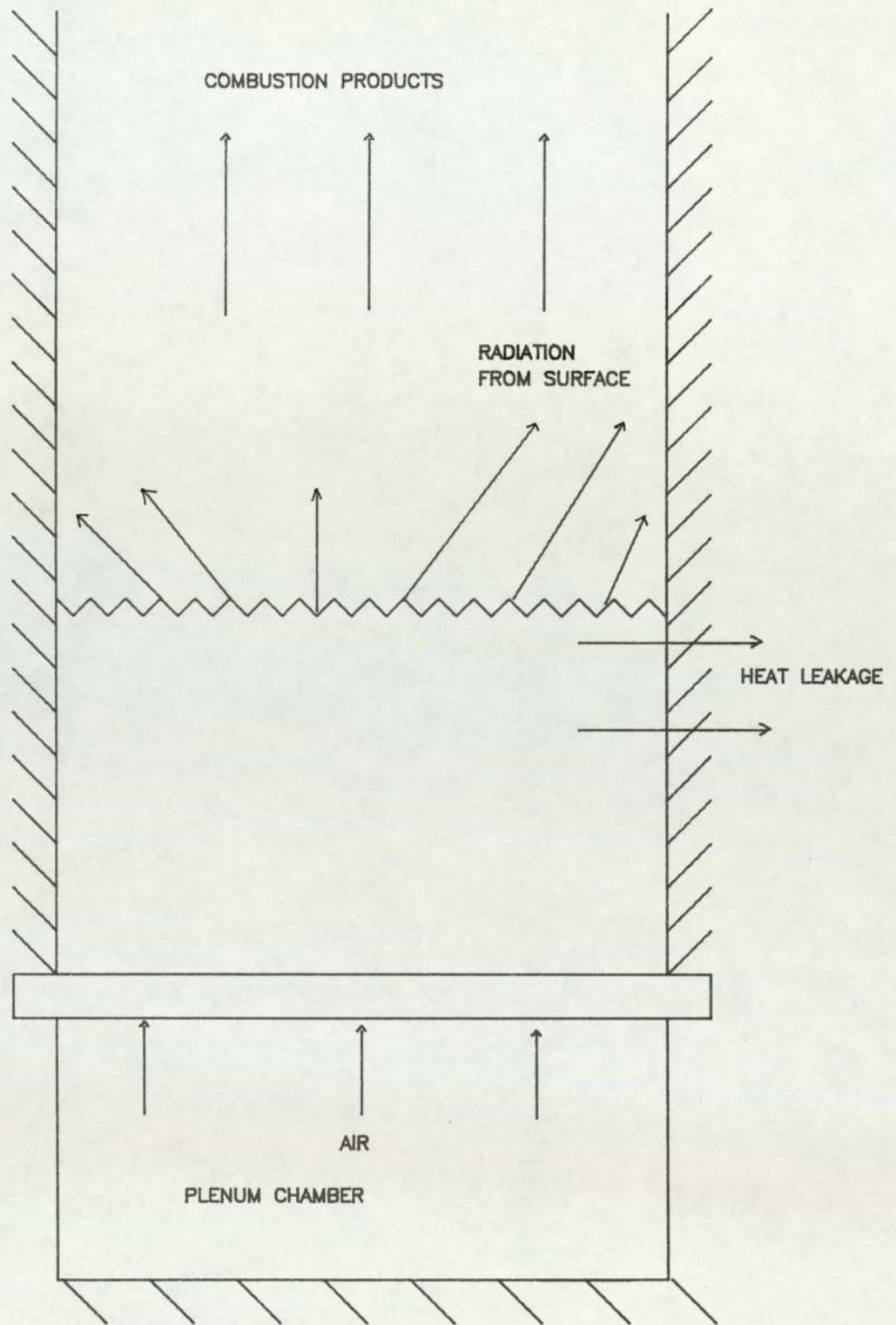


FIG.3.2 REFRACTORY LINED BED SHOWING HEAT LEAKAGE.

Composition as Fired	%	Molecular Mass	Kg mol.	Kg mol. of oxygen required
Moisture	12			
Ash	8			
Carbon	78.2	12	6.52	6.52
Hydrogen	2.4	2	1.2	0.6
Nitrogen	0.9	28	0.032	-
Sulphur	1.0	32	0.0313	0.0313
Oxygen	1.5	32	0.047	-0.047
Gross Calorific Value	27 MJ/Kg	Total Oxygen required		7.1043

NATIONAL COAL BOARD RANK 101 ANTHRACITE SUPPLIED AS WASHED

TABLE 3.1

PRODUCTS	MOL.	KJ/Kg Fuel	SPECIFIC ENTHALPY AT 850 °C (KJ/KgK)	ENTHALPY AT 850 °C (KJ/Kg Fuel)
CO ₂	0.065	2.86	978.48	2792.7
H ₂ O	0.012	0.216	1850.2	399.6
SO ₂	0.000313	0.02	NEGLECT	NEGLECT
O ₂	0.071043	2.273	899.46	2044.5
N ₂	0.33422	9.358	971.67	9092.9
Ash	0.08	--	619.5	49.6
TOTAL				14379.3 KJ/Kg Fuel

EQUILIBRIUM PRODUCTS OF COMPLETE COMBUSTION FROM COMBUSTION OF
COAL DESCRIBED IN TABLE (3.1) WITH 25% EXCESS AIR

TABLE 3.2

3.2 Heat Extraction Requirement.

For 832 KW. fuelling rate, ^{to a 1m² bed,} we are required to remove about 393 KW. heat from the bed to keep the temperature at 850° C

$$Q = UA\Delta T_m \quad (3.9)$$

The required heat loss from the bed of 393 kW. was arrived at on the basis of that the entire calorific value of the fuel was released within the bed. Thus the system boundary was shown in Fig. 3.4 below.

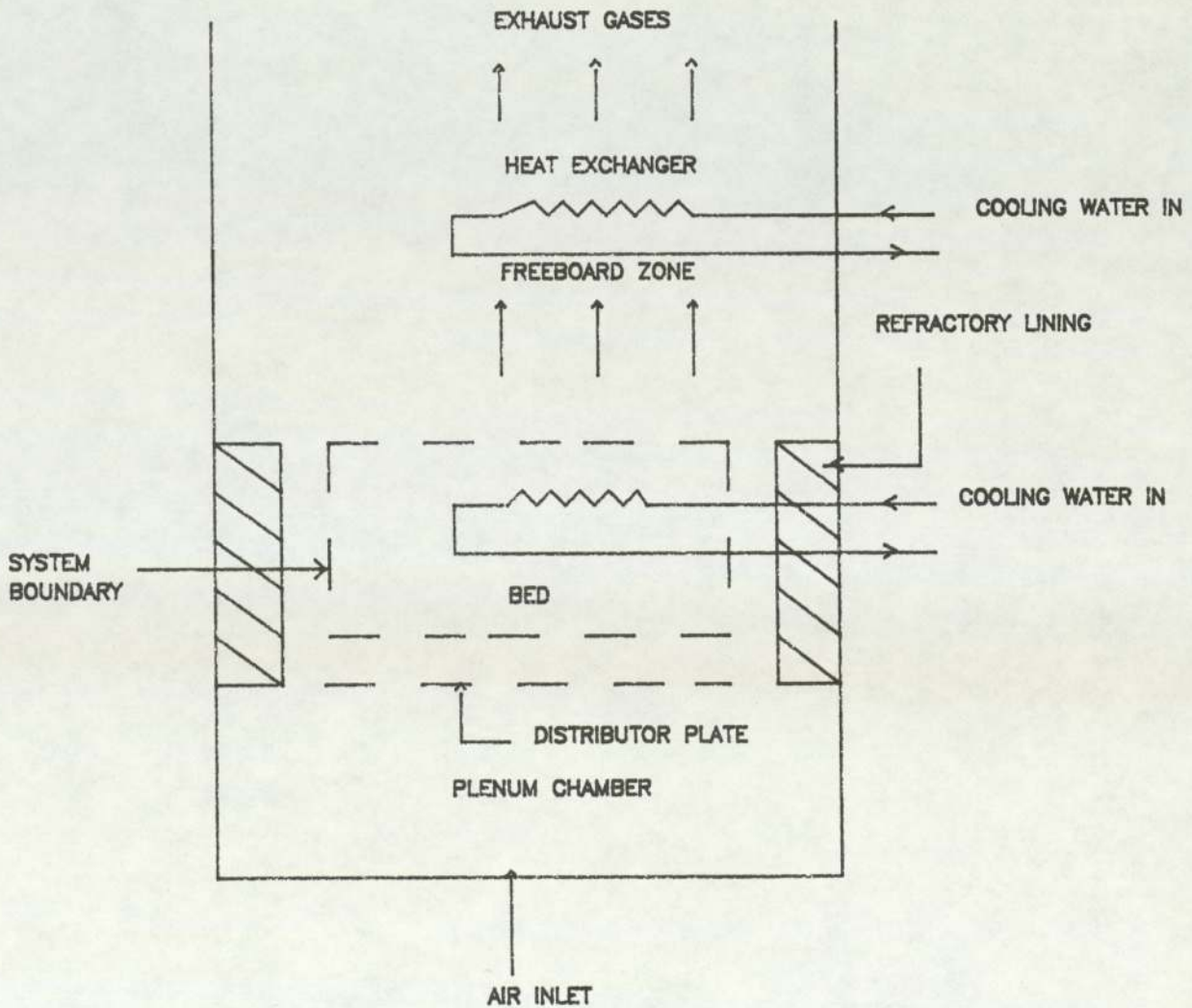


FIG.3.4 FLUIDIZED BED COMBUSTOR WITH HEAT TRANSFER TUBES IN THE BED AND A HEAT EXCHANGER IN THE OFF-GAS STREAM.

This condition of all energy released in the bed, may not be met. For example, suppose the coal contains a high proportion of volatile combustible matter and the bed is shallow. As soon as a coal particle enters the hot bed, many events occur (see section 2.10). For simplicity, however the whole process tends to be regarded as made up of two periods:

- (a) Evolution of moisture and volatiles.
- (b) Oxidation of residual char.

Combustion of most of the volatile matter occurs in the freeboard zone with a shallow bed, because of insufficient residence time to mix with oxygen, initiate and complete combustion. Thus sufficient height of freeboard zone must be provided to ensure satisfactory mixing and complete combustion of volatiles before they leave the combustion chamber.

Table 3.3 shows the results of calculating the surface area relative of tubes required in the bed \wedge to heat release. The detailed calculation is shown in Appendix A3.

FRACTION OF HEAT RELEASED IN BED	HEAT IN BED		AREA OF TUBE IN BED 2 (m)
	KJ/kg FUEL	KW	
.95	11590.8	356.986	3.0
.90	10427.4	321.164	2.7
.75	6937.2	213.666	1.8
.50	1124.2	34.625	0.3

TUBE SURFACE AREA REQUIRED TO MAINTAIN BED TEMPERATURE
 AT 850 °C

TABLE 3.3

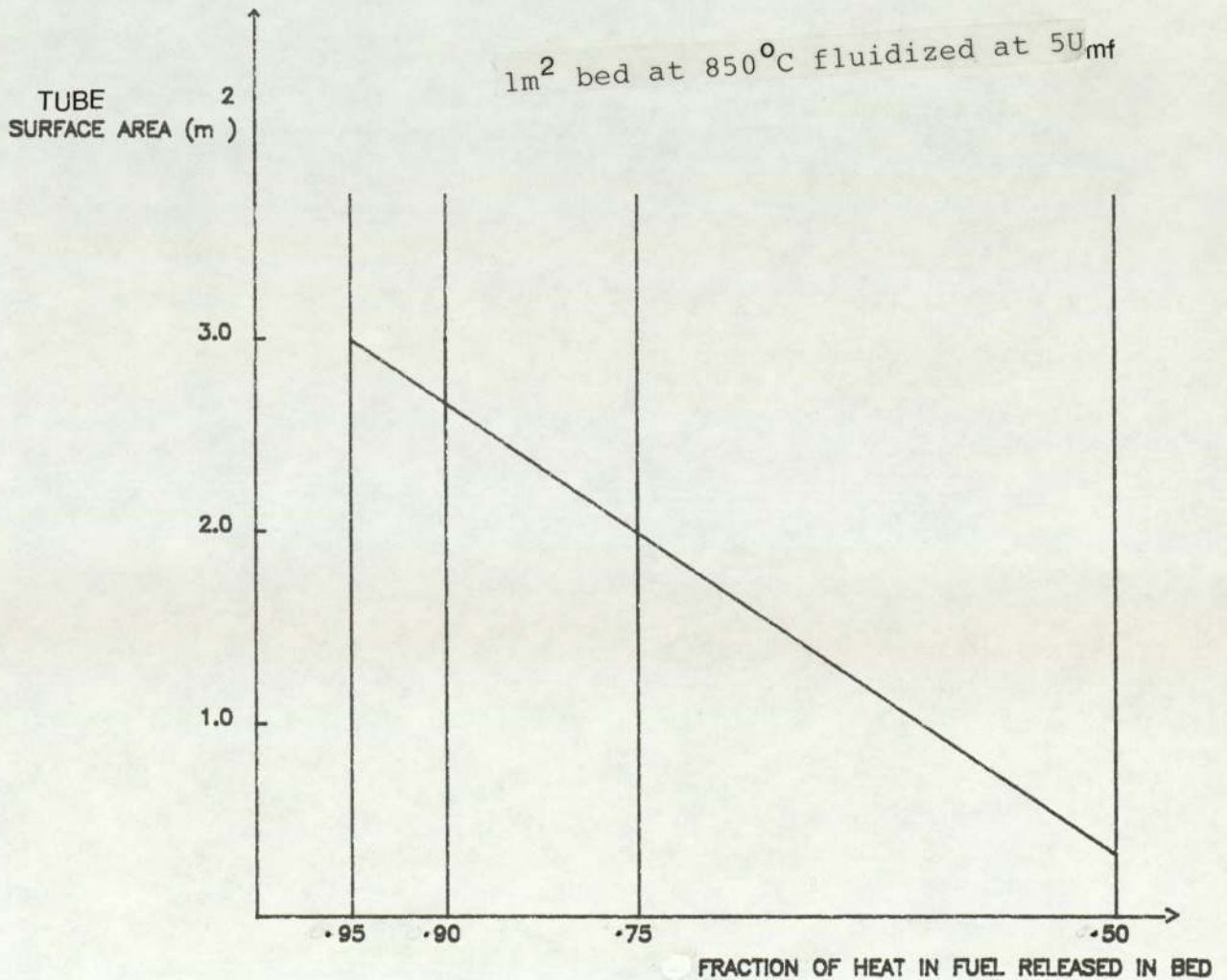


FIG.3.5 GRAPH OF SURFACE AREA AGAINST THE FRACTION OF HEAT IN FUEL RELEASED IN BED

3.3 Consequent Modification to Model.

Equations 3.3 and 3.4 therefore require modifications to allow for only part of the heat release (ΔH_o) occurring within the system boundary, defined by the bed. The amount of heat released within the bed would then be $CV(1 - XV)$ where XV is the fraction of the calorific value (CV) contributed by the volatiles, so that $(1 - XV)(\Delta H_o)$ could be written in place of (ΔH_o) in equation (3.4).

Assume coal to be of identical ultimate analysis and gross calorific value to rank 101 anthracite (Rose and Cooper page 302) (64) table 3.1 but that volatiles content accounts for 5%, 10%, 25% and 50% respectively of its gross calorific value.

Further assume that 95%, 90%, 75% and 50% respectively of the carbon and hydrogen are oxidized completely in the bed, and that the gross calorific value of the volatiles is the same as the char. Then only 95%, 90%, 75% and 50% respectively of the equilibrium CO_2 and H_2 emerge from the bed so that table 3.2 is modified to table 3.4.

It is also assumed that no oxidation of evolved volatiles within the bed.

Table 3.4 shows the analysis but details of calculations are in Appendix A2 and table A1.

PRODUCTS	MOL	Kg/kg Fuel	MASS OF CONSTITUENT FORMED Kg/Kg Fuel				SPECIFIC ENTHALPY AT 850 °C (KJ/KgK)	ENTHALPY AT 850 °C			
			FRACTION OF FUEL BURNT IN THE BED					FRACTION OF FUEL BURNT IN BED			
			0.95	0.90	0.75	0.5		0.95	0.90	0.75	0.50
CO 2	0.065	2.86	2.717	2.574	2.145	1.43	976.46	2513.4	2094.5	1386.3	
H O 2	0.012	0.216	0.205	0.194	0.162	0.108	1850.2	358.8	288.7	189.8	
SO 2	0.000303	0.02	NEGLECTED				NEGLECTED	NEGLECTED	NEGLECTED	NEGLECTED	
O 2	0.071043	2.273	2.159	2.046	1.705	1.137	898.46	1840.3	1533.6	1022.7	
N 2	0.33422	9.358	9.358	9.358	9.358	9.358	971.67	9092.9	9092.9	9092.9	
ASH	0.08						619.5	49.6	49.6	49.6	
EVOLVED VOLATILES FRACTION			0.05	0.1	0.25	0.5	1500	75.0	375.0	750.0	
TOTAL								14181.7	14005.1	13445.3	12511.3

EQUILIBRIUM PRODUCTS OF BURNING FRACTION OF FUEL IN THE BED FROM COMBUSTION OF COAL DESCRIBED IN TABLE 3.1 WITH 25% EXCESS AIR

TABLE 3.4

In the previous example, the ^{basic} fuel considered has a very low content of combustible volatile matter (< 5%). If a radically different type of fuel is burnt (table 3.4), e.g having 50% of more of its calorific value contributed by combustion of volatiles then it was shown that the heat loss required from the bed to maintain its temperature at 850°C will be about 35 KW. which is significantly less than the 393 KW. required if all the heat of combustion is released in bed.

It can be shown Figs. 3.6 and 3.7 that reduced heat extraction requirement from the bed would have to be accompanied by an increase in heat extraction in the region downstream of the bed surface.

$$ie \quad Q = q_{VZ} + q_b$$

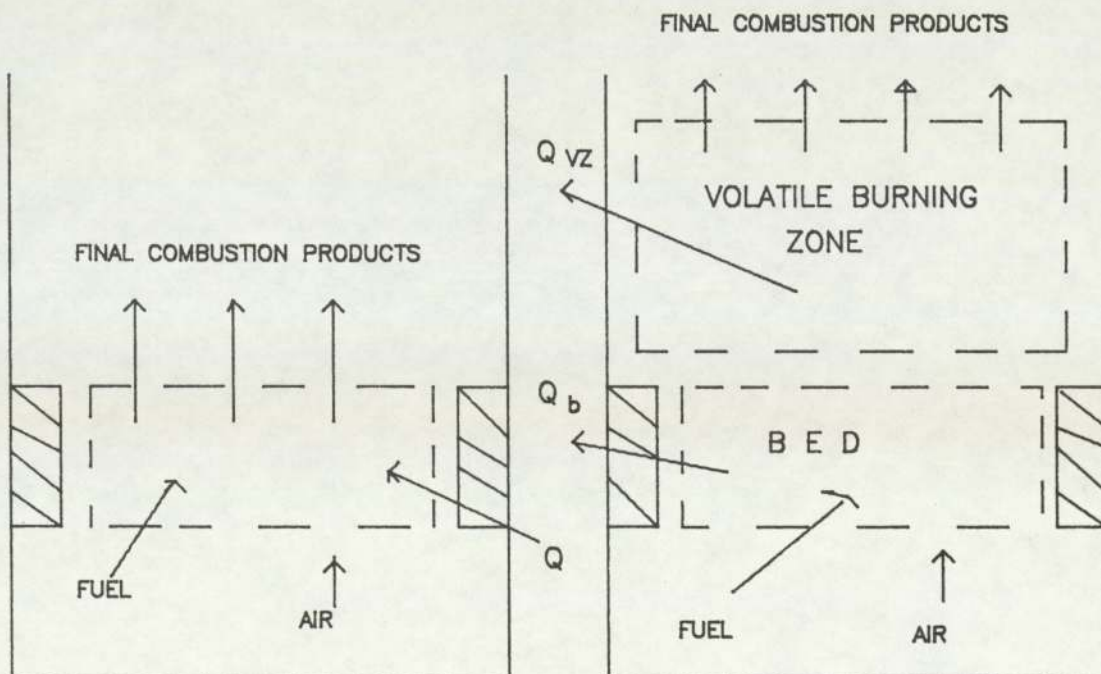


FIG. 3.6 SHALLOW BED BURNING
LOW VOLATILE FUEL

FIG. 3.7 SHALLOW BED BURNING
HIGH VOLATILE FUEL

3.4 Mixing Concepts.

Combustion in a fluidized bed combustor is a physically controlled process, in which the combustion of char is a slow process and that of gases is relatively rapid.

In a coal-fired fluidized bed combustor, solid fuel enters from one stream and air from another. There is further separation of the streams when volatiles are evolved. The degree of mixing between the volatiles and air determines the flammability locally and the potential for heat release rate from volatiles within the bed.

In the freeboard zone above the bed, combustion of volatiles will be physically controlled, with the chemistry effects being limited by extinction in region where the mixture strength and temperature are in appropriate for combustion (Westwood(66)).

Because the volatiles are released in a relatively cool region inside the coal particle, it is unlikely that volatiles will burn inside the coal during their release in form of laminar jets egressing from the particle surface. Rather they will mix with the surrounding turbulent gases and burn in a premixed or partially premixed state outside. This degree of mixing determines the temperature profile in the outlet stream which must nearly uniform and be controlled in order to avoid sintering arising from overheating of the bed arising from combustion gases radiating back to the bed.

However, flow mixing alone cannot ensure stable, continuous combustion, since conventional hydrocarbon fuels are not mutually self-igniting with air

Tringham (67)), at least within a few hundred degrees of standard ambient temperature.

Combustion of residual carbon formed by pyrolysis begins with chemisorption of oxygen on the carbon surface. The resulting surface oxides decompose to generate carbon monoxide which burns in the gas phase as it meets the oxygen. Carbon dioxide produced in this reaction either escapes into the off-gas stream or diffuses back to the carbon surface where it is reduced to carbon monoxide if it impinges on hot carbon residue.

Field et al (33) consider the controlling step of reaction sequence to be the oxidation of CO to CO₂. After the formation of volatiles, for coal particles in the 100um range, at temperatures of about 1000°C, it is estimated that about 7 milliseconds are required for diffusion of oxygen. The oxidation of CO to CO₂ which is assumed to be the controlling reaction step, takes about 3 milliseconds. Hence it is believed that diffusion of the oxygen is the controlling overall step since it is also generally assumed that the transport of products away will not be controlling.

It is also commented by Field et al (33) that though the ordinary diffusion relations are inappropriate for distances on the order of the mean free path of the gas, at combustion temperatures the mean free path is about 1 micron whereas pulverised fuel particle size is about 50 microns. Hence the customary equations for diffusion can be used for transport of the reactions.

Khitrin et al (68) noted that diffusion slows down the overall reaction rate at high temperatures. This infer that diffusion becomes rate controlling. Above 1000-1400°C

diffusion-limited combustion occurs (Golovina and Khaustovich (69)).

In the fluidized bed combustion of coke at 700°C Khirtin et al (68) found CO₂ to be the principle product and chemisorption of oxygen to occur.

Avedesian and Davidson (30) have assumed boundary layer type diffusion control for their 0.25- 0.26mm size particles. They also assumed that the carbon surface is oxidized by CO₂ and the resulting CO diffuses to a reaction zone surrounding the particle where it burns with oxygen to CO₂

Rajan and Wen (44) stated that for small particles, carbon monoxide formed during char combustion diffuses out fast because of rapid mass transfer and burns to form carbon dioxide outside the particle, whereas for large particles, because of slow mass transfer, carbon monoxide burns within the boundary layer of the particle, and carbon dioxide is transported out.

It is also commented by Rajan and Wen (44) that for smaller particles, diffusion of oxygen to the surface of the char particle is faster than the chemical reaction rate, while for large particles, diffusion of oxygen is slower than chemical ^{reaction} rate. Thus, the diffusional term tends to dominate for larger particles at high temperatures, while the chemical terms tends to dominate at low temperatures.

PART B

3.5. A MATHEMATICAL MODEL FOR COMBUSTION OF VOLATILE MATTER

MASS BALANCE

3.5.1. Introduction

Coal devolatilization, which occurs in all coal conversions, is a complex and perhaps the most difficult to model mathematically. Earlier attempts at the construction of mathematical models have been directed at the evolution and kinetic reaction rates of volatiles. A review of the models has been presented by Anthony and Howard (54) and others (33,56,57). They have modelled coal pyrolysis as a set of independent parallel reactions having a statistical distribution of the activation energies which has provided valuable insight into the overall or global kinetics of the process.

Accordingly, a model was developed which provided a computational procedure valid for the range of coal types, used for combustion, to predict the parameters required by the models of physical properties. Limitation imposed on the model is the requirement of the input data that has to be derived from the standard coal test method. Hence it was decided that only the composition of the coal in terms of carbon, hydrogen, oxygen, nitrogen and sulphur would be used. Other traces of elements which are known to occur in

the coal, but amount to less than 0.4% are therefore ignored.

3.5.2. DEVELOPMENT OF THE MODEL

3.5.2.1. Composition of Volatile Matter

The composition of the volatile matter is defined in the model in terms of the following five species: CO_2 , CO , HC , H_2O , O_2 . Although there is no restriction to the number of species to be considered to be sufficient for reasonable construction of accurate element balances, ^{For simplicity} it is assumed that the yields and composition of these species are independent of the heating rate as well as the carbonising environment. Although in fluidized bed combustion, the resident time of the primary decomposition products within the coal particles is shortened, thereby lessening the chance of secondary reactions within the coal matrix. This mechanism affects the total volatile matter yield.

When a sample of coal is dropped into the heated bed, both the coal substance and the mineral matter in the coal decompose and contribute to the total volatile matter evolved. The main reactions of these mineral matter in the coal are generally dissociations of the pyrites, carbonates and the water of crystallisation.

The present model is therefore based on dry, mineral matter free coal (dmmf), so that the volatile matter arising from the decomposition of the mineral matter are regarded as part

of coal. This convention is used to avoid problems of identifying the interactions between the volatile matter species from the mineral matter components and the pure coal substance, e.g. formation of carbon monoxide and hydrogen from the reduction of water of crystallisation by coke.

In using these species, it is assumed that the hydrocarbon (HC) can be dealt with as methane equivalent.

3.5.2.2. Assumptions

1. Humidity of air negligible.
2. H_2 and S come in the coal as written.
3. All the S is oxidized to SO_2 .
4. Fraction x_4 of H_2 in fuel is oxidized to H_2O .
5. Fraction x_5 of H_2 is converted to unburnt hydrocarbon (compositions unknown, but some reasonable assumptions might be made).
6. Fraction x_1 of carbon in fuel is oxidized to CO_2 .
7. Fraction x_2 of carbon in fuel is oxidized to CO.
8. Fraction x_3 of carbon is oxidized to unburnt hydrocarbon.
9. Fraction $(1-x_1-x_2-x_3)$ is not oxidized.
10. Part of the ^{fraction,} section 9 is transported as particles in exhaust gas. Part of it is retained in bed, gradually building up until an equilibrium composition in the bed is reached, after a very long time.
11. Mass of carbon in the bed ash is neglected.
12. About 20% of coal retained in bed.
13. ^{Quantity of} Elutriated sand ^{is} very small.

3.5.2.3. Structure of the Model

The development of mathematical models to describe the thermochemical process occurring in the combustion of volatiles in a fluidized bed involves setting up the mass and enthalpy balance equations. The total process is presented in terms of a set of independent equations which are solved simultaneously.

The approach adopted in the model to predict the combustion of the volatile species is to construct a set of five simultaneous linear equations with the mass fractions of carbon and hydrogen burnt to CO_2 , CO , HC and H_2O as the unknowns.

At any given time, the volatile composition is calculated thus:

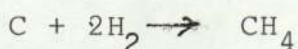
(i) The volume of carbon dioxide associated with unit mass of coal is given by

$$V_{\text{CO}_2} = 1/12 r_4 x_1 \quad (1)$$

(ii) The volume of carbon monoxide is given by

$$V_{\text{CO}} = 1/12 r_4 x_2 \quad (2)$$

(iii) The volume of HC assuming CH_4 , is derived from



Mass of H_2 that goes to $CH_4 = r_5 \times 5$

Volume of CH_4 produced for each mol of $H_2 = 1/2$ mol H_2

But molecular weight of $H_2 = 2$ kg

$$\text{kmol of } CH_4 = \frac{r_5 \times 5}{2 \text{ kg}} \text{ kg mol } H_2 \times \frac{1}{2} \text{ kmol } CH_4$$

$$V_{CH_4} = \frac{1}{4} r_5 \times 5 \quad (3)$$

(iv) The volume of water is derived:

$$V_{H_2O} = \frac{1}{2} r_5 \times 4 \quad (4)$$

(v) For nitrogen

$$V_{N_2} = 1/28 (r_2 + r_7) \quad (5)$$

(vi) For sulphur dioxide

$$V_{S_2} = 1/32 r_8 \quad (6)$$

(vii) The oxygen balance gives:

Excess $O_2 = (\text{Vol of oxygen in air + fuel}) - (\text{Vol of oxygen in } CO_2 + CO + H_2O + SO_2)$



$$VO_2 = 1/32 (r_1+r_6) - (1/12 r_4x_1 + 1/24 r_4x_2 + 1/4 r_5x_4 + 1/32 r_8)$$

(7)

The total dry gas volume is given by the sum of the constituent volumes:

$$VT = VCO_2 + VCO + VHC + VO_2 + VSO_2 + VN_2$$

$$= 1/24r_4x_2 - 1/4r_5x_4 + 1/4r_5x_5 + 1/32(r_1+r_6) + 1/28(r_2+r_7)$$

(8)

The individual fractions by volume are given by:

$$FO_2 = \frac{VO_2}{VT} \text{ etc.}$$

(9)

Thus the total mass of carbon and hydrogen consumed by chemical reaction can be obtained by solving the five equations obtained from equation (9).

These equations can be written as follows:

$$A_{ij}x_i = b_i \quad i = 1 \dots, 5 \quad (10)$$

where A_{ij} is a matrix of constants

x_i is the vector of unknown

and b_i is the measured combustion products.

The first four equations represent the element balances on the carbon, hydrogen and oxygen respectively. The values A_{ij} , $i = 1 \dots, 5$, $j = 0 \dots, 5$ therefore represent the

analysis of volatile matter species, expressed as volume of carbon dioxide, carbon monoxide, hydrocarbon and oxygen. Similarly, the values of b_i , $i = 1 \dots, 5$ represent the experimentally observed values of combustion products.

Equation five of the set is used to specify the carbon to hydrogen ratio of the hydrocarbon.

The equations can be represent in the matrix form as:

$$Ax = B \quad (11)$$

The values of the elements of the matrix A, and the vector B are calculated from the Ultimate Analysis of the coal and product of combustion.

The equations can be solved by inverting the matrix A.

$$[X] = [B][A]^{-1} \quad (12)$$

With the above set up and assumptions, the set of equations 10 can be completed and is shown in matrix form in Fig. 3.8.

The five equations are represented by the five rows of the matrix, each row comprising the coefficients of the five variables given in the column vector $[CO_2, CO, \text{etc.}]$. For example the first three equations are the carbon balances, and the entries in the first, second and third rows correspond to the carbon content of CO_2 , CO , and HC. Similarly, rows 4 and 5 represent the balances on hydrogen

contents of H_2O and HC respectively.

The solution of the above equations enables the fractions of burnt carbon to be predicted from the ultimate analysis [C,H,O,N and S] and carbon to hydrogen ratio of the coal.

$$\begin{bmatrix}
 -1/12r_4 & + 1/24r_4 & + 0 & - 1/4r_5 d_1 & + 1/4r_5 d_1 \\
 0 & + 1/24r_4 d_2 - 1/12r_4 & + 0 & - 1/4r_5 d_2 & + 1/4r_5 d_2 \\
 0 & - 1/24r_4 d_3 & + 0 & - 1/4r_5 d_3 & + 1/4r_5 d_3 \\
 1/12r_4 & + 1/24r_4 (d_4 + 1) & + 0 & - 1/4r_5 (d_4 - 1) & + 1/4r_5 d_4 \\
 0 & + 0 & - r_4 & + 0 & + r_5 (d_5 + 3)
 \end{bmatrix}
 \cdot
 \begin{bmatrix}
 x_1 \\
 x_2 \\
 x_3 \\
 x_4 \\
 x_5
 \end{bmatrix}
 =
 \begin{bmatrix}
 b_1 \\
 b_2 \\
 b_3 \\
 b_4 \\
 b_5
 \end{bmatrix}
 -
 \begin{bmatrix}
 1/32d_1 (r_1 + r_6) & + 1/28d_1 (r_2 + r_7) \\
 1/32d_2 (r_1 + r_6) & + 1/28d_2 (r_2 + r_7) \\
 1/32d_3 (r_1 + r_6) & + 1/28d_3 (r_2 + r_7) \\
 1/32 (r_1 + r_6)(d_4 - 1) & + 1/28d_4 (r_2 + r_7) + 1/32r_8 \\
 0 &
 \end{bmatrix}$$

NOTE : r_1, r_2, r_4 to r_6 are the mass of oxygen, nitrogen, carbon, hydrogen, oxygen, nitrogen and sulphur in the air and fuel respectively (dmmf)

d_1 to d_4 are the volume fraction of CO_2, CO, HC and O_2 in the dry products.

d_5 is the ratio by mass of carbon to hydrogen of the fuel

FIG. 3.8 SET OF LINEAR EQUATION FOR PREDICTING THE FRACTIONS OF BURNT CARBON AND HYDROGEN IN THE FUEL

3.5.3. Theoretical Investigation

The mathematical model for volatile matter combustion described in the previous sections is applicable to a fluidized bed of fixed height and having a constant cross-sectional area. For this type of combustor operating for a given feed rate of coal and fluidizing air, the model presented here can predict the following

- (1) the fraction of burnt carbon.
- (2) the fraction of burnt hydrogen.

The calculations described according to the mathematical model developed here will employ the parameter values given in Tables 3.5 and 3.6. The values of r used in the matrix are calculated as given in appendix E. The matrix computations are shown as printout in Table E2. page 228

Ultimate Analysis %		Proximate Analysis %	
Carbon	77.4	Moisture	5.1
Hydrogen	5.1	Volatile	35
Nitrogen	6.1	Ash	5.4
Sulphur	1.6		
Oxygen	4.4		

CHARACTERISTICS OF COAL USED.

TABLE 3.5

CO ₂	0.100495245138
CO	5.5830691743 x 10 ⁻³
HC	8.37471917380 x 10 ⁻⁴
O ₂	8.92783607438 x 10 ⁻²
H ₂ O	0

THEORETICAL VALUES OF PRODUCTS OF COMBUSTION

TABLE 3.6

x ₁ of C converted to	CO ₂	=	0.8999281143
x ₂ of C converted to	CO	=	0.0499960063016
x ₃ of C converted to	HC	=	0.00749920431601
x ₄ of H ₂ converted to	H ₂ O	=	0.91566059794
x ₅ of H ₂ converted to	HC	=	0.0379371512457
Unburnt Carbon		=	0.042576675952

FRACTION OF CARBON AND HYDROGEN CONVERTED AND UNBURNT CARBON

TABLE 3.7

3.5.4 VALIDATION OF THE MODEL

In order to validate the model, experiments were carried out in a 0.254 m diameter steel combustor. The combustor used

inert silica sand sized 500 μm to 355 μm as the bed material, fluidizing air was introduced via a ceramic tile distributor. Preheating of the bed was achieved by premixed air and propane gas which raised the temperature to the required temperature of 1173 K. The crushed coal of 1.67 mm was fed from the above into the bed.

Once the steady state conditions were established, measurements of bed freeboard and exhaust temperatures and the gas concentrations in the flue at the freeboard were made.

Experimental runs were carried out for a period of 1.5 to 1.75 hours. The ultimate and proximate analysis of the coal were shown in Table 3.8. The range of operating conditions used were, excess air levels from 50% to 55%, temperature from 850°C to 930°C. The fluidizing velocity was constant at 0.35 m/s, the static bed height was 100 mm.

3.5.4.1 EXPERIMENTAL RESULT AND DISCUSSIONS

The parameters needed for the numerical calculations of the elements of matrix A on the computer were obtained and entered into the computer. The value of HC was assumed since it was not measured.

The products of combustion as used in the matrix and the output from the computer of the fractions of carbon and hydrogen burnt to CO_2 , CO, HC and H_2O are shown in Tables 3.9 and 3.10 respectively.

It can be seen from Table 3.10 that increase in the amount of excess air affects both the combustion of carbon and hydrogen.

More hydrogen is being ^{oxidized} to H₂O in preference to carbon.

The increase in unburnt carbon and the decrease in the amount of carbon burnt to CO₂ in Table 3.10 prove this. This led to the explanation that there is a ^{preferential reaction} for the oxygen in the air between the two constituents of the coal, and hydrogen, ^{reaction} having the faster of the two, gets the oxygen first and is burnt to water.

Comparisons of the theoretical results with this limited experimental data for Daw Mill coal show that the predicted yields of carbon converted to carbon dioxide, carbon monoxide and hydrocarbon are in good agreement with the experimental yields. However, comparison for the yields of hydrogen converted to water and hydrocarbon are not favourable. Reliable determination of hydrocarbon gas from the flue was difficult due to the limitation of the hydrocarbon gas analyser.

3.5.5 CONCLUSIONS

In the proposed model, coal is used and the concentrations vary with the type and origin of the coal. Available analytical data were not sufficient to determine all the concentrations and had to be supplemented by assigned parameters on the basis of assumptions or treated as

adjustable parameters.

In view of the several adjustable parameters employed, the comparison given between the theoretical analysis and limited experimental data is not intended to show the validity of the assumptions used in the model; on the contrary, its ability to describe the experimental trends is shown, and is believed to be significant. In particular, the model attempts to quantify the likely conversion of carbon and hydrogen to hydrocarbon, which could be of considerable help to reactor designer.

In its present state, the model should not be considered as final and ready for use but rather as a source of information on various analytical techniques that may be combined in models. Further work should be directed towards improvement.

Ultimate % Analysis		Proximate % Analysis	
Carbon	83.6	Moisture	7.9
Hydrogen	5.5	Volatile Matter	35.0
Nitrogen	1.2	Ash	5.4
Sulphur	0.9		
Oxygen	8.8		

CHARACTERISTICS OF COAL USED: BITUMINOUS COAL, DAW MILL COLLIERY

TABLE 3.8

	RUN 1	RUN 2
Excess air %	29.5	43
CO ₂	0.105	0.09
CO	0.0011	0
HC	0.001	0.001
O ₂	0.085	0.09
H ₂ O	0	0

PRODUCTS OF COMBUSTION

TABLE 3.9

	RUN 1	RUN 2
x ₁ of C - CO ₂	0.97698	0.82516
x ₂ of C - CO	0.01024	0
x ₃ of C - HC	0.00930	0.00917
x ₄ of H ₂ - H ₂ O	1.25119	1.87273
x ₅ of H ₂ - HC	0.04714	0.04645
Unburnt Carbon	0.00348	0.16568

FRACTION OF CARBON AND HYDROGEN CONVERTED AND UNBURNT CARBON

TABLE 3.10

CHAPTER FOUR

4. DEVOLATIZATION RATES OF COAL PARTICLES IN SHALLOW FLUIDIZED BEDS

4.1. Introduction

Combustion experiments with batch charges of coal particles of different size ranges and mass, to determine devolatilization rates of coal are described in this section.

Rate of devolatilization of charge was obtained by.

- (i) Visual observation.
- (ii) Continuous recording of bed temperature against time.

The influence of the following variables on devolatilization rate was explored.

- (1) Coal particle size over the range 1-2 mm.
Mean diameter 1 mm.
Batch sizes 3, 10, 20, 30 grams.
- (2) Bed temperature over the range 800-900°C.
- (3) Inert particle size over the range 355-850µm.
- (4) Bed diameter 0.254 m.
- (5) Bed static depth 50 mm.

4.2. Experimental Equipment

4.2.1. Experimental Fluidized Bed Combustor

The fluidized bed combustor Fig. 4.1. consisted of a refractory lined steel cylinder of approximately 0.254 m

internal diameter and 1.2 m in height. The porous distributor plate was made of ceramic and the bed material was closely graded sand with particles of mean diameter 549.3 μ m and size range 355 to 850 μ m.

4.2.2. Fluidizing Gas

Air was used as fluidizing gas. A calibrated rotameter (metric sizes tube, size 65 Aluminium float; supplied by Rotameter Manufacturing Company Ltd, Croydon, England) was used to measure the air flow rate.

4.3. Rate of Devolatization Experiments - Test Procedure

At the beginning of each experimental run, about 1,414 grams of sand particles of a particular size range were placed into the bed to obtain a static bed depth of 50 mm. The bed was fluidized with air; propane gas premixed with the air was used to light up and heat the bed to the required temperature (800 - 900 C). When the bed approached this temperature, the air flow rate was adjusted to obtain a particular fluidizing velocity and the gas flow rate was finally adjusted to keep the bed at the required steady temperature. The bed reached a steady state in about 45 minutes.

4.3.1. Batch Burning Experiments

Batch burning experiments were done in order

(a) To establish the amount of fuel required to reside in the bed (and in freeboard) to meet the output. For example, if 2.5 kW output is required then, conceptually,

(1) Number of carbon particles in bed
x the burning rate of 1 particle
(kg/s) x Calorific value of carbon
= Rate of heat release in the bed.

(2) EITHER Mass of Volatiles
in freeboard x

Burning rate
of volatiles x

Calorific value
of volatiles

= Rate of heat release in free-
board zone.

OR Rate of emission of volatiles
(kg/s) x Calorific Value of
volatiles.

= Rate of heat release in free-
board zone.

Hence addition of (1) + (2) will give 2.5 kW.

(b) To establish bed (and freeboard) temperature history during changes in fuelling rate.

When the bed was running steadily, a weighed amount of coal particles of a particular size range was dropped into the bed from the top and two stop watches were started

simultaneously. Prior to dropping the batch charge, the recorder for recording the bed temperature was started. The recorder was set to the speed of 25 mm per minute. Immediately after the charge was dropped into the bed, smoky yellow flames appeared at the top of the bubbling bed indicating the burning of volatile matter. This lasted for about 10 to 52 seconds depending on the coal particle size, charge mass, bed temperature, inert particle size and superficial fluidizing velocity used. The flame was initially tall about 300 mm high, but decreased gradually in height as evolution and combustion of volatile matter slowed down, finally disappearing at completion of volatile evolutions and combustion. This data was used to calculate the rate of heat release from the volatiles.

4.3.2. Devolatilisation Rate Experiments; Results and Discussion

The burning rate and specific emission rate at various bed temperatures are shown in Fig. 4.4. for different design operating conditions of the bed.

The data were found to be substantially affected by bed temperature and mass charge, which are discussed below.

4.3.2.1. Effect of Bed Temperature

The variation of burning rate and specific emission rate of volatiles at bed temperatures of 800°C and 900°C is shown in Fig. 4.4. The results show that the burning rate and specific emission rate increase substantially with bed temperature.

This suggests that the increased agitation in the bed arising from the increase in bubble frequency, due to higher superficial fluidizing velocity and also the higher rate of energy transfer from the bed to the fuel charge at the higher superficial velocity caused faster emission of volatiles of the batch charge.

4.3.2.2. Effect of Charge Mass

The burning rate of volatiles of batch charge always increased with the mass charge of the coal, Fig.4.4, but the specific emission rate decreased with increase in mass charge of coal.

This increase in the burning rate is due to the increase in the number of coal particles in the bed, as shown in Table 4.1. below. This exposes more active surface area and hence consumes an increasing amount of oxygen available. The decrease in the specific burning rate kg/m^2 may be due to the large surface area with lower average oxygen concentration in the bed.

Volatile Matter (%)	37 754.3 mm Hg 23.5 °C 800 °C					37 758.5 mm Hg 23.5 °C 900 °C				
	3	10	20	30	50	3	10	20	30	50
Barometric Pressure										
Ambient Temperature										
Bed Temperature										
Mass charge of coal particles (g)	3	10	20	30	50	3	10	20	30	50
Mass of volatiles (g)	1.11	3.7	7.4	11.1	18.5	1.11	3.7	7.4	11.1	18.5
Time for Volatiles to burn (s)	19.5	20	20	21.5	52.5	7	11	10.2	16.5	52.5
Burning Rate of Volatiles (g/s)	0.057	0.185	0.37	0.516	0.352	0.159	0.336	0.725	0.673	0.352
Specific Emission Rate (g/am ²)	12.67	12.33	12.37	11.49	4.69	35.34	22.4	24.25	14.99	4.69
Gas flow rate (L/min)	9.71	9.71	9.71	9.71	9.71	10.75	9.71	9.71	9.71	9.71
Air flow rate L/min	361.9	361.9	361.9	361.9	361.9	364.2	364.2	364.2	364.2	364.2
A/F Ratio	37.3	37.3	37.3	37.3	37.3	33.9	37.5	37.5	37.5	37.5
A/F Ratio (Stoichiometric)	23.80	23.8	23.8	23.8	23.8	23.8	23.8	23.8	23.8	23.8
Excess air (%)	36.2	36.2	36.2	36.2	36.2	29.8	36.5	36.5	36.5	36.5
Exhaust Temp. before combustion (°C)	248	230	280	230	280	460	240	300	320	300
Exhaust Temp. after combustion (°C)	430	300	380	450	510	500	300	400	550	600
Fluidizing Velocity (m/s)	0.44					0.49				

TABLE 4.1 EXPERIMENTAL RESULTS OF BATCH CHARGE OF COAL PARTICLES AT BED TEMPERATURES OF 800 & 900 °C

CONCLUSION

The experimental investigations made so far show that volatiles burn at the freeboard zone and that the heat released by combustion of volatiles is about half of the total heat released from the raw coal. Most of this is released in the freeboard zone. It should be possible to put extra heat transfer surfaces in the freeboard zone and less in the bed provided that heat extracted by these surfaces does not lead to quenching of combustion and hence large amounts of unburnt fuel.

4.5. DEVELOPMENT OF PLUME OF VOLATILES

A well designed fluidized bed-combustor should

- (i) operate with a minimum of excess air,
- (ii) reduce pollution,
- (iii) reduce loss of unburned coal.

In order to compromise with all the above requirements in different fluidized bed combustor designs, it is necessary to have a model to predict bed operating conditions. In the development of such a model, one should have a pictorial assessment ^{of events} occurring in the bed. Such a picture includes the flow of gases and solids in the bed, coal devolatilization, attrition of solids in the bed, the elutriation of unburnt chars and bed inert particles, solid to gas reaction and gas to gas reaction within and above the bed.

Since a general model to incorporate all these features is too complex and difficult to use, a simplified practical

model is now proposed. The interest of this present work is limited to the devolatilisation of coal.

4.5.1. Plume Model

Because models of fluidized bed coal combustion that have been developed so far differ according to the combination of assumptions they make, here a plume model is proposed which gives the general pictorial features of fluidized bed combustion of volatiles.

4.5.2. Assumptions of the Plume Model

The main assumptions of the plume model are as follows:

- (1) The gas flow is plug flow.
- (2) Devolatilization is instantaneous at the coal feed point to give a plume of unburnt combustible gases which rises through the bed at the velocity of the surrounding gas.
- (3) The unburnt volatiles in the plume mix with air at the freeboard region to burn completely.
- (4) The devolatilized solids mix well throughout the bed and burn everywhere in the bed except in the plume.
- (5) The plume and bed temperatures are uniform throughout.

Typical  profile of volatiles emitted by a mechanically restrained coal particle in the plume is shown

in Fig. 4.2.

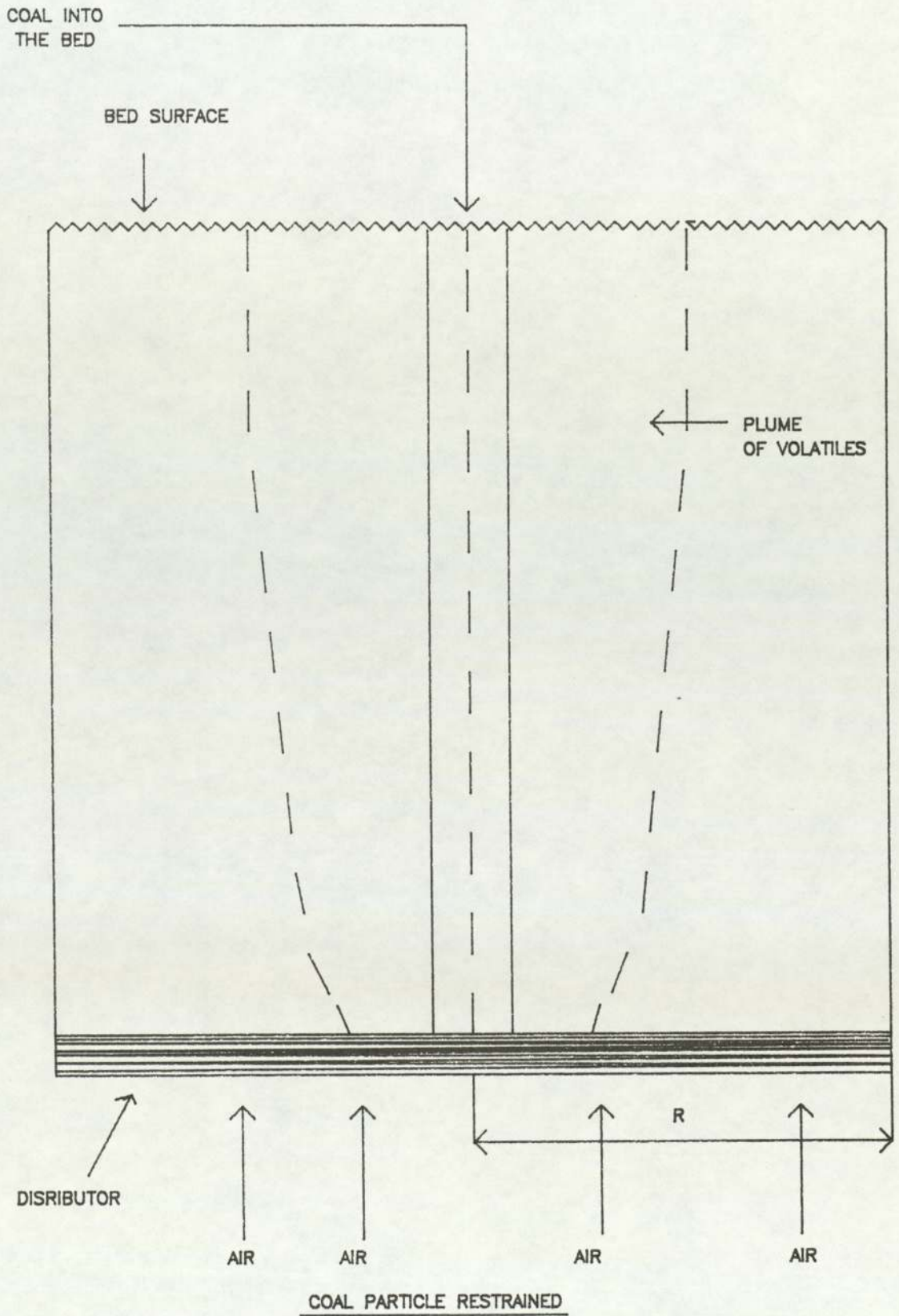


FIG.4.2 TYPICAL PROFILE OF VOLATILES IN THE PLUME

Upon entering the bed, the coal devolatilizes and, once devolatilized, undergoes char combustion. Therefore, depending on comparative devolatilization and mixing times, regions of fuel (volatiles) rich gas may exist in the vicinity of the injected coal, giving rise to combustion.

Whether or not combustion occurs depends on how the volatiles are transported within the bed as they are formed.

Some understanding of volatiles transport is provided by the experiments of Jovanovic(71) who determined the gas flow patterns associated with the slow bubble regime. Those experiments show that a tracer gas injected at the bottom of a large-particle bed rises as a plume. Though this is contrary to the observations in vigorously bubbling small-particle beds, the results suggest that the volatiles will rise as plumes with the same velocity as the fluidizing air. Thus a plume of volatiles is envisaged as rising from each coal entry port and burning in a diffusion flame with the surrounding oxygen at the plume boundary as depicted in Fig. 4.2. This combustion of volatiles, accounting for as much as 50 per cent of the coal heating value, can be completed either in the bed or, if the plume breaks through the bed surface, in the freeboard as suggested by Park et al (60) in an explanation of widely varying freeboard species measurements. The latter circumstance results in an abrupt temperature jump in the gas space above the bed. Volatiles combustion may therefore lead to depletion of oxygen in the bed and will thus have a direct bearing on the rate of combustion of the char in the bed.

However, little experimental data have yet been published with which to test the plume model.

4.6. EXPERIMENTS TO OBTAIN BETTER INSIGHT INTO MIXING OF VOLATILES WITH COMBUSTION AIR IN ABOVE BED REGION

4.6.1. Introduction

In order to obtain better insight into the mixing of volatiles with combustion air in ^{the} above-bed region, experiments were conducted with ^{subliming} blocks of solid CO₂ in air in a fluidized bed at ambient temperature and bed temperature of 900° C respectively.

Although the physical properties (density, conductivity etc.) of ^{solid} CO₂ and coal differ, CO₂ block was used because it could give an easily detectable and quick assessment of the air/volatiles mixing pattern, which can then be related to the combustion of volatiles in the freeboard zone.

Four water-cooled gas sampling probes were placed at the heights of 152.4, 304.8, 457.2 and 609.6 mm above the bed. Each probe was connected to a selector valve which could direct sampled gas from each probe to an Infra Red gas analyser. A chart recorder was used to record the concentrations of CO₂ sampled by each probe during the time the CO₂ block sublimed. Two tests were done; namely in a bed fluidized at ambient temperature and a bed in which premixed propane and air was burnt.

4.6.2. Cold bed test with solid CO₂ block-free and restrained in the bed

The bed was fluidized with air at room temperature i.e. 20° C and when the bed became steady, approximately 25.4 mm diameter of solid block of CO₂ was dropped into the centre of the bed and later into the 38.1 x 38.1 mm stainless steel wire mesh basket already hung into the centre of the bed from above.

Concentrations of CO₂ were measured at 7 different transverse locations in the freeboard at 4 axial locations. This was done in two separate conditions of motion of the CO₂ block,

- (a) restrained in a basket and
- (b) free to move in the bed.

4.6.3. Results and Discussion sublimation

The results of ^{sublimation} of solid blocks of CO₂ in combustion air were analysed. To analyse the data, calibration curves were first used to convert chart readings and then average concentrations were calculated.

The results obtained for the two tests are discussed below. It is evident from Figs. 4.5, 4.6 and 4.13 that there are differences in patterns of concentration up the freeboard zone. These differences can only arise due to different mixing in the freeboard zone and the movement of the block in the bed.

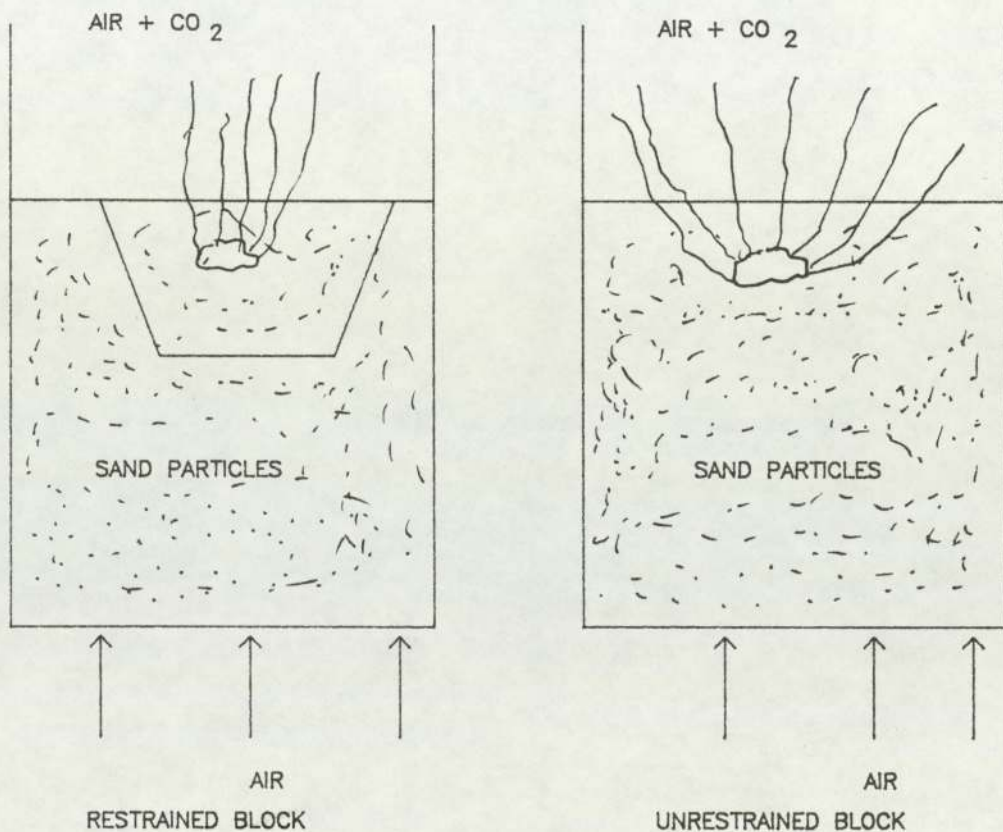


FIG. 4.3 TO SHOW QUALITATIVELY THE SIGNIFICANT DIFFERENCES IN FREEBOARD MIXING PATTERNS

Fig. 4.7 also shows that there are differences in the average concentration. The differences may be attributed to slower ^{sublimation} in the restrained block. However, lateral motion of the free block helps to distribute CO₂ across the freeboard but it has no significant effect in this present test.

It is clear that whether the CO₂ block is restrained or not, complete mixing of the emitted CO₂ with the air is not achieved in the bed. Indeed a definite "mixing length" is required in the freeboard. Therefore bed mixing when ^{the} block is free assists uniformity of CO₂ concentration in the freeboard zone.

It is implicit from these figures that the mixing length required to give uniform composition under

(a) free block conditions is about

457 mm above the bed surface and

(b) restrained block conditions is

about 610 mm above the bed surface. .

This represents a slow devolatilization case and this may set a minimum height of freeboard unless some provision is made to promote mechanical mixing of the volatiles and unburnt oxygen in the freeboard so as to reduce the height required.

In this case the flow in the freeboard region is laminar. Reynold's Number based on particle diameter is 8

4.6.4. Experiments with solid blocks of CO₂ in hot bed
-Analogous to more rapid devolatilisation

The above experiments were repeated in a gas fired fluidized bed at 900° C. The results shown in Tables 4.2A and 4.2B_A are discussed below.

From Figs. 4.9, 4.10 and 4.14 it could be seen that there was no significant effect due to positioning of solid CO₂ block. The test needs further investigation.

Figs. 4.8 and 4.12 show that (see the lateral concentration graphs) as the probe moves up the freeboard, CO₂ diffuses and mixes well with the combustion air especially with the free block. "Mixing length" agrees with the ambient temperature tests. This suggests that there is much more rapid heat input to CO₂ block when free in the bed. This is due to higher particle convective component of heat transfer when CO₂ block is totally free to move in the bed. In the restrained block case, the total surface area of the CO₂ block is not exposed to the sand and also particle convection partly suppressed by screening effect of gauze basket. However, there are errors though small, in data processing to averaging ^e_A the concentration time curves; mass balance closes well for the freeblock case but less completely with restrained block in the two experiments performed.

A question arises "Is mixing length greatly affected by rapidity of devolatilization?"

The results suggest that U/U_{mf} is approximately the same for all the tests. It has been suggested earlier (page 91) that

the flow in the above bed region is laminar, Reynold's Number is 2596. However, the effect of increasing temperature on the gas physical properties leads to a reduction in operating Reynold's Number which may be sufficient to reduce the flow condition from turbulent through transitional to laminar according to the mean bed particle size and range of operating temperature. Thus according to Botterill (4) this could be experienced with particles in the size range $3 \text{ mm} > d_p > 800 \text{ um}$ and for beds operating between ambient and 900° C .

AVERAGE COMPOSITION OF CO₂

Probe distance above the bed (m)	COLD TEST		HOT TEST	
	Freeblock	Restrained	Freeblock	Restrained
0.1524	0.203	0.203	0.133	0.165
0.3048	0.208	0.190	0.138	0.163
0.4572	0.135	0.083	0.0875	0.108
0.6096	0.175	0.145	0.100	0.110
Av. Conc.	0.180	0.160	0.120	0.140

TABLE 4.2A AVERAGE COMPOSITION OF CO₂ AT EACH LEVEL

	COLD TEST		HOT TEST	
	Freeblock	Restrained	Freeblock	Restrained
Av. Melting Time (min) (Vis. observed)	19.85	29.5	16.35	10.48
Av. Conc. of CO ₂ in air by vol.	0.136	0.1	0.243	0.379

TABLE 4.2B TIME AVERAGE CONCENTRATION OF CO₂ IN AIR BY VOLUME

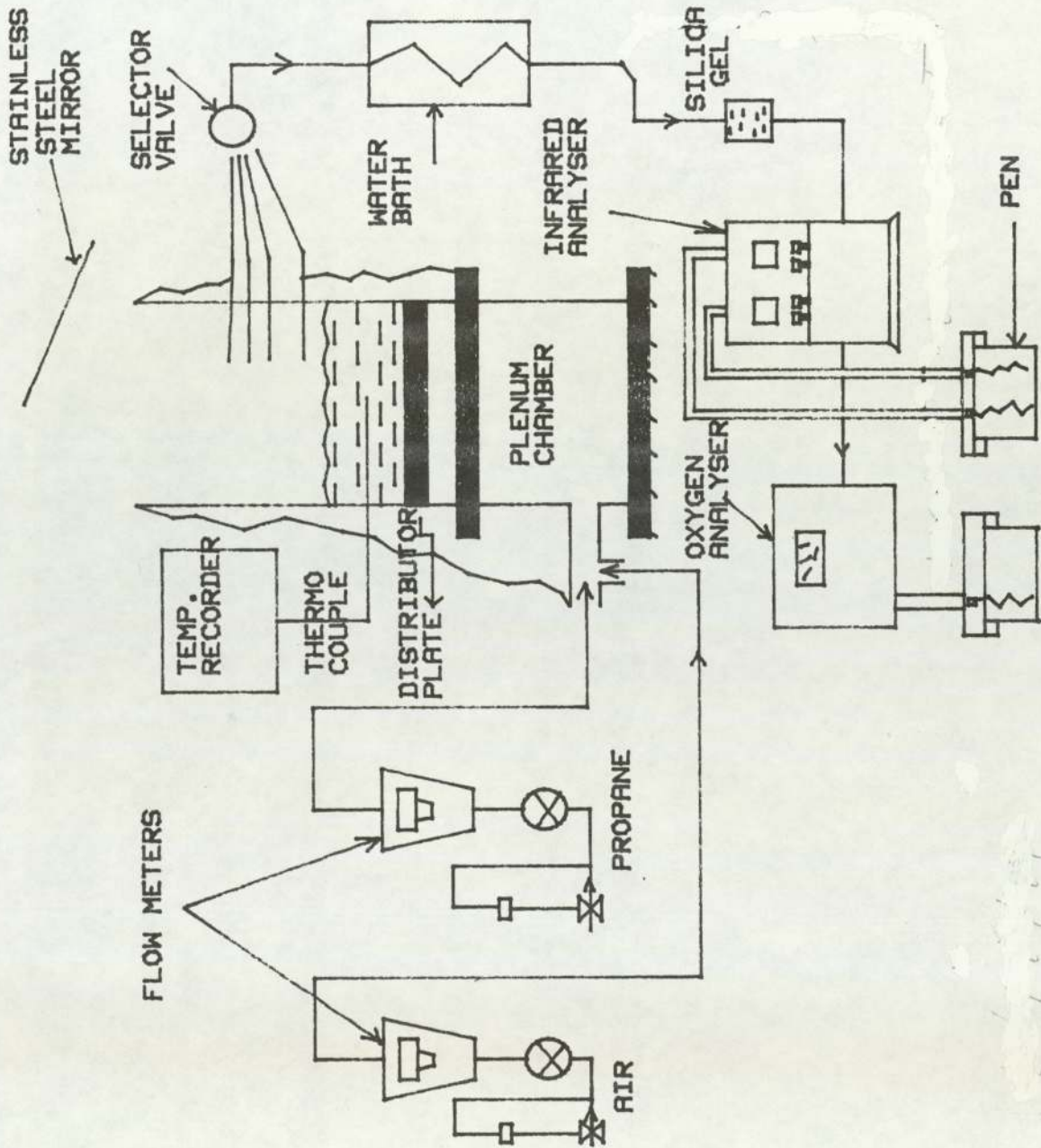


FIG. 4.1 EXPERIMENTAL FLUIDIZED BED COMBUSTOR

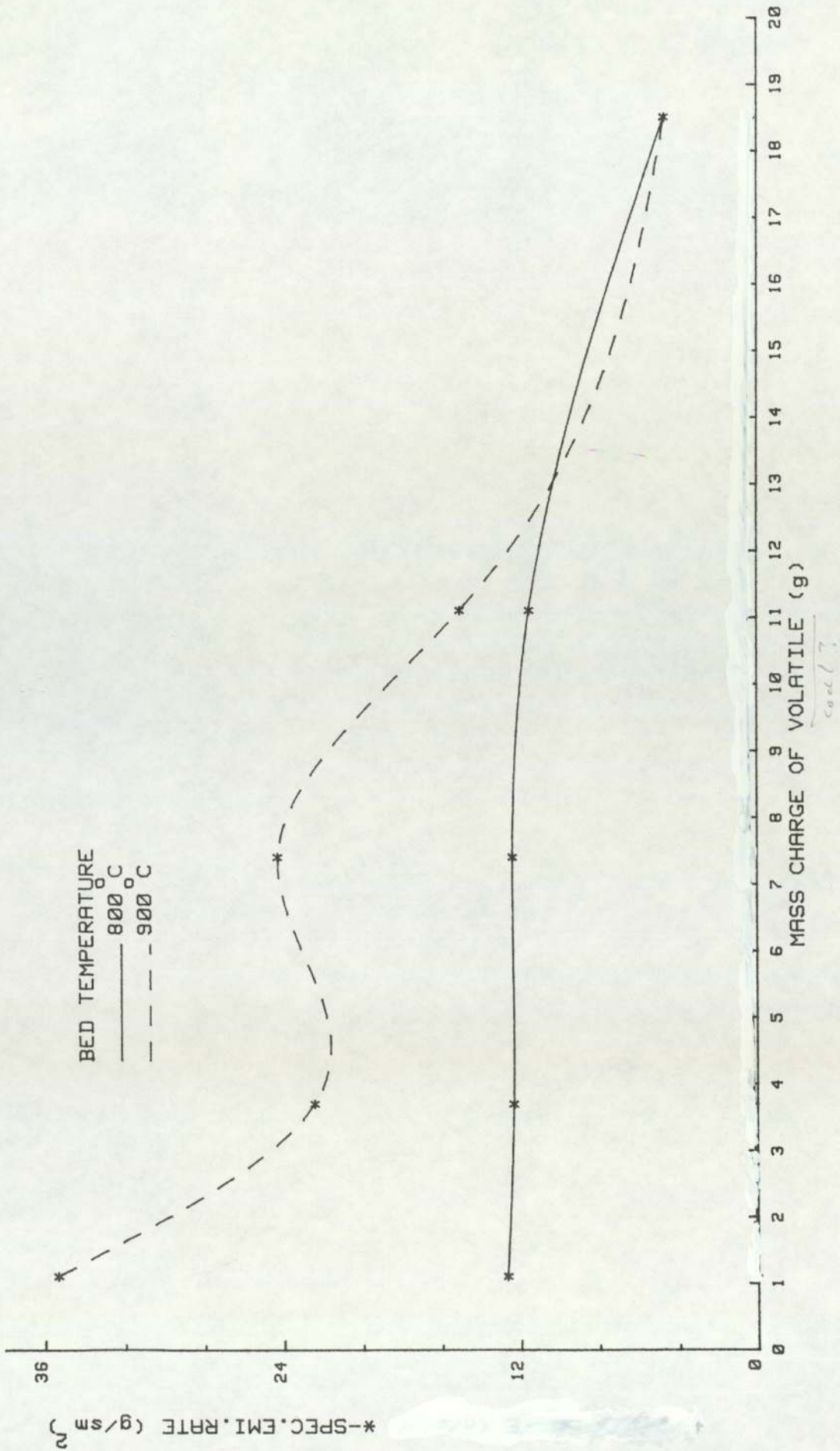


FIG.4.4 EXP.RES.OF BATCH CHARGE OF COAL PART. AT BED TEMP. 800 & 900 °C

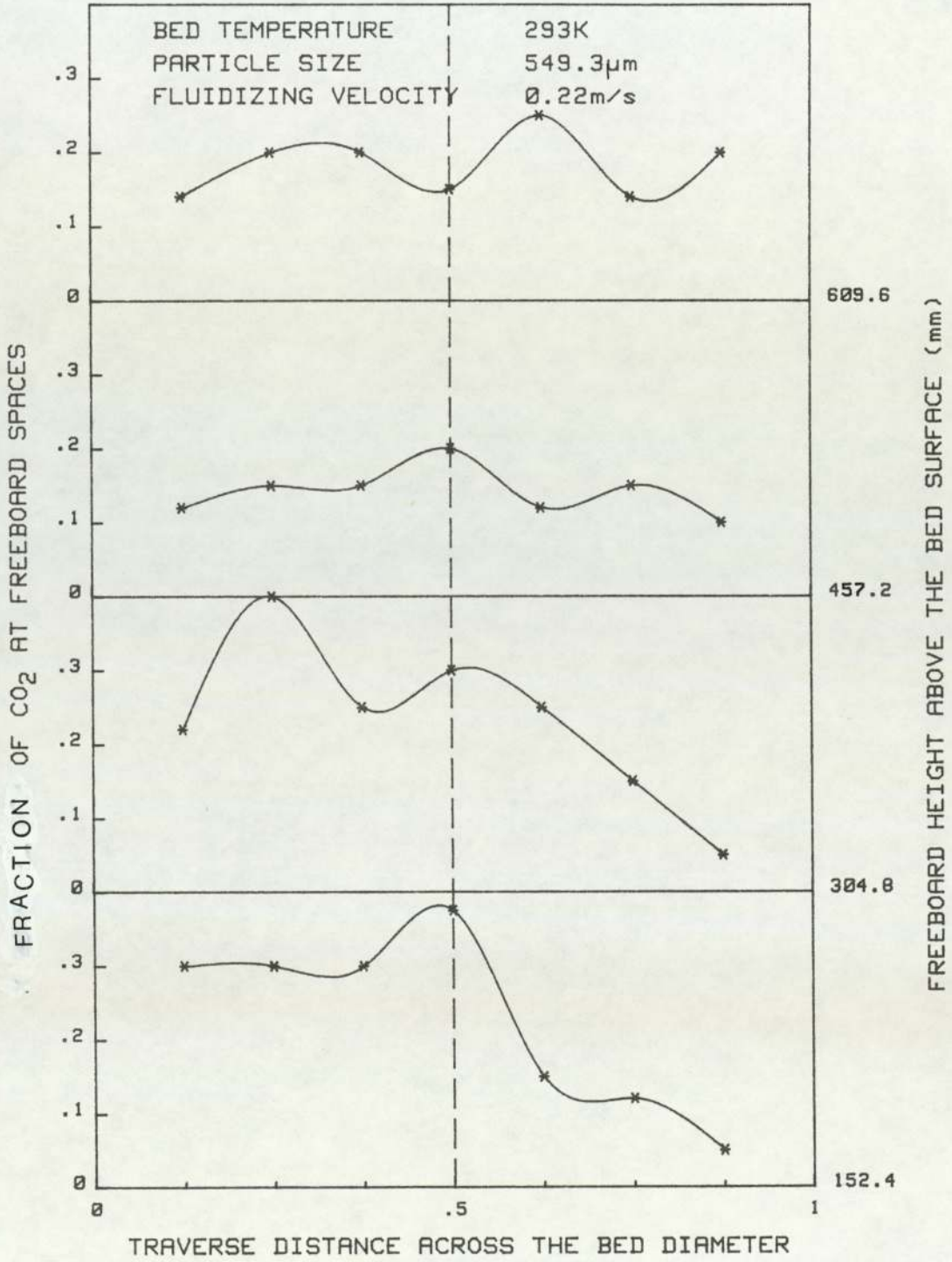


FIG.4.5 CONCENTRATION OF CO₂ AT VARIOUS FREEBOARD LEVELS WITH CO₂ BLOCK UNRESTRAINED

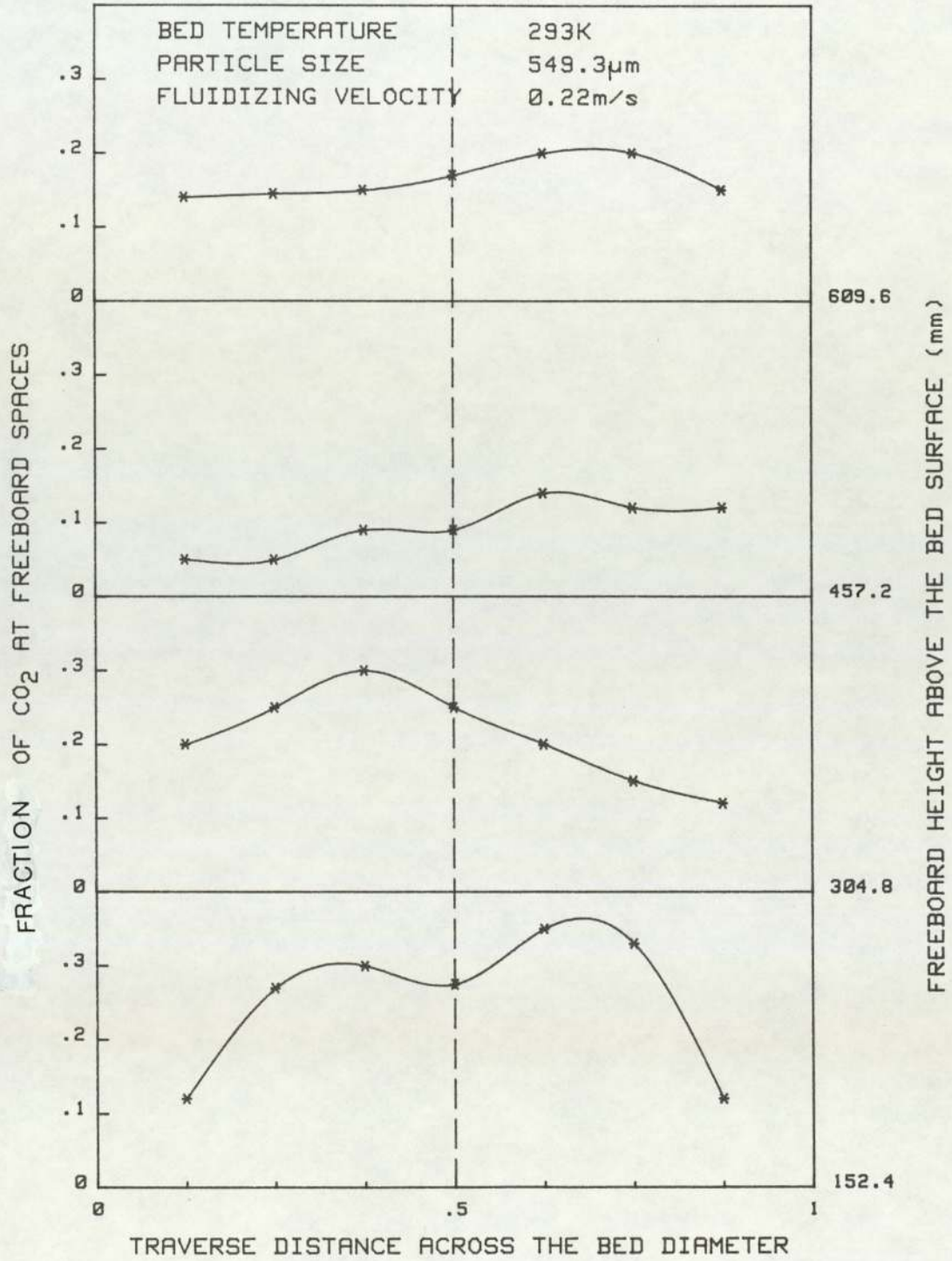


FIG.4.6 CONCENTRATION OF CO₂ AT VARIOUS FREEBOARD LEVELS WITH CO₂ BLOCK RESTRAINED

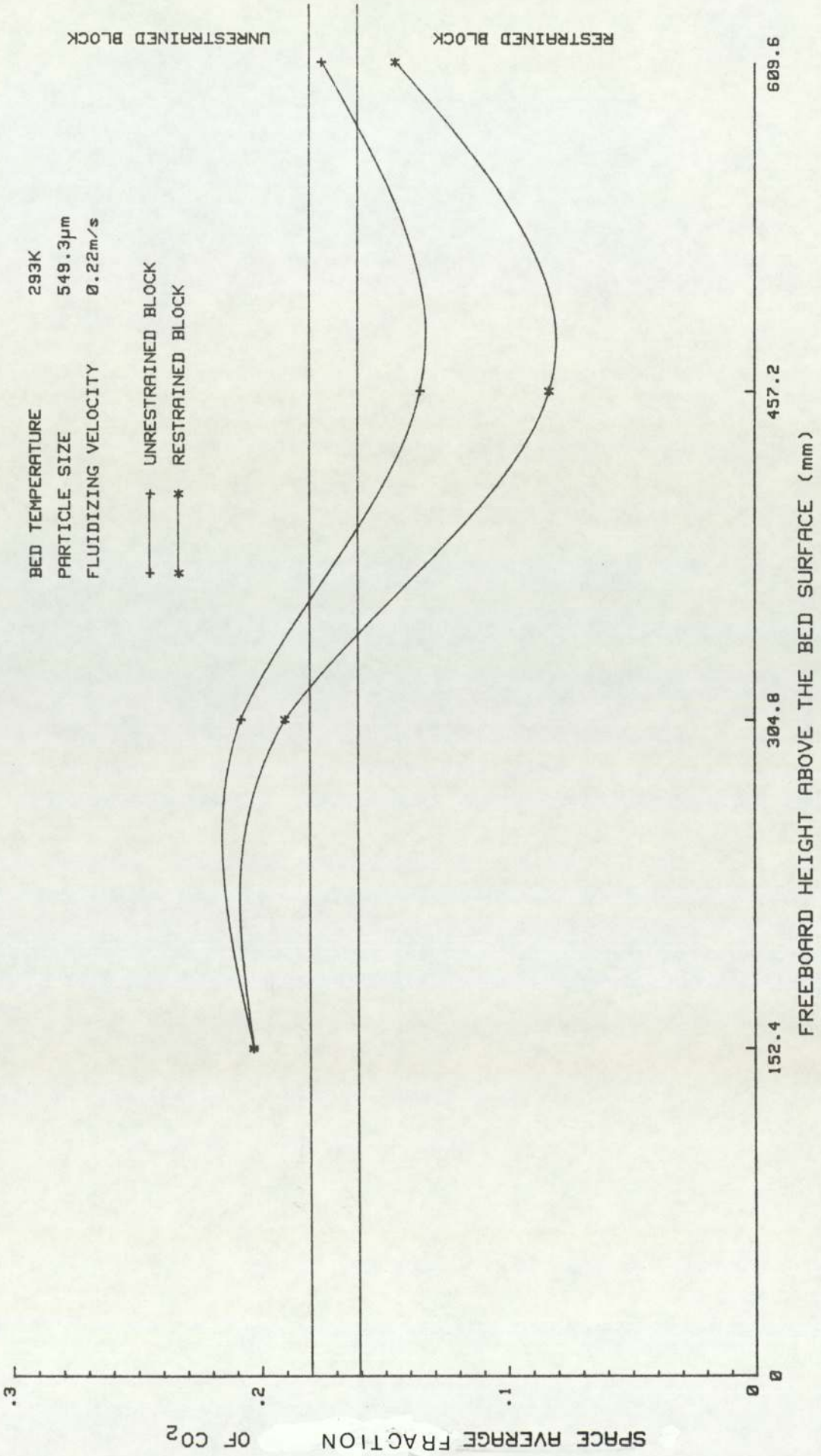


FIG. 4.7 AVERAGE FRACTION OF CO₂ AT EACH LEVEL

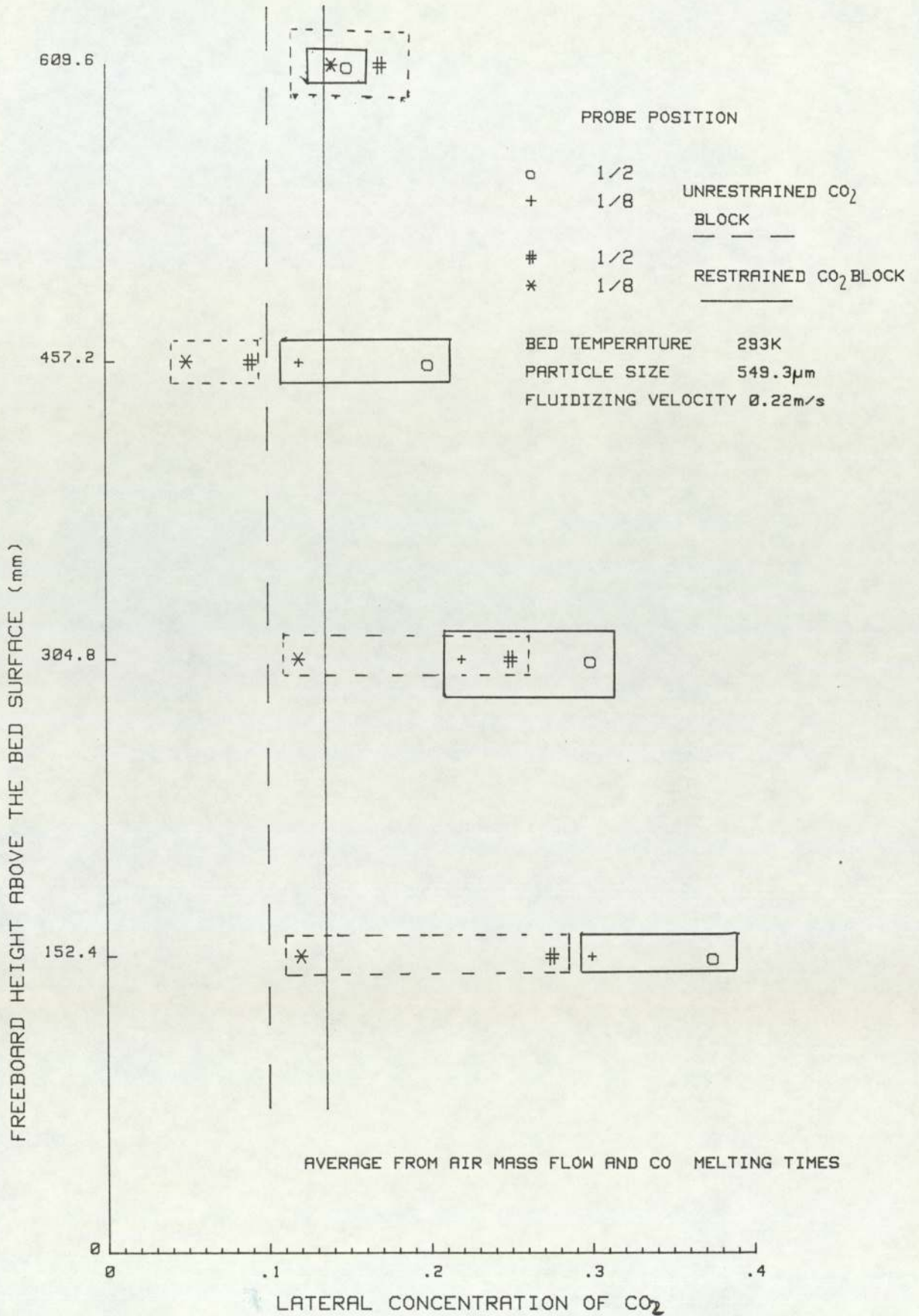


FIG. 4.8 TIME AVERAGE CONCENTRATION OF CO₂ IN AIR BY VOLUME

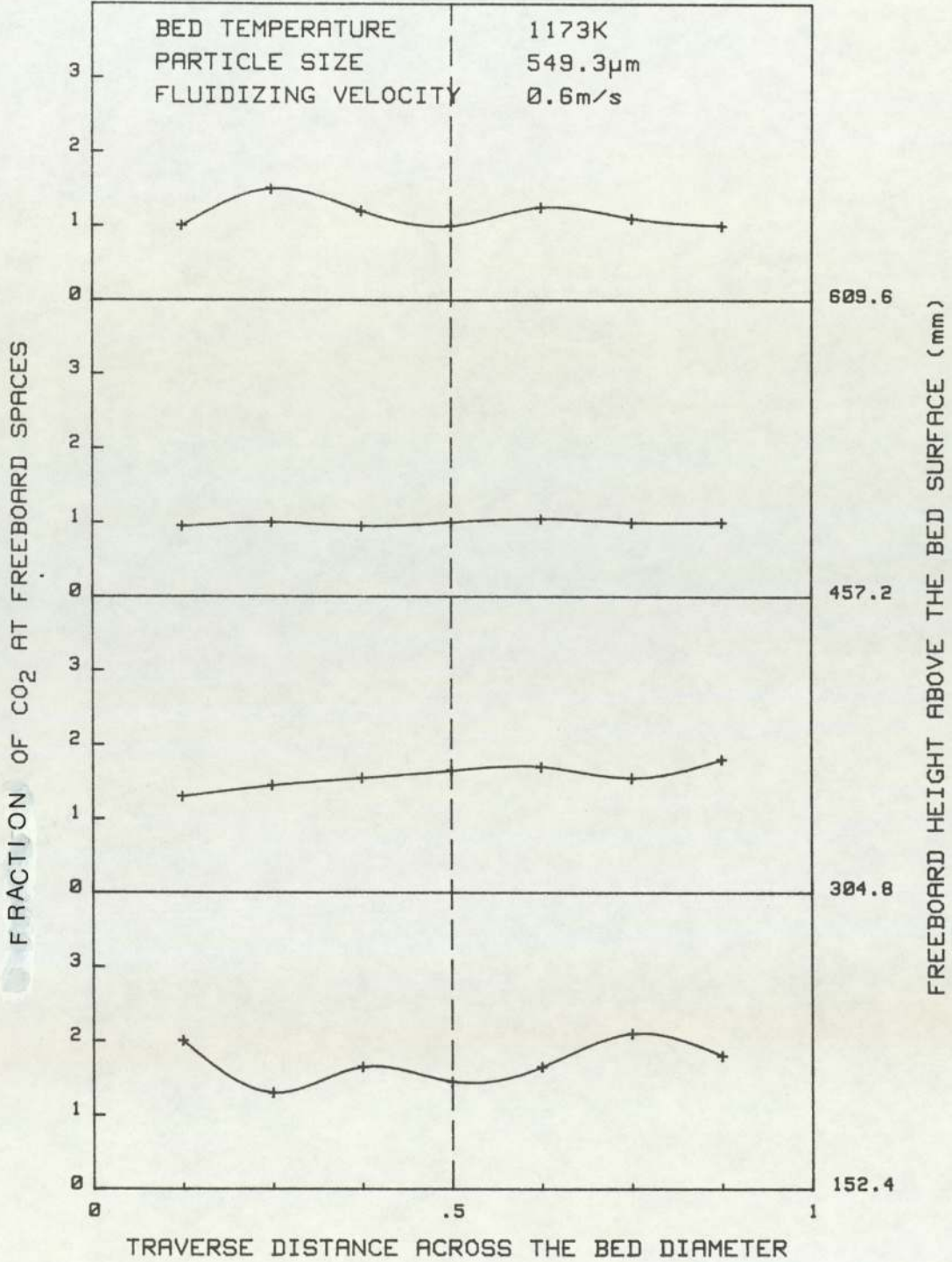


FIG.4.9 CONCENTRATION OF CO₂ AT VARIOUS FREEBOARD LEVELS WITH CO₂ BLOCK UNRESTRAINED

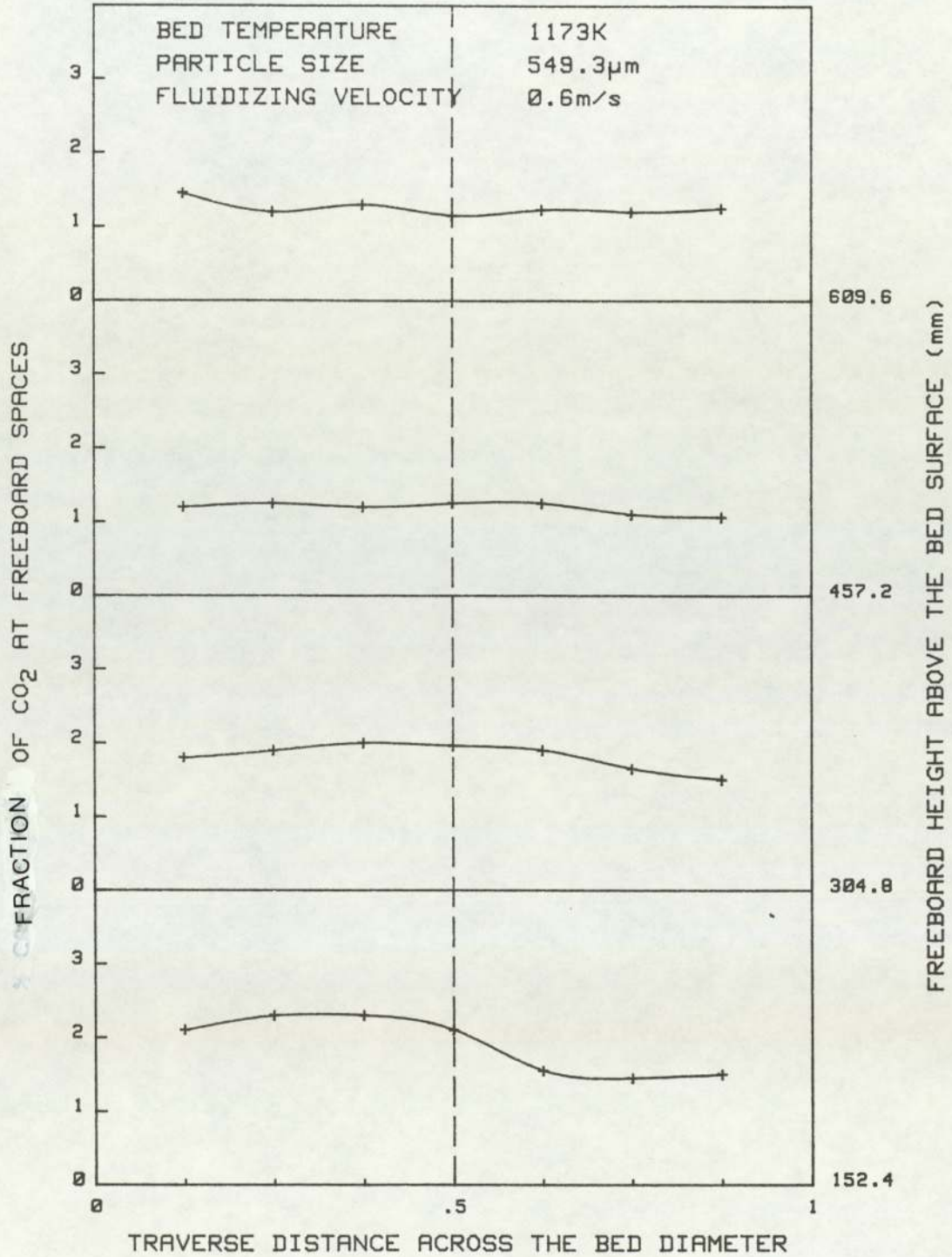


FIG.4.10 CONCENTRATION OF CO₂ AT VARIOUS FREEBOARD LEVELS WITH CO₂ BLOCK RESTRAINED

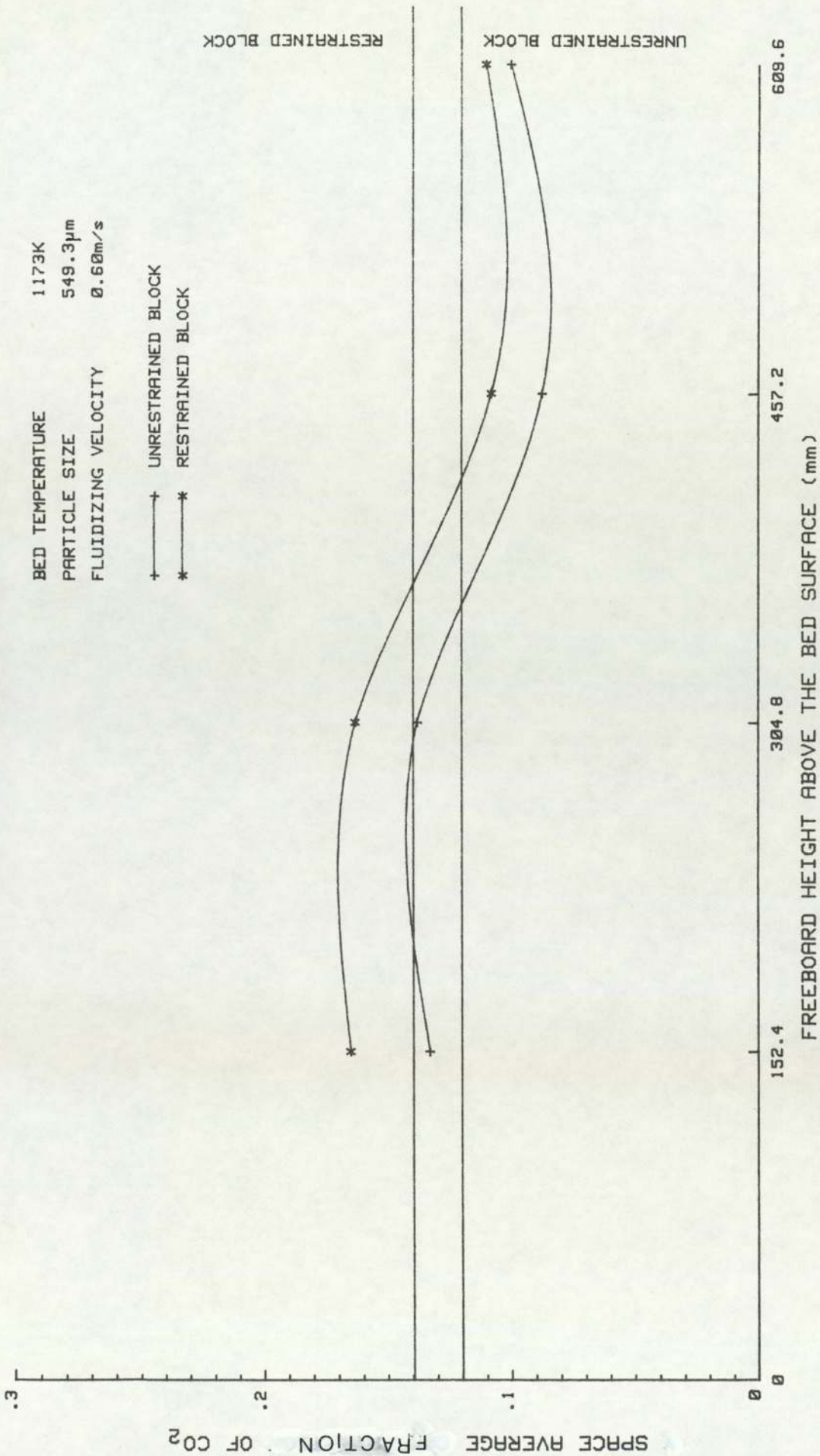


FIG.4.11 AVERAGE FRACTION OF CO₂ AT EACH LEVEL

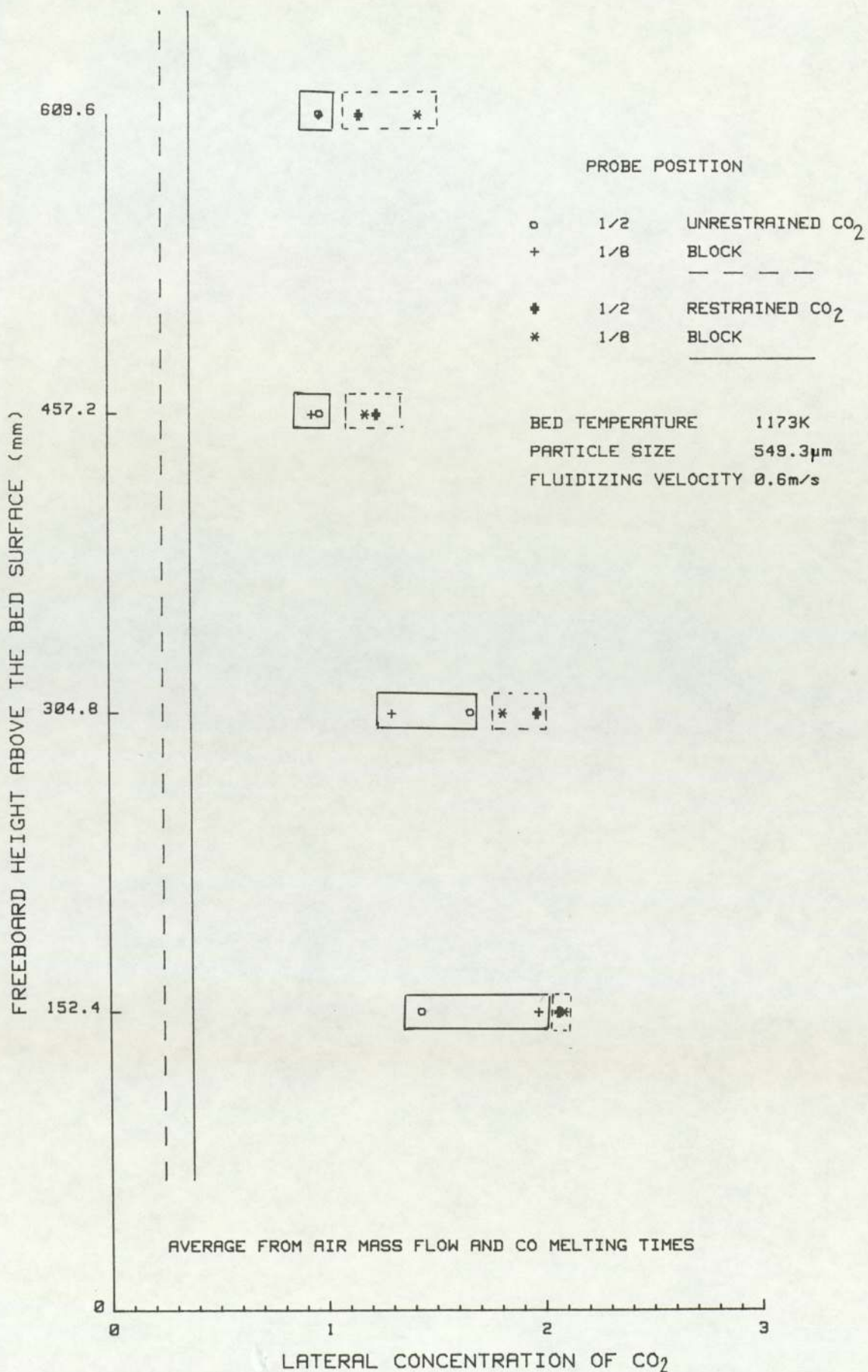


FIG. 4.12 TIME AVERAGE CONCENTRATION OF CO₂ IN AIR BY VOLUME

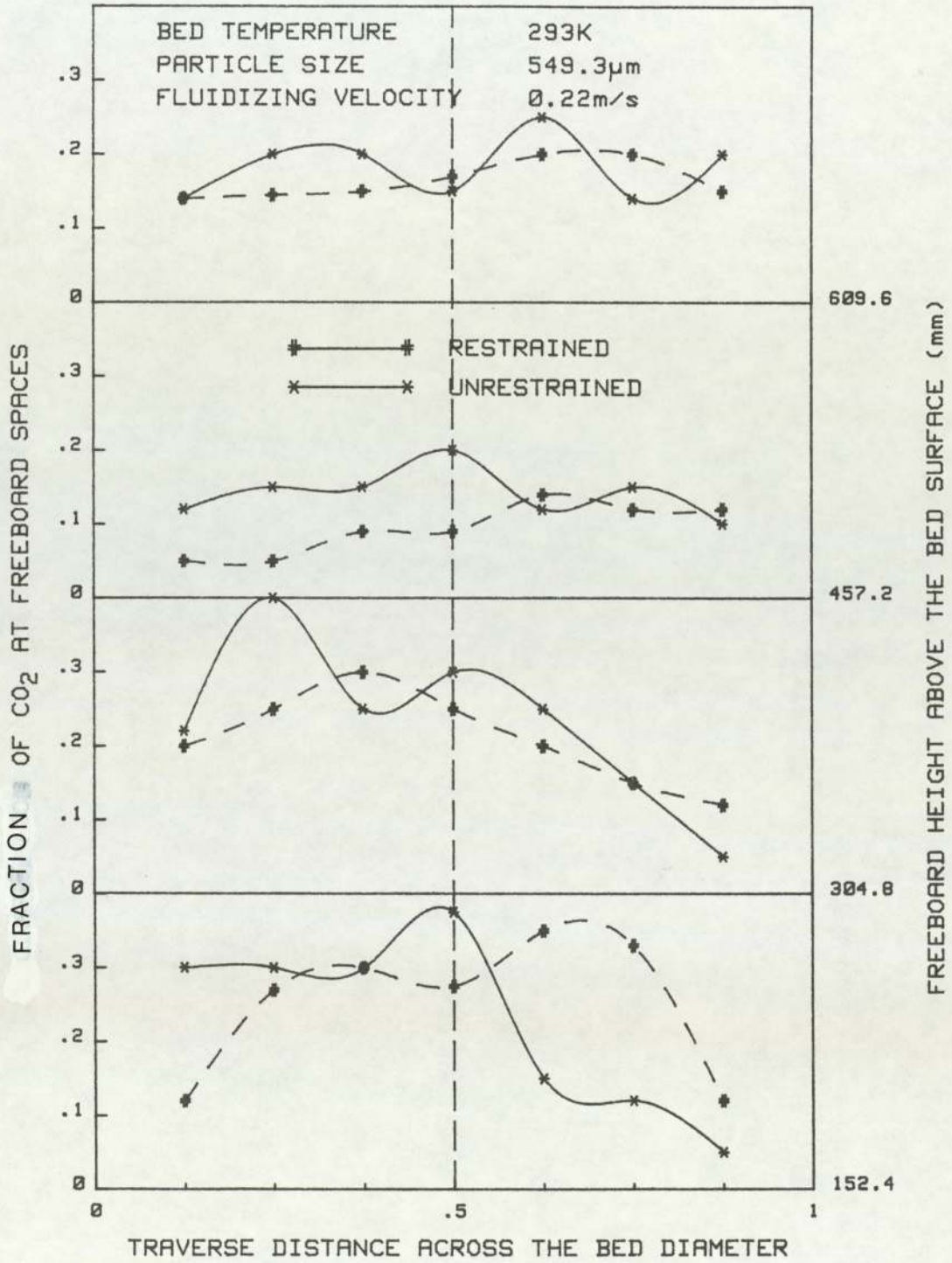


FIG.4.13 COMP.BETWEEN RESTRAINED WITH UNRESTRAINED BLOCK OF CO₂ (SAME BED TEMPERATURE)

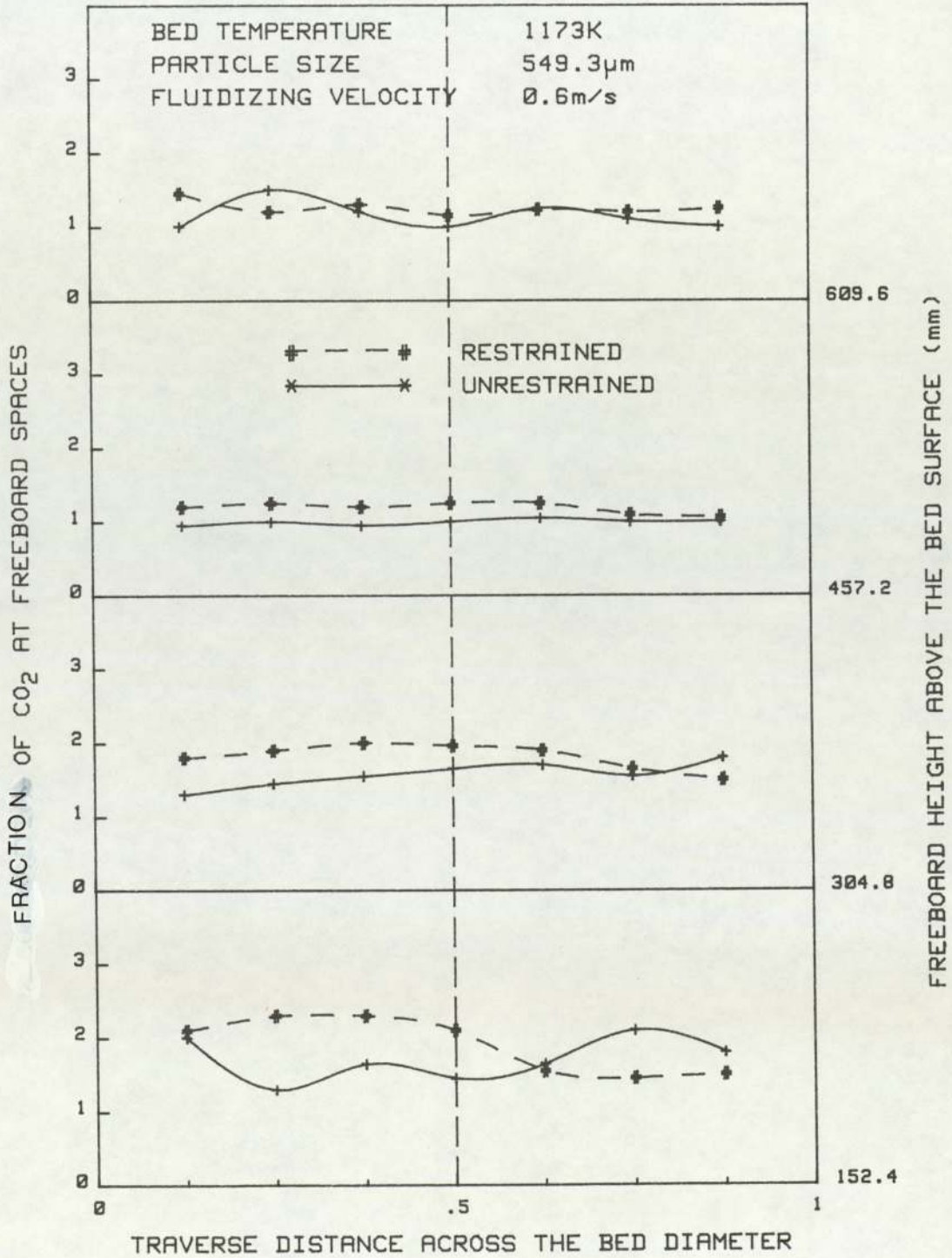


FIG. 4.14 COMPARISON BETWEEN RESTRAINED WITH UNRESTRAINED BLOCK OF CO₂ (SAME BED TEMP.)

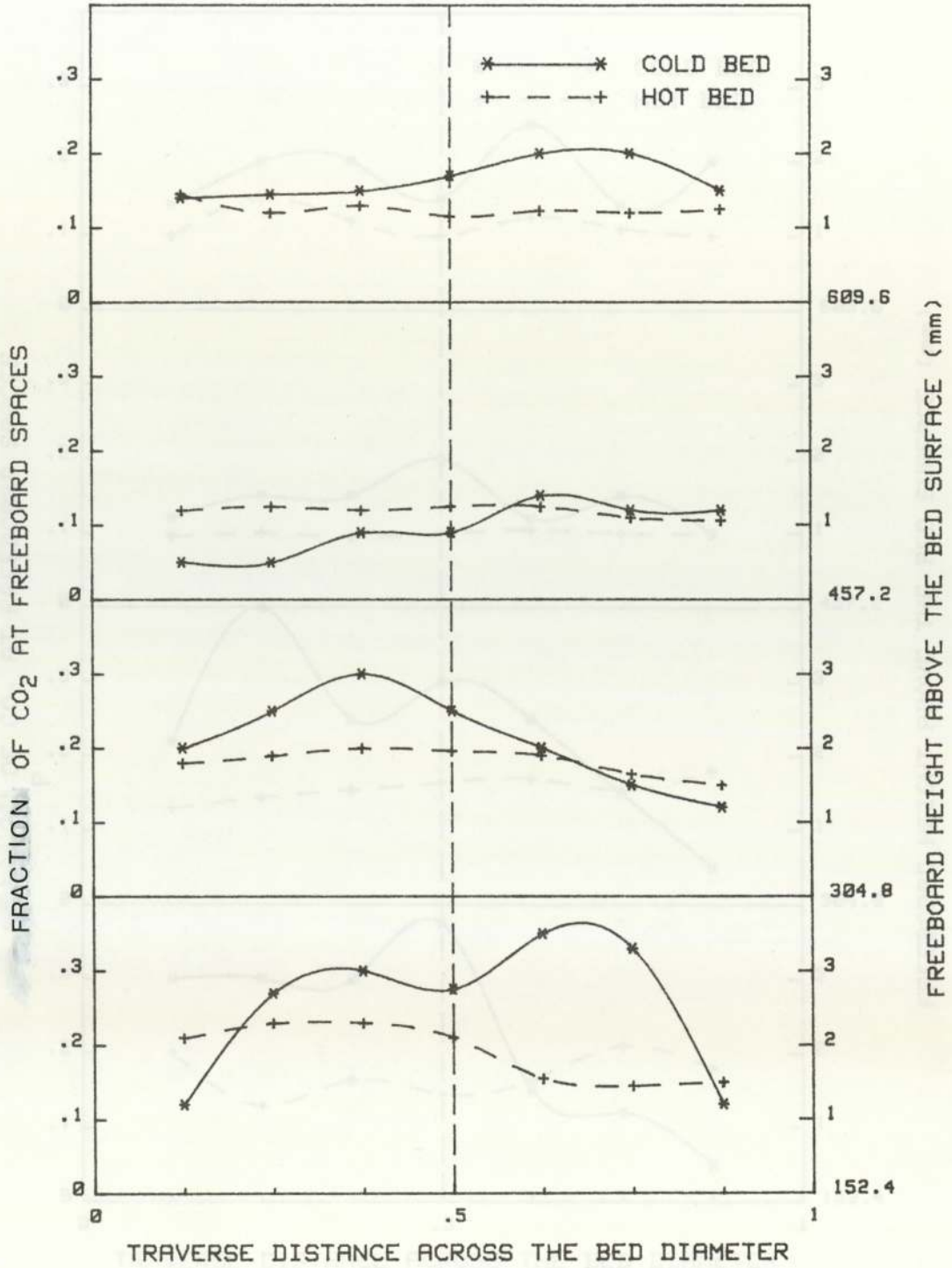


FIG.4.15 RESTRAINED BLOCK OF CO₂ IN HOT BED COMPARED WITH RESTRAINED BLOCK IN COLD BED.

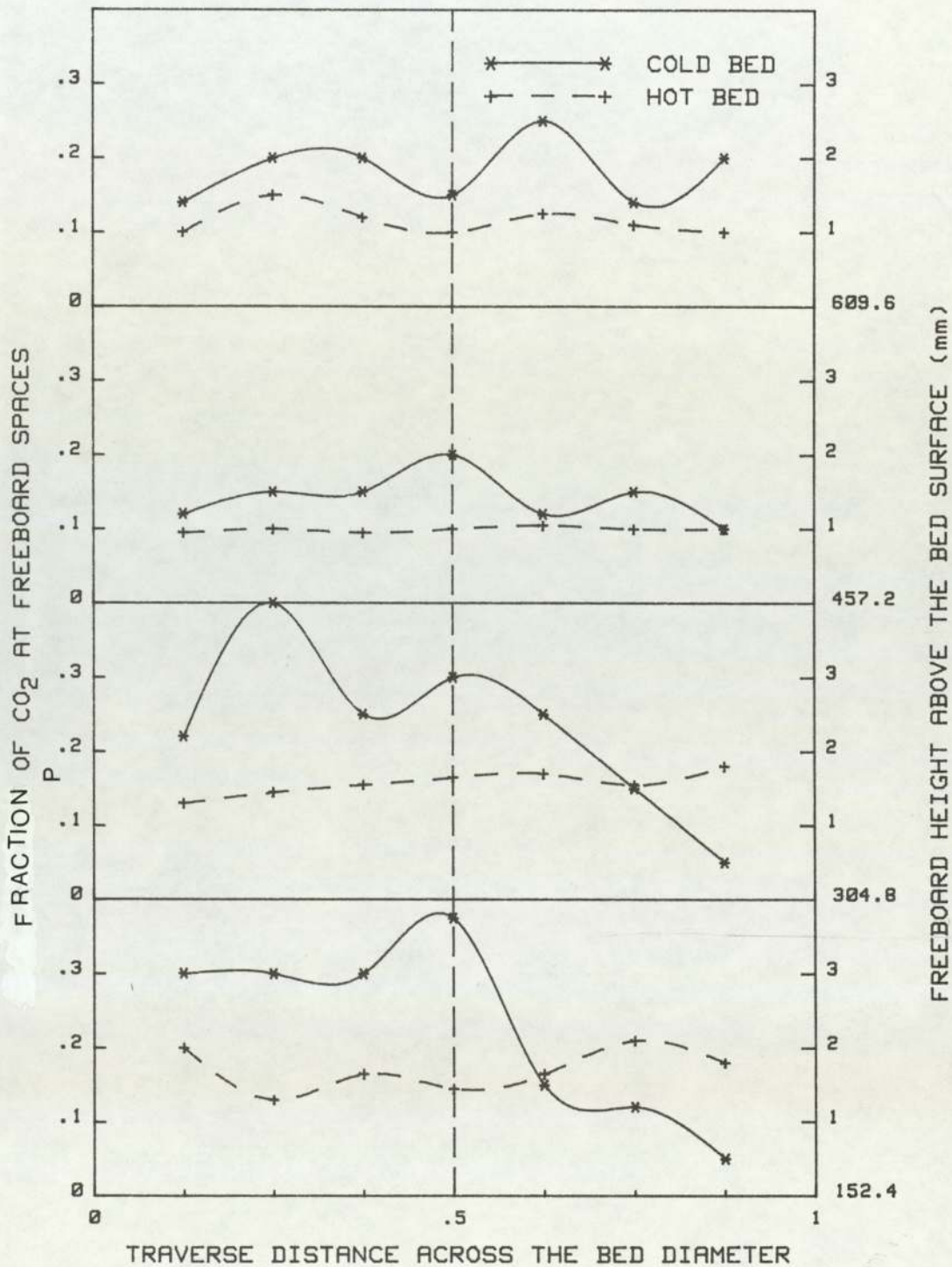


FIG.4.16 UNRESTRAINED BLOCK OF CO₂ IN HOT BED COMPARED WITH UNRESTRAINED BLOCK IN COLD BED.

CHAPTER FIVE

5. COMBUSTION EXPERIMENTS WITH CONTINUOUS FEEDING OF COAL PARTICLES IN FLUIDIZED BEDS

5.1. Introduction

To support a continued and stable combustion condition, a steady feed rate of coal has to be introduced into the combustor. This is carried out to determine the maximum combustion rate attainable for various bed temperatures, excess air and fluidizing velocities.

Items (i), (ii) and (v) were fixed and item (iv) was varied.

- (i) Bed temperature; 900 C constant
- (ii) Inert particle size; 355 μ m to 500 μ m. constant
- (iii) Static bed depth; 100mm constant
- (iv) Excess air. variable; 3% to 30%
- (v) Coal particle size; 1 - 2.8 mm constant
6.7 - 8.0 mm constant.

5.2. Experimental Equipments

5.2.1. Experimental Fluidized Bed Combustor

The fluidized bed combustor already described in section four and shown in Fig. 5.1 was also used for these experiments with some necessary modifications. Since there was lots of air entrainment from the surroundings, the cone

shaped chimney Figs. 5.1 and 5.2 was built to avoid the dilution of combustion products.

A 1.5 mm Porous Stainless Distributor made to the bed diameter (supplied by Pall Process Filtration Ltd., Porous Metals Division, Europa House, Portsmouth, England) was fitted onto the top of the ceramic tile. This helped to achieve a more evenly distributed flow of fluidizing gas entering the bed.

Above the bed are eight sets of four 7.94 x 10⁻³ mm diameter tangential and radial nozzles through which secondary air is introduced. The nozzles are evenly disposed around the combustion chamber at ^{heights of} about 200, 315, 400, 470, 500, 610, 700 and 800 mm above the bed shown in Fig. 5.3. The purpose of the nozzle injection of secondary air is to create turbulence and thereby promote mixing of combustible gases and volatiles with the secondary air in the above bed region so as to ensure that combustion is complete before gases pass out of the chimney. This method of injection of air would enable the investigation of how much air would be required through the bed and how much above the bed for satisfactory combustion.

5.2.2. Distribution of Coal Particles in the Bed

The performance of a combustor depends on proper distribution of fuel and mixing of fuel, inert particles and air. In fluidized beds the axial mixing of particles in a fluidized bed is normally very good; lateral mixing is however considered to be poor as the rising bubbles

discharge their wake solid almost vertically above their point of eruption. For good fluidization the distributor is designed in such a way that bubbling occurs uniformly over the whole cross section of the fluidized bed. If the cross section is very large then the fuel is fed at a number of points over the cross-section. Hence, the method of coal feed and the positioning of the discharge point(s) play an important role in the distribution of coal.

Reference (73) shows that a rule of thumb for number of coal distribution points is one per 0.8m^2 of bed plan area. If however, the coal is discharged as uniformly as possible over the whole bed surface area, then the variation in lateral mixing encountered in a bubbling bed is reduced giving more uniform combustion.

5.2.3. Effect of Coal Feed System on Distribution of Coal Particles in the Bed

The fluid mechanics of the freeboard region influence the dynamics of the particles there. Baulev and Troyankin (72) in their work on velocity profiles in the cylindrical sections of a cyclone indicated that in the turbulent core region the fluid flows radially outward except near the axis of rotation where the direction of flow is reversed. If the coal is discharged in the turbulent core region where the gases are leaving the combustor it is likely that some of this coal may be entrained even before it reaches the bed surface. Therefore the preferred position for the coal feed point is outside the turbulent core.

5.2.3.1 ANCILLARY EXPERIMENTS

The effect of coal discharge chute end-piece on coal distribution was studied ^{page 113.} photographically. See Figs. 5.8 - 5.9. A bed with a bowl of water with a wire mesh was used initially Figs. 5.4 - 5.6, ^{page 155/6.} A fine wire mesh about the same diameter of the bed was placed in the bowl of water. This allowed the distribution pattern shown in Figs. 5.4-5.6 to be seen clearly. Also water was used because it is lighter than coal particles so that when coal particles drop into the bowl of water, they all sink onto the mesh. Later trials were conducted using a bed of sand fluidized with air, Fig. 5.7.

^{page 113,} It was found with the bowl of water technique Fig. 5.8, above that when coal was discharged under gravitational force directly onto the bed surface, almost all coal ended either on the centre or within a few centimetres from the centre to one side of the bed surface see Figs. 5.4 and 5.5, ^{page 155/6.}

When the chute was extended further towards the bed surface ^{as in} with a cone shape attached to the end Fig. 5.9, it was found that coal dispersed over most of the bed surface see Figs. 5.6 and 5.7. This spread of coal would obviously depend on the bed height, diameter of the coal feed pipe and the coal particle diameter. In these experiments, dispersion of coal was regarded as sufficiently uniform see Figs. 5.29 to 5.32 for temperature and gas concentration distribution.

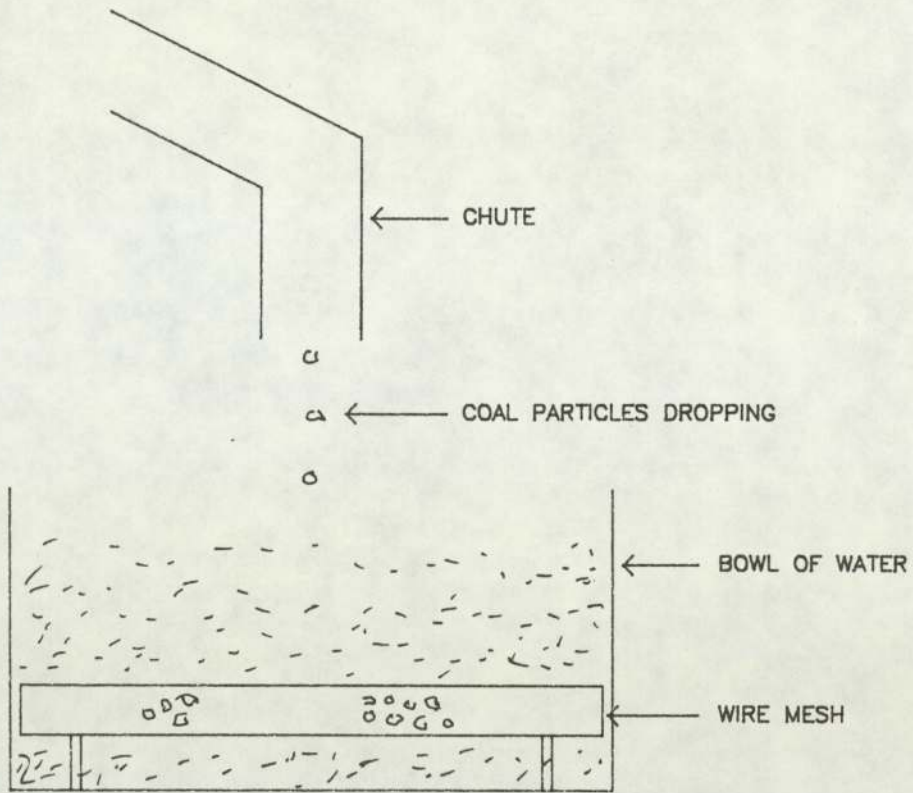


FIG. 5.8 SCHEMATIC DIAGRAM OF THE WATER TECHNIQUE APPARATUS

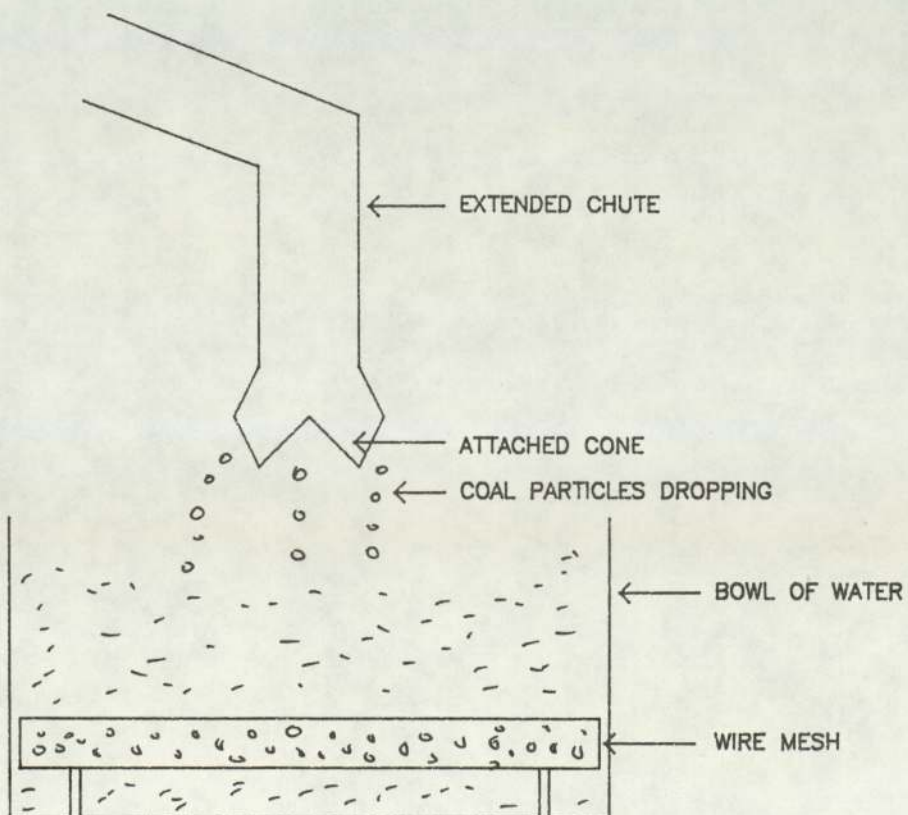


FIG. 5.9 SCHEMATIC DIAGRAM OF WATER TECHNIQUE APPARATUS
WITH THE EXTENDED CHUTE AND THE ATTACHED CONE

5.2.4. Bed Inert Material

Silica sand particles were used as the bed inert materials in every case as they do not sinter at temperatures lower than 1150° C. The particles used in the experiments were sized into narrow ranges using British Standard sieves.

5.2.5. Fluidizing Gas

Air was used as the fluidizing gas during combustion experiments. A calibrated rotameter (Metric Series Rotameter, Tube size 35, float type Korannite; manufactured by Rotameter Manufacturing Co. Ltd., Croydon, England) was used to measure the air flow rate.

5.2.6. Analysis of the Products of Combustion

During the continuous feed experiments, the products of combustion were sampled continuously by using water cooled probes for CO, CO₂, O₂ and heated probes for unburnt hydrocarbons, placed 800 mm above the bubbling surface of the fluidized bed. The limitations of ^{the} unburnt hydrocarbon detector is that oven temperature must not exceed between $100-200^{\circ}$ C; hence high boiling point hydrocarbons may be missed. Therefore it is not an entirely satisfactory instrument but the best available commercially. This is a constraint in the measurement of unburnt hydrocarbon. An infra red analyser (Mexa-310 infra red analyser, manufactured by Horiba Limited, Kyoto, Japan) was used to analyse the concentrations of carbon dioxide and carbon monoxide, a paramagnetic oxygen analyser (oxygen analyser type OA,272, manufactured by Taylor Servomex Ltd., Crowborough, Sussex

England) was used to analyse the concentration of oxygen while a high temperature flame Ionisation Detector Hydrocarbon Analyser (Hydrocarbon analyser, Model 523 II, manufactured by Analysis Automation Ltd., Southfield House, Eynsham, Oxford, England) was used to analyse the concentrations of unburnt hydrocarbon. The concentration of carbon dioxide, carbon monoxide, oxygen and the unburnt hydrocarbon were continuously recorded on chart recorders. Fig. 5.10 shows a photograph of the experimental apparatus.

5.2.7. Response Time of the Instruments

5.2.7.1. Introduction

Inconsistencies from the ideality assumed in developing the basic reactor design theories are often present in practical reactors and the extent of non-ideality varies considerably, depending on the scale, and type of reactor. Important types of these inconsistencies are

- (1) non-uniform distribution of fluidizing gas due to channelling of the reacting fluid through the bed material and the presence of the stagnant fluid pockets.
- (2) the presence of velocity and temperature gradients in the radial direction.
- (3) changes of properties in the direction of flow or effect of backmixing as the result of

fluid turbulence, thermal convective transport and molecular diffusion.

The various types of behaviour listed above imply that different positions of the reacting fluid follow separate flow patterns through the reacting vessel, resulting in a wide distribution of residence times. Such deviations from ideality lead to inefficiency in the reactor performance.

5.2.7.2 RESPONSE OF INSTRUMENTS

The flow, turbulence characteristics and particle dynamic properties of gases play a dominant role in the mixing and hence combustion characteristics of the system. The response of instruments will therefore depend upon where in the reactor the probe receives that mixture which combustion products indicate.

If for example coal particles on entering the hot bed, devolatilize instantaneously, the volatiles will rise in plug flow as plumes from each coal entry port and burning with air at the plume boundary in the above bed region as in the case of a diffusion flame. If well mixed with the sufficient air, the gases picked up by the probe will be uniform. On the other hand, because of the bubbling and agitation activities of the bed, coal particles do not stay in one place, hence there is fluctuation in the position of the plume of volatiles as they rise from the particles while dancing about in the bed. In this circumstance, there is periodic exposure of the probe to the plume and the air as it is being

traversed across the bed diameter.

In examining these conditions, a response/residence time experiment was performed. Information obtainable from this transient-response technique is the distribution times of reacting fluid across the planform of the bed.

5.2.7.3 EXPERIMENTAL PROCEDURE

Two mild steel tubes each of 23 mm diameter and 555 mm high were brazed together with two probes each inserted at the centre of the tubes. The probes were each connected to a solenoid valve operated by a common switch Fig. 5.11.

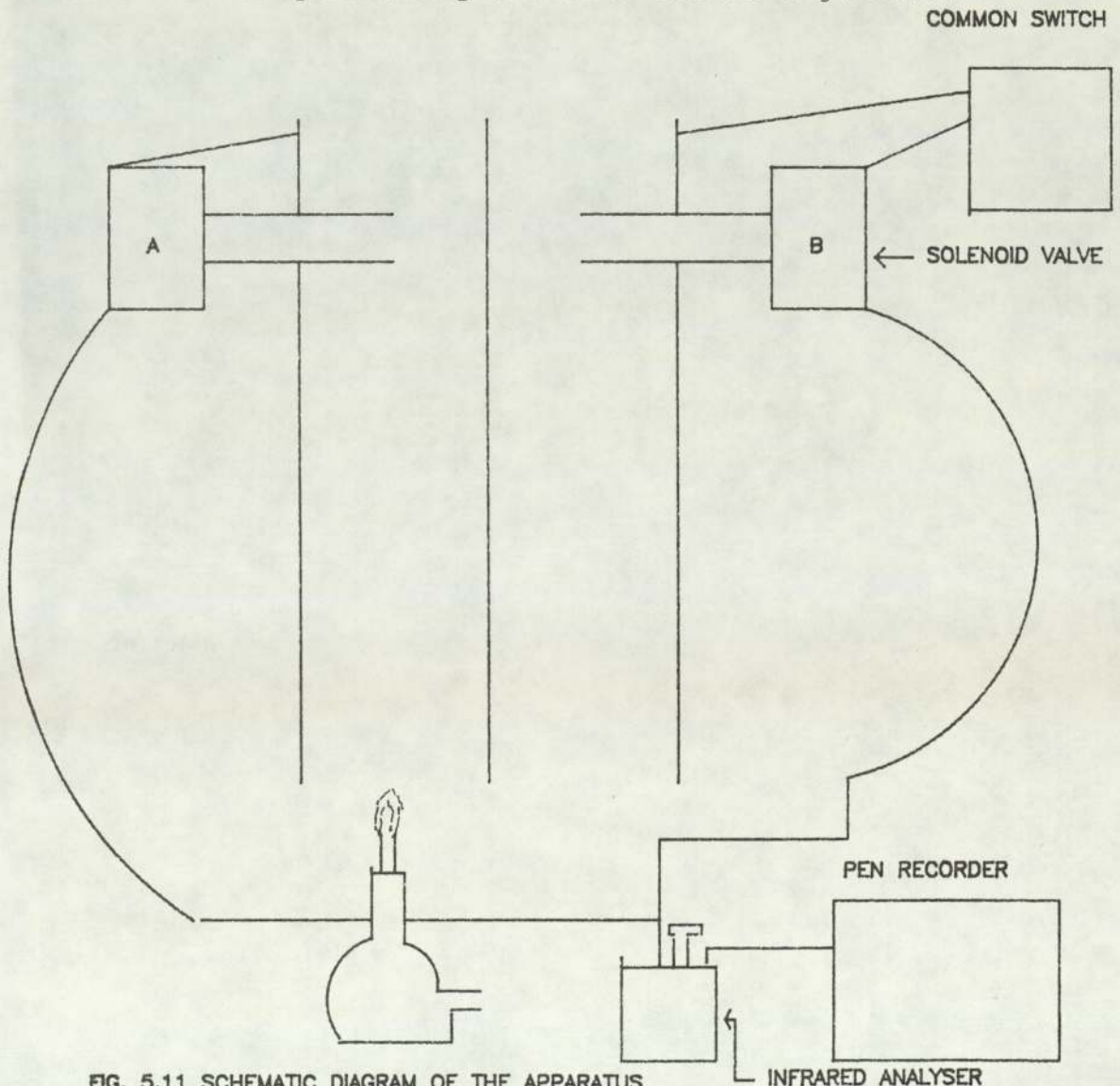


FIG. 5.11 SCHEMATIC DIAGRAM OF THE APPARATUS

The bunsen burner was ignited and placed under tube A while the end of tube B was opened to the atmosphere. The air was then quickly replaced by the CO₂ from the combustion products of the bunsen burner by operating the common switch of the two separate solenoid valves placed in air and CO₂ lines (see Fig. 5.11). The switch was left at this position for one second and later switched back to the air line for another nine seconds, thereby completing a 10 seconds cycle.

The above cycle was repeated for 2,3,4,5,6, 7,8 and 9 seconds with the switch on CO₂ line opened while that on air line closed and 8,7,6,5,4,3,2 and 1 seconds with the switch on air line opened while that on CO₂ line closed.

It was found that it took about seven seconds for the response time to be steady and constant Figs. 5.12 and 5.13.

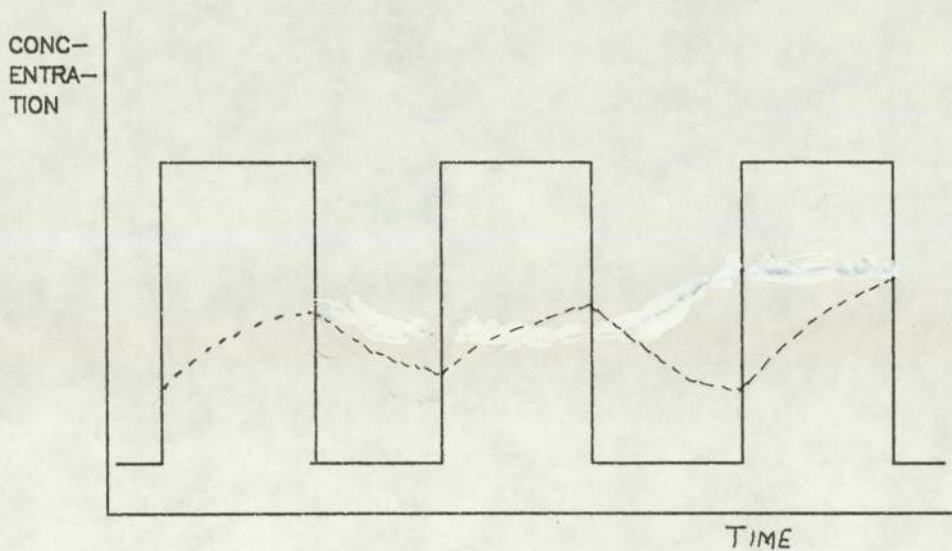
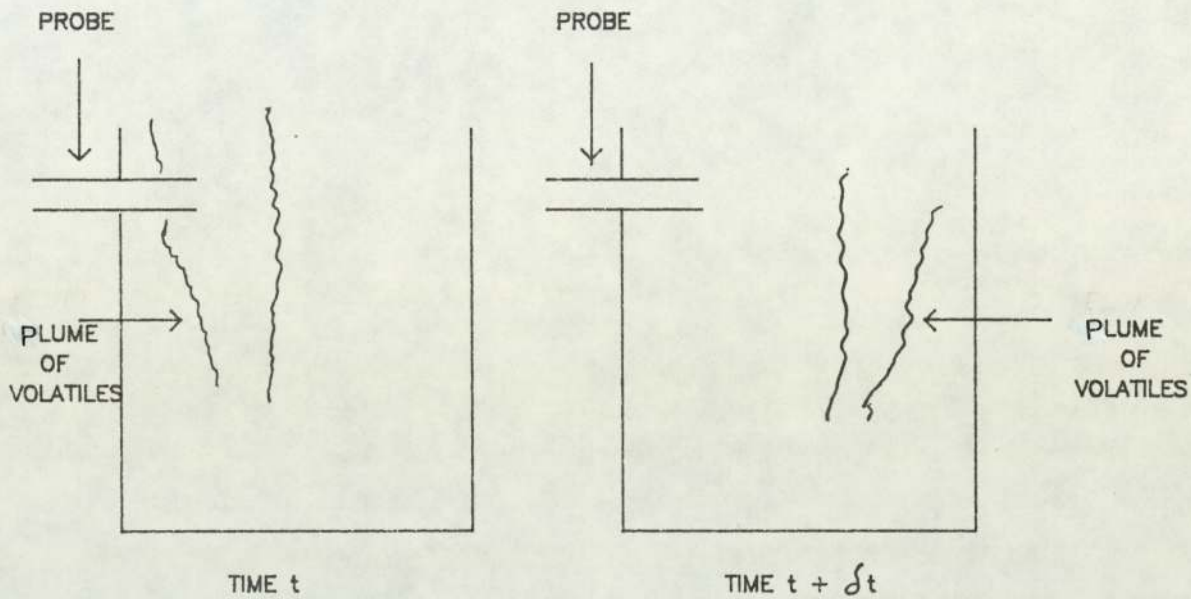


FIG. 5.12 CO 2 OUTPUT RESPONSE CURVES TO AIR/COMBUSTION PRODUCTS INPUT

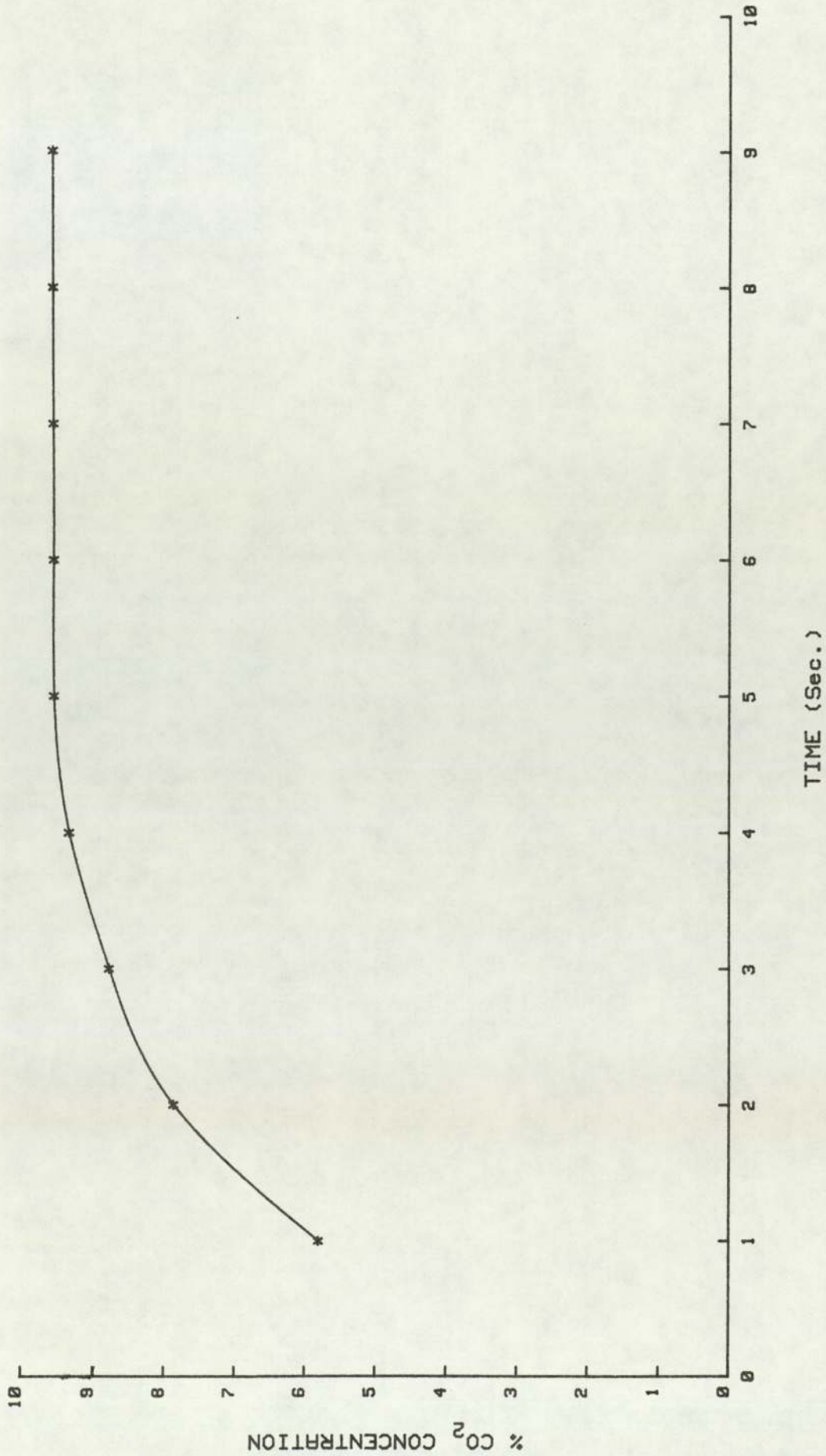


FIG.5.13 RESPONSE TIME OF SAMPLING PROBE IN THE COMBUSTOR

5.3 COMBUSTION EXPERIMENTS

5.3.1 Combustion Test Procedures

The fluidized bed was first heated to operating temperature by burning the premixed air and propane gas. The coal feed was then started and the gas gradually turned off. The feed rate of coal was adjusted to keep the bed at the desired temperature. The coal was metered from a coal hopper by a vibratory feeder and dropped down a chute onto the surface of the bed. The vibratory feeder could not be maintained at an absolutely steady feed rate; hence the average feed rate was determined by weighing the coal hopper before and after each experimental run and noting the time taken for this weight change.

When the bed temperature was steady at the desired value, probes at 800 mm above the bed surface were transversed across the bed diameter (which had been divided into 15 equal areas), sampling the concentrations of CO_2 , CO , O_2 and unburnt hydrocarbons and also measuring the temperature (a) at each sampling point and (b) at the exhaust, see Fig. 5.10.

A series of test runs were done with excess air through the bed and through the secondary air injector nozzles (tangential and radial). Bituminous and anthracite coals were used in separate experiments.

5.3.2 EXPERIMENTAL RESULTS AND DISCUSSIONS

5.3.2.1 Freeboard Reaction

The highest combustion efficiency in the fluidized bed can only be achieved if the coal particles and oxygen are well distributed and well mixed in the fluidized bed and if the period of time required for obtaining the complete combustion is shorter than the retention time of coal particles and volatile products in the system. Highley and Merrick (73) noted that unless the fuel is well distributed in the fluidized bed, reduction zones may develop by local over concentrations of coal particles and this will cause carbon monoxide to be produced. Part of this carbon monoxide may not necessarily be oxidized, with attendant loss of heat release.

During the tests with bituminous coal, the volume concentrations of CO_2 , CO , O_2 and unburnt HC in the exhaust gas measured at 800 mm above the bed surface were always less than 12%, 0.1%, 14% and 140 ppm respectively. At the bed temperatures 900 and 1000^oC, the ^{maximum} flue gas temperature measured in the freeboard at 800 mm above the free surface Fig.5.14 was  about 500^oC.

5.3.2.2 INITIAL TESTS

In the first series of tests the air flow through the bed was held constant at a value approximately the stoichiometric air flow. Excess air was supplied at the

desired rate through the secondary air nozzles. The temperature of the air supplied to the secondary air nozzles was 30°C.

As the excess air (through the secondary air nozzles) increased, it was found that the extent of freeboard combustion was reduced.

5.3.2.3 SECOND TESTS

In these tests the excess air was passed through the bed only. The fluidizing velocity was thus increased; but it was observed that the amount of heat released rises. This effect was confirmed by the increase (>88°C) in freeboard temperature at 800 mm above the bed surface. Fig.5.15

It could then be insinuated that the increase in heat release in the freeboard zone takes place when the fluidizing velocity is increased. The increased heat release could be due to oxidation of CO to CO₂ or oxidation of unburnt volatile hydrocarbons.

It is difficult to establish which of these two oxidations is dominant. The amount of unburnt HC_^ analyser is not necessarily the actual amount, because of the limitation upon the instrument oven temperature, 100-200 °C. Thus the amount of high boiling point hydrocarbons cannot be determined.

Nevertheless these alternative oxidations may be considered unlikely because CO_2 and CO levels, though increased slightly at the higher velocity, were still not sufficiently high to account for the increased activity in the freeboard. There is thus a third possibility, namely that the increased heat release results from increased coal or char particle concentration in the freeboard, which are then oxidized.

This implies that fuel particles themselves are thrown up into the freeboard region to react and eventually burn out with any volatiles released being consumed, hence no large changes of volatiles concentration was measured.

Fourthly it can be speculated that the concentration of CO_2 and high concentration of O_2 detected are due to either part of the fuel being swept out of the bed unburnt or being diluted by the excess air.

The choice of overbed feeding may also contribute to the increased freeboard reaction occurring because some particles may devolatilise before they fall into the bed.

5.3.2.4 TESTS WITH BITUMINOUS COAL

(a) Effect of air feed above the bed.

The role of excess air, as indicated by the flue gas oxygen concentration is shown in Fig. 5.16. Feeding the air above the bed decreases the CO_2 concentration and increases the flue gas oxygen concentrations for all the test runs. This results from the excess air acting as a

diluent, and of course moisture in it may contribute.

(b) Effect of air feed into the bed.

Feeding air into the bed leads to an increase in CO₂

5.3.2.5 TESTS WITH ANTHRACITE COAL

(a) Effect of air feed above the bed.

Feeding air above the bed only acts as a diluent with loss of combustion efficiency. This may be due to the ~~with~~ low volatile matter content (<10%) being released and burnt in the bed and also the large amount of carbon being consumed in the bed.

(b) Effect of air feed into the bed.

It was found that flue gas concentration of CO₂ was far less than expected while those of CO and O₂ were more, Fig. 5.17. This is a loss in combustion efficiency. The loss is thought to be due to a smaller size of feed and to the low reactivity of anthracite; ^{fuel} particle breakage and abrasion presumably occurred during the longer residence time in the bed. Another reason may be due to overbed feeding in which fines are delivered into the rising gas stream of the overbed region. This indicates that larger particle size coal must be used in order that most of it gets down the bed.

5.3.2.6. Effect of Insulation when burning small Coal Particles

(a) Heat Loss from Freeboard

In the freeboard, temperatures were measured by a thermocouple mounted on to the gas sampling probe through the axis of symmetry of the bed. A heat balance of the freeboard for both the insulated and uninsulated combustors were made. The heat of reaction was obtained from the flow of coal particle volatiles and its heating value, assuming complete combustion by equation 3.3 in chapter 3

The enthalpy of gases entering and leaving the freeboard zone was computed, given the gas composition and temperature.

The datum temperature taken for enthalpies was 298 K. The heat loss from the freeboard was calculated from the model outlined earlier in chapter three of this thesis. Table 5.1 page ¹²⁸ shows the results, but details of calculation in Appendix A.

From the results, it was concluded that in ^{an} uninsulated combustor, 50% of the total heat supplied by the fuel was lost in the freeboard through enthalpy transfer, out of which 27% was lost through radiative and convective losses, see Sankey diagram fig.5.18. After a layer of insulation (about 0.0254 m thick) was applied, loss through enthalpy transfer was 44%, out of which 5% was lost through radiative and convective losses, Fig.5.19.

The apparently high "heat loss" figure for both cases arises from

(a) Heat leakage

(b) The assumption that all volatiles have burnt.

If only a fraction of the volatiles have burnt then the calculation of heat loss may show a substantial heat loss, equation 3.1, chapter 3.

(b) Heat Release in the Freeboard

Heat released in the freeboard is generally proportional to the amount of volatiles burn^{-ed} in the freeboard. Some deviation from this proportionality may occur due to carbon monoxide combustion and carbon-steam reaction. Thus heat release in the freeboard depends not only on volatile concentration but also on the other factors that will influence the oxygen, carbon monoxide and steam concentrations entering the freeboard. As expected increased heat release in the freeboard zone increases the freeboard temperatures. However, increase in heat release speeded up gas flow velocity, thereby reducing residence time for volatile matter and oxygen; on the other hand the increased temperature leads to more active combustion of volatiles. Higher gas velocity entrains more particles of coal in the freeboard region.

5.3.2.7. Effects of using large Coal Particles - only with Insulated Bed on

(a) Heat Loss

Large coal particles have a significant effect on conditions in both the freeboard and bed.

With larger size coal particles a larger fraction of volatiles burns in the freeboard.

Bed Temperature K	1239	1241	1323
Freeboard Temperature K	748	827	1042
AirFlowrate (litre/min)	355.6	365	544.6
(kg/min)	.408	.439	.643
Fluidizing Vel.(m/s)	0.5	0.5	0.61
%Gas Analysis by volume			
Oxygen	10.1	5.0	5.0
Carbon dioxide	10.05	10.5	10.1
Carbon monoxide	0.11	0.16	0.3
% Excess Air	3	11	15
Coal feed rate(kg/s)	.000667	.000667	.000942
Coal size (mm)	1-2.8	1-2.8	6.7-8
Heat released rate(kW)			
in the bed	10.21	10.18	14.42
in the freeboard	12.74	12.7	18
Heat loss (kW)			
in the bed	3.0	2.4	5.2
in the freeboard	9.3	8.3	4.8

SUMMARY OF RESULTS WITH COAL

TABLE 5.1

The rate of heat production in the bed due to combustion of residual carbon would be a function of the coal surface temperature and of the exposed coal surface area available for reaction. Larger area of particles fed to the bed means faster release of volatiles.

$$\begin{aligned} \text{i.e. Heat release rate} &= \\ &\text{Specific burning rate [kg/sm}^2\text{]} \times \\ &\text{Exposed surface area [m}^2\text{]} \times \\ &\text{Calorific Value [kJ/kg}_{\text{carbon}}\text{]} \end{aligned}$$

If we assume ^{the} bed to be heated by residual carbon only, then, [active area of carbon resident in the bed \times Specific burning rate \times Calorific value] is the same irrespective of size of coal particles being fed to the bed. This ~~total~~ ~~of~~ resident carbon has already emitted all its volatile matter. The size distribution of this resident carbon in the bed will be much wider for the larger size coal feed than small size (shrinking carbon particle).

Now consider the particles just as they enter the bed.

Suppose \dot{n} coal particles of small size enter per unit time then mass of coal per second = $\dot{n} \rho_c \pi d^3 / 6$ where ρ_c = coal density

If \dot{N} particles of large size enter per unit time then mass of coal per second = $\dot{N} \rho_c \pi D^3 / 6$.

Therefore for a given feed rate of coal the mass of volatiles released per second must be the same irrespective of coal particle size.

If the fraction of f_v of the coal is volatile matter the rate of feed of volatile matter is $\dot{n} f_v \rho_c \pi d^3 / 6$ and $\dot{N} f_v \rho_c \pi D^3 / 6$.

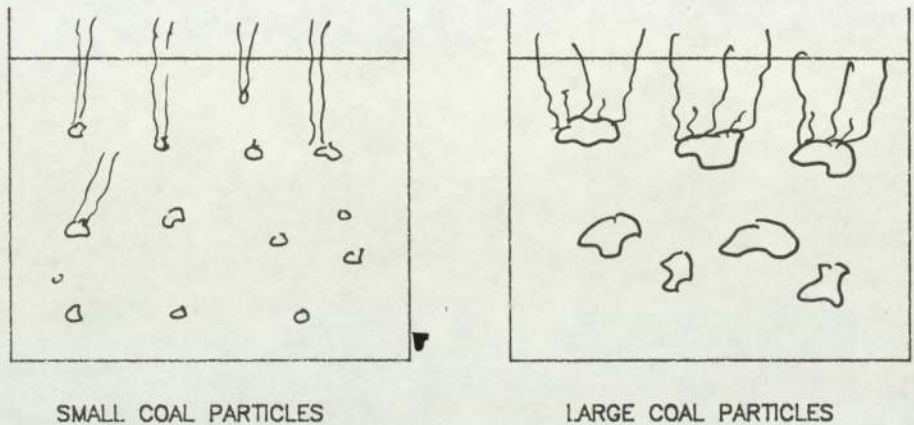
If these rates of feed are the same then the fraction f_b of them burning in the bed must be the same.

$$\text{i.e. } (\dot{n} f_v \rho_c \pi d^3 / 6) f_{b_d} = (\dot{N} f_v \rho_c \pi D^3 / 6) f_{b_D}$$

But this is not so in that a greater fraction f of them are burnt in the bed when large coal particles are fed to the combustor.

$$\text{i.e. } (\dot{n}f_v \rho_c \pi d^3 / 6) f_{b_d} < (\dot{N}f_v \rho_c \pi D^3 / 6) f_{b_D}$$

This is due to the time taken for volatiles to be released from the same mass of coal. The same mass of volatiles is emitted by both particles, but the emission requires more time when coal particle is large. However, it is where the volatiles burn that matters.



Assume same exposed area of carbon in the bed so that heat released due to residual carbon combustion is the same.

FIG.5.20 THE EFFECT OF HEAT RELEASE IN THE TWO ZONES

5.3.2.8. Influence of Excess Air

The role of excess air, as indicated by the flue gas oxygen concentration is shown in Fig.5.21.

The excess air could be supplied (a) into the bed (b) directly to the freeboard zone, (c) part through the bed and part directly to the freeboard zone.

(a) Comparison between supplying all Excess Air through the Bed with all direct to Freeboard Zone

When all excess air (1%) was supplied through the bed, it was

found that there was low^{-er} concentration of oxygen and greater concentration of carbon dioxide concentrations in the exhaust gases[^] when the excess air was supplied to the freeboard[^] than all. When the air is supplied to the bed it contacts a very large surface area of particles and becomes heated rapidly, so that it is heated up to the bed temperature before reaching the freeboard. The volatiles in the freeboard are therefore fed with hot air rather than cold air. They therefore burn more rapidly than when fed with cold air with attendant effect on CO₂ and O₂ concentrations.

The exhaust gas temperature increases as a consequence of the additional combustion.

However, elutriation of bed materials imposes a constraint upon putting more air through the bed. Adding excess air solely to the freeboard zone tends to cool the gases and dilute them rather than increase the amount of combustion.

(b) Part of Excess Air through Main Bed and part through the Secondary Air Pipes

Putting part of the excess air through the main bed and part through the secondary air pipes increased the oxygen concentration further but reduced the carbon monoxide concentration to zero. This can be attributed to air not being used but acted as a diluent. The average concentration of oxygen reported in this experiment was 12.8%. Pritchard and Caplin (74) in their tests on peat combustion with primary air of about 2500 kg/h and secondary air of about 741kg/h reported the variation in oxygen content of the hot gas between 2.0% and 3.2%. They

concluded that good combustion could be achieved by putting less air through the bed and more through the secondary air nozzles. This was not the case with the experiment described in this thesis, where good combustion was achieved by putting all the excess air through the bed especially when burning coal. However, what Pritchard and Caplin (74) did not say was whether their secondary air was preheated or not.

(d) Quenching of Combustion Products

Combustion reactions are a balance ^{between} (on the one hand), high reaction or flame temperatures, which favours carbon monoxide at equilibrium, and (on the other hand) of the use of excess air, which drives the conversion to carbon dioxide. Relative to these counter-acting facets, rates of reaction are generally controlling, manifested by short residence times with rapid heat transfer such that the system temperature is lowered before equilibrium can occur. From practical point of view, the amount of excess air can be viewed as the determining feature of combustion. It not only affects combustion rates, but flame temperatures and the heat balance as well.

As can be seen in Fig. 5.16, too much excess air diluted the combustion products. The water vapour formed as an inert, affects the combustion characteristic of the gases. The flame temperature for combustion of hot gases is higher than for combustion of cold gas, thus achieving higher heat transfer rates. The cooling effects of these gases will tend to lower flame temperatures and subsequently reduces

the heat release rate.

5.3.2.9. Effect of using large coal particles on

(a) Bed Sintering

The main special feature of fluidized bed combustion is the constraint imposed by the relatively narrow temperature range within which the bed must be operated. With coal combustion there is a risk of sintering the bed if the temperature exceeds 950°C . If the temperature is too low combustion will cease.

In order to operate the bed below 950°C , the bed has to be cooled, (but not too much).

Although the inert material used in this test has a low melting point of about 1015°C , it was discovered when burning large coal particles (6.7 mm - 8.0 mm) that the bed surface was sintered, Fig. 5.22. This bed sintering may be attributed to ash melting temperature lower than sand melting temperature, and high local heating.

(b) Burn out of Pilot Burner

Fig. 5.23 shows the pilot burner which became burnt out by exposure to high temperature zone. The burner was about 50 mm above the bed surface. Insulating the flow into such components, constitutes a problem.

5.3.3 Energy Balance

Figs. 5.18 and 5.19 page 162/3

The Sankey diagrams Δ show the energy balance which is an arithmetic account of the various forms of energy entering and leaving the combustor.

The energy difference between the reactants and the products indicates firstly whether the process requires a nett energy input or whether is a nett producer of energy and secondly the minimum level of energy required or maximum level of energy produced.

page 162/3

Figures 5.18 and 5.19 Δ show the energy sources and losses for a variety of postulated situations. This type of energy balance corresponds to application of the First law of Thermodynamics Δ to an isothermal system with shaft work $W_s = 0$.

Most of the energy changes that occur in thermochemical conversion processes are a result of the lib^eration or absorption of energy by the chemical reaction. The heat of reaction is the enthalpy change between the products of the reaction and the reactants.

For an exothermic reaction, the heat of reactions are negative, the enthalpy of the products is less than the enthalpy of the reactants and heat is released to the surroundings during reaction. For an endothermic reaction in which heat is absorbed the heats of reaction are positive.

At high reaction temperatures, gaseous enthalpy is high (i.e total enthalpy of formation at that temperature of the individual molecules making up the gas) and low at a low reaction temperatures. For example, for inert particles such

as nitrogen ~~and water vapour~~ and water vapour, the only source of energy is the energy of the molecule due to its thermodynamic temperature (i.e gaseous enthalpy) and for non-inert materials such as hydrocarbons, the energy can be released by breaking down and oxidising the molecules thereby releasing the energy of an exothermic chemical reaction. This combustion energy, depending in the particular molecule involved can be so high as to greatly exceed the gaseous enthalpy of molecules of the oxidant entering the reactor.

Thus a low temperature gas stream containing hydrocarbons in significant quantities will be a source of high temperature combustion products.

Energy loss from the combustor comes from different ways. The only heat loss accounted for in this study is the heat losses from the bed to the surroundings. The estimated heat losses amounted to $1.5 \frac{\text{kW}}{\wedge}$ and $0.4 \frac{\text{kW}}{\wedge}$ in the bed and $2.5 \frac{\text{kW}}{\wedge}$ and $0.3 \frac{\text{kW}}{\wedge}$ in the freeboard. The estimated values of the heat transfer in both insulated and uninsulated situation do not include heat transfer from the pipe work associated with secondary air supply. These pipes would act as fin and some estimate of the effect is desirable.

The other possibility is losses through the elutriated carbon or coal, but this has been found to be negligible. (Bomb calorimeter tests of the collected elutriated particles show calorific value to be $4.5 \frac{\text{kJ}}{\text{kg}}$, compared with 28000 $\frac{\text{kJ}}{\text{kg}}$ for the fuel)

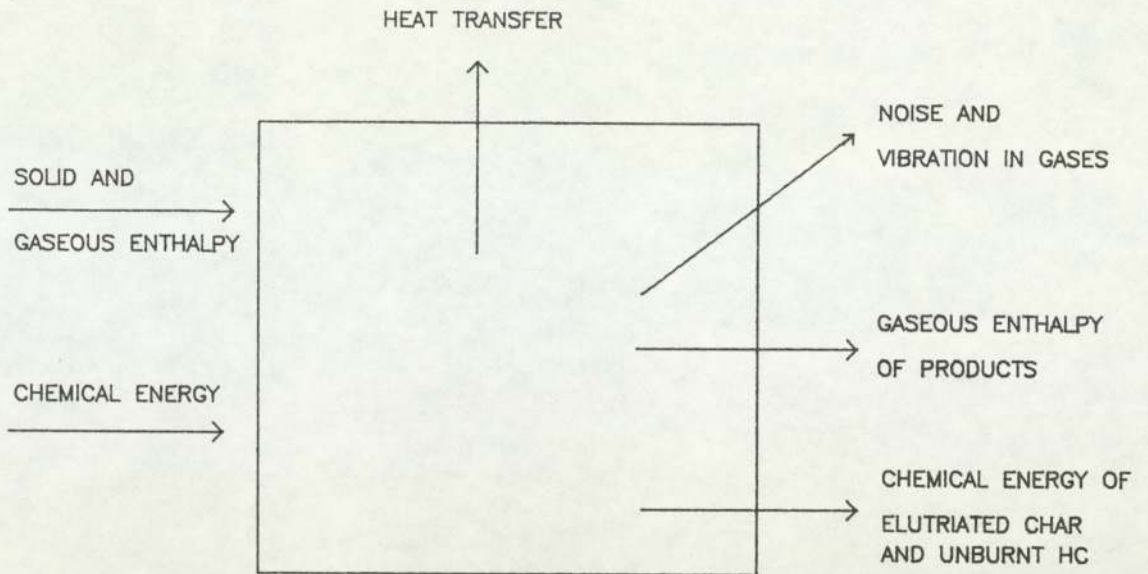


FIG.5.24 FLOW DIAGRAM SHOWING ENERGY LOSSES IN THE REACTOR

5.3.4 Comparison of combustion enthalpy balance with intrinsic limit (Merrick's data)

In the present study, evaluation of enthalpy balance using the author's model and experimental results were compared with Merrick's data⁽⁷³⁾ using author's experimental results. Good agreement was achieved in the freeboard for both the insulated and uninsulated conditions_^ with enthalpies of unburnt hydrocarbons of 9.3 and 8.3 kW. from author's model and 7.6 and 7.5 kW. from Merrick's data respectively. see Figs. 5.18 and 5.19 page 162/3

Because of the limitation imposed by the unburnt hydrocarbon analyser's oven temperature (between 100 to 200°C), the author assumed the volatiles to be methane equivalent; while Merrick's data gave a complete composition of volatiles and tar (assumed to be C₁₀H₂₂) at 500 to 550°C.

In contrast, at a bed temperature of about 900°C, the results are characterized by the comparatively small amounts of enthalpies ~~of unburnt hydrocarbons~~ of unburnt hydrocarbons from the bed from author's model (3 and 2.4 kW.) and larger amounts from Merrick's data (7.3 and 8.5 kW.).

These differences may be attributed to time-temperature rate of heating. The gaseous products obtained are dependent on both the temperature and technique.

In fluidized bed combustion, different species of volatiles and less tar may be produced due to rapid heating rate as compared with low heating rate reported by Merrick.

Desypris et al (112) in their fluidized bed and electrically heated grid experiments on flash pyrolysis of coal reported that the production of unsaturated hydrocarbons increased considerably with temperature in fluidized bed compared with ^{the} electrically heated grid.

At higher temperatures >900K gaseous hydrocarbon and tar crack and production decreases as the temperature increases.

Keains^r and Morris (104) in their studies of devolatilization of coals in fluidized bed reported that increasing the temperature from 872 to 982°C caused a moderate increase in the quantity of methane and little change in the evolution time. They did not analyse the tar, but Hesp and Waters (113) who ^{did} analyse the tar reported that the major products of thermal cracking of tar, aside from solid carbon, are hydrogen and methane. They found that the maximum yield of methane occurred between 850 and 900°C.

5.4. COMBUSTION EXPERIMENT WITH WOOD

5.4.1. Introduction

Of the various ways in which biomass can be utilised, the simplest and most direct is by the combustion of wood. Wood is of course not a new fuel and until the middle of the 19th century, combustion of wood formed the major source of energy in the world. At the present, wood is still an important source of energy in the third world particularly in African and Asian countries.

The detailed process of the combustion of wood is more complicated than the combustion of any common liquid or gaseous fuel. The reasons are:-

- (i) Wood is chemically complex.
- (ii) Wood is a solid, and in most home applications, fairly large pieces are used, so combustion can be quite inhomogeneous, parts of each piece being reduced to ash; while other parts are just beginning to warm and
- (iii) The heating necessary to get wood to the temperature at which it can burn causes very complex reactions in the wood. In a sense, raw, natural wood itself does not burn; its chemistry is so fragile that substantial changes take place due to the heating necessary to get whatever products of wood which do burn, up to the ignition temperature. The major chemical components of wood are cellulose and lignin which are made of carbon, hydrogen and oxygen. Because of its high oxygen content and a lower calorific value and

density than coal, it imposes a weight and volume penalty if wood has to be transported any distance before it is utilised. On the other hand wood also has low sulphur content and therefore any gaseous pollutants produced are relatively sulphur free. Most of these compounds were not in the wood originally, but were formed from wood's chemical structure. In a typical wood fire, these gases and droplets burn when they move out of the solid wood. However, the major problem which arises from the burning of these compounds is that it results in the formation of smoke which should be prevented because it is the main pollutant problem. These generated gases (volatiles) and smoke prevent oxygen from getting in and hence making combustion inside the bed impossible.

Total yields from the pyrolysis of wood depend critically on conditions under which pyrolysis takes place. Generally the quicker the heating of the wood, the larger is the yield of charcoal. The fraction will be different in different fires, depending on the fire's intensity and the type of wood, its moisture content and the sizes of the pieces.

5.4.2 EXPERIMENTAL TECHNIQUE

5.4.2.1 Wood-burning Unit

A fluidized bed combustor as shown in Fig.5.1 was used for the investigation. Because of the problems of blocking the chute by pieces of wood experienced at the initial stage, the vibratory feeder was connected to the upper part of the chimney. The amount of combustion air entering the bed was controlled by passing some through the bed and some through the secondary air nozzles. The combustion of the wood could be conveniently observed through the stainless steel mirror placed above the bed.

The bed temperature for the two tests were 850°C and 700°C respectively, before starting to feed the wood.

5.4.2.2. Wood Sample used

Redwood Deal wood was used as the fuel. Redwood Deal wood was selected because of its availability as sawn lengths of small dimension. The wood was then sawn into 8x8x10 mm sizes. A complete analysis of a sample of Redwood Deal wood was carried out to obtain its calorific value, moisture content, ash and volatile matter.

5.4.2.3. Analytical Method

Samples of the flue gas were analysed continuously using

Infra Red gas analyser for carbon dioxide and carbon monoxide and using ^a Paramagnetic gas analyser for oxygen.

5.4.3. Experimental Results

5.4.3.1. Analysis of wood

The Redwood Deal wood was analysed according to the British Standard 1016 and the following results were obtained:

Volatile Matter content	80.3%
Moisture content	7.5%
Ash content	0.15%
Calorific Value	2.278×10^4 kJ/kg
Carbon	48.6%
Hydrogen	6.3%
Oxygen	44.3%
Nitrogen	0.8%

5.4.3.2. General Behaviour of Wood Combustion and Gas Analysis

At the start of the experiment, the combustion air was passed through the bed, its behaviour was observed through the stainless steel mirror.

As the wood undergoes pyrolysis, considerable smoke was

produced. It was then decided to carry out the combustion with part of the combustion air through the bed and part through the secondary air nozzles. This enabled the wood to burn long enough to allow a good analysis of the flue gas to be made. The bed was heated up to 850°C before the wood feeding started. After 15 minutes of continuous feeding on wood alone, the bed became fairly stable at about 750°C , but rose slowly as the experiment continued.

In the second experiment the wood was added when the bed temperature was a little over 700°C . The bed temperature decreased initially, and later became fairly stable at about 660°C , rising slowly as the experiment proceeded.

Analysis of the flue gases (CO_2 , CO , and O_2) for the two experiments with the bed temperature, gas temperature and exhaust temperature are shown in Figs. 5.25 to 5.28.

Table 5.2 shows the summary of the results and the detail calculations is in Appendix D.

	RUN 1	RUN 2
Bed Temperature(K)	1124.2	1060.7
Air Flow Rate (L/min)	464.18	470.37
(kg/min)	0.5483	0.5657
Gas Analysis by volume(%)		
O_2	4.5	5.9
CO_2	11.8	11.02
CO	0.25	0.13

N ₂	83.45	82.95
% Excess Air	20	28.5
% through the bed	13.6	19.4
% through sec.air nozzles	6.4	9.1
Wood Feed rate kg/sec.	0.0013	0.0013
Fuelling rate kW.		
to the bed	4.0795	4.0795
to the freeboard	52.345	52.345
Heat loss/gained kW.		
by the bed	18.074gain	18.434 gain
by the freeboard	23.53 loss	22.64 loss

SUMMARY OF RESULTS WITH WOOD

TABLE 5.2.

5.4.4. Discussion of the Results

5.4.4.1. General Nature of Wood Combustion

As wood undergoes pyrolysis, combustion takes place if oxygen is available.

When a new piece of wood is added to a fire, it is heated up by its hot surroundings. Since wood is a moderate^{-ly} good thermal insulator, the heat cannot be conducted quickly into the interior of the wood; so only a very thin layer at the surface is affected initially. It dries very quickly and decomposes into volatile matter and char. Heating rates appear to be important.

Wood is normally burned either in the open or in open fireplaces. It could also be used in a fluidized bed combustion unit of the type used here.

In addition, good mixing of particles promoted by bubbling or turbulent action provides excellent conditions for heating and combustion of any carbonaceous material. Ideally, this latter type is preferable.

The studies undertaken here were carried out with excess air. With limited amounts of air the results are relevant to both direct complete combustion and partial combustion (gasification).

5.4.4.2. Effect of Secondary Air

Complete combustion of wood is a desirable objective, and this does require the burning of both the evolved gases and solid wood. This requires a certain minimum amount of air, sufficiently high temperatures, and adequate distribution and mixing of the air with the combustible materials.

As the wood was added to the hot bed and the secondary air inlets were closed; there was a considerable pyrolytic decomposition of wood, but little combustion and little air to dilute the smoke. But as the air was introduced, directly into the freeboard zone, smoke reduced.

In fluidized bed of the type used here, plenty of air through the bed would be needed to burn these gases as well as the wood. In practice, putting plenty of air through the

bed did not seem to burn the gases but only increase the particle elutriation rate and diluting the combustion products. The former point is in contrast to burning of coal.

In the case of the above observations, air through the bed was admitted at a point where there is very little flame. Since wood contains about 80% volatile matter, volatile matter loss from the bed is likely to occur and travels up to the freeboard region above the bed to burn there ^{if} _^ enough oxygen ^{is} there ^{with} which ^{to} ignite the smoke.

The rough rule of thumb with other types of wood burner, Shelton (75), is that secondary air will only help if admitted into a region where flame already exists. This seems to be the case for fluidized beds too, because when flames filled the freeboard region, the supply of secondary air led to more complete combustion.

The amount of secondary air admitted was also critical. Visual observation of the combustion behaviour at the start of the experiment showed that when it was too little, not much of the combustible gas was burnt. When it was too much, its cooling and diluting effects inhibited combustion. Thus, combustion in the freeboard was only possible over a moderately wide range of secondary air flow.

5.4.4.3. Effects of Bed Temperature

Figures 5.25 and 5.26 show the bed, flue gas and exhaust temperatures. For the two test runs, the bed was heated to 850°C and 700°C respectively before wood feeding started. The bed temperatures became stable at 750°C and 660°C respectively within 25 minutes of wood feeding. Bed temperatures continued to rise as the combustion progressed. It was found that as long as the bed temperature was about 600°C or higher, combustion would sustain and be nearly complete when burning wood. This may be attributed to the good mixing of bed inert particles promoted by bubbling or particles to receive turbulent action which allows the inert radiant energy from the flame and convective heating which helps to maintain bed temperatures.

5.4.4.4. The Nature of Combustion Products

The products of combustion obtained were CO_2 , CO and O_2 and CH_4 (Heavier hydrocarbons could not be detected due to limitations imposed by the hydrocarbon analyser for higher boiling point hydrocarbons. This does not mean that none were produced).

The extent of the reactions possible between these species, could be dependent on residence time, temperature in the fluidized bed and the equilibrium conversion conditions.

According to Lian et al (76), methane must be produced from the pyrolysis of wood or tar and not by the reaction of CO and H₂.

The products of reactions obtained indicate that oxygen is reacting with pyrolysis products faster than they are formed in the later periods of reaction (when char and tar are being converted).

As expected the amounts produced by the two test runs were not significantly different. In addition their variation with combustion conditions followed the expected pattern. The levels of CO₂, CO produced increased generally with increase in bed temperature. Thus, the formation of carbon monoxide was evidently due to partial combustion at low temperatures. Should excess air cause CO formation, then it probably does so by ^{the} lowering of bed temperature. This is an unresolved matter.

5.4.4.5. Heat in the Bed and Freeboard

Table 5.2 shows the heat released both in ^{the} bed and freeboard as well as heat generated or consumed in the bed and the freeboard. The heat released in the bed by combustion of carbon alone was 4.0795 kW and the heat transferred into the bed ^{consumed} was 18.074 kW. This explains the complexity of wood combustion. As the wood entered the hot bed, the major effect of heat is to drive out moisture which was present in the wood. This is an endothermic reaction since evaporation of water requires energy. As the temperature increases more

water is driven off and probably many other compounds are evolved out of the wood. The processes are still endothermic - heat is consumed and not generated. All of the compounds except water and carbon dioxide are combustible, but the actual mixture including the water vapour and carbon dioxide, may not be ignitable due to excessive dilution with non-combustible gases.

The bulk of pyrolysis occurs ^{in the bed} between 280°C and 500°C. The reactions ^{in the freeboard} evolve heat - they are exothermic. Hence the temperature in the freeboard starts to rise. Large amounts of gases are released in the bed and undergo further changes in the freeboard. The amount of heat released by volatiles alone was 52.345 kW while heat lost from ^{the freeboard zone} by these gases was 23.53 kW. Wood tar is another product of heating wood, and although the tar molecules do not exist as a vapour, some tar in the form of tiny droplets is carried out of the wood by the moving gases and thrown into the freeboard region above the bed. This mixture is rich in combustibles ⁱⁿ that it is ignitable and serves as the fuel source for wood flame.

After pyrolysis, the final solid product is charcoal ^{which} is stable to very high temperatures - melting point 3480°C and its boiling point 4200°C Shelton (75), much more higher than the highest temperature achievable in a fluidized bed combustor.

In wood burning, wood is not so heated slowly and uniformly as was thought. On the contrary the inside of a piece of wood may not even be warm when the outside is already fully

charred and burning. Additional pyrolysis reactions then take place. Gases and tar generated below the wood's surface must pass through the surface layers on their way out of the wood. Water vapour can react with carbon in charred layers and become carbon monoxide and hydrogen gases. Carbon dioxide can be similarly transformed into carbon monoxide. These reactions consume heat. Similarly the tar droplets from inside the wood also can react with charcoal and this reaction evolves heat.

Internal heat generation is small for wood - low carbon, very porous carbon, easily blown out of bed. Yet bed temperature is steady at 750°C, therefore heat must come into the bed through fuel surface.

5.4.4.6 Modes of heat transfer

(1) Radiation to a bubbling surface, new particles are exposed continuously. Lewin (89)

(2) Bubbles burst throwing sand particles into a hot zone and then they fall back to the bed.

If radiation is greater than particle convection, this may be because fluidizing velocity is low, therefore not so many particles^{are} being transported into the hot zone.

Heat transfer required to keep bed hot is found from combustion of propane where all heat is released in bed.

There is not enough carbon being burnt in the bed to supply the losses, therefore additional heat must be entering bed from another source e.g back radiation, particle from bubbles being thrown into hot flame freeboard and returning to bed.

5.4.4.7 Freeboard Reaction

Assuming that everything is burnt in freeboard zone. But it may not be, however; sufficient heat may be being released in freeboard ^{23.53kW in table 5.2} to supply heat losses from freeboard (through walls) and to supply back heat flow to bed ^{in table 5.3.} 18.074kW [^]. Equation (I) in the Appendix D is sensitive to unburnt fuel. If 10% fuel is unburnt, heat loss 23.53KW would be significantly reduced.

5.4.4.8 Comparison of Fluidized bed combustion of wood with fixed grate.

This experiment was done with soft wood hence it was compared with **Evans et al(77)**'s soft wood experiment.

Comparison of macroscopic performance of fluidized bed with fixed grate by Evans et al (77) show devices to give similar performance. Both produce ^{the} same smoke and exhaust gas analysis.

Evans et al (77) showed that their wood burner was not sensitive to changes of wood grade. Coal may behave differently.

FUEL	REMARKS ABOUT FREEBOARD COMBUSTION	EFFECT ON EXTERNAL HEAT INPUT IN BED
Wood	Smoke, luminous yellow flame high radiation	Lots of back radiation

Anthracite Coal		
Large particles	No visible flame	
Small particles	No visible flame	
Bituminous Coal		
Large particles	Lots of flame and smoke	Lots of back radiation
Small particles	Slightly visible yellow flame, smoke	

OBSERVATIONS OF COMBUSTION IN FREEBOARD

TABLE 5.3

5.4.4.9 Conclusion from the table

Bed temperatures are approximately the same for all fuels, therefore heat loss is approximately the same. Back heat flow provides greater heat input to bed when wood or large bituminous coal is used than when anthracite is used.

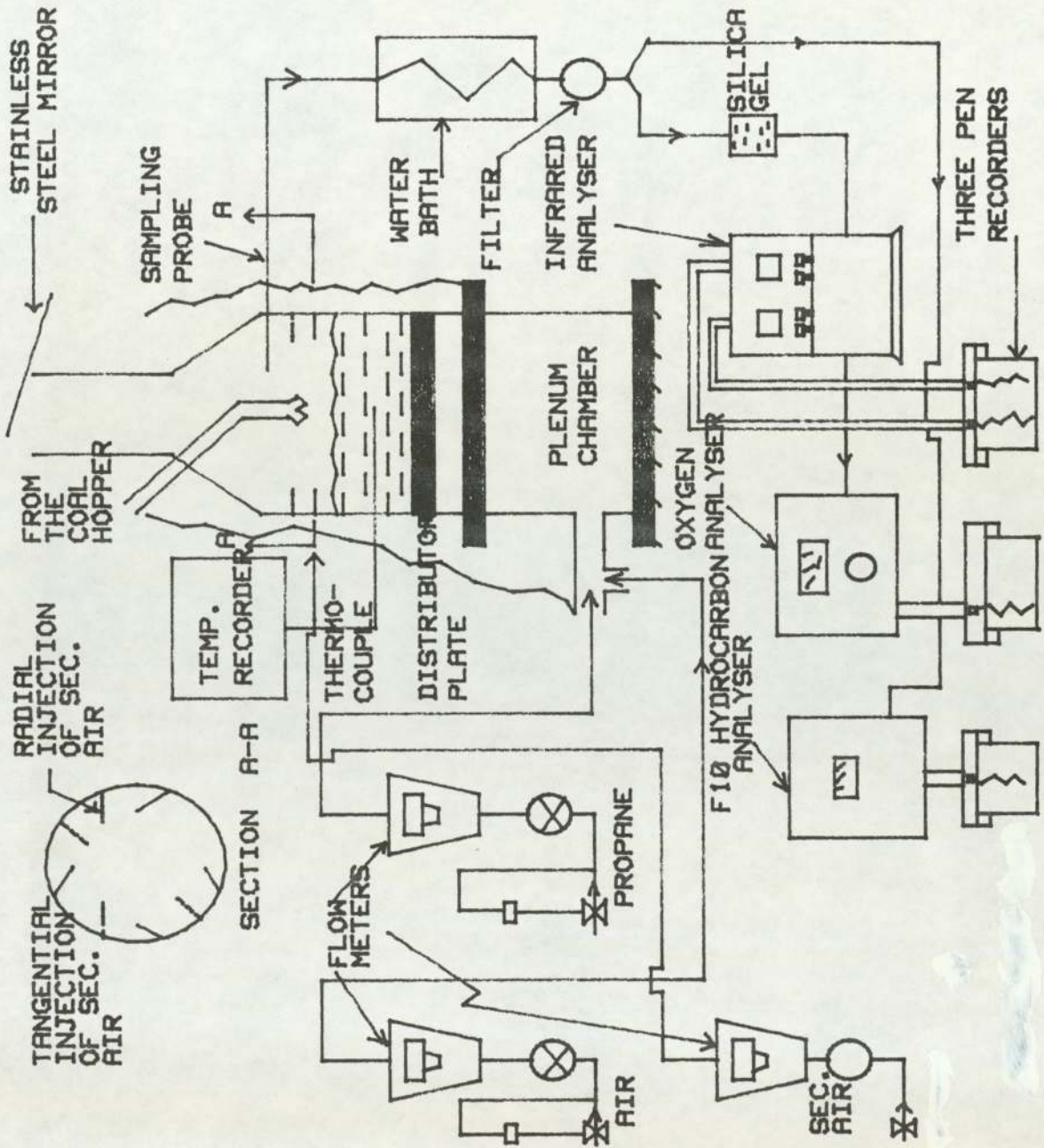


FIG. 5.1 EXPERIMENTAL FLUIDIZED BED COMBUSTOR



FIG. 5.2 PHOTOGRAPH SHOWING THE CONE SHAPED CHIMNEY WITH THE ATTACHED CONE FOR COAL DISTRIBUTION

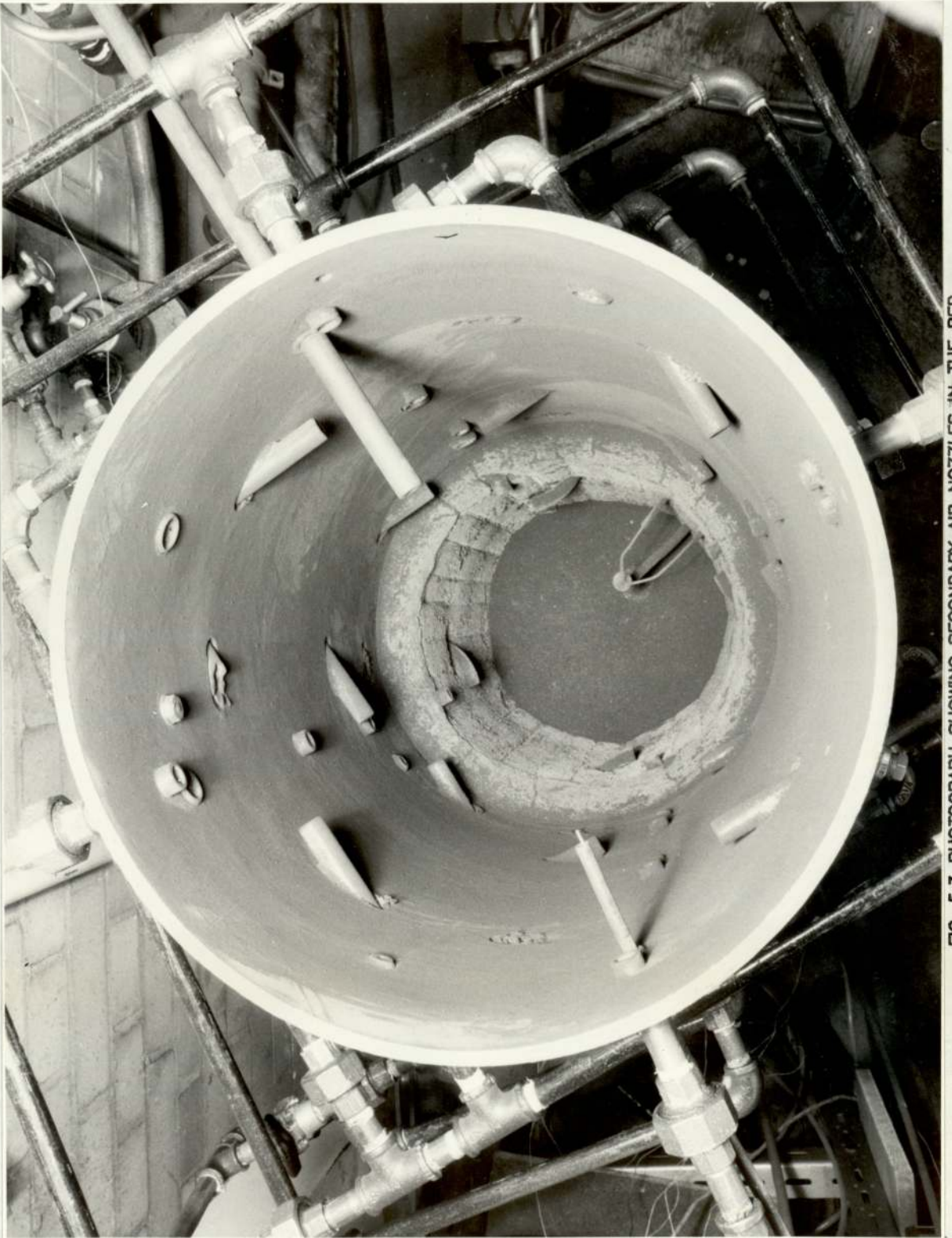


FIG. 5.3 PHOTOGRAPH SHOWING SECONDARY AIR NOZZLES IN THE BED

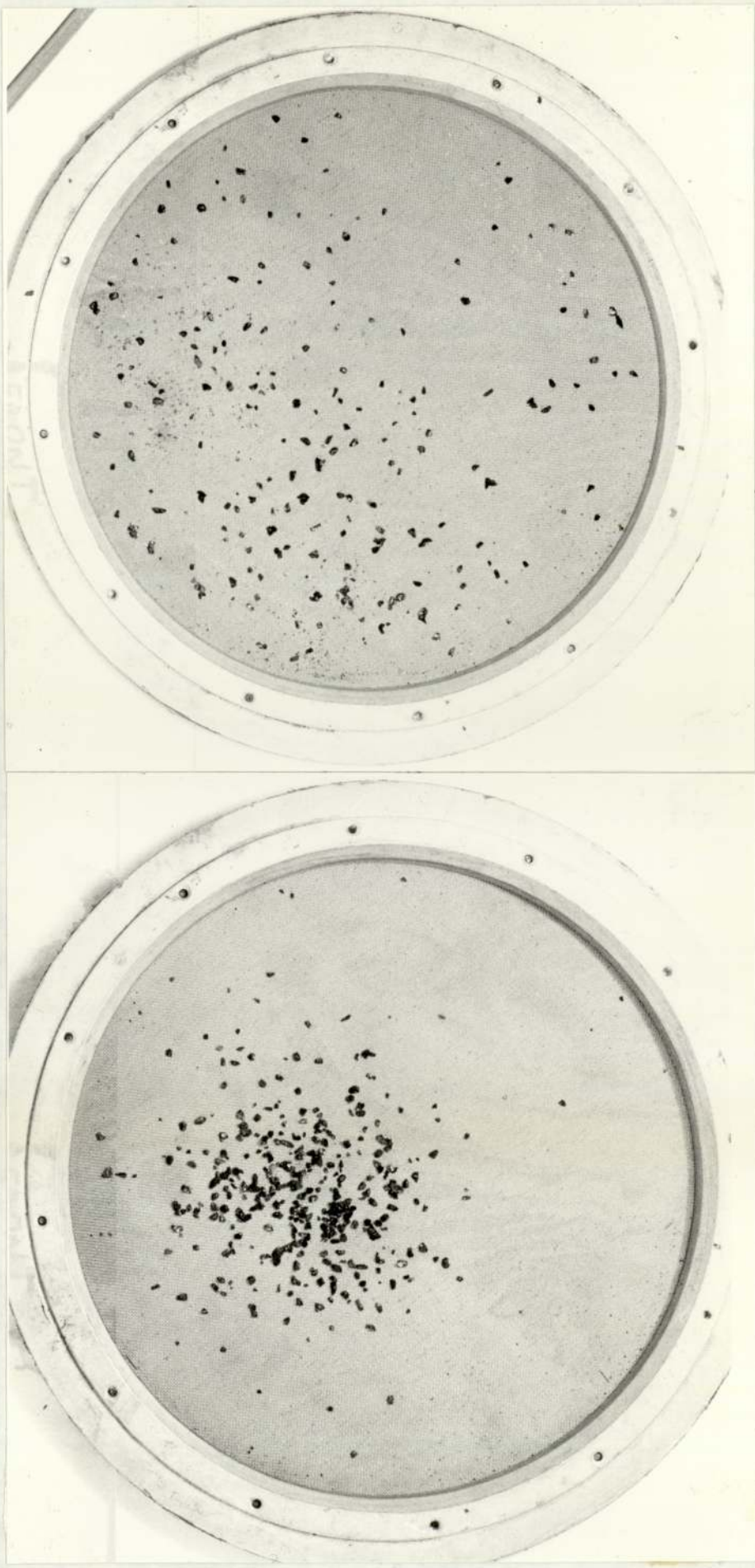


FIG. 5.4

PHOTOGRAPHS SHOWING COAL DISPERSION IN THE BOWL OF WATER BEFORE THE EXTENSION OF THE CHUTE AND THE ATTACHED CONE
(Long vertical chute, no cone)

FIG. 5.5

PHOTOGRAPHS SHOWING COAL DISPERSION IN THE BOWL OF WATER BEFORE THE EXTENSION OF THE CHUTE AND THE ATTACHED CONE
(Short vertical chute, no cone)

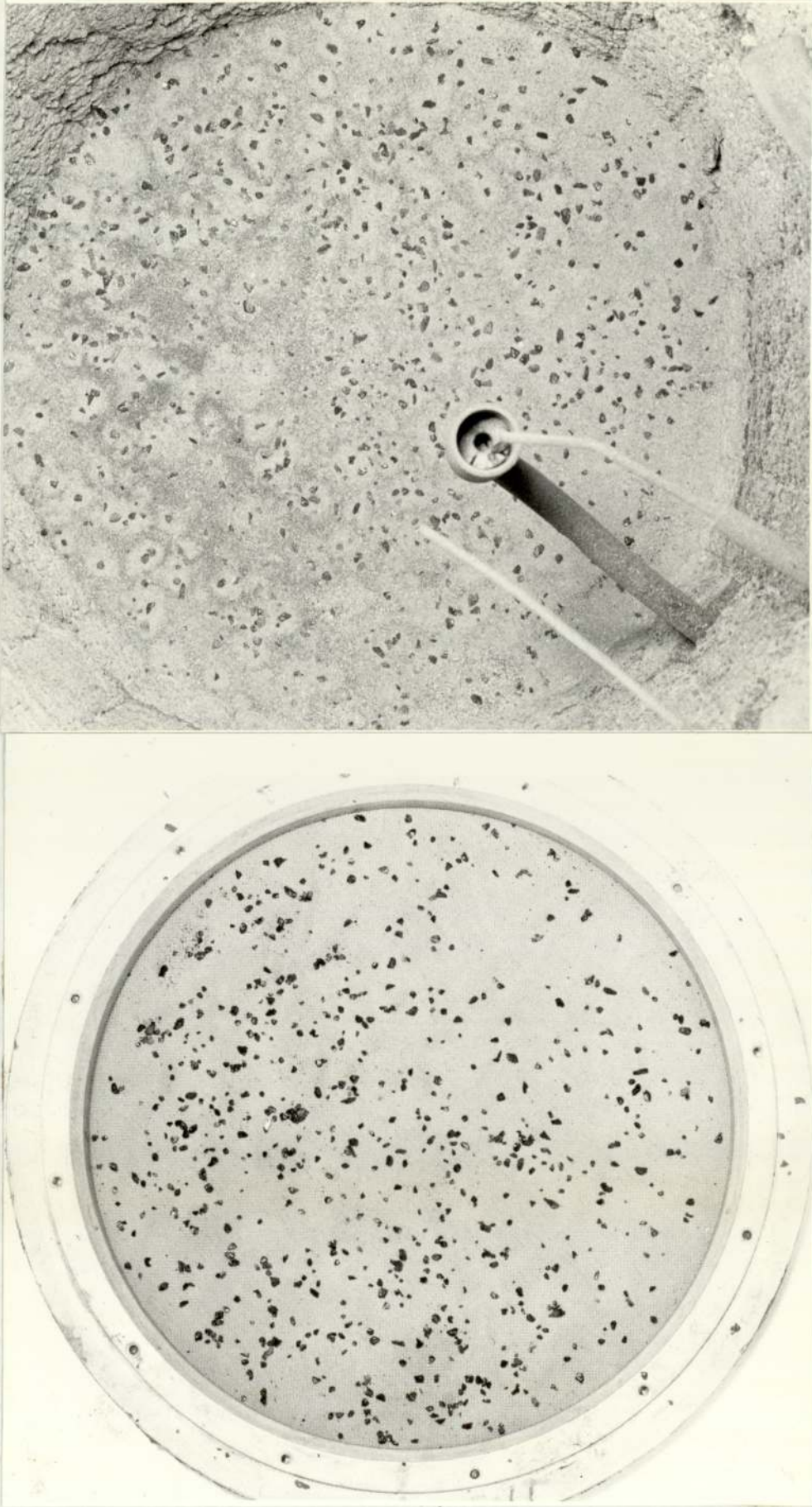


FIG. 5.6

PHOTOGRAPHS SHOWING COAL DISPERSION IN THE BOWL OF WATER AND IN THE BED OF SAND FLUIDIZED WITH AIR AFTER THE EXTENSION OF THE CHUTE AND THE ATTACHED CONE
(Long chute, with cone)

FIG. 5.7

(Long chute, with cone)

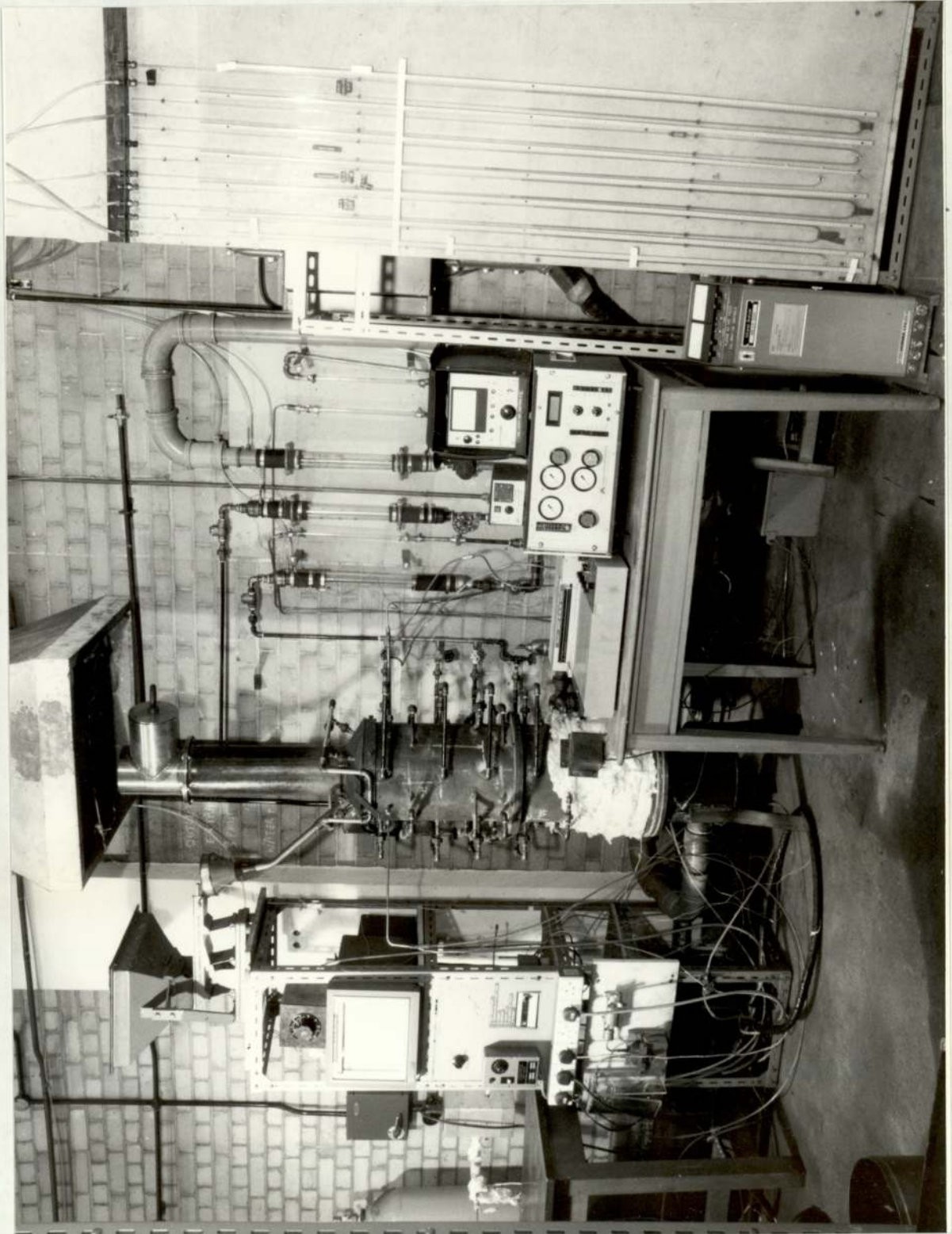


FIG. 5.10 PHOTOGRAPH OF THE EXPERIMENTAL APPARATUS

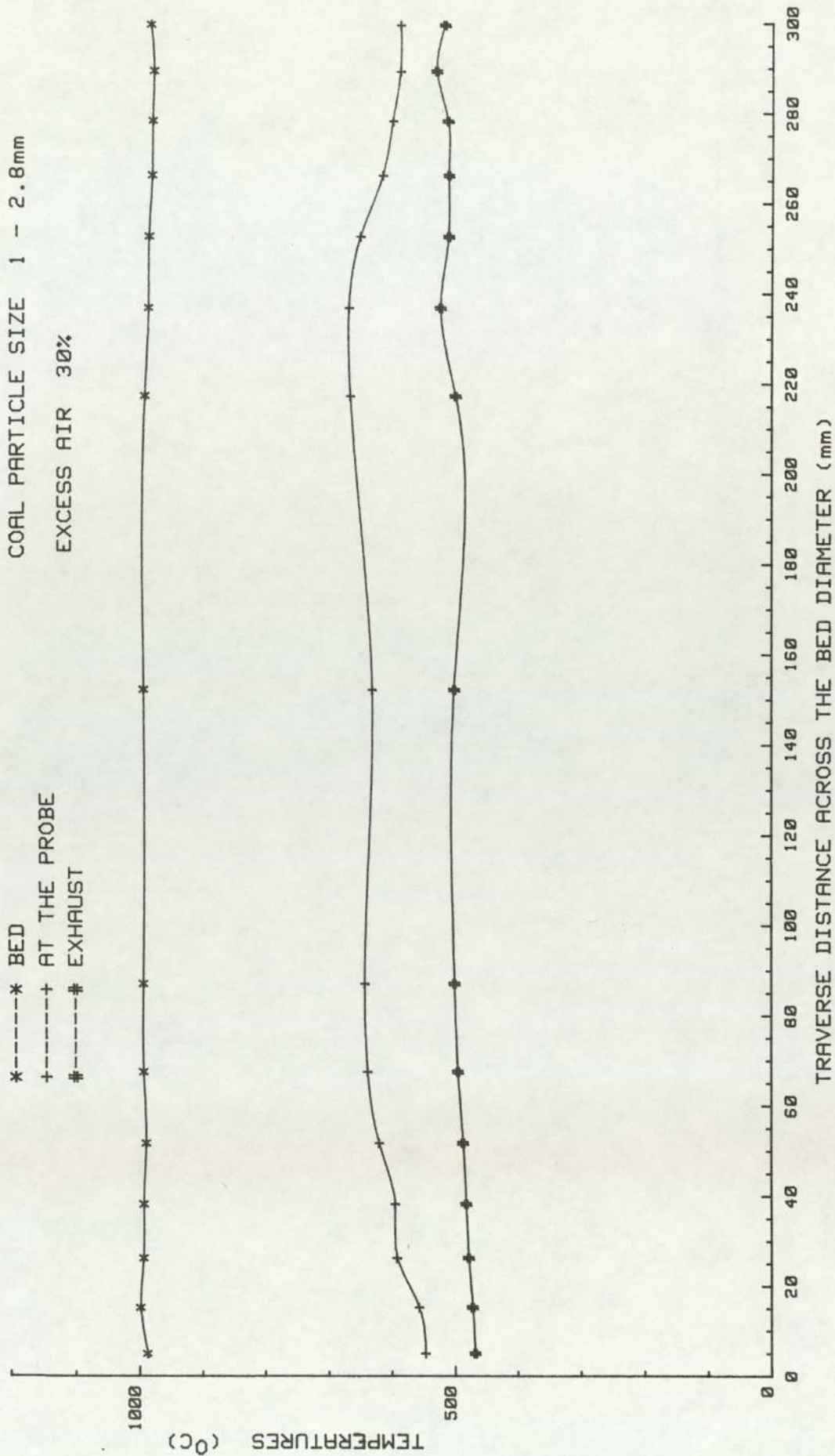


FIG. 5.14 TEMPERATURE MEASUREMENT FROM BURNING BITUMINOUS COAL EXPERIMENT
(UNINSULATED CONDITION)

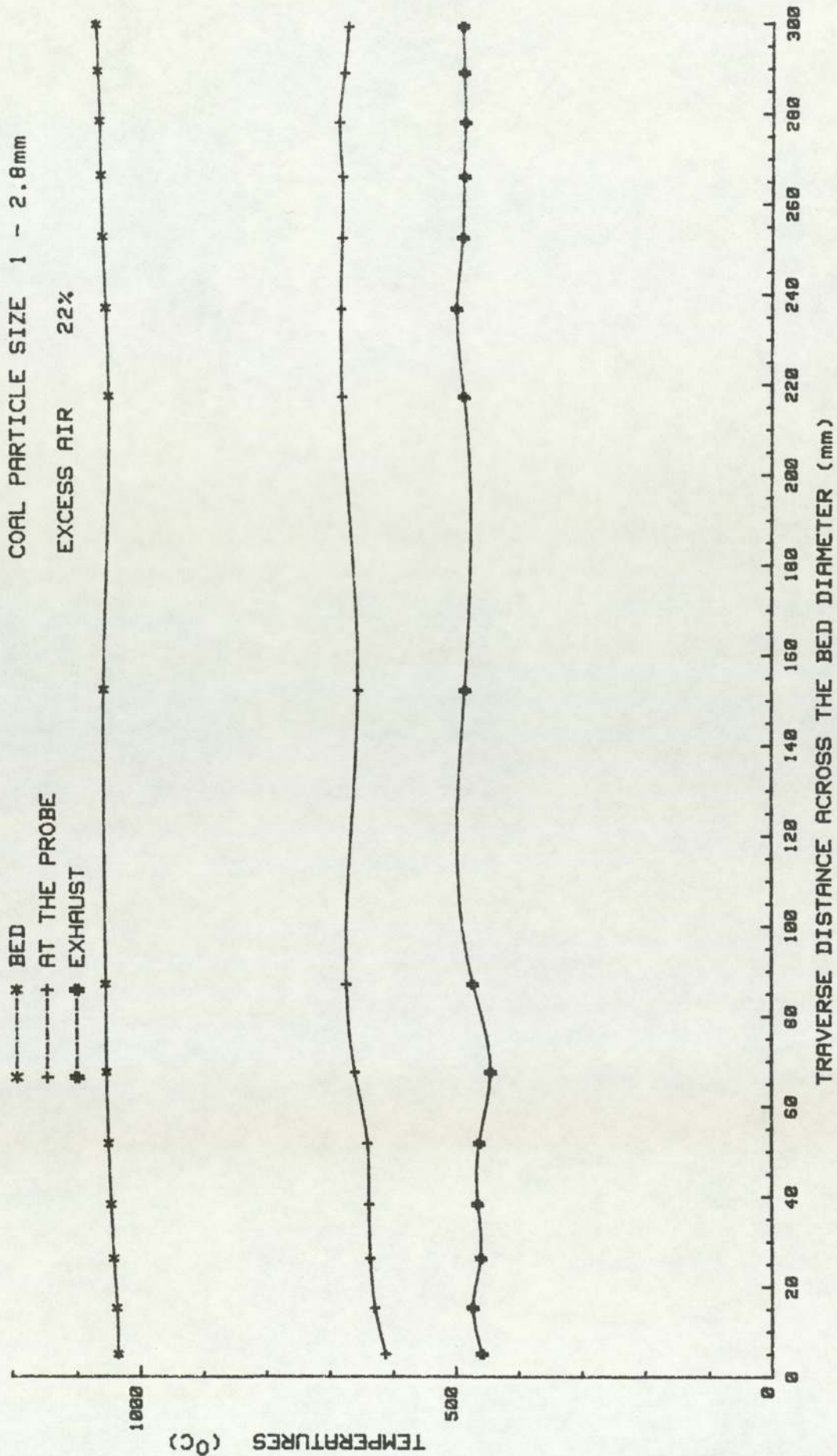


FIG.5.15 TEMPERATURE MEASUREMENT FROM BURNING BITUMINOUS COAL EXPERIMENT
(INSULATED CONDITION)

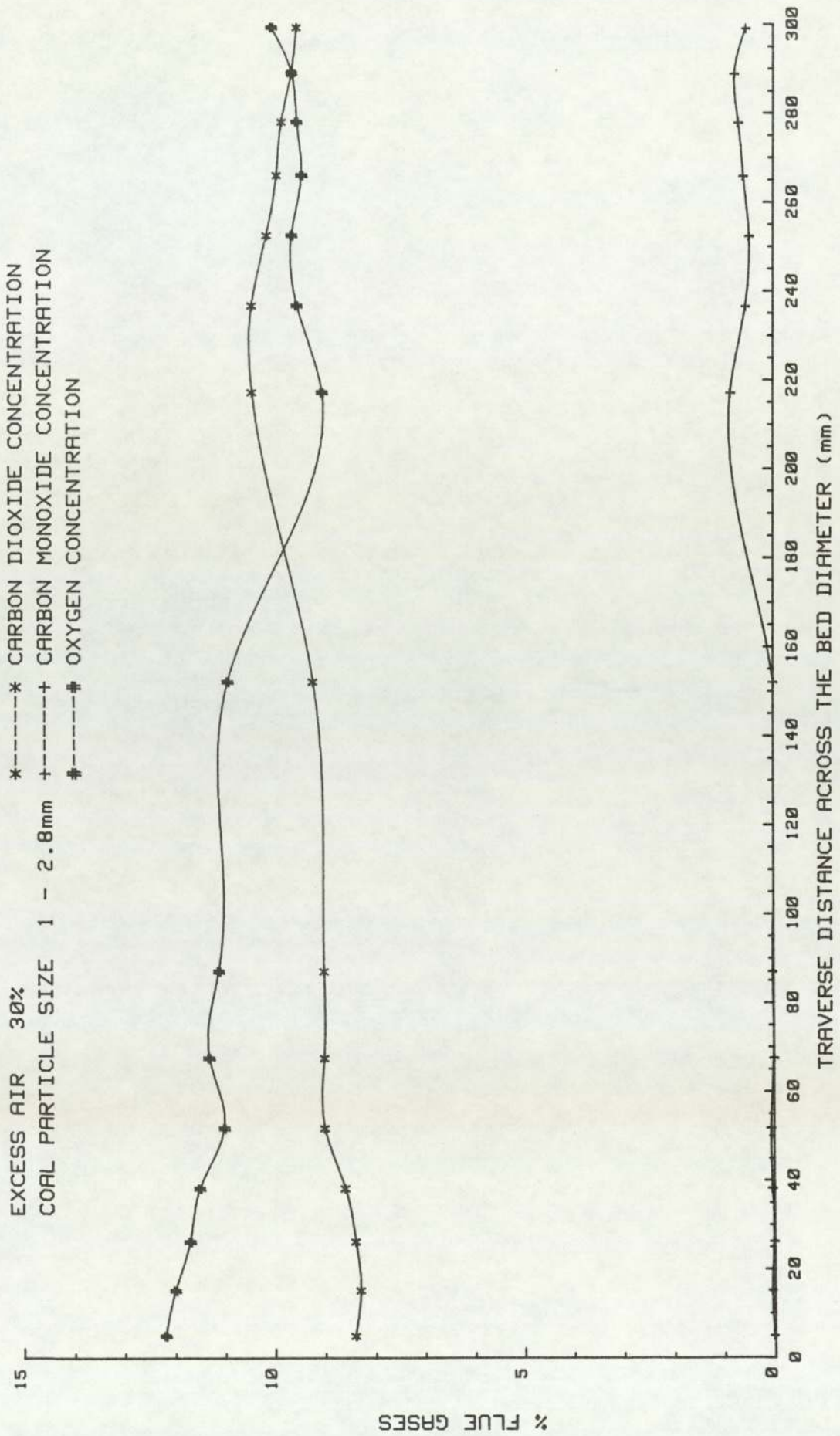


FIG.5.16 GAS CONCENTRATIONS FROM BURNING BITUMINOUS COAL EXPERIMENT
(UNINSULATED CONDITION)

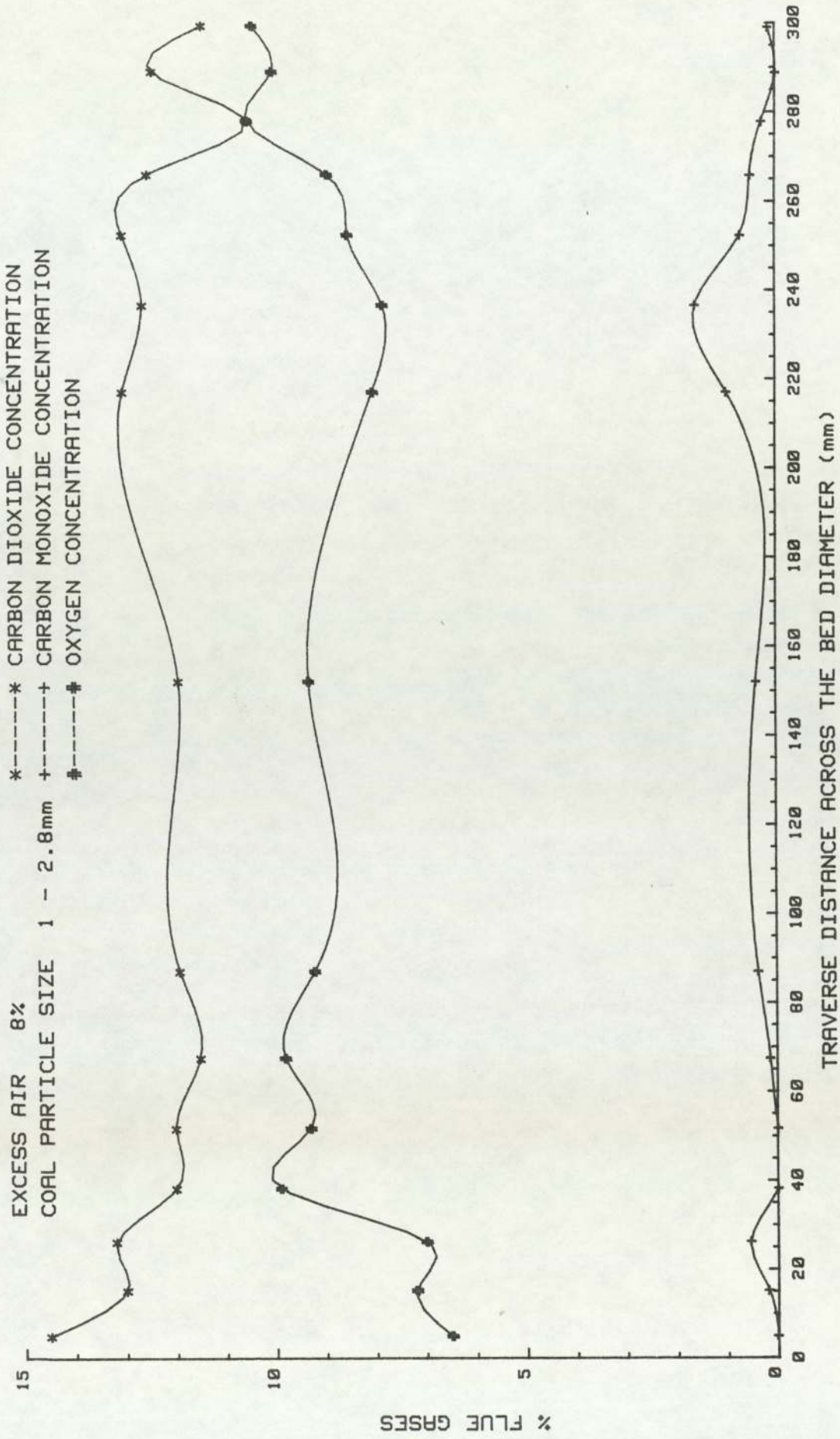
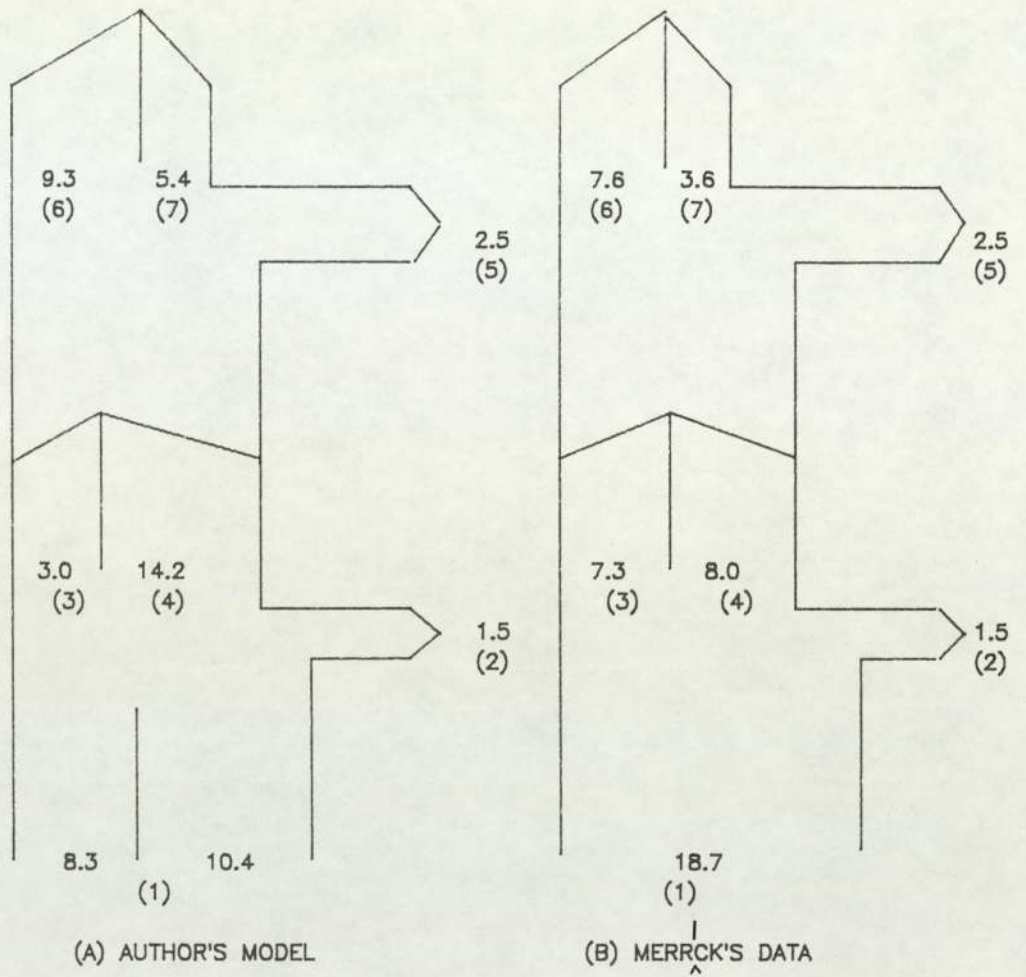


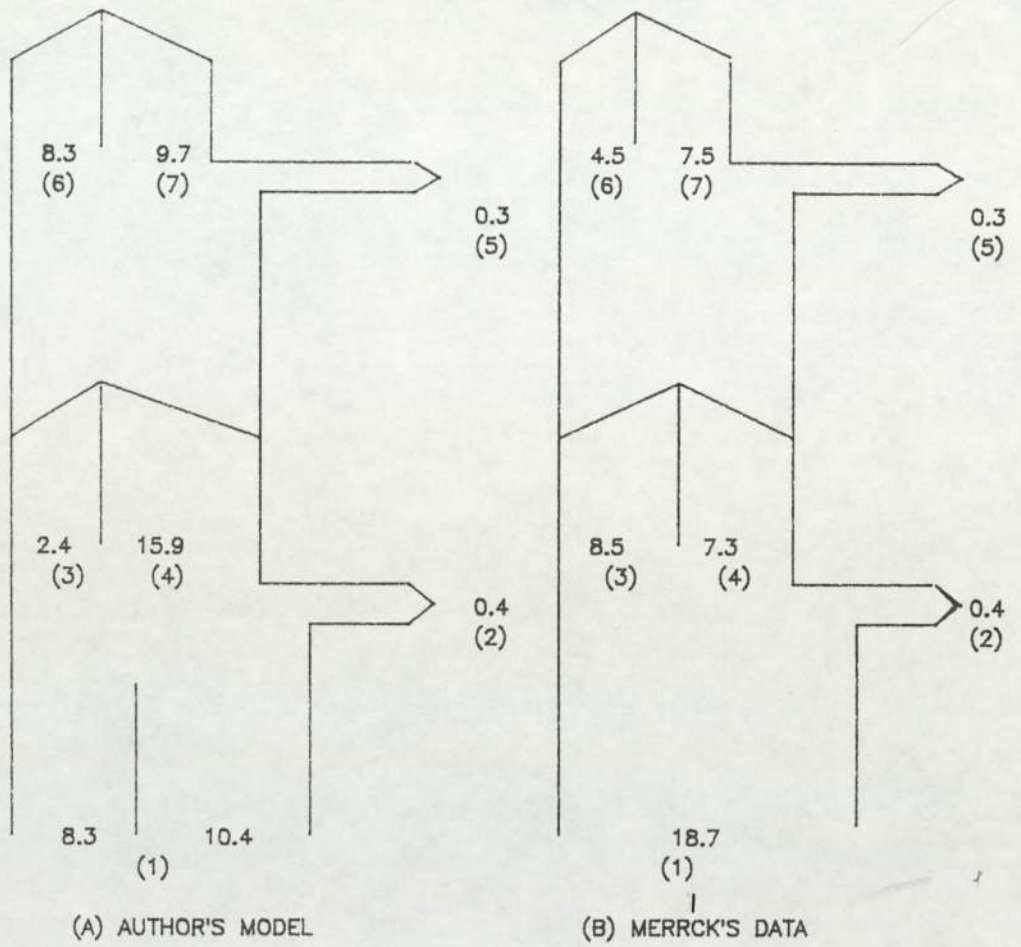
FIG.5.17 GAS CONCENTRATIONS FROM BURNING ANTHRACITE COAL EXPERIMENT (UNINSULATED CONDITION)



ALL QUANTITIES ARE IN KW.

- (1) Energy in the fuel
- (2) Heat loss by radiative and convective losses ^{from} the bed
- (3) Enthalpy of unburnt HC ^{leaving} the bed
- (4) Enthalpy of hot gases and unburnt volatiles
- (5) Heat losses by radiative and convective losses in the freeboard
- (6) Enthalpy of unburnt HC at the freeboard temperature
- (7) Enthalpy of hot gases

FIG. 5.18 SANKEY DIAGRAM USING AUTHOR'S MODEL AND MERRICK'S DATA
(UNINSULATED CONDITION)



ALL QUANTITIES ARE IN KW.

- (1) Energy in the fuel
- (2) Heat loss by radiative and convective losses ^{from} the bed _{leaving}
- (3) Enthalpy of unburnt HC ^{at} the bed
- (4) Enthalpy of hot gases and unburnt volatiles
- (5) Heat losses by radiative and convective losses in the freeboard
- (6) Enthalpy of unburnt HC at the freeboard temperature
- (7) Enthalpy of hot gases

FIG. 5.19 SANKEY DIAGRAM USING AUTHOR'S MODEL AND MERRICK'S DATA
(INSULATED CONDITION)

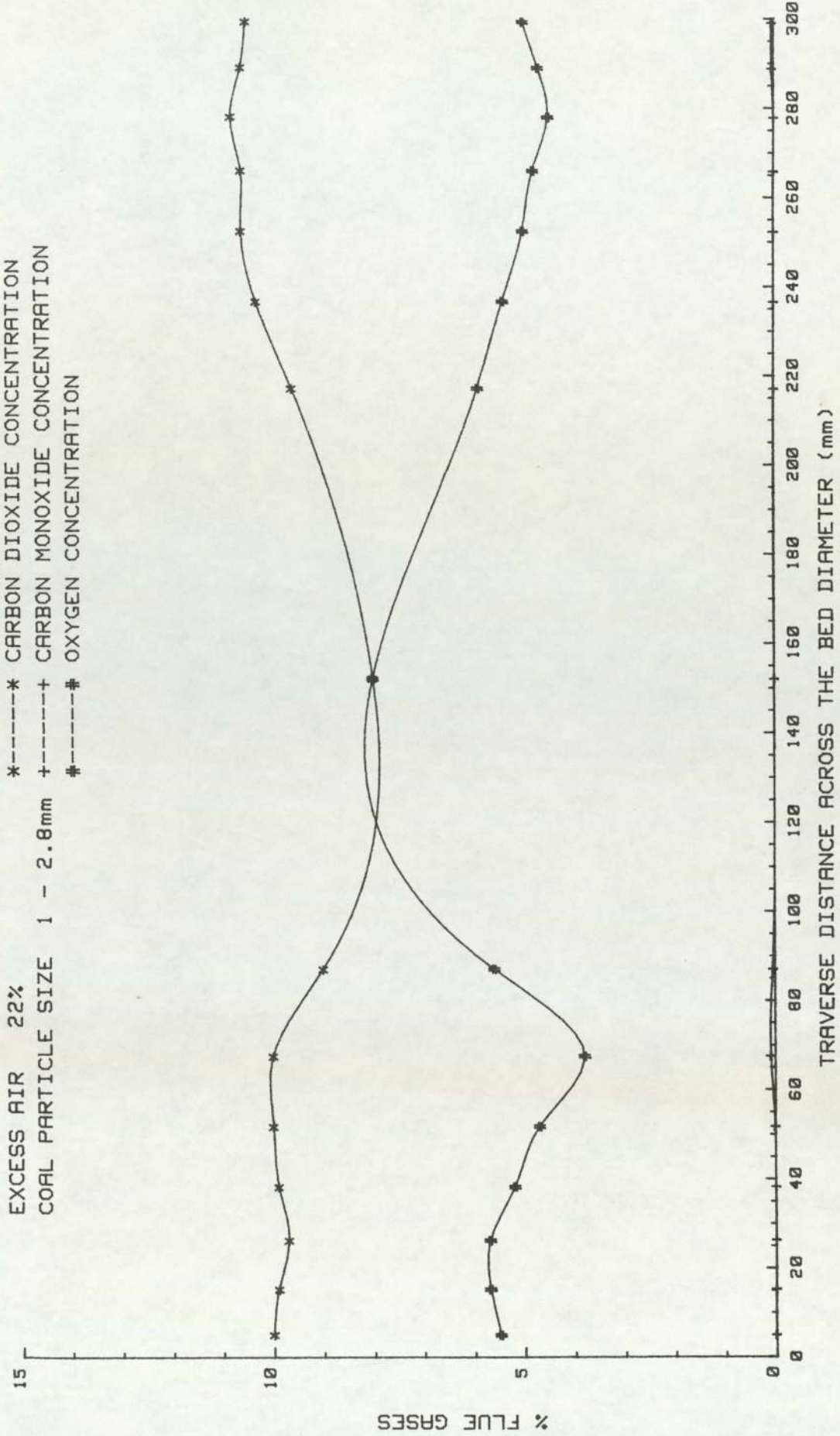


FIG.5.21 GAS CONCENTRATIONS FROM BURNING BITUMINOUS COAL EXPERIMENT
(INSULATED CONDITION)



FIG. 5.22 PHOTOGRAPH SHOWING THE SINTERED BED SURFACE



FIG. 5.23 PHOTOGRAPH SHOWING THE BURNOUT OF THE PILOT BURNER

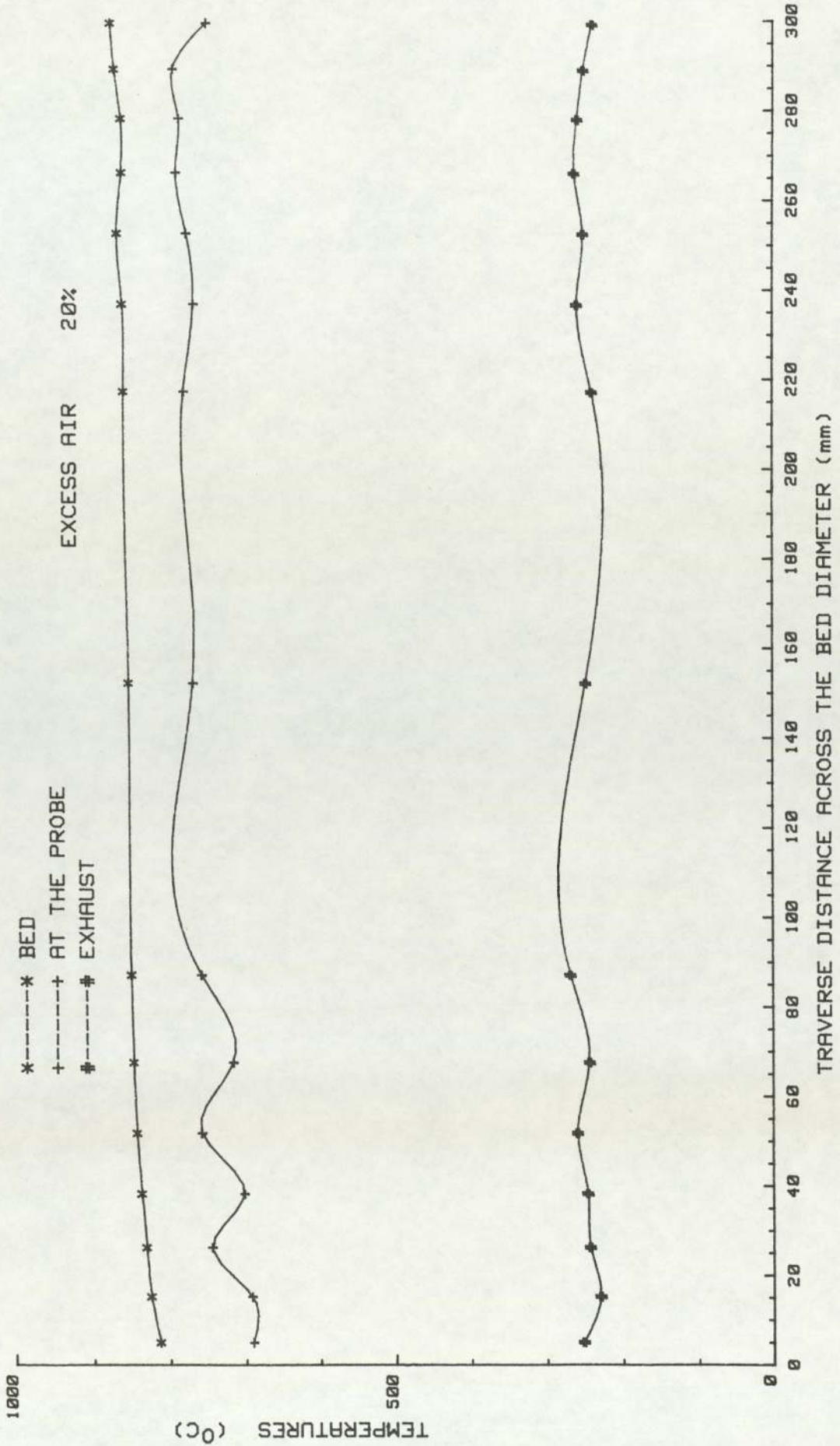


FIG.5.25 TEMPERATURE MEASUREMENT FROM BURNING WOOD EXPERIMENT
(INSULATED CONDITION)

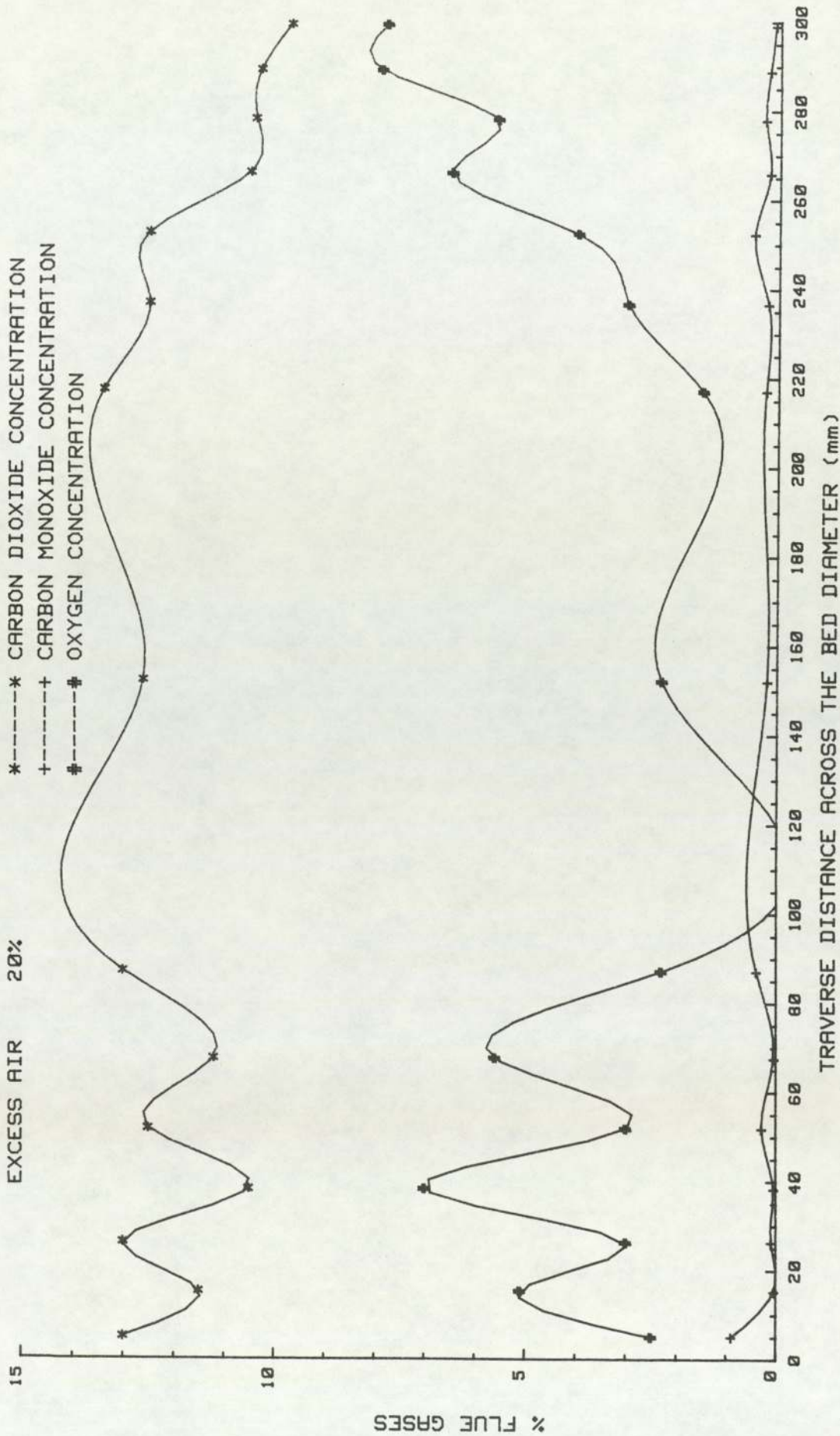


FIG.5.26 GAS CONCENTRATIONS FROM BURNING WOOD EXPERIMENT (INSULATED CONDITION)

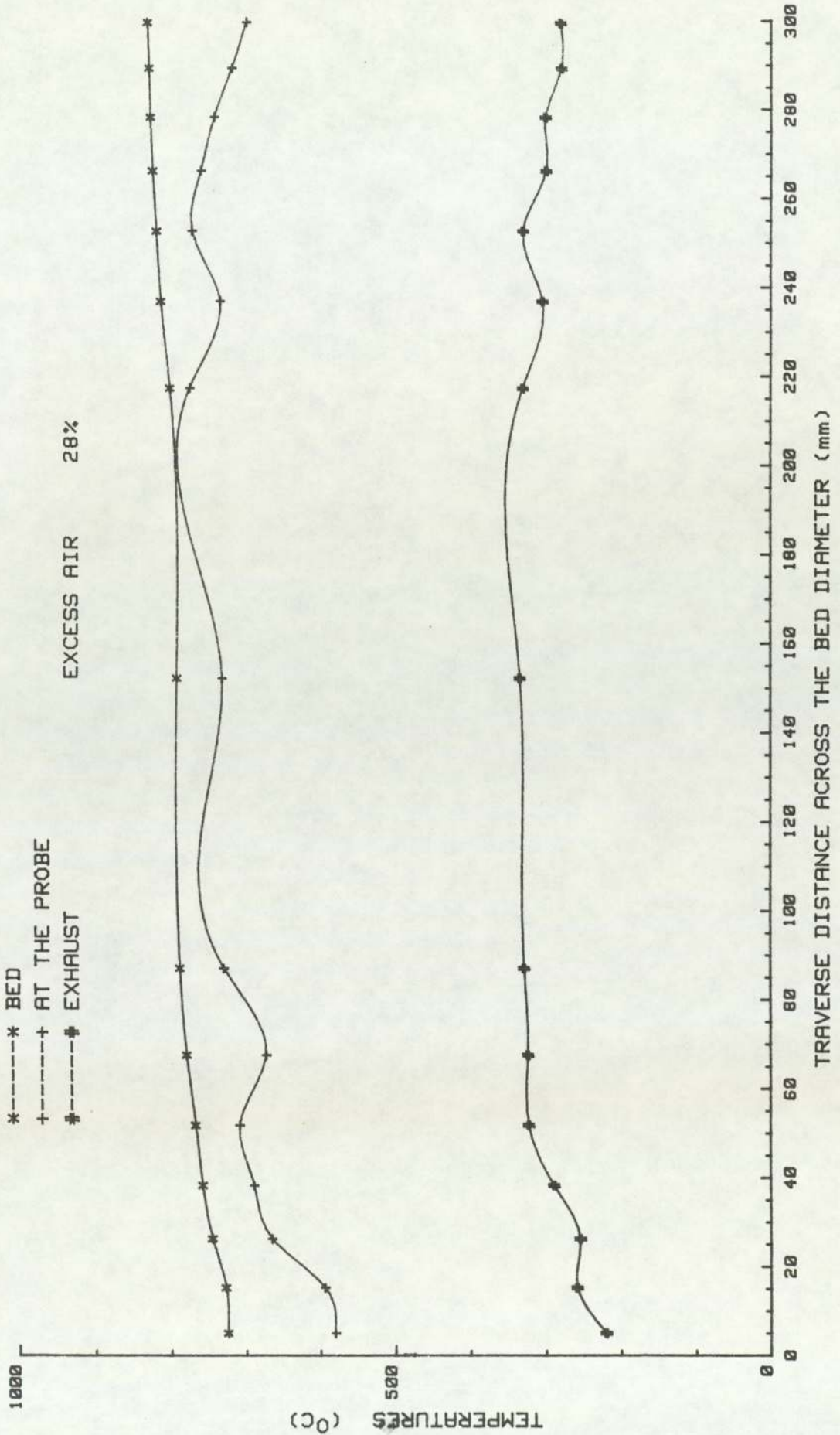


FIG.5.27 TEMPERATURE MEASUREMENT FROM BURNING WOOD EXPERIMENT
(INSULATED CONDITION)

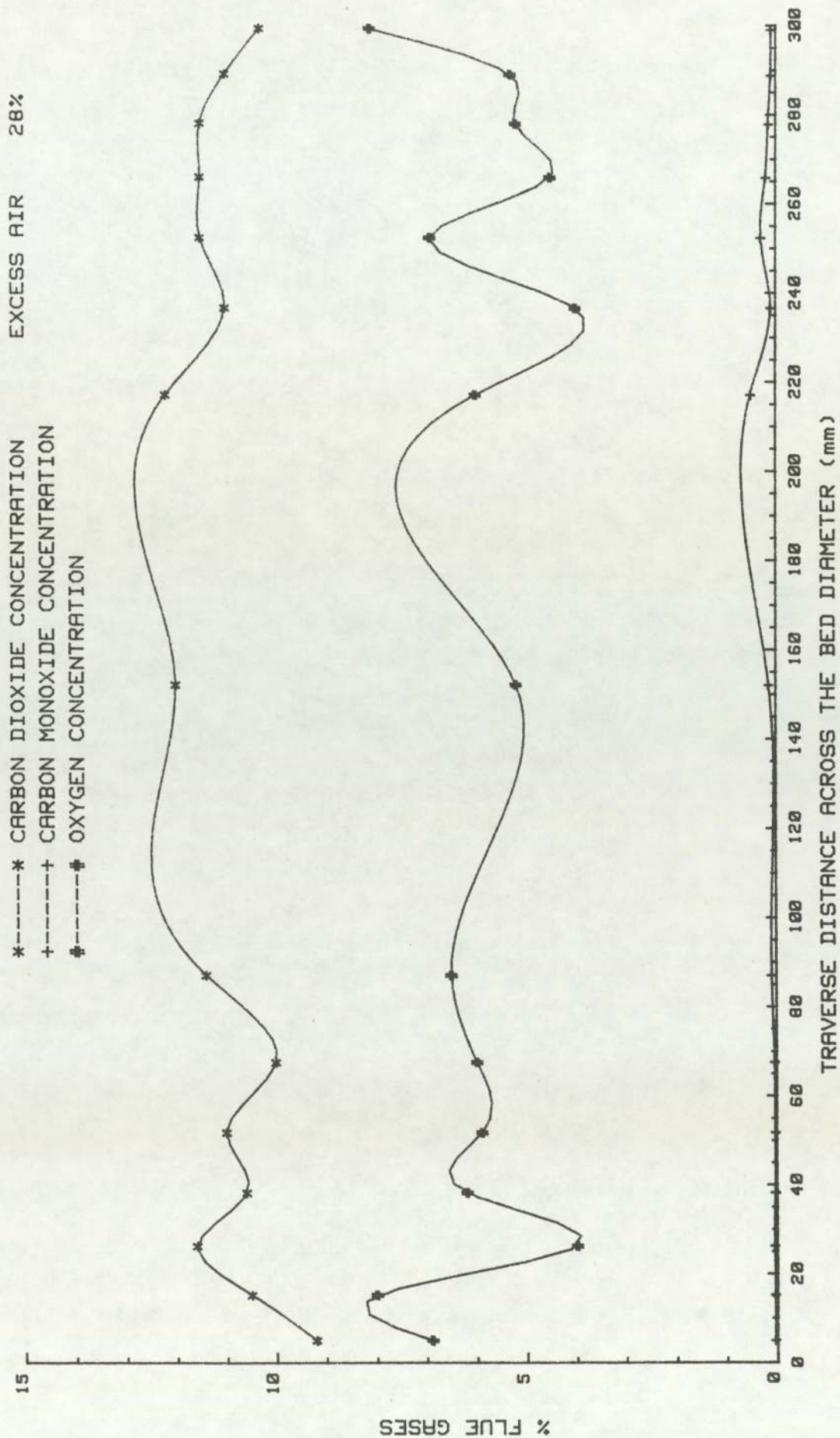


FIG. 5.28 GAS CONCENTRATIONS FROM BURNING WOOD EXPERIMENT
(INSULATED CONDITION)

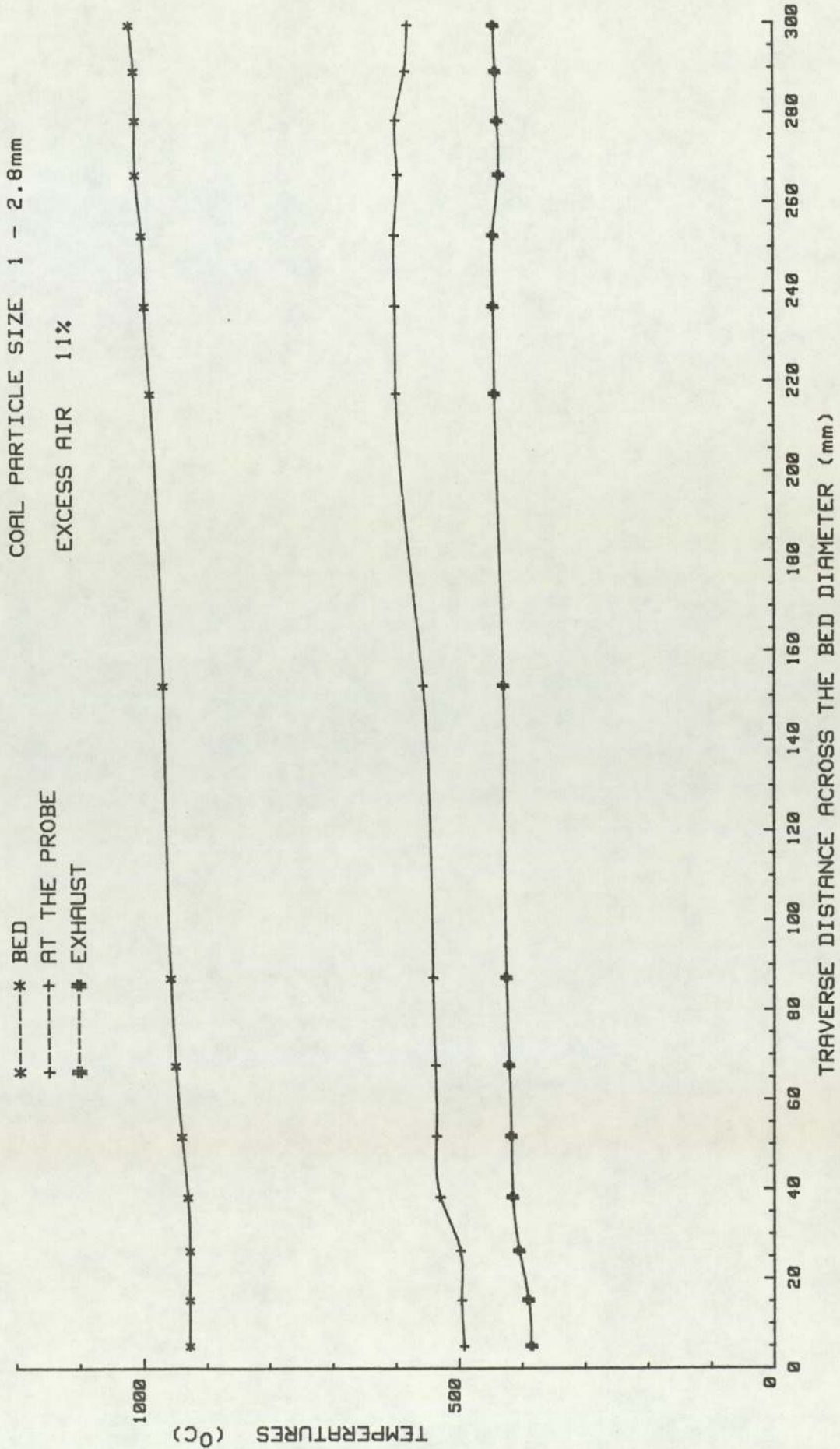


FIG.5.29 TEMPERATURE MEASUREMENT FROM BURNING BITUMINOUS COAL EXPERIMENT
(INSULATED CONDITION)

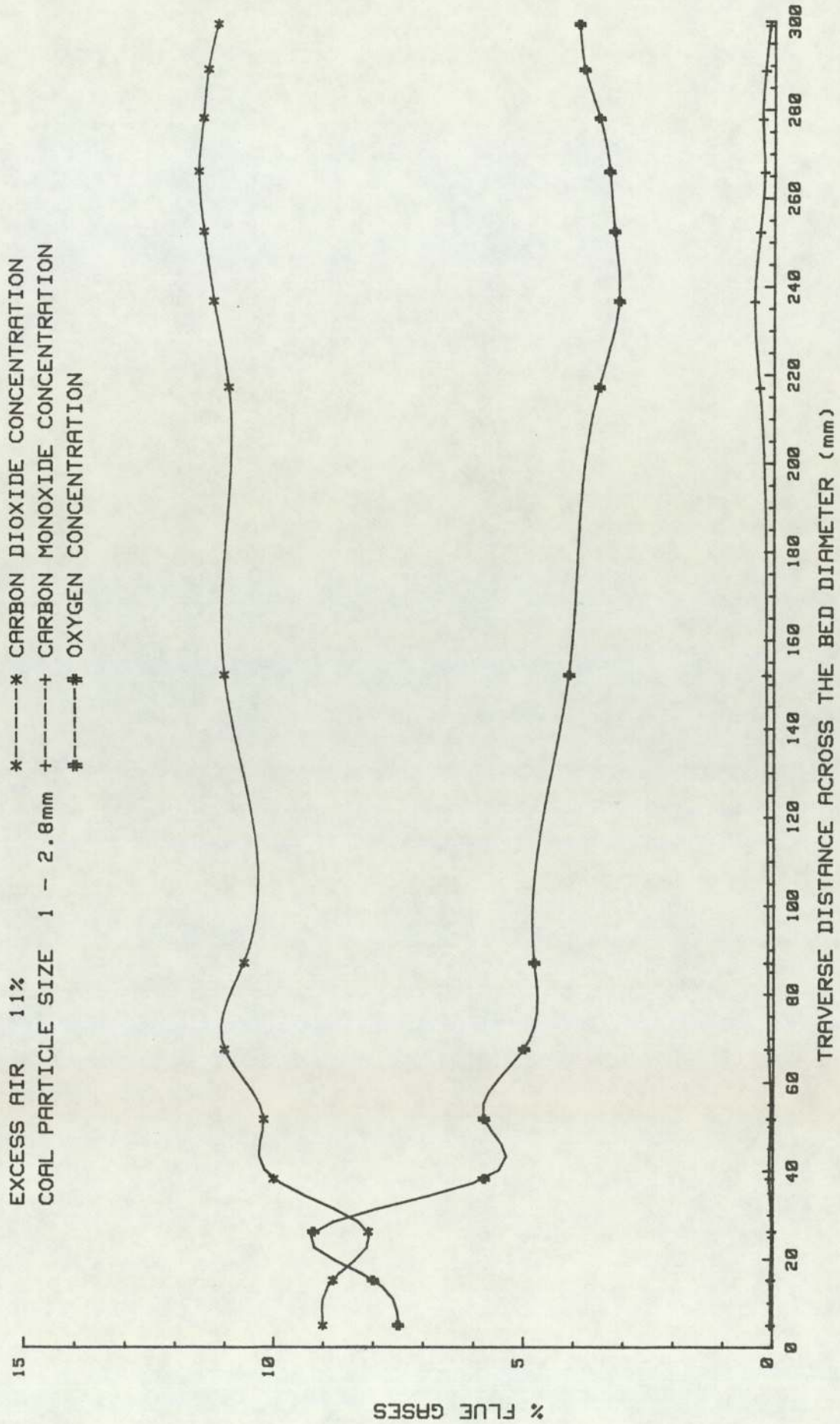


FIG.5.30 GAS CONCENTRATIONS FROM BURNING BITUMINOUS COAL EXPERIMENT
(INSULATED CONDITION)

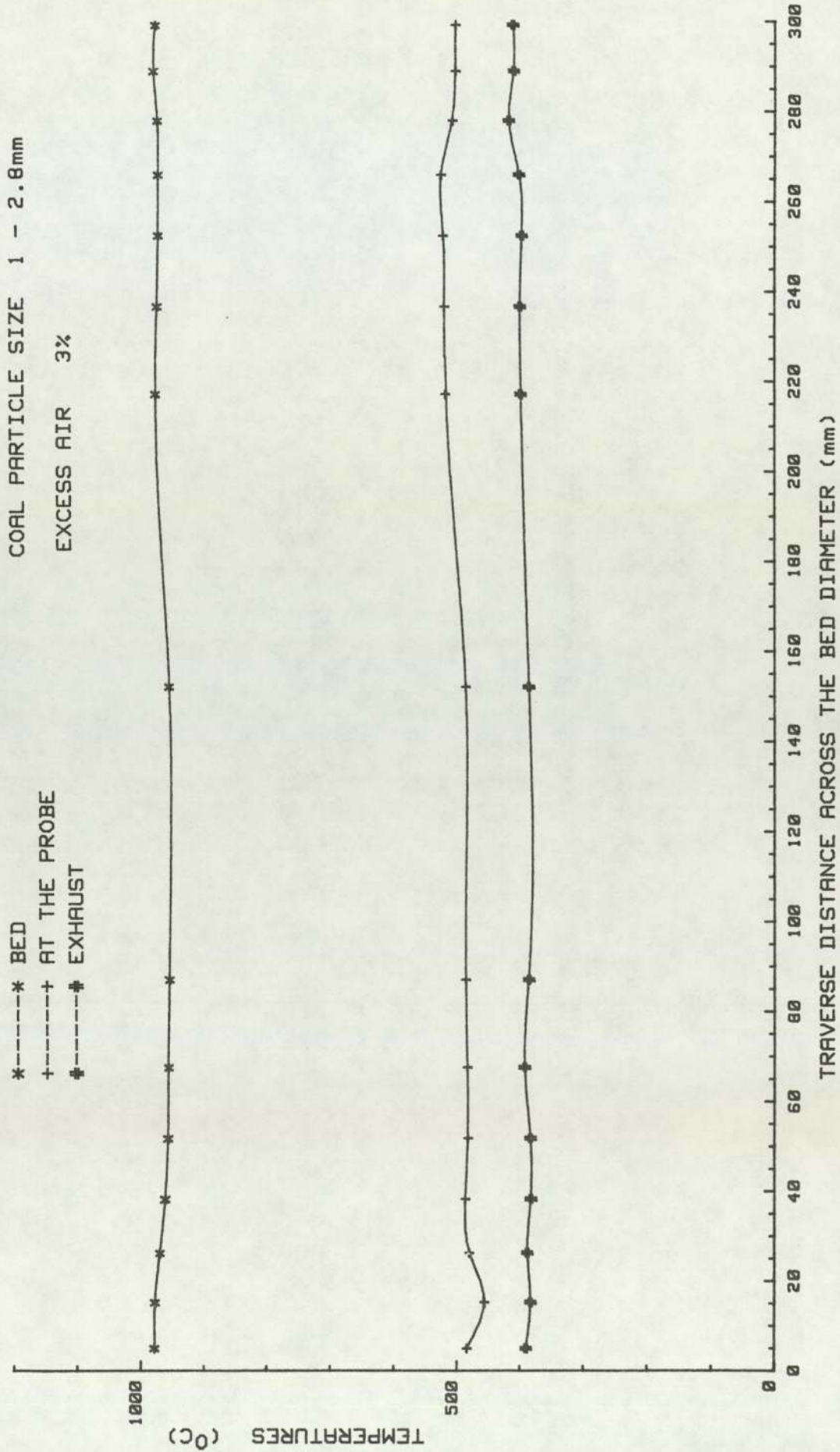


FIG.5.31 TEMPERATURE MEASUREMENT FROM BURNING BITUMINOUS COAL EXPERIMENT
(UNINSULATED CONDITION)

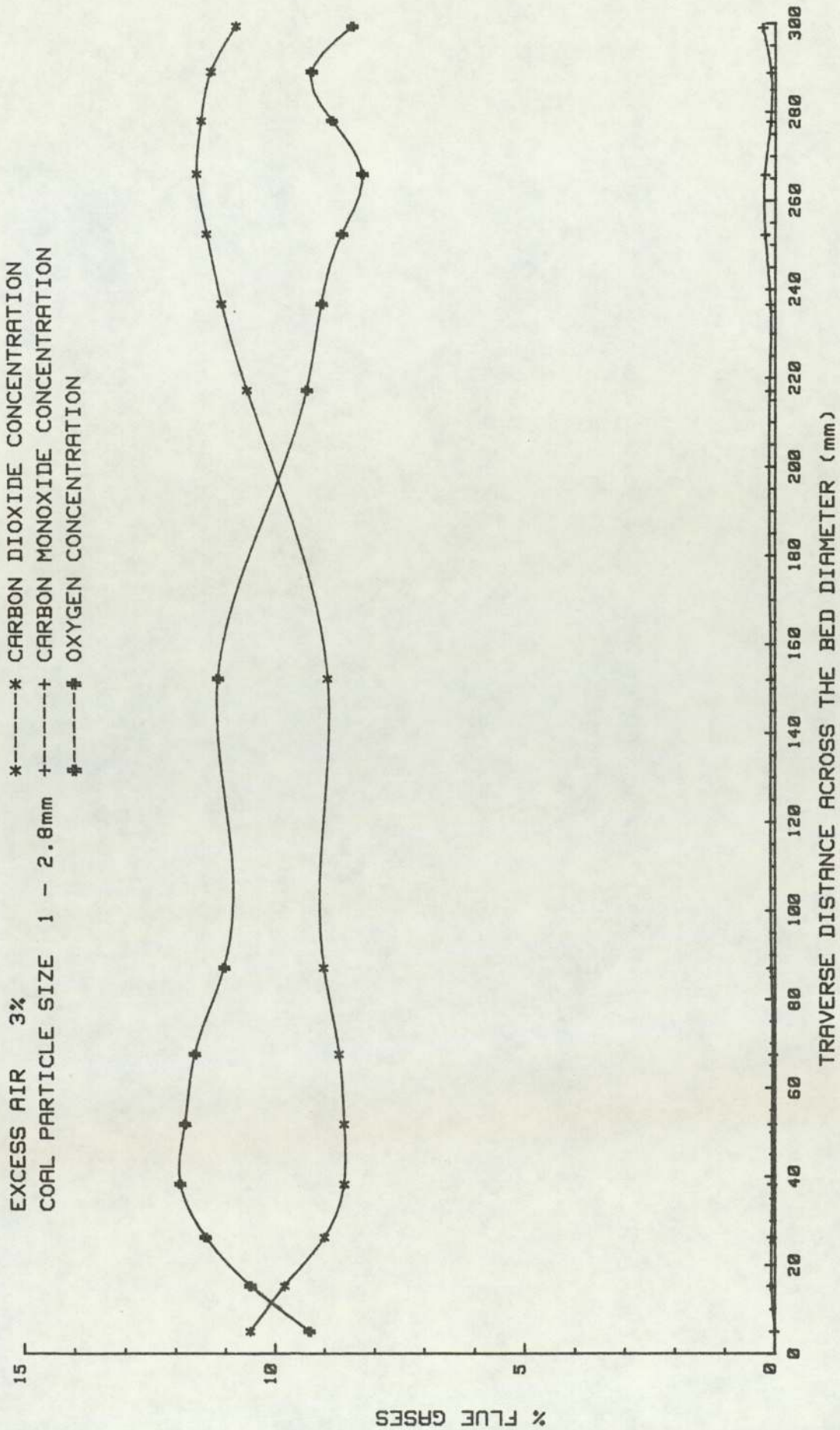


FIG.5.32 GAS CONCENTRATIONS FROM BURNING BITUMINOUS COAL EXPERIMENT
(UNINSULATED CONDITION)

CHAPTER SIX

GENERAL DISCUSSION ON PRESENT EXPERIMENTAL FINDINGS

1. In chapter three, part A of this thesis, a theoretical assessment of the combustion of solid fuel was undertaken to ascertain the constraints which might determine the manner of combustion of coal and wood in fluidized beds. The assumptions used are discussed further in the light of the experimental findings reported in chapters 4 and 5.

Tables 5.1 and 5.2 showed that in a fluidized bed combustor burning high volatile fuels, more heat is released in the freeboard than in the bed. This can only be because although combustible volatiles are emitted in the bed, insufficient mixing of air and volatiles and inadequate residence time restricts the extent of their combustion. Burning of volatiles occurs in the freeboard zone above the bed where conditions are more favourable; but the combustion may still not proceed to completion.

As expected the behaviour was similar when the combustor was fuelled by wood. However, there was dissimilarity between the way in which wood and coal burnt, because wood contains about 80% volatiles and less fixed carbon than coal. This reduced the quantity of carbon burning in the bed and generated very little heat. That heat is possibly being consumed by the endothermic reactions of water vapour with carbon in the charred layers of the wood, to become carbon monoxide and hydrogen gases, Shelton (75).

2. Directly above the bed region, volatiles, elutriated carbon particles and carbon monoxide from the dense phase are poorly mixed with air from bursting bubbles. This mixing could probably be improved by any mechanical mixing device.

3. The coarser sizes of entrained carbon particles, representing the main loss, would normally require at least 25-30 seconds depending on size of particle for effective burnout, but this condition could not be obtained with velocities of about 0.4 - 0.5 m/s and a disengaging height of 800 to 900 mm.

4. There were no cooling tubes in the fluidized bed. Thus the heat generated was removed

- i by heat transfer to the side walls
- ii by radiation to the walls and roof of the combustion chamber and
- iii by the heated off-gas.

Mechanism (i) and (ii) removed relatively little heat.

5. Excess air was passed through the bed for combustion of volatiles.

CHAPTER SEVEN

SUMMARY OF CONCLUSIONS

A study of the major process in the combustion of volatile matter in a solid fuel fired fluidized bed combustor has been made.

1. Volatiles evolution time increases with increase in fuel size and it may take over a minute for a very large coal particle (6.7 - 8 mm). A significant extent of combustion of volatile matter is unlikely to occur within a shallow fluidized bed, even if under-bed feeding and/or many feed points are employed. Thus combustion of some volatile matter in the freeboard region above the bed is inevitable when burning high volatile fuels.
2. More heat is released in the freeboard than bed.
3. Excess air supplied through the bed improves volatiles combustion when coal is burnt. Excess air supplied through secondary air ports does not improve combustion without preheat.
4. When burning wood, excess air is best supplied above the bed.
5. Validity of Merrick's model (57) based on slow heating appears extendable beyond his range of experiments to fluidized beds where there are bigger ^{gas} velocities and higher particle heating rates.

CHAPTER EIGHT

RECOMMENDATIONS FOR FURTHER WORK

The present investigation has brought to light ^a number of important problems relevant to the design of a fluidized bed combustor. There are areas where more reseach and development are needed to define these ^{problems} _{more} clearly.

1. Further information is required on how volatiles are evolved and their subsequent combustion both theoretically and experimentally to develop a complete model of combustion of coal in fluidized beds. In particular the difficulties of getting more accurate mass balance and sampling gaseous ^{products} _{have} to be overcome.

^{in the pilot unit are required using}
2. Further tests ^{different} fuels of high volatile matter contents ^{to assess the validity of the} concept expressed in chapter three of this thesis, to establish design and operating characteristics and to provide a firm engineering base for full-scale industrial units. In particular, ^{the suggested} _{distribution} of heat transfer surfaces require validation.

Further of
3. ^{study} _{the} reactivity of coal in fluidized beds with combustion tests using coals of wider range of reactivity, and ^{with} detailed and careful analysis of the obtained data.

Further
4. ^{experiments} with removal of heat from the bed and/or the

freeboard will be very helpful to further strengthen the validity of the model in chapter three, (part A) for the combustion of volatiles and to control the bed temperature. Also the effect of temperature of secondary air should be studied.

5. Use of recycled combustion products to control bed temperature and elutriation of unburnt carbon or char should be studied.

6. Improved diagnostic and analytic techniques for the measurement of time average and fluctuating concentrations of gases, temperatures and velocities in continuously fed fluidized bed combustors and estimation of concentration of higher hydrocarbons will be very helpful especially for the experimental research in which mathematical models and the predicted values of combustion gases are tested.

7. This work assumes no coal particle swelling or breaking which often occurs when a coal particle is fed into the bed. Pecanha (79) did a lot of work on this. It is suggested that allowance for this in subsequent work should be attempted.

8. Study should concentrate on the space directly above the bed, heavily laden with particles from bursting bubbles, many of these particles dropping back into the bed. Conditions in this zone can be quite different dependent on whether the freeboard is highly cooled or not but its importance should not be overlooked as a region in which

heat release can occur, some of the heat returns to the bed in the particles falling back to the bed after disengagement.

10. There may be advantages in a fluidized bed system for combustion of wood over conventional system. Its use in municipal and rural electrification requirements especially in African and Asian countries where wood supply is in abundance is worthy of consideration.

11. Limiting primary air through the bed and striving for secondary air through the nozzles for combustion of gases is more practical in wood combustion than in coal combustion. Such systems have the potential for high efficiency and steady heating. Further experimental study on this will be more helpful.

APPENDIX A

Theoretical Investigation.

A1 Thermodynamic analysis of heat release.

Using a fuel based upon Rose and Cooper (51), National Coal Board rank code number 101 and considering a coal fired fluidized bed boiler operating with 25% excess air, a bed temperature of 850C, the following assumptions are made.

Heat being released in the freeboard zone.

1. Gross calorific value to be 27MJ/kg. but that volatile contents account for 5%, 10%, 25%, and 50% of this gross calorific value respectively.
2. 95%, 90%, 75%, and 50% respectively of carbon and hydrogen are oxidized in the bed.
3. Gross calorific value of the volatiles is the same as the fuel.

Figures 3.2 and 3.1 show fluidized bed schematically and the system boundary enclosing the bed respectively. The flow of reactants, products of combustion, heat and ash are indicated.

From table 3.1 chapter 3, total oxygen required = 7.1043 kmol/kg fuel

Stoichiometric air/fuel ratio = $7.1043 \times 32/23.2 = 9.8 : 1$

Air/fuel ratio with 25% excess air = $1.25 \times 9.8 = 12.25:1$

Considering a bed of plan area 1m^2 , the mass flow rate of air M_a is given by

$$M_a = \rho_a U \quad (\text{A1.1})$$

where $\rho_a = 0.3139 \text{ kg/m}^3$ = air density at temperature and pressure, i.e 1 atmospheric and 850°C .

$$U = 1.2 \text{ m/s} = \text{velocity}$$

The corresponding mass flow rate of fuel M_f is also given by

$$M_f = M_a / (St + 0.25St) \quad (\text{A1.2})$$

where St = Stoichiometric air/fuel ratio by mass bed

From equations A1.1 and A1.2

$$M_a = 0.3139 \text{ kg/m}^3 \times 1 \text{ m}^2 \times 1.2 \text{ m/s} = 0.3767 \text{ kg/s} \quad (\text{A1.3})$$

$$M_f = M_a / St(1 + 0.25) = 0.3767 / 9.8 \times 1.25 = 0.0308 \text{ kg/s} \quad (\text{A1.4})$$

A2 Thermodynamic Considerations.

From equation 3.6 chapter 3, $(H_{p2} - H_{p0})$ is obtained by adding the last column of table 3.2 thus

$$(H_{p2} - H_{p0}) = 14379.3 \text{ kJ/kg fuel} \quad (\text{A2.1})$$

also from equation 3.5 chapter 3

$$(H_{RO} - H_{RL}) = (1 \times 0.94 + 1.25 \times 9.8 \times 1.005)(15 - 25) = -132.5 \text{ kJ/kg} \quad (\text{A2.2})$$

and from equation 3.7 chapter 3

$$\Delta H_0 = \text{Higher calorific value of the fuel} = -27 \text{ MJ/kg fuel} \quad (\text{A2.3})$$

Heat transfer Q to the bed from the surroundings is the addition of equations (A2.1), (A2.2) and (A2.3) giving

$$Q = 14379.3 + (-132.5) + (-27000) \text{ kJ/kg} \\ = -12753.2 \text{ kJ/kg fuel} \quad (\text{A2.4})$$

As with equations (A2.1), (A2.2) and (A2.3), but this time with 5%, 10%, 25% and 50% of the coal gross calorific value accounted for by the volatiles content, equation (A2.1) is

modified to

$$(H_{p2} - H_{p0}) = (1 - XV)H_{CO_2} + (1 - XV)H_{H_2O} + (1 - XV)H_{O_2} + (1 - XV)H_{N_2} + XH + XVH \quad (A2.5)$$

where XV is the fraction of volatiles evolved from the coal.

H is the enthalpy of the combustion products.

X is the fraction of ash in the coal.

From equation (A2.3) above

$$\Delta H_0 = -27000 \text{ kJ/kg fuel}$$

of which only 95%, 90%, 75% and 50% respectively are liberated in the bed, so that $(1 - XV)(\Delta H_0)$ could be written in place of (ΔH_0) in equation (A2.3). The heat transfer Q, from the bed is given by

$$Q = (H_{p2} - H_{p0}) + (1 - XV)(\Delta H_0) + (H_{RO} - H_{R1}) \quad (A2.6)$$

Table A1 shows the results of calculating the heat transfer Q from the bed using equation (A2.6).

The remaining 5%, 10%, 25% and 50% of all the fuels respectively oxidized in the freeboard zone.

Also for a fuel flow rate of 0.0308 kg/s from equation (A1.4) above, the rate of heat loss Q from the whole system must be

$$\begin{aligned} Q &= 0.0308 \text{ kg/s} \times 12753.2 \text{ kJ/kg fuel} \\ &= 393 \text{ kW.} \end{aligned} \quad (A2.7)$$

Assuming radiant heat loss and heat leakage through the bed containment to be 120 ^{kw} and 10 kw. respectively. The cooling requirements in the bed will then be

$$[393 - (120 + 10)] \text{ kw.}$$

$$= 263 \text{ kw.}$$

The rate of heat supplied by the fuel = $M_f \times \text{Calorific Value}$
 $= 0.0308 \text{ kg/s} \times 27000 \text{ kJ/kg}$
 $= 832 \text{ kw.}$

Therefore $(263/832 \times 100\%) = 32\%$ of the total heat supplied has to be removed by tubes in the bed.

FRACTION OF FULL BURST IN BED	COMBUSTION PRODUCTS							EVOLVED VOLUMES
	CO ₂	H ₂ O	O ₂	N ₂	ASH	(H ₂ O - H ₂)	(H ₂)	
0.25	0.080 Kg/Kg fuel	0.012 0.216	0.071043 2.073	0.31472 8.350	0.09	14101.7	0.05, 0.1 0.23, 0.20	
0.50	2.717 2053.0	0.209 376.3	2.108 1041.8	8.359 9092.9	40.8	14025.1	79.0	
0.75	2.574 2013.1	0.196 358.9	2.048 1046.5	8.258 9092.9	48.8	13448.3	100.0	
0.90	2.168 2094.5	0.162 299.7	1.705 1533.8	8.259 9092.9	48.8	12511.3	379.0	
	1.43 1386.3	0.105 199.9	1.137 1022.7	8.258 9092.9	40.8	12511.3	730.0	

HEAT TRANSFER FROM THE BED BY BURNING FRACTION OF FUEL IN THE BED FROM COMPOSITION OF COAL DESCRIBED IN TABLE 3.1 WITH 25% EXCESS AIR

TABLE A1

FRACTION OF FUEL BURNT IN BED	COMBUSTION PRODUCTS							EVOLVED VOLATILES	ASH	N ₂	O ₂	H ₂ O	CO ₂	MOL Kg/Kgfuel	Kg/Kgfuel ENTHALPY (KJ/KgK)	(HP -HP) ₂₀	(ΔH) ₀	(HR -HR) ₁₀	Q
	0.065	0.012	0.071043	0.33422	0.08	0.05, 0.1	0.08												
0.95	2.86	0.216	2.273	9.358	-	0.25, 0.50	-	0.08	9.358	2.159	0.205	0.012	0.065	2.717	379.3	14191.7	- 25650	- 132.5	-11590.8 KJ/Kgfuel supplied
0.90	2513.4	358.9	1840.3	9092.9	49.6	150.0	-	49.6	9092.9	1840.3	358.9	0.194	2.574	2653.0	379.3	14005.1	- 24300	- 132.5	-10427.4 KJ/Kgfuel supplied
0.75	2094.5	289.7	1533.6	9092.9	49.6	375.0	-	49.6	9092.9	1533.6	289.7	0.162	2.145	2094.5	289.7	13445.3	- 20250	- 132.5	-6937.2 KJ/Kgfuel supplied
0.50	1396.3	188.8	1022.7	9092.9	49.6	750.0	-	49.6	9092.9	1022.7	188.8	0.108	1.43	1396.3	188.8	12511.3	- 13500	- 132.5	- 1121.2 KJ/Kgfuel supplied

HEAT TRANSFER FROM THE BED BY BURNING FRACTION OF FUEL IN THE BED FROM COMPOSITION OF COAL DESCRIBED IN TABLE 3.1 WITH 25% EXCESS AIR

TABLE A1

A3 Area of tube required to remove about 356.986 kW. heat from the bed to keep the temperature at 850 C.

Assumptions: Water in at 15°C
Water out at 90°C

$$Q = UA\Delta T_m$$

where Q = heat transferred from the bed
= 356.986 kW.

$$U = 150 \text{ W/m}^2 \text{ K}$$

U = overall heat transfer coefficient
= 150 W/m²K

A = area of the tube

$$\Delta T_m = \text{LMTD} = \frac{\theta_1 - \theta_2}{\text{Log } \theta_1 / \theta_2}$$

$$\text{where } \theta_1 = 850 - 15 = 835$$

$$\theta_2 = 850 - 90 = 760$$

$$\therefore \Delta T_m = (835 - 760) / \text{Log } 835 / 760$$

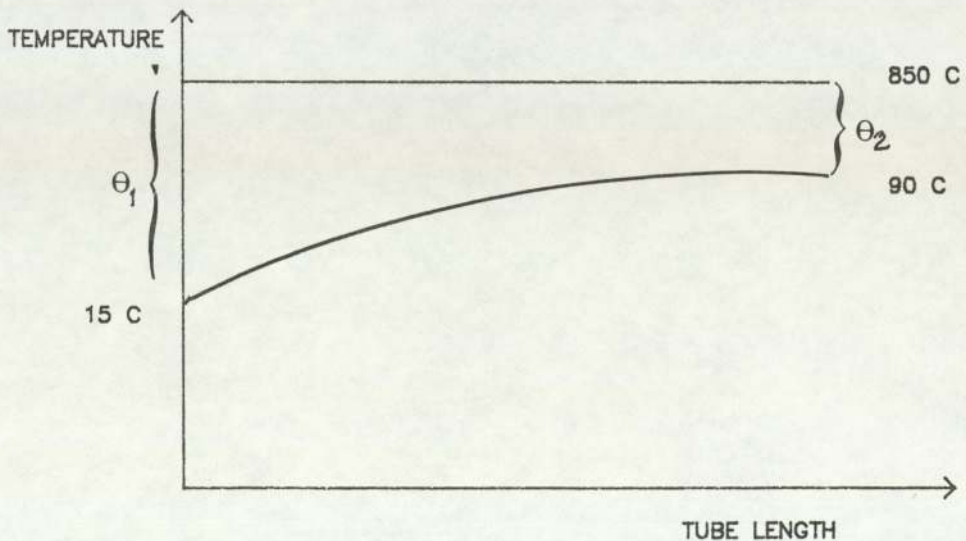
$$= 769.9 \text{ K}$$

$$Q = UA\Delta T_m$$

$$A = Q / U\Delta T_m$$

$$= 356.986 / 150 \times 769.9 \text{ [(kW} \times \text{m}^2 \text{K) / W K]} \times \text{[(10}^3 \text{W) / WK} \times \text{kW}]$$

$$= 3 \text{ m}^2$$



APPENDIX B

COMBUSTION EXPERIMENT WITH COAL

$$\text{Number of particles } N = \frac{M}{\frac{4}{3}\pi r^3 \rho_p}$$

where M = Mass of coal particles.

r = radius of particle.

ρ_p = density of particles.

$$= \frac{10 \times 10^3}{\frac{4}{3} (1.25 \times 10^{-3})^3 \times 1600} = 763.9$$

$$\text{Surface Area} = N \times 4 \pi r^2 = 0.0150$$

$$\text{Burning rate} = \frac{\text{Mass}}{\text{Time}} = \frac{\text{g}}{\text{s}} = \frac{3.7}{20} = 0.185$$

$$\begin{aligned} \text{Specific Emission rate} &= \text{Mass/Time} \times \text{Area} \\ &= \frac{\text{g}}{\text{sm}^2} = \frac{0.185}{0.0150} \\ &= 12.33 \end{aligned}$$

Fluidizing velocity at 800°C =

$$\begin{aligned} & \frac{361.9 \text{ Lit/min} \times ((800+273)/288) \times 4}{0.254^2 \text{ m}^2 \times [m^3/10^3 \text{ Lit.}] \times [\text{min}/60 \text{ sec}]} \\ & = 0.44 \text{ m/s} \end{aligned}$$

B1 HEAT RELEASED

30 gram of coal into the bed.

Moisture Content = 5.3%.

Mass of moisture = $0.053 \times 30 = 1.59$.

Mass of coal in the bed less moisture content = $(30 - 1.59) = 28.41$ g.

Out of this, $0.370 \times 30 = 11.1$ gram is the Volatile Matter.

After combustion, what remains is 7.78 grams.

Solid matter lost from the system = $28.41 - 7.78 - 11.1 = 9.53$ grams.

This is the total loss of solid matter and it comprises

(a) oxidized carbon.

(b) elutriated material.

Calorific value of coal = 27600 kJ/kg

Calorific value of residue (Bomb Calormeter Test)

$$= 40961.1 \text{ kJ/kg}$$

From equation 3.4 Chapter 3.

$$M_{vm}(CV)_{vm} + M_{res}(CV)_{res} = M_{rc}(CV)_{rc}$$

$$11.1 \times 10^{-3} (CV)_{vm} + 7.78 \times 10^{-3} \times 40961.1 = 28.41 \times 10^{-3} \times 27600$$

$$\begin{aligned}(\text{CV})_{\text{Vm}} &= 28.41 \times 10^{-3} \times 27600 - 7.78 \times 10^{-3} \times 40961.1 \\ &\quad 11.1 \times 10^{-3} \\ &= 41931.41 \text{ kJ/kg}\end{aligned}$$

$$\begin{aligned}\text{Heat released by combustion of volatiles} &= 11.1 \times 10^{-3} \text{ kg} \times \\ &41931.41 \text{ kJ/kg} \\ &= 465.44 \text{ kJ.}\end{aligned}$$

$$\begin{aligned}\text{Heat released from raw coal} &= 28.41 \times 10^{-3} \text{ kg} \times 27600 \text{ kJ/kg} \\ &= 784.12 \text{ kJ.}\end{aligned}$$

APPENDIX C

EXPERIMENTS WITH SOLID CO₂

Average height = 3.6 vertical division x 0.05 units/division
= 0.18% CO₂

Average concentration = Average of Average of 4 graphs.

Average mass of CO₂ blocks = 32 grams.

Air flow rate (uncorrected) = 660 litres/min.

Average time taken to sublime

At 6 inches above bed = 11.4 min

12 " " " = 18.4

18 " " " = 26.4

24 " " " = 23.2

Average of averages = 19.85 min

Average rate of emission of CO₂ = 32 g/19.85 min
= 1.61 g/min

Average air flow = $660 \frac{\text{L}}{\text{min}} \times 1.18 \frac{\text{kg}_3}{\text{m}^3} \times \frac{10^3 \text{g}}{\text{kg}} \frac{\text{m}^3}{10^3 \text{L}}$
= $779 \frac{\text{g}}{\text{min}}$

.. % CO₂ by mass = $\frac{1.61}{779} \times 100 = 0.2066$

% CO₂ by vol. = $\frac{V_{\text{CO}_2}}{V_{\text{air}}} = \frac{M_{\text{CO}_2}}{M_{\text{air}}} \frac{\text{air}}{\text{CO}_2} = 0.2066 \times \frac{29}{44}$

= 0.136

Compared with 0.18 above.

APPENDIX D

CALCULATION OF ENTHALPY BALANCE

In Chapter 3 of this thesis, thermodynamic analysis of heat release was expressed by equation 3.2 which is written below

$$Q = H_P - H_R \quad (3.2)$$

The calculation of heat release for a number of cases is given below.

SECTION 1

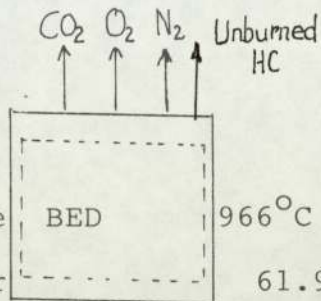
Case 1: Experimental conditions (UNINSULATED COMBUSTOR)

Bed temperature:	966°C
Inert sand particle size:	355 - 500 μm
Static bed depth:	100 mm
Superficial fluidizing velocity: (at bed temperature)	0.5 m/s
Coal particle size:	1-2.8 mm
Freeboard temperature:	475°C
Air Flow rate	355.6 L/min
Excess air	3%

Under the above experimental conditions the heat release

rate both in the bed and in above bed region are found.

(a) Bed only (Assuming all hydrogen leaves in volatile compounds)
 Assuming 61.9% of the total carbon is burnt in the bed. No H₂O is evolved except that due to moisture.



For 1kg of fuel BED 966°C = 1239K.

10.2 kg of air is used N₂ O₂ 61.9% carbon

is used

N₂ O₂

∴ Mass of carbon

= 61.9% of 75.4% of kg of fuel

= 0.47 kg

GASES LEAVING THE BED SURFACE AT 1239 K.

Const.	Mass kg	SP.Enthalpy kJ/kg	Enthalpy kJ/kg fuel
CO ₂	0.47x44 = 1.72	1060.98	1824.886
O ₂	(.23x10.2)- 32/44x1.72 = 1.095	973.29	1065.753
N ₂	.77x10.2 = 7.854	1051.23	8248.506
			11139.145 kJ/kg fuel

$$Q_{bed} = [H_{P2} - H_{Po}] + [\Delta H_o] + [H_{Ro} - H_{Rl}]$$

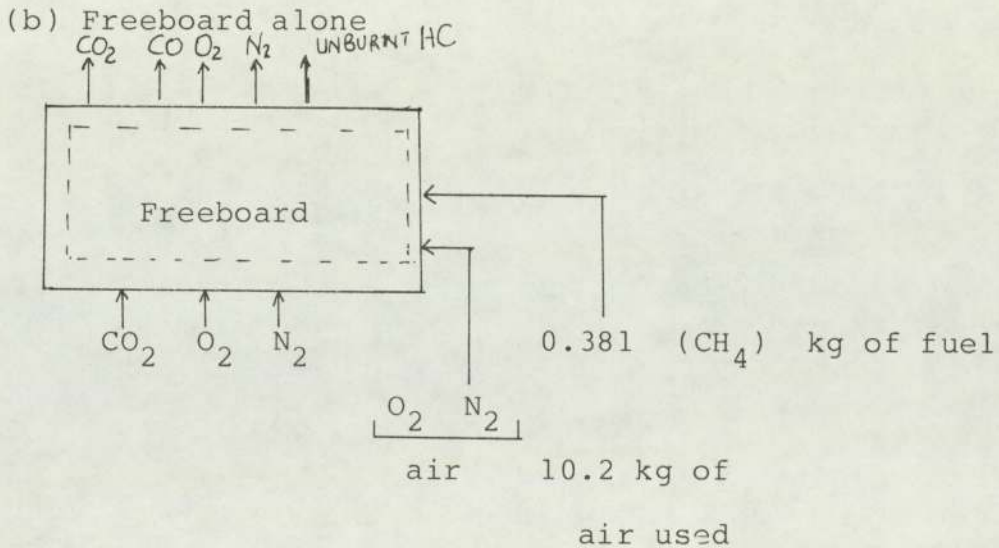
$$= 11139.145 + [0.47 \times -32791] + [1.802 \times 105 + [18.36 \times 1.005][15 - 25]]$$

= - 4476.064 kJ/kg fuel.

$Q_{bed} = - 4476.064 \text{ kJ/kg fuel} \times 0.000667 \text{ kg/5 [kW5/kJ]}$
 $= -2.986 \text{ kW.}$

Fuelling rate of carbon only

= 0.000667 kg/5 x 0.619 x 075 x 32791 kJ/kg fuel
 = 10.21 kW.



GASES LEAVING THE FREEBOARD AT 748 K

Const.	Mass Kg	Sp. Enthalpy kJ/kg	Enthalpy kJ/kg fuel
CO ₂	.381x44/16 = 1.04775	457.95	479.817
CO	0.381x28/16 = .66675	484.013	322.716
H ₂ O	.381x18/16 = .4286	891.138	381.942

O ₂	1.095-[0.23 x10.2] - [32/44 x 1.04775] -[32/28 x 0.667] - [32/18 x 0.4286] = 1.035	440.908	456.340
N ₂	0.77x10.2 = 7.858	480.149	3771.09
			5412.567 kJ/kg fuel

$$Q_{FB} = [H_{P2} - H_{PO}] + [\Delta H_O] + [H_{RO} - H_{R1}]$$

$$= 5412.507 + [0.381 \times (50143.75)] + [(1.82 \times 1.05) + (18.36 \times 1.005)][15-25]$$

$$= - 13895.701 \text{ kJ/kg fuel.}$$

$$\dot{Q}_{FB} = -13895.701 \times 0.000667 \text{ kg/s [KWs/kJ]}$$

$$= - 9.27 \text{ kW.}$$

Fuelling rate of volatiles (CH₄) only

$$0.000667 \text{ kg/s} \times .381 \times 50143.75$$

$$= 12.743 \text{ kW} \approx 13 \text{ kW}$$

Case 2 EXPERIMENTAL CONDITIONS - (INSULATED COMBUSTOR)

Bed temperature:	968 ^o C
Inert sand particle size:	355-500 μm
Static bed depth:	100 mm
Superficial fluidizing velocity at bed temperature	0.52 m/s
Coal particle size	1-2.8 mm
Freeboard temperature	554 ^o C
Coal feed rate	0.000665 kg/s
Air flow rate	365 L/min
Excess air	11%

Under the above experimental conditions the heat release rate in the bed and in the above bed region are found as in Case 1 above.

	$[H_{P2} - H_{PO}]$ kJ/kg	$[\Delta H_o]$ kJ/kg	$H_{RO} - H_{R1}]$ kJ/kg	Q kJ/kg	Q kW	F/Rate kW
Bed	12001.5	-15411.8	-195.9	-3606.2	-2.4	10.18
FB	6771.2	-19104.8	-195.9	-12529.4	-8.3	12.7

Case 3 EXPERIMENTAL CONDITIONS (INSULATED COMBUSTOR)

Bed temperature:	1050°C
Freeboard temperature:	769°C
Inert sand particle size:	355-500 μm
Static bed depth:	100 mm
Superficial fluidizing velocity:	
at bed temperature:	0.6 m/s
Coal particle size:	6.7-8.00 mm
Coal feed rate:	0.000942 kg/s
Air flow rate:	544.6 L/min
Excess air:	15%

Under the above experimental conditions the heat release rate in the bed and in the above bed region are found as in Case 1 above.

	$[H_{P2} - H_{P0}]$ kJ/kg	$[\Delta H_0]$ kJ/kg	$[H_{R0} - H_{R1}]$ kJ/kg	Q kJ/kg	Q kW	F/Rate kW
Bed	10199.2	-15411.8	-320.9	-5533.5	-5.2	14.4
FB	14315.8	-19104.8	-320895	-5109.9	-4.8	18.0

Case 4 EXPERIMENTAL CONDITION - WOOD (INSULATED COMBUSTOR)

Bed temperatures:	851.2°C
	787.7°C
Freeboard temperatures:	751.6°C
	703.5°C
Inert sand particle size:	355-500 μm
Static bed depth:	100 mm
Superficial fluidizing velocity at bed temperature:	0.4 m/s
Wood size:	8 x 8 x 10 mm
Wood feed rate:	0.013 kg/s
Air flow rate:	464.18 L/min
	470.37 L/min
Excess air:	20%, 28.5%

Under the above experimental conditions the heat release rate in the bed and in the above bed region are found as in Case 1 above.

	$[H_{P2} - H_{P0}]$ kJ/kg	$[\Delta H_0]$ kJ/kg	$[H_{R0} - H_{R1}]$ kJ/kg	Q kJ/kg	Q kW	F/Rate kW
(a) Bed	17233.03	-3138.1	-191.7	13903.18	18.07	4.08-(I)
FB	22356.6	-40265.4	-191.7	-18100.6	-23.5	52.3
(b) Bed	17531	-3138.1	-191.7	14180.1	18.4	4.1
FB	230161.42	-40265.4	-191.7	-17416.9	-22.6	52.3

SECTION 2

In this section heat transfer by radiation and natural convection are calculated for both insulated and insulated combustors.

CASE I. UNINSULATED COMBUSTOR

Experimental conditions are identical to Case I of the previous section (section 1).

Using Wong (85)'s expression for free convective heat transfer of vertical cylinder with large diameter the following equations are used. The bed is divided into five equal areas.

$Nu = C(Gr.Pr)^n K$ where K is a dimensionless correction function.

$$q = hA(\theta_w - \theta_3) \quad (W)$$

Prandtl no. = $\mu c_p / k$ where μ = viscosity of fluid (kg/ms)

$$= 1.8169 \times 10^{-5}$$

C_p = Specific heat of fluid (kJ/kg C).

$$= 0.757$$

k = fluid thermal conductivity

$$= 0.0241 \text{ kW/mK}$$

$$\text{Pr No.} = \frac{1.8169 \times 10^{-5} \text{ kg} \times \text{kJ} \times \text{mk}}{0.0241 \text{ ms} \quad \text{kgk} \quad \text{W} \quad \text{kw}} \frac{10^3 \text{ W}}{\text{kw}}$$

$$= 1.005 \text{ kJ/kgK}$$

$$\text{Nu} = \frac{hx}{k} = 55.178$$

$$\begin{aligned} \therefore h &= \frac{55.178 \text{ k}}{x} = \frac{55.178 \times 0.0241 \text{ W} \times \frac{1}{\text{mk}}}{166.66 \times 10^{-3} \text{ m}} \\ &= 7.979 \text{ W/m}^2\text{K}. \end{aligned}$$

$$h = \frac{q}{A(\theta_w - \theta_s)}$$

$$\begin{aligned} q &= hA(\theta_w - \theta_s) \\ &= 7.979 \frac{\text{W}}{\text{m}^2\text{K}} \times 0.1596 \text{ m}^2 [543 - 294] \text{ K} \\ &= 0.317 \text{ kW}. \end{aligned}$$

Radiative heat transfer $q = A\epsilon\sigma(T_w^4 - T_s^4)$

where $A = 0.1596$

$$\epsilon = 0.95$$

$$\sigma = 5.67 \times 10^{-8} \text{ W/m}^2\text{K}^4$$

$$q = 0.1596 \text{ m}^2 \times 0.95 \times 5.67 \times 10^{-8} \text{ W/m}^2\text{K}^4 (543^4 - 294^4) \text{ K}^4$$

$$= 0.683 \text{ kW}.$$

∴ Total Q = 0.317 + 0.683 = 1.0 kW.

Similarly the remaining areas are calculated as above.

Convective	Radiative	Total
0.317	0.683	1.0
0.286	0.579	0.865
0.225	0.404	0.629

∴ Total heat lost by convection and radiation in the freeboard 2.494 kW

0.288	0.563	0.851
0.241	0.438	0.679

∴ Total heat lost through the refractory in the bed 1.530 kW

$$\text{Grashof No.} = \frac{g\beta\rho^2\Delta\theta X^3}{\mu^2}$$

where g = gravitational acceleration
= 9.81 m/s²

β = coefficient of volumetric thermal expansion

$$= 1/T_f \text{ for gases (K}^{-1}\text{)}$$

T_f = absolute bulk temperature of fluid(K)
= 294

ρ = density of fluid (kg/m³)
= 1.20268 (kg/m³)

Δθ = temperature difference

$$[\theta_w - \theta_s]^\circ\text{C}$$

$$\theta_w = 270, 250, 210, 210, 185^\circ\text{C}$$

$$\theta_s = 21^\circ\text{C}$$

$$X = 500 \text{ and } 465 \text{ mm.}$$

$$\begin{aligned} \text{Gr.no.} &= 9.81 \times 1 / 294 \times 1.20268^2 [270 - 21] 166.66^3 \times (10^{-3})^3 \times \\ & (1.81696 \times 10^5)^2 \\ &= 1.68509581 \times 10^8 \end{aligned}$$

For large diameter cylinder

$$38(\text{Gr})^{-1/4} = 6.40336 \times 10^{-16}$$

$$D = 0.3048 = 0.31585$$

$$L = 965 \times 10^{-3}$$

$$\therefore \frac{D}{L} = 38(\text{Gr})^{-1/4}$$

$$c = 0.8$$

$$n = 0.25.$$

$$K = [1 + (1 + \frac{1}{\sqrt{\text{Pr}}})^2]^{-1/4}$$

$$= [1 + (1 + \frac{1}{.725})^2]^{-0.25} = 0.649$$

$$\text{Nu} = C(\text{Gr.Pr})^n K.$$

$$= 0.8(1.68509581 \times 10^8 \times 757)^{0.25} \times 0.649$$

$$= 55.178$$

CASE II. INSULATED COMBUSTOR

Experimental conditions are identical to Case II of Section 1.

Using the same method adopted in Case I, Section 2 above the total heat transfers are calculated in the bed and freeboard zone.

Convective kW	Radiative kW	Total kW
0.0584	0.0787	0.1371
0.0317	0.0434	0.0751
0.0459	0.0618	0.1077
Total heat transfer in the freeboard		0.3199 kW
0.0652	0.0954	0.1606
0.0917	0.1355	0.2272
Total heat transfer in the bed		0.3878 kW

CASE III. HEAT TRANSFER TO BED THROUGH FREE SURFACE
INTERFACE - COMBUSTION OF WOOD

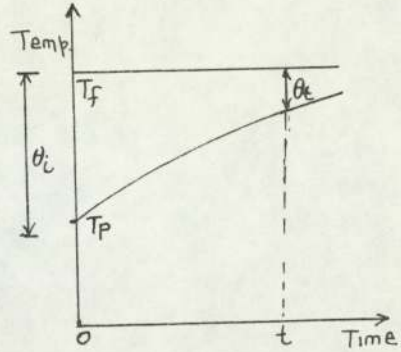
Time constant of sand particle

$$\theta_i = T_f - T_p$$

$$\theta_t = T_f - T_p$$

$$\frac{\theta_t}{\theta_i} = e^{-t/\tau}$$

where $\tau = \frac{mcp}{hs}$



Value of τ

Sand particle density = 2640 kg/m^3

$$C_p = 1 \text{ kJ/kgK}$$

$$h = 60 \text{ W/m}^2\text{K}$$

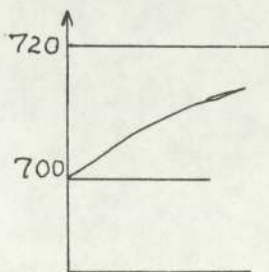
$$s = 4\pi r^2 = d_p^2 \rho$$

$$d_p = 425 \text{ } \mu\text{m}$$

$$= \left[\frac{(4/3\pi r^3 \rho C_p)}{(h \times 4\pi r^2)} \right] = \rho d_p / 6 C_p / h$$

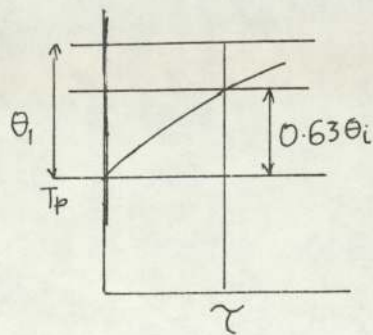
$$= \frac{2640 \text{ kg}}{\text{m}^3} \times 425 \times 10^{-6} \times \frac{1 \text{ kJ}}{\text{kg}} \times \frac{1}{60} \times \frac{\text{m}^2 \text{ K}}{\text{W}} \times \frac{10^3 \text{ W s}}{\text{kJ}}$$

$$= 3.1 \text{ secs}$$



$$\theta_1 = 20$$

$$0.63 \theta_1 = 12.6 \text{ K.}$$



Suppose particles rise to height 0.15 m above bed and fall back

$$S = \frac{1}{2} g t^2 \quad t = \frac{\sqrt{0.15}}{\sqrt{0.5 \times 9.81}} = 0.17 \text{ s}$$

$$\therefore \theta_t = \theta_{ie}^{[-.34/-3.1]}$$

$$= \theta_{ie}^{-0.11} = 0.896 \theta_i$$

$$t = 0.896 \times 20 \text{ K} = 17.92 \text{ K.}$$

For 1 kW heat transport by particles No. of particle/sec.

$$N = (1 \text{ kW} \times \text{m}^3 / 2640 \text{ kg}) \times 6/\pi [10^6/425 \text{ m}^3]^3 \times \text{kgK}/1\text{kJ} \times 1/17.92\text{K} \times [\text{kJ}/\text{kWs}]$$

$$= 525887.$$

If wood flame exchange factor is 0.1 (gas flame 0.05)

$$F = \epsilon \times \text{shape factor}$$

$$Q = \sigma (\epsilon \times \text{shape factor}) \text{ Area } (T_f^4 - T_p^4)$$

$$\text{Radiative flux} = \frac{Q}{\text{area}}$$

(Free surface is a cloud of particles (not a flat plate).

Flame temperature say $1000^{\circ}\text{C} = 1300\text{K}$.

$$\sigma = 5.67 \times 10^{-8} \text{ W/m}^2 \text{ K}^4$$

$$\begin{aligned} \text{Radiation flux} &= \frac{5.67 \text{ kW}}{10^{11} \text{ m}^2 \text{ K}^4} \times 1.3^4 \times (10^3)^4 \\ &= 162 \text{ kW/m}^2 \end{aligned}$$

$$\begin{aligned} \text{Back radiation} &= \frac{200 \text{ kW}}{\text{m}^2} \times \frac{\pi}{4} \times 0.2542 \text{ m}^2 \\ &= 8 \text{ kW.} \end{aligned}$$

Inert particle size 355 μm to 500 μm
 Type of fuel Bituminous Coal
 Fuel size 1 - 2.8mm
 Fuel feed rate 0.00048 kg/sec.
 Air flow rate 220.94 L/min
 Excess air 10%
 Fluidizing velocity 0.31 m/s

PROBE POSITION (mm)	TEMPERATURES ° C			% FLUE GASES			
	BED	PROBE	EXHAUST	CO ₂	CO	O ₂	HC
5	857	395	309	9.7	0.35	10.0	0.014
15.25	856	400	293	8.6	0.3	11.5	0.0072
26.25	885	444	304	9.7	0.45	10.4	0.0085
38.25	896	456	307	8.3	0.10	13.0	0.0063
51.75	904	482	317	9.0	0.31	12.1	0.0083
67.5	931	474	307	6.0	0.35	15.9	0.0094
87.0	950	477	303	10.8	1.7	10.0	0.0134
152.0	958	232	313	4.4	0.41	20.0	0.0084
217.0	972	422	318	7.4	0.5	14.6	0.0080
236.5	974	428	320	7.1	0.6	14.6	0.0073
252.25	978	437	324	7.9	0.9	13.9	0.0092
265.75	986	430	318	8.9	1.6	12.5	0.0088
277.75	989	437	323	10.0	1.0	11.5	0.0136
288.75	989	417	310	8.2	2.0	12.2	0.0137
299.0	981	422	327	9.2	3.5	11.5	0.0115

TABLE D1 EXPERIMENTAL RESULTS FROM COMBUSTION OF BITUMINOUS COAL
 (UNINSULATED CONDITION)

Inert particle size 355 μm to 500 μm
 Type of fuel Anthracite Coal
 Fuel size 1 - 2.8mm
 Fuel feed rate 0.0006 kg/sec.
 Air flow rate 336.25 L/min
 Excess air 8%
 Fluidizing velocity 0.5 m/s

PROBE POSITION (mm)	TEMPERATURES ° C			% FLUE GASES		
	BED	PROBE	EXHAUST	CO ₂	CO	O ₂
5	964	395	370	14.5	0.02	6.5
15.25	967	435	389	13.0	0.2	7.2
26.25	983	518	416	13.2	0.55	7.0
38.25	1008	480	394	12.0	0	9.9
51.75	988	497	398	12.0	0	9.3
67.5	998	510	407	11.5	0.15	9.8
87.0	1001	518	424	11.9	0.38	9.2
152.0	998	524	437	11.9	0.4	9.3
217.0	991	619	468	13.0	0.98	8.0
236.5	1001	623	484	12.6	1.6	7.8
252.25	987	615	462	13.0	0.7	8.5
265.75	999	558	447	12.5	0.5	8.9
277.75	1011	494	429	10.5	0.28	10.5
288.75	1029	453	405	12.4	0	10.0
299.0	973	378	395	11.4	0.15	10.4

TABLE D2 EXPERIMENTAL RESULTS FROM COMBUSTION OF ANTHRACITE COAL
 (UNINSULATED CONDITION)

Inert particle size < 355 μm to 500 μm
 Type of fuel Bituminous Coal
 Fuel size 1 - 2.8mm
 Fuel feed rate 0.0007 kg/sec.
 Air flow rate 470.3 L/min
 Excess air 30%
 Fluidizing velocity 0.47 m/s

PROBE POSITION (mm)	TEMPERATURES ° C			% FLUE GASES		
	BED	PROBE	EXHAUST	CO ₂	CO	O ₂
5	987	547	468	8.4	0.03	12.2
15.25	998	557	472	8.3	0.06	12.0
26.25	993	592	478	8.4	0.02	11.7
38.25	992	595	482	8.6	0.05	11.5
51.75	988	620	487	9.0	0.07	11.0
67.5	992	638	495	9.0	0.01	11.3
87.0	992	642	500	9.0	0.03	11.1
152.0	992	630	500	9.2	0.1	10.9
217.0	990	665	498	10.4	0.85	9.0
236.5	984	667	522	10.4	0.55	9.5
252.25	983	649	509	10.1	0.48	9.6
265.75	978	614	509	9.9	0.6	9.4
277.75	977	598	511	9.8	0.7	9.5
288.75	975	586	529	9.6	0.78	9.6
299.0	980	586	516	9.5	0.55	10.0

TABLE D3 EXPERIMENTAL RESULTS FROM COMBUSTION OF BITUMINOUS COAL
 (UNINSULATED CONDITION)

Inert particle size 355 μ m to 500 μ m
 Type of fuel Bituminous Coal
 Fuel size 1 - 2.8mm
 Fuel feed rate 0.000667 kg/sec.
 Air flow rate 355.6 L/min
 Excess air 3%
 Fluidizing velocity 0.5 m/s

PROBE POSITION (mm)	TEMPERATURES ° C			% FLUE GASES		
	BED	PROBE	EXHAUST	CO ₂	CO	O ₂
5	978	484	390	10.5	0.01	9.3
15.25	977	456	383	9.8	0.08	10.5
26.25	969	480	388	9.0	0.07	11.4
38.25	960	486	382	8.6	0.06	11.9
51.75	955	482	383	8.6	0.06	11.8
67.5	954	483	392	8.7	0.05	11.6
87.0	952	485	385	9.0	0.08	11.0
152.0	952	485	385	8.9	0.09	11.1
217.0	973	517	398	10.5	0.11	9.3
236.5	970	518	399	11.0	0.1	9.0
252.25	968	520	396	11.3	0.21	8.6
265.75	968	523	400	11.5	0.21	8.2
277.75	969	505	416	11.4	0.09	8.8
288.75	975	500	408	11.2	0.09	9.2
299.0	972	500	409	10.7	0.25	8.4

TABLE D4 EXPERIMENTAL RESULTS FROM COMBUSTION OF BITUMINOUS COAL
 (UNINSULATED CONDITION)

Inert particle size 355 μ m to 500 μ m
 Type of fuel Bituminous Coal
 Fuel size 1 - 2.8mm
 Fuel feed rate 0.000665 kg/sec.
 Air flow rate 364.97 L/min
 Excess air 11%
 Fluidizing velocity 0.52 m/s

PROBE POSITION (mm)	TEMPERATURES ° C			% FLUE GASES		
	BED	PROBE	EXHAUST	CO ₂	CO	O ₂
5	927	492	385	9.0	0.05	7.5
15.25	927	496	390	8.8	0.05	8.0
26.25	927	498	405	8.1	0.03	9.2
38.25	930	530	415	10.0	0.08	5.8
51.75	939	535	417	10.2	0.05	5.8
67.5	948	537	420	11.0	0.10	5.0
87.0	955	540	424	10.6	0.12	4.8
152.0	965	554	427	11.0	0.16	4.1
217.0	984	595	440	10.9	0.30	3.5
236.5	992	596	442	11.2	0.4	3.1
252.25	996	597	442	11.4	0.29	3.2
265.75	1006	592	432	11.5	0.21	3.3
277.75	1006	595	435	11.4	0.25	3.5
288.75	1008	580	438	11.3	0.19	3.8
299.0	1015	576	441	11.1	0.10	3.9

TABLE D5 EXPERIMENTAL RESULTS FROM COMBUSTION OF BITUMINOUS COAL
 (INSULATED CONDITION)

Inert particle size 355 μ m to 500 μ m
 Type of fuel Bituminous Coal
 Fuel size 1 - 2.8mm
 Fuel feed rate 0.000665 kg/sec.
 Air flow rate 402.5 L/min
 Excess air 22%
 Fluidizing velocity 0.61 m/s

PROBE POSITION (mm)	TEMPERATURES ° C			% FLUE GASES		
	BED	PROBE	EXHAUST	CO ₂	CO	O ₂
5	1035	612	459	10.0	0.02	5.5
15.25	1037	629	473	9.9	0.01	5.7
26.25	1042	636	460	9.7	0.01	5.7
38.25	1046	638	465	9.9	0.01	5.2
51.75	1050	640	462	10.0	0.02	4.7
67.5	1053	660	440	10.0	0.1	3.8
87.0	1054	673	472	9.0	0.05	5.6
152.0	1057	654	484	8.0	0.01	8.0
217.0	1049	680	486	9.6	0.01	5.9
236.5	1054	682	498	10.3	0.01	5.4
252.25	1059	680	488	10.6	0.01	5.0
265.75	1062	680	486	10.6	0.01	4.8
277.75	1064	685	485	10.8	0.01	4.5
288.75	1067	677	487	10.6	0.05	4.7
299.0	1070	671	489	10.5	0.05	5.0

TABLE D6 EXPERIMENTAL RESULTS FROM COMBUSTION OF BITUMINOUS COAL
 (INSULATED CONDITION)

Inert particle size 355 μ m to 500 μ m
 Type of fuel Bituminous Coal
 Fuel size 6.7 - 8.0mm
 Fuel feed rate 0.000942 kg/sec.
 Air flow rate 544.6 L/min
 Excess air 15%
 Fluidizing velocity 0.61 m/s

PROBE POSITION (mm)	TEMPERATURES ° C			% FLUE GASES		
	BED	PROBE	EXHAUST	CO ₂	CO	O ₂
5	1045	718	502	9.2	0	6.9
15.25	1053	717	502	9.0	0	8.0
26.25	1049	814	527	11.0	0.29	2.9
38.25	1052	825	505	11.2	0.9	2.1
51.75						
67.5						
87.0						
152.0						
217.0						
236.5						
252.25						
265.75						
277.75						
288.75						
299.0						

TABLE D7 EXPERIMENTAL RESULTS FROM COMBUSTION OF BITUMINOUS COAL
 (INSULATED CONDITION)

Inert particle size = 355µm to 500µm
 Type of fuel Wood
 Fuel size 8 X 8 X 10 mm
 Fuel feed rate 0.0013 kg/sec.
 Air flow rate 464.2
 Excess air 20%
 Fluidizing velocity 0.41 m/s

PROBE POSITION (mm)	TEMPERATURES ° C			% FLUE GASES		
	BED	PROBE	EXHAUST	CO ₂	CO	O ₂
5	813	690	252	13.0	0.9	2.5
15.25	825	692	230	11.5	0.05	5.1
26.25	831	745	244	13.0	0.1	3.0
38.25	837	702	247	10.5	0.05	7.0
51.75	843	758	260	12.5	0.29	3.0
67.5	847	716	244	11.2	0.05	5.6
87.0	850	758	269	13.0	0.4	2.3
152.0	853	768	248	12.6	0.2	2.3
217.0	860	781	240	13.4	0.25	1.5
236.5	862	768	260	12.5	0.22	3.0
252.25	869	778	252	12.5	0.5	4.0
265.75	863	792	264	10.5	0.20	6.5
277.75	864	788	260	10.4	0.3	5.6
288.75	873	796	252	10.3	0.21	7.9
299.0	878	752	240	9.7	0.1	7.8

TABLE D8 EXPERIMENTAL RESULTS FROM COMBUSTION OF WOOD
 (INSULATED CONDITION)

Inert particle size 355µm to 500µm
 Type of fuel Wood
 Fuel size 8 X 8 X 10mm
 Fuel feed rate 0.0013 kg/sec.
 Air flow rate 470.73
 Excess air 28%
 Fluidizing velocity 0.4 m/s

PROBE POSITION (mm)	TEMPERATURES ° C			% FLUE GASES		
	BED	PROBE	EXHAUST	CO ₂	CO	O ₂
5	724	580	220	9.2	0.05	6.9
15.25	727	594	259	10.5	0.05	8.0
26.25	745	665	255	11.6	0.06	4.0
38.25	758	689	290	10.6	0.04	6.2
51.75	767	708	323	11.0	0.04	5.9
67.5	779	672	324	10.0	0.05	6.0
87.0	788	729	329	11.4	0.1	6.5
152.0	791	730	334	12.0	0.15	5.2
217.0	800	773	330	12.2	0.5	6.0
236.5	812	732	304	11.0	0.1	4.0
252.25	818	770	330	11.5	0.3	6.9
265.75	823	758	299	11.5	0.2	4.5
277.75	826	740	300	11.5	0.15	5.2
288.75	828	716	279	11.0	0.1	5.3
299.0	830	697	280	10.3	0.1	8.1

TABLE D9 EXPERIMENTAL RESULTS FROM COMBUSTION OF WOOD
 (INSULATED CONDITION)

APPENDIX E

CALCULATION OF 'r's FROM THE FUEL AND THE AIR

Mass of air used = 8.23 g/s x 3416 sec

$$= 28.11368 \text{ kg.}$$

Mass of coal used = 0.489 g/s x 3416 sec = 1.67042 kg.

This mass of coal includes

7.9% of moisture)

5.5% of ash) 13.3%

∴ Mass of dry mineral matter free coal used

$$= \frac{1.67042}{1.133} = 1.474333628 \text{ kg}$$

$r_1 = 0.232 \times 28.114 = 6.52 \text{ kg}$ - Mass of oxygen in the air.

$r_2 = 0.768 \times 28.114 = 21.59 \text{ kg}$ - " " nitrogen " " "

$r_3 = 0$

$r_4 = 0.836 \times 1.47 = 1.23 \text{ kg}$ - Mass of carbon in the fuel.

$r_5 = 0.055 \times 1.47 = 0.081 \text{ kg}$ - " " hydrogen " " "

$r_6 = 0.088 \times 1.47 = 0.13 \text{ kg}$ - " " oxygen " " " "

$r_7 = 0.012 \times 1.47 = 0.018 \text{ kg}$ - " " nitrogen " " "

$r_8 = 0.009 \times 1.47 = 0.013 \text{ kg}$ - " " sulphur " " "

INPUT ELEMENT	MOL. WEIGHT	INPUT MASS kg	PRODUCTS	MOL. WEIGHT	MASS OF PRODUCT	VOLUME OF PRODUCT
C	12	r_4	CO ₂	44	$44/12(r_4x_1)$	$1/12(r_4x_1)$
			CO	28	$28/12(r_4x_2)$	$1/12(r_4x_2)$
			UnburntHC			$1/12(r_4x_3)$
			Unburnt C	12	$r_4(1-x_1-x_2-x_3)$	ZERO
H ₂	2	r_5	H ₂	18	$18/2(r_5x_4)$	
			UnburntHC		(r_5x_5)	$1/2(r_5x_5)$
			Unburnt H	2	$r_5(1-x_4-x_5)$	
*O ₂	32	r_6	Excess O ₂		$[r_1/32+r_6/32]$ $-1/12r_4x_1$ $-1/24r_4x_2$ $-1/32r_8$	
**N ₂	28	r_7	N ₂	28	r_7	$1/28r_7$
S	32	r_8	SO ₂	64	$64/32r_8$	$1/32r_8$
Ash		r_9	Ash			
Moisture		r_{10}	H ₂ O			
*O ₂	32	r_1				
**N ₂	28	r_2	N ₂		r_2	$1/28r_2$
Traces Elements		r_3	Traces		r_3	

* Excess O_2 = Mass of oxygen in air and fuel - Mass of oxygen used to convert carbon, hydrogen and sulphur to CO_2 , CO , H_2O and SO_2 .

∴ Excess O_2 by volume =

$$[\frac{1}{32}r_1 + \frac{1}{32}r_6] - \frac{1}{12}r_{4x1} - \frac{1}{24}r_{4x2} - \frac{1}{4}r_{5x4} - \frac{1}{32}r_8$$

** Total N_2 = $\frac{1}{28} [r_2 + r_7]$

Dry Products = $\frac{1}{12}r_{4x1} + \frac{1}{12}r_{4x2} + \frac{1}{4}r_{5x5} + \frac{1}{32}(r_1 + r_6) - \frac{1}{12}r_{4x1}$

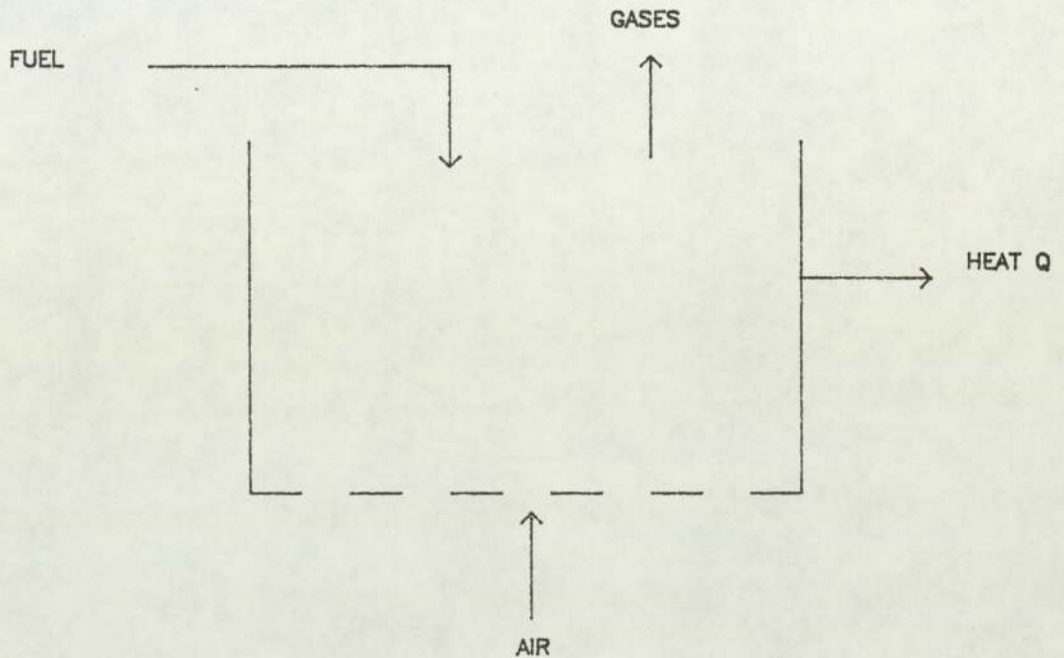
$$- \frac{1}{24}r_{4x1} - \frac{1}{32}r_8 + \frac{1}{28}(r_2 + r_7) + \frac{1}{32}r_8$$

$$= \frac{1}{24}r_{4x2} - \frac{1}{4}r_{5x4} + \frac{1}{4}r_{5x5} + \frac{1}{32}(r_1 + r_6) + \frac{1}{28}(r_2 + r_7)$$

TABLE E1.

APPENDIX F

EVALUATION OF ENERGY BALANCE USING MERRICK (57)'s DATA



Steady state energy equation gives

$$Q - W + H_i + H_o = 0.$$

H_i = enthalpy of air and fuel, the reactants at inlet temperature T_i

H_o = enthalpy of combustion products at temperature T_o .

$H_{iR} - H_{oR}$ = enthalpy of formation of all constituents at T_o
plus enthalpy of solid fuel above T_o .

$$= hf_o + Cp(T_i - T_o) \text{ kJ/mol for all constituents and the}$$

same for air as O₂ and N₂ separately.

Similarly the same is true for all the combustion products in the exhaust.

If the fuel burns incompletely, then the exhaust contains volatiles, CO, CO₂, H₂O, etc., so $n_j [hf_o + (h-h_o)_j]$ must be input for each gas or vapour in the exhaust. Suppose the coal is of Merrick's type i.e. 35% volatiles - coal C on page 539, Fuel, vol. 62, 1983

C	H	O	N	S	
84.7	5.3	7.8	1.3	0.9	% wt d.a.f

(Merrick's coal was taken because he has correlated the species in terms of ultimate analysis and total volatile proportion (see printout Table F5.)

If the proximate analysis is known then 1 kg coal will contain C kg carbon, H kg hydrogen, W kg water, O, S, N and ash masses. The water and minerals together represent (W+A) kg/kg fuel and the remaining (1-(W+A)) is to be divided into Merrick's proportion of 35% volatile coal. i.e. Taking 1 kg coal as supplied, it will contain

$$1-(W+A) \quad \frac{84.7}{12} \text{ mol C} + \frac{5.3}{2} \text{ mol H}_2 + \frac{7.8}{32} \text{ mol O}_2 + \frac{1.3}{28} \text{ mol N}_2 + \frac{0.9}{32} \text{ mol S}$$

$$+X[\text{O}_2 + 3.79 \text{ N}_2] \text{ mol air} + \frac{W_a}{100} \frac{x}{18} \text{ mol H}_2\text{O}$$

where W_a = absolute humidity

X = is the mols of air per kg fuel.

W = moisture content in the fuel.

A = Ash content in the fuel

This then forms $\text{CO}_2 + \text{CO} + \text{H}_2\text{O} + \text{N}_2 + \text{SO}_2 +$ unburned hydrocarbons. In the molar proportions it becomes $a\text{CO}_2 + b\text{CO} + d\text{H}_2\text{O} + e\text{O}_2 + f\text{N}_2 + g\text{SO}_2 + p\text{CH}_4 + q\text{C}_2\text{H}_6 + r\text{tar}$ and the molar equations require to be balanced between reactants and products. Merrick has predicted the mass proportion of p, q, r etc. and gives their enthalpies of formation at $T_{p_{\text{out}}}$ °C so that an energy balance becomes possible.

The situation is then specified and the results examined.

From Merrick's work the following are derived

$$p = [1-(W+A)] \times 6.943/16 \text{ mol CH}_4;$$

$$q = [1-(W+A)] \times 1.166/30 \text{ mol C}_2\text{H}_6; \text{ etc.}$$

so the enthalpy of CO_2 for instance is

$$a_{\text{CO}_2} [hf_o + (h_T - h_o)]_{\text{CO}_2}$$

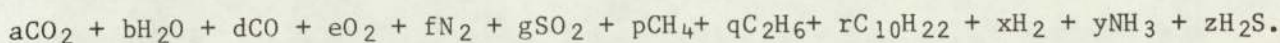
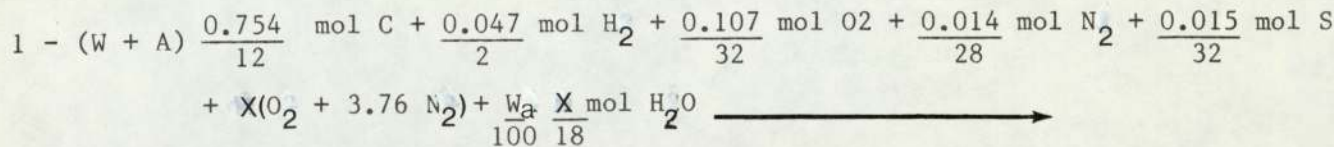
where T is the temperature of the gases at any point in the bed,

and similarly for each constituent.

Merrick gives the whole of $[hf_o + (h_T - h_o)]$ for the volatiles and tar in polynomial form on Page 544 of the reference (57), but the polynomials for O_2 , N_2 and SO_2 were taken from references 82, 84.

The above process was then used to evaluate the energy balance on the coal used in this work.

$$\begin{aligned}
 M_s &= \left[1 \frac{(0.754)}{12} + 0.5 \frac{(0.047)}{2} + \frac{0.015}{32} \right] - \frac{0.107}{32} \\
 &= 1(0.0628) + 0.05(0.0235) + 0.000469 - 0.00334. \\
 &= 0.0717 \text{ Kmol/Kg fuel.}
 \end{aligned}$$



where $W = 0.042$

$$A = 0.064$$

$$1 - (W + A) = 0.894$$

$$W_a = 60\%$$

$$X = 1.03 \times M_s = 1.03 \times 0.0717 = 0.07385.$$

$$p = 0.894 \times \frac{0.06943}{16} = 0.00388$$

$$q = 0.894 \times \frac{0.01166}{30} = 0.00035$$

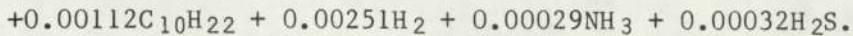
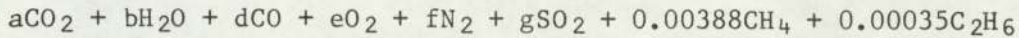
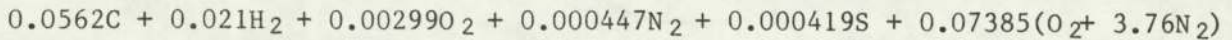
$$r = 0.894 \times \frac{0.1773}{142} = 0.00112$$

$$x = 0.894 \times \frac{0.00562}{2} = 0.00251$$

$$y = 0.894 \times \frac{0.00997}{31} = 0.00029$$

$$z = 0.894 \times \frac{0.01223}{34} = 0.00032$$

The general combustion equation then becomes



$$\text{Carbon balance : } a + b = 0.0562 - 0.00388 - 0.0007 - 0.0112 = 0.04042 \quad (A)$$

$$\begin{aligned} \text{Hydrogen balance : } b &= 0.021 + 0.00246 - 0.00776 - 0.00105 - 0.01232 - 0.00251 \\ &\quad - 0.000435 - 0.00032 \\ &= -0.000935 \end{aligned}$$

$$\text{Sulphur balance : } g = 0.000419 - 0.00032 = 0.000099$$

$$\begin{aligned} \text{Oxygen balance : } a + b/2 + d/2 + e + g &= 0.00299 + 0.07385 + 0.00123 \\ e + a + d/2 &= 0.00299 + 0.07385 + 0.00123 + 0.0004675 - 0.000099 \\ e + a + d/2 &= 0.07844 \quad (B) \end{aligned}$$

$$\begin{aligned} \text{Nitrogen balance : } f &= (0.07385 \times 3.76) + 0.000447 - 0.000145 \\ &= 0.278 \end{aligned}$$

Product analysis gives

$$d/a = 0.11/10.05 = 0.0109$$

$$\text{From (A) } a(1 + d/a) = 0.04042$$

$$a = 0.04042/0.0109 = 0.04$$

$$\text{and } d = 0.04042 - 0.04 = 0.00042$$

$$\begin{aligned} \text{From (B) } e &= 0.07844 - (0.04 + 0.00042/2) \\ &= 0.03823. \end{aligned}$$

ENTHALPY BALANCE

With 3 % Excess Air

		FREEBOARD		BED	
Constituents	Kmol/kg (n)	Molar Enthalpy	Specific enthalpy	MW[h _P -h _R] KJ/kg-mol	n[MW(h _P -h _R)] KJ/kg
		MW[h _P -h _R] KJ/kg-mol	n[MW(h _P -h _R)] KJ/kg		
CO	0.00042	-27603.12	-116.22	-266340.47	-111.86
CH ₄	0.00388	-772450.31	-2997.11	-740679.37	-2873.84
C ₂ H ₆	0.00035	-1376396.88	-481.74	-1322193	-462.77
C ₁₀ H ₂₂	0.00112	-6099634.31	-6831.59	-5893466.85	-6600.82
H ₂	0.00251	-239793.19	-601.88	-234544.73	-588.71
NH ₃	0.00029	-498817.5	-144.66	-482831.47	-140.02
H ₂ S	0.00032	-595829.2	-190.67	-571281.86	-182.81
			-11363.85		-10960.83
			= -7.6 KW		= -7.3 KW

TABLE F1. ENTHALPY OF UNBURNT HC IN THE BED AND FREEBOARD

(UNINSULATED CONDITION)

constituents	Kmol/kg (n)	BED		FREEBOARD	
		MW[h _P -h _R] KJ/kg-mol	n[MW(h _P -h _R)] KJ/kg	MW[h _P -h _R] KJ/kg-mol	n[MW(h _P -h _R)] KJ/kg
CO ₂	0.04	46614.85	1864.59	20044.62	801.79
CO	0.00042	29710.08	12.48	13559.45	5.7
CH ₄	0.00388	56535.8	219.36	21516.98	83.49
C ₁₀ H ₂₂	0.00112	428258.51	479.65	147516.33	165.22
H ₂ O	-0.000935	36126.71	-33.78	16016.95	-14.98
O ₂	0.03823	31092.95	1188.68	14119.56	39.79
N ₂	0.278	29383.33	8168.57	13444.88	3737.68
H ₂ S	0.00032	38915.5	12.45	16782.88	5.37
NH ₃	0.00029	46552.07	13.5	19088.44	5.54
H ₂	0.00251	27993.83	70.27	13037.41	32.72
			11995.77		5362.31
			= 8 KW		= 3.6 KW

TABLE F2. ENTHALPY OF HOT GASES IN THE BED AND FREEBOARD

(UNINSULATED CONDITION)

With 11% excess air

Constituents	Kmol/kg (n)	FREEBOARD		BED	
		MW[h _P -h _R] KJ/kg-mol	n[MW(h _P -h _R)] KJ/kg	MW[h _P -h _R] KJ/kg-mol	n[MW(h _P -h _R)] KJ/kg
CO	0.00062	-275166.56	-170.6	-266295.97	-165.1
CH ₄	0.00388	-767142.78	-2976.51	-740557.58	-2873.36
C ₂ H ₆	0.00035	-1367288.27	-478.55	-1321987.91	-462.7
C ₁₀ H ₂₂	0.00112	-6062381.26	-6789.87	-5892770.22	-6599.9
H ₂	0.00251	-239111.78	-600.17	-234518.18	-588.64
NH ₃	0.00029	-496187.32	-143.89	-482764.87	-140.003
H ₂ S	0.0032	-592040.89	-189.45	-571178.52	-182-.78
			-11352.05		-11012.49
			= -7.5 KW		= -7.3 KW

TABLE F3. ENTHALPY OF UNBURNT HC IN THE BED AND FREEBOARD

(INSULATED CONDITION)

Constituents	Kmol/kg (n)	FREEBOARD		BED	
		MW[h _P -h _R] KJ/kg-mol	n[MW(h _P -h _R)] KJ/kg	MW[h _P -h _R] KJ/kg-mol	n[MW(h _P -h _R)] KJ/kg
CO ₂	0.0398	24087.08	958.67	46728.54	1859.8
CO	0.00062	16063.44	9.96	29778.62	18.46
CH ₄	0.00388	26326.34	102.15	56704.07	220.01
C ₁₀ H ₂₂	0.00112	184097.2	206.19	429668.8	481.23
H ₂ O	-0.000935	19054.16	-17.82	36214.89	-33.86
O ₂	0.044	16755.24	737.23	31164.61	1371.24
N ₂	0.2995	15917.1	4767.17	29451.01	8820.58
H ₂ S	0.00032	21509.21	6.88	39014.03	12.48
NH ₃	0.00029	23035.22	6.68	46678.6	13.54
H ₂	0.00251	15396.55	38.65	28056.3	70.42
			6815.75		12833.9
			= 4.5 KW		= 8.5 KW

TABLE F4. ENTHALPY OF HOT GASES IN THE BED AND FREEBOARD

(INSULATED CONDITION)

```
10 ! RE-STORE"FOA4B:F8"
20 OPTION BASE 0
30 PRINTER IS 0
40 REM ****COMPUTATION OF MATRIX A AND VECTOR B
50 REM ***
60 REM OBTAINING NUMERATOR
70 DIM Nu(10,10),De(10,10),D(10),A(10,10),B(10),X(10),X1(10)
80 READ R1,R2,R3,R4,R5,R6,R7,R8,R9,R10
90 READ D1,D2,D3,D4,D5,D6
100 INPUT "ENTER THE NUMBER OF EQUATIONS",N
110 REDIM Nu(N,N),De(N,N),D(N)
120 REDIM A(1:N,1:N),B(1:N),X(1:N),X1(1:N)
130 FOR I=1 TO N
140 PRINT "This is equation no. ";I
150 FOR J=0 TO N
160 INPUT "Enter numerator",Nu(I,J)
170 NEXT J
180 FOR J=0 TO N
190 PRINT Nu(I,J);
200 NEXT J
210 IF I=1 THEN GOTO 260
220 DISP "IS Denominator the same for the equation number ";I;"
"
230 INPUT Y#
240 IF Y#="Y" THEN GOTO 320
250 IF Y#<>"N" THEN GOTO 230
260 DISP "ENTER DENOMINATOR FOR THE ";I;"th EQUATION"
270 FOR J=0 TO N
280 INPUT De(I,J)
290 PRINT De(I,J);
300 NEXT J
310 GOTO 360
320 FOR J=0 TO N
330 De(I,J)=De(I,J)
340 PRINT De(I,J);
350 NEXT J
360 INPUT "ENTER CONSTANT",D
370 FOR J=0 TO N
380 Final(I,J)=D*De(I,J)-Nu(I,J)
390 NEXT J
400 PRINT " D IS"
410 PRINT D
420 NEXT I
430 FOR I=1 TO N
440 FOR J=0 TO N
450 PRINT Final(I,J);" ";
460 NEXT J
470 PRINT CHR$(10)&"NEXT EQUATION"
480 NEXT I
490 FOR I=1 TO N
500 FOR J=1 TO N
510 A(I,J)=Final(I,J-1)
520 NEXT J
530 B(I)=Final(I,N)
540 NEXT I
550 PRINT "MAT A IS"
560 FOR I=1 TO N
570 FOR J=1 TO N
580 A(I,J)=A(I,J)*10000
590 NEXT J
```

```
600 NEXT I
610 FOR I=1 TO N
620 B(I)=B(I)*10000
630 NEXT I
640 MAT PRINT A
650 Deta=DET(A)
660 MAT A=INV(A)
670 MAT X1=B*(-1)
680 MAT X=A*X1
690 PRINT "INVERSE OF MAT A IS"
700 MAT PRINT A
710 PRINT "DETERMINANT OF MAT A: ";Deta
720 PRINT "MAT B IS"
730 MAT PRINT B
740 PRINT "MAT X IS"
750 MAT PRINT X
760 REM ****OBTAINING UNBURNT CARBON
770 C1=1-X(1)-X(2)-X(3)
780 PRINT " C1 IS"
790 PRINT C1
800 END
810 DATA 9.61222,31.81978,0,1.37095,0.08546,0.19455,0.02546,0.027
27,0,0
820 DATA 0.056,0.0005,0.000062,0.16,0,0
```

```
1  I RE-STORE "VOL%:F8"
10  REM ***VOLATILES FORM PROX. ANAL***
20  OPTION BASE 1
30  DIM A(10,10),C(10),C$(10),V(10),D(10,10)
40  MAT READ C$
50  MAT READ A
60  READ P
70  FOR I=1 TO 5
80  READ C(I)
90  NEXT I
100 C(6)=1-P
110 C(7)=1.31*C(2)
120 C(8)=.22*C(2)
130 C(9)=.32*C(3)
140 C(10)=.15*C(3)
150 MAT D=INV(A)
160 MAT V=D*C
170 PRINT "VOLATILE MATTER ";100*P;"%"
180 FOR I=1 TO 10
190 PRINT C$(I);" = ";V(I)
200 NEXT I
210 FOR I=2 TO 10
220 S=S+V(I)
230 NEXT I
240 PRINT "TOTAL VOLATILES = ";S
250 S=0
260 GOTO 60
270 DATA "CHAR","CH4","C2H6","CO","CO2","TAR","H2","H2O","NH3","H2
S"
280 DATA .98,.8,.75,.4286,.2727,.85,0,0,0,0
290 DATA .002,.25,.2,0,0,.082,1,.1111,.1765,.0588
300 DATA .002,0,0,.5714,.7273,.049,0,.8889,0,0
310 DATA .01,0,0,0,0,.009,0,0,.8235,0
320 DATA .006,0,0,0,0,.01,0,0,0,.9412
330 DATA 1,0,0,0,0,0,0,0,0,0
340 DATA 0,1,0,0,0,0,0,0,0,0
350 DATA 0,0,1,0,0,0,0,0,0,0
360 DATA 0,0,0,1,0,0,0,0,0,0
370 DATA 0,0,0,0,1,0,0,0,0,0
380 DATA .15,.918,.043,.023,.01,.006
390 DATA .25,.894,.049,.037,.012,.008
400 DATA .35,.847,.053,.078,.013,.009
410 DATA .381,.754,0.047,0.107,0.014,0.015
```

Print Out Table F5

REFERENCES

1. ANSON, D. Prog. Energy Combustion Science, Vol. 2, pp 61-82 (1976).
2. SKINNER, D G. The Fluidized Combustion of Coal, NCB, London, 1970.
3. THURLOW, G G. Process Engineering and Steam Plant Groups, Proceedings of The Institution of Mechanical Engineers, Vol. 192, No. 15, 1978.
4. BOTTERILL, J S M. Fluidized Beds Combustion and Applications - by J R Howard, Applied Science Publishers, London and New York (1983).
5. MATHESON, G L. HERBST, W A and HOLT, P H. Industrial and Engineering Chemistry, June 1949.
6. GELDART, D. Powder Technology, 1, 355 (1967/68).
7. DAVIDSON, J F and HARRISON, D. Fluidized Particles, Cambridge University Press, 1963.
8. ERGUN, S. Chemical Engineering Progress, 48, 89 (1952).
9. ALLEN, T. Particle Size Measurement, pp 110-113, 3rd Edition, Chapman and Hall, London and New York (1981).
10. WEN, C Y and YU, Y H., A I Chem. Eng. J. 12, 610 (1966).
11. GOROSHKO, V D, ROZENBAUM, R B and TODDES, O M. Izvetiya Vizzor, Neft'e Gras I, 125 (1958).
12. BOTTERILL, J S M. Fluid Bed Heat Transfer, Academic Press, London (1975).
13. ZABRODSKY, S S. Int. J. Heat Mass Transfer, Vol. 6, pp 23-31 (1963).
14. BOTTERILL, J S M. Thermal Applications of Fluidized Bed Technology - Notes on a short course, Department of Mechanical Engineering, The University of Aston in Birmingham, 1982.
15. BASKAKOV, A P, BERG, B V, VITT, O K, FILLIPPORSKI, N F, KIRAKOSYAN, V A, GOLDOBIN, J M and MASKEAR, V V. Powder Technology, 8, 273 (1973).
16. ROWE, P N. The effect of bubbles on gas-solid contacting in fluidized beds. Chem. Engng. Progr. Sympos. Ser. 1962, 58, N38, 42-56.
17. ROWE, P N and SUTHERLAND, K S. Solid mixing studies in gas fluidized beds, Part II: The behaviour of deep beds of dense materials, Trans. Instn. Chem. Engrs., Vol. 42, 1964.

18. ROWE, P N, PARTRIDGE, B A, CHENEY, A G, HENWOOD, G A and LYALL, E. The Mechanisms of solids mixing in fluidized beds, Trans. Instn. Chem. Engrs., Vol. 43, 1965.
19. SUTHERLAND, K S. Solids Mixing Studies in Gas Fluidized Beds, Part I. A Preliminary Comparison of Tapered and Non-tapered Beds. Trans. Instn Chem. Engrs, Vol. 39, 1961.
20. LEWIS, W K, GILLILAND, E R and GIRONARD, H. Heat Transfer and solids mixing in beds of fluidized solids - Chem. Engng. Progress Sympos. Ser. No. 38, Vol. 58.
21. TAILBY, S R and COCQUEREL, M A T. Some studies of solids mixing in fluidized beds, Trans. Inst. Chem. Engrs. Vol. 39, 1961.
22. FAN, L T, CHEN, S J and WATSON, C A. Industrial and Engineering Chemistry, Vol. 62, No. 7, 1970.
23. BROUGHTON, J. Gas combustion in shallow fluidized beds. Applied Energy pp 61 (1965).
24. PILLAI, K K. Premixed gas combustion in shallow fluidized beds, Journal of the Institute of Fuel, Dec. 1976.
25. GILLILAND, E R and MANSON, E A. Gas and solid mixing in fluidized beds - Industrial and Engineering Chemistry, pp 1191 (1949).
26. GILLILAND, E R, MANSON, E A and OLIVER, R C. Gas-flow patterns in beds of fluidized solids - Industrial and Engineering Chemistry, pp 1177, 1953.
27. BROUGHTON, J and HOWARD, J R. Fluidized Beds Combustion and Applications, by J R Howard, Applied Science Publishers, London and New York (1983).
28. PILLAI, K K. Journal of the Institute of Energy (1981).
29. CHAKRABORTY, R K and HOWARD, J R. Journal of the Institute of Energy, 1981.
30. AVEDESIAN, M M and DAVIDSON, J F. Trans. Inst. Chem. Engrs., Vol. 51 (1973).
31. CAMPBELL, E K and DAVIDSON, J F. Inst. of Fuel Symposium, Series No. 1 (1975), Fluidized Bed Combustion Conference.
32. BASU, P. Fuel, Vol. 56 (1977).
33. FIELD, M A, GILL, D W, MORGAN, B B, HAWKSLEY, P G W. Combustion of Pulverized Coal, BCURA, Leatherland (1967).
34. ESSENHIGH, R H and PERRY, M G. Combustion and Gasification: A Review - Residential conference on science in the use of coal. Proceeding at the conference 15th to 17th April 1958. Held at University of Sheffield. Published by the Institute of Fuel.

35. MULCAHY, M F R and SMITH, I W. Kinetics of combustion of pulverized fuel: A review of theory and experiment, Rev. Pure and Appl. Chem. 19, 81 (1969).
36. BASU, P., BROUGHTON, J. and ELLIOTT, D E. Combustion of single coal particles in fluidized beds, Institute of Fuel Symposium, Series No. 1 (1975), Fluidized Bed Conference.
37. GIBBS, B M and HEDLEY, A B. Fluidization, Cambridge University Press pp 235-240 (1978).
38. SINHA, P K, DATTA, A B, NANDI, S S and BHADURI, D. Fuel 1980, Vol. 59, July pp 527-531.
39. PYLE, D L. Rapporteur's Report, Institute of Fuel Symposium, Series No. 1: Fluidized Combustion Conference (1975)
40. HORIO, M and WEN, C Y. An Assessment of Fluidized Bed Modelling, AIChE Symposium Series No. 161, Vol. 73.
41. GIBBS, B M, PEREIRA, F J and BEER, J M. Coal Combustion and NO Formation in an Experimental Fluidized Bed, Institute of Fuel Symposium Series No. 1: Fluidized Combustion 1975.
42. GIBBS, B M. A mechanistic model for predicting the performance of a fluidized bed coal combustor. Inst. of Fuel Symposium Series No. 1: Fluidized Combustion 1975.
43. BEER, J M. The Fluidized Combustion of Coal, Proceeding 16th Symposium (International) Combustion, p 439, The Combustion Institute 1977.
44. RAJAN, R R and WEN, C Y. A comprehensive model for fluidized bed coal combustors, AIChE Journal Vol. 26, No. 4, 1980.
45. SMITH, I W. Combustion and Flame, 17, 303-314 (1971).
46. FIELD, M A. Combustion and Flame, 14, 237-248 (1970).
47. GARBETT, E S and HEDLEY, A B. Combustion rates in a fluidized bed combustor - Fluidized Combustion Systems and Applications. Proceedings of the Institute of Energy, Nov. 1980.
48. JUNG, K and LaNAUZE, R D. Particle Size and Density changes during Fluidized Bed Combustion - The Canadian Journal of Chemical Engineering, Vol. 61, 1983.
49. YAGI, S and KIRUI, D. Combustion of Solids - Fifth Symposium (International) on Combustion. The Combustion Institute, 1955.
50. MENSTER, M, O'DONNELL, H J, ERGUN, S and FRIEDEL, R A. Coal Gasification: A symposium sponsored by the division of fuel chemistry at the 165th meeting of the American Chemical

Society, Dallas Texas (April 9-10) 1974, Series 131, Editor, Lester G. Massey - Washington.

51. LEIGHTON, L H and TOMLINSON, R C. Fuel, Vol. 39 (1960).

52. BADZIOCH, S and HAWKSLEY, P G W. Ind. Engng. Chem. Process. Devel. Vol. 9, No. 4 pp 521-530 (1970).

53. NEUFIELD, L F and BERKOWITZ, Fuel Vol. 43 (1964).

54. ANTHONY, D B and HOWARD, J B. AI Chem. Journal, Vol. 22, No. 4, pp 625-656 (July 1976).

55. THURGOOD, J R and SMOOTH, L Douglas. Pulverized - Coal Combustion and Gasification by L Douglas Smooth and David T Pratt - Plenum Press, New York and London.

56. HOWARD, J B and ESSENHIGH, R H. Eleventh Symposium (International) on combustion. Combustion Institute, pp 399-408.

57. MERRICK, D. Fuel, Vol. 62, May 1983, pp 534-546.

58. STUBINGTON, J F. Journal of the Institute of Energy, pp 191-195, Dec. 1980.

59. ATIMTAY, A. Fluidization - Plenum Press, New York and London, 1980.

60. PARK, D, LEVENSPIEL, O and FITZGERALD, T J. Fuel Vol. 60 (1981)

61. PATTIPATI, R R and WEN, C Y. Devolatilization and Combustion of Coal in Fluidized Bed Combustion, - 2nd World Congress of Chemical Engineering, Oct. 1981, Vol.2.

62. YATES, J G, MacGILLIVRAY, M and CHEESMAN, D J. Coal Devolatilization in Fluidized Bed Combustors - Chemical Engineering Science, Vol. 35, pp 2360-2361.

63. LaNAUZE, Robert D. Coal Devolatilization in Fluidized Bed Combustors. Fuel 1982, Vol. 61, pp 771.

64. ROSE, J W and COOPER, J R. Technical Data on Fuel, Scottish Academic Press, Seventh Edition 1977.

65. FLINT, W L. Tables of Enthalpy of Undissociated Gases - Department of Mechanical Engineering, The University of Aston in Birmingham.

66. WESTWOOD, C R. PhD Thesis, The University of Aston in Birmingham.

67. TRINGHAM, D J. PhD Thesis, University of Leeds, 1982. The Combustion of Methane in Shallow Fluidized Beds.

68. KHITRIN, L N, RATVITCH, M B and KATOVA, L L. The characteristics of the combustion of the coke residue of solid fuels. Eighth Symposium on Combustion (1962) pp 793-800.
69. GOLOVINA, E S and KHAUSTOVICH, G P. The interaction of carbon with carbon dioxide and oxygen at temperatures up to 3000 K. Eighth Symposium on Combustion (1962) pp 784-792.
70. BYWATER, R J. The effects of devolatilisation kinetics on the injector region of fluidized beds: The proceedings of the Sixth International Conference on Fluidized Bed Combustion, Vol. III 1980, Atlanta Hilton, Atlanta, Georgia, USA.
71. JOVANOVIC, G. PhD Thesis, Oregon State University, USA.
72. BAULEV, E D and TROYANKIN, Y V. Study of the Aerodynamic Structure of Gas Flow in a Cyclone Chamber. Thermal Eng. Vol. 4, 1969.
73. HIGHLEY, J and MERRICK, D. 1971, Chem. Eng. Prog. Symposium, Series 67, 116, 219.
74. PRITCHARD, A B and CAPLIN, P B. Experience with a fluid bed test rig - fluidization combustion: Systems and Applications, 1980.
75. SHELTON, J. The Woodburner's Encyclopedia, 1976. Vermont Crossroads Press, Waitsfield, Vermont, USA.
76. LIAN, C K, FINDLEY, M E and FLANIGAN, V J. Air-blown wood gasification in a large fluidized bed reactor. Ind. Eng. Chem. Process Des. Dev. 1982, 21, 699-705.
77. EVANS, M, VITHANADURAGE, I and WILLIAMS, A. An investigation of the combustion of wood.
78. PECANHA, R P. PhD Thesis, University of Leeds, 1984.
79. ROBERTS, A F. Problems associated with the theoretical analysis of the burning of wood - 13th Symposium (International) on Combustion 1971. Combustion Institute
80. MURGAI, M P, RAM, S and NAGAR, P S. A study of design parameters of simple and complex wood cookstoves - Energy Research, Vol. 8, 139-150 (1984).
81. WAY, R J B. Combustion Engines Group. Proc. Inst. Mech. Engrs. Vol. 190, 60/76.
82. STULL, D R and PROPHET, H. JANAF Thermochemical Tables - Second Edition.
83. McBRIDE, B, HEIMEL, S, EHLERS, J G and GORDON, S. Thermodynamic Properties to 6000 K for 210 substances involving the first 18 elements - National Aeronautics and Space Administration 1963.

84. BAUM, M M and STREET, P J. Predicting the Combustion Behaviour of Coal Particles -Combustion Science and Technology 1971, Vol. 3, pp 231-243.
85. WONG, H Y. Heat Transfer for Engineers, Longman Group Limited, London 1977.
86. McADAMS, W H. Heat Transmission, McGraw-Hill Publishing Company Ltd, New York, London and Toronto.
87. HAMBLIN, F D. Abridged Thermodynamic and Thermochemical Tables SI Units, Pergamon Press, Oxford (1971).
88. KUNII, D and LEVENSPIEL, O. Fluidization Engineering, Wiley, New York, (1969).
89. LEWIN, D A. Thermal radiation characteristics of fluidized solids. PhD thesis, The University of Aston in Birmingham, 1975.
90. MARTENS, F J A. The behaviour of the freeboard region of a fluidized bed coal combustion. The Seventh International Conference on Fluidized Bed Combustion, October 25-27, 1982, Philadelphia, Pennsylvania, USA. US Dept. of Energy
91. STONE, H N, BATCHELOR, J D and JOHNSTONE, H F. Low temperature carbonization rates in a fluidized bed. Industrial and Engineering Chemistry, Vol. 46, No.2, Feb. 1954.
92. PITT, G J. The kinetics of the evolution of volatile products from coal: Fuel 41, 267 (1962).
93. BERKOWITZ, N. Mechanisms of coal pyrolysis on the nature and kinetics of devolatilization. Fuel, Vol. 39 (1960).
94. PILLAI, K K. A schematic for coal devolatilization in fluidized bed combustors.
95. SHAPATUNA, E A, KALYUZHNYI, V V and CHUKHANOV, Z F. Rate of Evolution of Volatile substances in the Thermal Decomposition of the Organic Mass of coal. - Akademii Nank, SSSR, 72(5), 869-972 (1950).
96. ZABRODSKY, S S. Hydrodynamics and Heat Transfer in Fluidized Beds. The MIT Press Cambridge (1966).
97. BASU, P. Combustion of coal in shallow fluidized beds. PhD thesis 1976. University of Aston
98. CHAKRABORTY, R K. Some aspects of combustion of coal in fluidized beds. PhD thesis 1979. University of Aston
99. JONES, J F, SCHMID, M R and EDDINGER, R T. Fluidized bed pyrolysis of coal. Chemical Engineering Progress, Vol. 60, No. 6, June 1964.
100. ROSS, I B and DAVIDSON, J F. The combustion of carbon

particles in a fluidized bed. Trans. IChemE, Vol. 59, 1981.

101. KIMBER, G M and GRAY, M D. Rapid Devolatilization of small coal particles. Combustion and Flame, Vol. 11 (1967).

102. ZIELINSKI, E. The evolution of volatile matter from pulverized coal particles. Fuel, 46, 329 (1967).

103. BEER, J M, BARON, R E, BORGHI, G, HODGES, J L and SAROFUN, A F. A model of coal combustion in fluidized bed combustors. Fifth Int. Conference on Fluidized Bed Combustion, Washington DC, Dec. 1977.

104. KEAIRNS, D L and MORRIS, J P. Coal devolatilization studies in support of the Westinghouse fluidized bed coal gasification process. Fuel, 1979, Vol. 58, pp 465.

105. STUBINGTON, J F and DAVIDSON, J F. Gas-phase combustion in fluidized beds. AIChE Journal Vol. 27, No. 1 Jan. 1981.

106. STUBINGTON, J F and LaNAUZE, R D. The combustion of non-premixed gas in fluidized beds. CHEMECA 81 - 9th Australasian Conference in Chemical Engineering, Christchurch, New Zealand, Aug. 30 - Sept. 4, 1981.

107. LEIGHTON, L H and TOMLINSON, R C. Estimation of the volatile matter of pure coal substance. Fuel, Vol. 39 (1960).

108. HOWARD, J R. Short Course Notes on Fluidized Bed Combustion System Design - University of Aston in Birmingham, 1982.

109. HOUGEN, O A and WATSON, K M. Chemical Process Principles, Part 3, John Wiley and Sons Inc.

110. HOWARD, J R. Fluidized Bed Combustion and Heat Treatment, Engineering, Dec. 1978.

111. FLINT, W L. Private communication, Department of Mechanical and Production Engineering, The University of Aston in Birmingham.

112. DESYPRIS, J., MURDOCH, P., and WILLIAMS, A. Investigation of the flash pyrolysis of some coals. Fuel 1982, vol. 61.

113. HESP, W.R. and WATERS, P.L., Thermal Cracking of tars and Volatile Matter from coal Carbonization. Ind. Eng. Chem., Prod. Res. Dev. 1970,9,194.

114. MARTENS, F J A., OP den BROUW, H., and VAN KOPPEN, C W J. Upwind Heat Transfer from the freeboard to the Fluidized Bed by recirculating particles. XVIth ICHMT International Symposium, Dubrovnik, Yugoslavia. 3 - 7 Sept. 1984.

115. OKA, S. Kinetics of coal combustion in Fluidized Bed. XVIth ICHMT International Symposium, Dudrovnik, Yugoslavia. 3 - 7 Sept. 1984.